



**MONASH** University

**Understanding liposomal drug nanocrystal  
formulations and their potential in oral drug  
delivery**

Tang Li

A thesis submitted for the degree of *Doctor of Philosophy* at  
Monash University in 2019

Drug Delivery, Disposition and Dynamics  
Monash Institute of Pharmaceutical Sciences  
Parkville, Victoria, Australia

For my parents C.X Li, Jin Tang  
And my fiancé Bo Chu

## Copyright Notice

© Tang Li (2019).

I certify that I have made all reasonable efforts to secure copyright permissions for third-party content included in this thesis and have not knowingly added copyright content to my work without the owner's permission.

## Table of contents

Copyright Notice .....	III
Abstract .....	VIII
Declaration of authorship .....	X
Publications during enrolment.....	XI
Thesis Including Published Works Declaration.....	XII
Acknowledgements .....	XIV
List of Abbreviations .....	XV
<b>Chapter 1: Introduction .....</b>	<b>1</b>
Statement of problem .....	2
Hypotheses .....	2
Aims .....	3
Investigate the <i>in vitro</i> drug release behaviour for ciprofloxacin liposomes with and without nanocrystallisation. Drug nanocrystallisation within liposomes.....	4
Abstract .....	4
1.1 Introduction .....	4
1.2 Liposomes as drug delivery systems .....	5
1.3 Drug loading methods .....	8
1.4 Structural characterisation techniques for the state of drugs inside liposomes	
14	
1.4.1 Cryogenic transmission electron microscopy (Cryo-TEM)/Cryogenic electron tomography.....	14
1.4.2 Small/Wide angle X-ray scattering (SAXS/WAXS) .....	15
1.4.3 Differential scanning calorimetry (DSC) .....	15
1.4.4 Other techniques.....	16
1.5 Precipitation of drug within liposomes .....	25
1.5.1 Doxorubicin .....	25
1.5.2 Vincristine, vinorelbine and vinblastine.....	27
1.5.3 Topotecan .....	28
1.5.4 Other drugs.....	29
1.6 Drug release from nanocrystallised drug within liposomes .....	30
1.7 Future applications of nanocrystallised liposomes and conclusions .....	34
Conflict of Interest .....	36
References .....	37
<b>Chapter 2: Solid state characterisation of ciprofloxacin liposome nanocrystals.....</b>	<b>54</b>
Solid state characterisation of ciprofloxacin liposome nanocrystals.....	55
Abstract .....	55
2.1 Introduction .....	56

<b>2.2 Hypotheses and aims.....</b>	<b>59</b>
<b>2.3 Experimental section .....</b>	<b>59</b>
2.3.1 Materials.....	59
2.3.2 Sample preparation .....	59
2.3.3 Cryogenic transmission electron microscopy (Cryo-TEM) .....	61
2.3.4 Solid state characterisation of the ciprofloxacin liposome nanocrystals in dispersion .....	61
2.3.5 Temperature-dependent SAXS measurements of the solid state of drug nanocrystals .....	62
2.3.6 pH-dependent SAXS measurements of the solid state of drug nanocrystals.....	62
<b>2.4 Results and Discussion .....</b>	<b>63</b>
2.4.1 Morphology of liposomal nanocrystals .....	63
2.4.2 Solid state characterisation of liposomal ciprofloxacin nanocrystals.....	66
2.4.3 Temperature-dependent structure of ciprofloxacin hydrate nanocrystals within liposomes.....	68
2.4.4 Effect of pH on the solid state of the ciprofloxacin nanocrystals upon dissolution	70
2.4.5 Implications for the use of ciprofloxacin liposomal nanocrystals <i>in vivo</i> .....	73
<b>2.5 Conclusion.....</b>	<b>74</b>
<b>Conflict of Interest .....</b>	<b>75</b>
<b>Acknowledgments .....</b>	<b>75</b>
<b>Supporting information.....</b>	<b>76</b>
<b>References .....</b>	<b>80</b>
<b><u>Chapter 3: Engineering the dimension of nanocrystals inside liposomes.....</u></b>	<b>86</b>
<b><u>Chapter 3 A: Direct comparison of standard TEM and cryogenic TEM in imaging nanocrystals inside liposomes .....</u></b>	<b>86</b>
<b>Abstract.....</b>	<b>87</b>
<b>3A.1 Introduction .....</b>	<b>88</b>
<b>3A.2 Hypotheses and aims.....</b>	<b>90</b>
<b>3A.3 Experimental section.....</b>	<b>91</b>
3A.3.1 Materials .....	91
3A.3.2 Sample preparation for thawing temperature effect study .....	91
3A.3.3 Standard transmission electron microscopy (standard TEM).....	92
3A.3.4 Cryogenic transmission electron microscopy (cryo-TEM) .....	92
3A.3.5 Microscopy image data analysis and visualisation .....	92
3A.3.6 Dynamic light scattering measurement (DLS).....	93
<b>3A.4 Results and discussion.....</b>	<b>93</b>
<b>3A.5 Conclusion.....</b>	<b>99</b>
<b>Acknowledgements .....</b>	<b>100</b>
<b>Conflict of Interest .....</b>	<b>100</b>
<b>Supporting information.....</b>	<b>101</b>
<b>References .....</b>	<b>103</b>
<b><u>Chapter 3 B: Controlling the size and shape of liposomal ciprofloxacin nanocrystals by varying the lipid bilayer rigidity and drug to lipid ratio.....</u></b>	<b>108</b>

Abstract .....	109
3B.1 Introduction.....	110
3B.2 Hypotheses and aims .....	111
3B.3 Materials and Methods .....	112
3B.3.1 Materials .....	112
3B.3.2 Sample preparation .....	112
3B.3.3 Cryogenic transmission electron microscopy (cryo-TEM) .....	114
3B.3.4 Standard transmission electron microscopy (standard TEM).....	114
3B.3.5 Small angle x-ray scattering (SAXS) measurements and analysis .....	115
3B.3.6 Particle size analysis from RT-TEM images.....	117
3B.4 Results and Discussion .....	117
3B.4.1 Effect of lipid composition on the size and shape of the ciprofloxacin nanocrystals .....	117
3B.4.2 Effect of cholesterol content on the size and shape of the ciprofloxacin nanocrystals .....	122
3B.4.3 Effect of drug to lipid ratio on the size and shape of the ciprofloxacin nanocrystals .....	126
3B.4.4 Comparing the results from standard TEM and SAXS size distribution analyses 129	
3B.4.5 Difference in the size of the liposomal ciprofloxacin nanocrystals and applications.....	130
3B.5 Conclusion .....	131
Acknowledgements .....	133
Conflict of Interest .....	133
Supporting Information.....	134
References .....	146
<b>Chapter 4: Exposure of nanocrystallised ciprofloxacin liposomes to digestive media induces solid-state transformation and altered <i>in vitro</i> drug release .....</b>	<b>151</b>
<b>Exposure of nanocrystallised ciprofloxacin liposomes to digestive media induces solid-state transformation and altered <i>in vitro</i> drug release .....</b>	<b>152</b>
<b>Abstract.....</b>	<b>152</b>
<b>4.1 Introduction .....</b>	<b>154</b>
<b>4.2 Experimental section .....</b>	<b>156</b>
4.2.1 Materials.....	156
4.2.2 Preparation of digestion medium, bile salt buffers and enzymes .....	156
4.2.3 Preparation of liposomal ciprofloxacin nanocrystals for SAXS analysis.....	157
4.2.4 Small angle X-ray scattering (SAXS) .....	158
4.2.4.1 <i>Ex Situ</i> digestion SAXS study.....	158
4.2.4.2 <i>In Situ</i> bile salt titration SAXS study .....	160
4.2.4.3 Temperature dependent SAXS study.....	160
4.2.5 Cryogenic Transmission Electron Microscopy (Cryo-TEM).....	160
4.2.6 Isolation of Ciprofloxacin bile salt precipitate .....	161
4.2.7 FTIR to investigate formation of ciprofloxacin salt .....	162
4.2.8 Cross polarized light microscopy (CPLM) and hot stage microscope .....	162
4.2.9 Preparation of sample for <i>in vitro</i> drug release studies .....	162
4.2.10 <i>In vitro</i> drug release studies.....	163

4.2.11	Quantification of ciprofloxacin using HPLC .....	164
4.3	Results and discussion .....	164
4.3.1	<i>Ex situ</i> solid state transformation of liposomal ciprofloxacin nanocrystal during <i>in vitro</i> digestion.....	164
4.3.2	<i>In situ</i> polymorphic transformation of nanocrystallised ciprofloxacin liposomes upon exposure to biorelevant media .....	167
4.3.3	pH dependent CIPTDC crystallisation .....	172
4.3.4	FTIR assessment of ciprofloxacin and sodium taurodeoxycholate salt formation.....	175
4.3.5	Thermal properties of crystalline CIPTDC salt .....	176
4.3.6	<i>In vitro</i> drug release from liposomal ciprofloxacin formulation in simulated digestive environment .....	178
4.4	Conclusion.....	181
	Acknowledgments .....	182
	Supporting Information .....	182
	References .....	184
	<b>Chapter 5: Summary and Future Outlook.....</b>	<b>188</b>
5.1	Summary and Findings.....	189
5.2	Future Outlook .....	193
	References .....	195

## Abstract

Liposomes are spherical colloidal systems that have been used as drug delivery nanocarriers for decades. Whilst most research into liposomes focuses on their benefits in modulating the pharmacokinetics of the encapsulated drug molecules, the physical states of the drug within liposomes are poorly understood. The physical state of encapsulated drug within the liposomes, whether it is in solution or forms an amorphous or crystalline precipitate, would affect the amount of free drug dissolved inside the liposomes, hence affecting the rate of drug release from liposomes. The ability to manipulate the physical state of the drug inside the liposomes can provide a platform for the investigation of how the drug solid state inside the liposome would affect drug release and digestion. In this project, we specially focus on liposomes with crystalline precipitate known as liposomal drug nanocrystal formulations, prepared with ciprofloxacin as a model drug crystallised inside the liposomes.

The first part of the work characterises the physical state of the liposomal ciprofloxacin nanocrystals. Using cryogenic transmission electron microscopy (cryo-TEM) and small angle X-ray scattering (SAXS), the physical state and the crystal form of ciprofloxacin nanocrystals inside the liposomes were confirmed. The thermotropic behavior of the nanocrystals and the changes to the solid state under different pH conditions were also investigated. The ability to monitor the change in physical state with respect to pH is important for design towards oral drug application. This is because the gastro-intestinal (GI) tract has different pH environments which could affect the amount of solubilised drug inside the liposomal formulation with and without drug nanocrystals as it moves along the GI tract and hence influence the drug release rate and availability for absorption.

The relevance of the dimension of the drug nanocrystal to different formulation parameters were investigated to engineer the growth of the nanocrystals. A quantitative room temperature TEM method was developed and validated against the cryo-TEM method and this quantitative TEM method was then used along with SAXS modelling to explore how different formulation parameters can influence on the size and growth of drug nanocrystals inside the liposome. It is evident that factors such as thawing temperature, lipid composition, bilayer elasticity and drug to lipid ratio can affect the size of the crystal growth inside the liposome. The quantitative TEM assay was then used to provide a faster, less expensive and more statistically favourable way to screen for changes in the shape

and size distribution of the nanocrystal as different formulation parameters were introduced. Moreover the ability to manipulate the growth, shape and size of drug nanocrystals inside liposomes is significant in designing towards tailored drug release liposomal systems.

Lastly, the effect of exposure of the liposomes to simulated intestinal environment and digestion conditions *in vitro* on the physical state of drug inside the liposomes were investigated using SAXS. The observation of a new ciprofloxacin-bile salt crystal transformation was crucial in understanding the drug release behaviour under the different environments. For liposomes with drug nanocrystals, the digestion-stimulated drug release was observed, which further proves the importance of the physical state of the drug inside the liposome in controlling the drug release rate from liposomes.

---

## Declaration of authorship

I hereby declare that this thesis contains no material which has been accepted for the award of any other degree or diploma at any university or equivalent institution and that, to the best of my knowledge and belief, this thesis contains no material previously published or written by another person, except where due reference is made in the text of the thesis.

The thesis included two original papers published in peer-reviewed journal and three manuscripts in preparation. The inclusion of co-authors reflects the fact that the work came from active collaboration.

The core theme of the thesis is the development and understanding of liposomal ciprofloxacin nanocrystal formulations and their applications in oral drug delivery. The ideas, development and writing up of all the papers included within the thesis were principal responsibility of myself, the PhD candidate, working within the Drug Delivery, Disposition and Dynamics unit under the supervision of Professor Ben J. Boyd.

Signature:

Print Name: Tang Li

Date: 27/02/2019

## Publications during enrolment

**Li T**, Cipolla D, Rades T, Boyd B J. Drug nanocrystallisation within liposomes. *Journal of Controlled Release*. 2018. 288: 96-110

**Li T**, Mudie S, Cipolla D, Rades T, Boyd B J. Solid state characterization of ciprofloxacin liposome nanocrystals. *Molecular Pharmaceutics*. 2019. 16. 1: 184-194

**Li T**, Nowell C J, Cipolla D, Rades T, Boyd B J. Direct comparison of standard transmission electron microscopy (TEM) and cryogenic-TEM in imaging nanocrystals inside liposomes. *Molecular Pharmaceutics*. (Accepted for publication)

**Li T**, Clulow A J, Nowell C J, Hawley A, Cipolla D, Rades T, Boyd B J. Controlling the size and shape of liposomal ciprofloxacin nanocrystals by varying the lipid bilayer rigidity and drug to lipid ratio. *Journal of Controlled Release* (Submitted manuscript)

**Li T**, Hawley A, Rades T, Boyd B J. Exposure of nanocrystallised ciprofloxacin liposomes to digestive media induces solid-state transformation and altered *in vitro* drug release. *Journal of Controlled Release* (Submitted manuscript)

Xiao Y X, Liu Q T, Clulow A J, **Li T**, Manohar M, Gilbert E, De Campo L, Hawley A, Boyd B J. PEGylation and surface functionalization of liposomes containing drug nanocrystals for cell-targeted delivery. *Journal of Physical Chemistry B* (Submitted manuscript)

## Thesis Including Published Works Declaration

Thesis Chapter and Publication Title	Publication Status	Nature and % of student contribution	Co-author name(s) Nature and of Co-author's contribution	Co-author(s), Monash student
<b>Chapter 1</b> Drug nanocrystallisation within liposomes	Published	90% Literature research and manuscript preparation	1. David Cipolla (Collaborator) 1% Revision of Manuscript 2. Thomas Rades 4% (Co-supervisor) Preparation of Manuscript 3. Ben J.Boyd 5% (Main Supervisor) Preparation of Manuscript	No No No
<b>Chapter 2</b> Solid state characterization of ciprofloxacin liposome nanocrystals	Published	80% Research design, data collection and analysis, and manuscript preparation	1. Stephen Mudie (Beamline Scientist) 3% Assistance with Experiment 2. David Cipolla (Collaborator) Revision of Manuscript 2% 3. Thomas Rades (Co-supervisor) Preparation of Manuscript 5% 4. Ben J.Boyd (Main supervisor) Guidance in research design and Preparation of Manuscript 10%	No No No No
<b>Chapter 3 A</b> Direct comparison of standard transmission electron microscopy (TEM) and cryogenic-TEM in imaging nanocrystals inside liposomes	Accepted	80% Research design, data collection and analysis, and manuscript preparation	1. Cameron J. Nowell (Collaborator) Assistance in Image analysis script 3% 2. David Cipolla (Collaborator) Revision of Manuscript 2% 3. Thomas Rades (Co-supervisor) Preparation of Manuscript 5% 4. Ben J.Boyd (Main supervisor) Preparation of Manuscript 10%	No No No No
<b>Chapter 3 B</b> Controlling the size and shape of liposomal ciprofloxacin nanocrystals by varying the lipid bilayer rigidity and drug to lipid ratio	Submitted	60% Research design, data collection and analysis, and manuscript preparation	1. Andrew J. Clulow SAXS modelling and preparation of manuscript 25% 2. Cameron J. Nowell (Collaborator) 1% 3. Adrian Hawley (Beamline Scientist) 2% Assistance with Experiment 4. David Cipolla (Collaborator) 1% 5. Thomas Rades (Co-supervisor) Preparation of Manuscript 5% 6. Ben J.Boyd (Main supervisor) Preparation of Manuscript 6%	No No No No No No

<b>Chapter 4</b>	Submitted	80%	1. Adrian Hawley (Beamline Scientist) 5%	No
Exposure of nanocrystallised ciprofloxacin liposomes to digestive media induces solid-state transformation and altered <i>in vitro</i> drug release		Research design, data collection and analysis, and manuscript preparation	Assistance with Experiment	No
			2. Thomas Rades (Co-supervisor) Preparation of Manuscript 5%	No
			3. Ben J.Boyd (Main supervisor) Guidance in research design and Preparation of Manuscript 10%	No

I have renumbered sections of submitted or published papers in order to generate a consistent presentation within the thesis.

**Student signature:**

**Date:** 27/02/2019

The undersigned hereby certify that the above declaration correctly reflects the nature and extent of the student's and co-authors' contributions to this work. In instances where I am not the responsible author I have consulted with the responsible author to agree on the respective contributions of the authors.

**Main Supervisor signature:**

**Date:** 27/02/2019

## Acknowledgements

I would like to first give my sincere thank you to my main supervisor Professor Ben Boyd for his continuing guidance and support during the course of my Ph.D study. You have been the most valuable adviser and role model for my research journey. Thanks for always been patient to provide feedbacks and guidance on my research works as well as my writing skills, despite your busy schedules. I am also very grateful for your support in providing the international and national conferences and technical workshop opportunities, these have given me the ability to network and learn from other academic leaders in the field. Your understanding and mental support when I was going through personal rough patches have motivated and helped me to regain my focus back to my Ph.D study. I'd also like to thank my co-supervisor Professor Thomas Rades for his time to provide valuable ideas, expert's advices and discussions that helped with the research design of this thesis and the publications generated from this thesis. Thanks to my second co-supervisor Dr. Cornelia Landersdorfer for your encouraging words during my study. I'd also like to thanks to my external collaborator Dr. David Cipolla, without you, this project would not have existed, thank you for your valuable advices and discussions during my research project.

Thanks to Dr. Adrian Hawley and Dr. Stephan Mudie from the Australian Synchrotron for your assistance and expertise with the small angle X-ray scattering experiment setup on the SAXS/WAXS beamline. Thanks to Dr. Andrew Clulow for your valuable advises and your expertise in SAXS modelling that shaped the engineering chapter of this thesis and your guidance in the Boyd research group. Also would like to thanks to Dr. Cameron J. Nowell in your assistance in image analysis, Dr. Lynne Waddington, Dr. Tim Williams, Dr. Emily Chen for your help and training in electron microscopy.

I would also like to thanks to the rest of the Boyd group members for your assistance and support in both the lab, as well as making the work environment such a pleasant experience during my Ph.D studies. I 'd like to thank Linda Hong, Nicole Bisset, Kristian Tangso, Jamal Khan, Joanne Du, Nicolas Alcaraz, Kapil Vithani, Anna Pham, Kellie May, Cindy Xiao, Mubtasim Murshed, Stephanie Rietwyk, Gisela Raminez, Angel Tan, Malinda Salim, Jason Liu, Charlie Dong, Khay Fong and Xiaohan Sun for your friendship.

Most importantly I'd like to specially thank my family and friends, in particular, my parents and my fiancé for the love and support during my studies.

This research was supported by an Australian Government Research Training Program (RTP) Scholarship.

## List of Abbreviations

ANOVA	One-way analysis of variance
AR	Aspect ratio
ATR	Attenuated total reflectance
CaCl <sub>2</sub> ·2H <sub>2</sub> O	Calcium chloride dihydrate
Chol	Cholesterol
Cip	Ciprofloxacin
CIPH <sub>2</sub> O	Ciprofloxacin hydrate
CIPHCl	Ciprofloxacin hydrochloride
CIPTDC	Ciprofloxacin bile salt crystals
CPLM	Cross polarised light microscopy
Cryo-ET	Cryogenic electron tomography
Cryo-TEM	Cryogenic transmission electron microscopy
D/L	Drug to lipid
DDLS	Dynamic depolarised light scattering
DLS	Dynamic light scattering
DMPC	1,2-Dimyristoyl-sn-glycero-3-phosphocholine
DOPC	1,2-Dioleoyl-sn-glycero-3-phosphocholine
DOX	Doxorubicin
DPPC	1,2-Dipalmitoyl-sn-glycero-3-phosphocholine
DSC	Differential scanning calorimetry
EDTA	Ethylenediaminetetraacetic acid
EE	Encapsulation efficiency
EGFR	Epidermal growth factor receptor
EPR	Electronic paramagnetic resonance spectroscopy
FDA	U.S. Food and Drug Administration
FTIR	Fourier-transform infrared spectroscopy
GI tract	Gastrointestinal tract
GMP	Good manufacturing practices
HBS	Hydroxybenzenesulfonate
HCl	Hydrochloric acid
HER2	Human epidermal growth factor receptor 2
HPLC	High-performance liquid chromatography
HSPC	Hydrogenated soy phosphatidylcholine
K <sub>sp</sub>	Solubility product constant
LBF	Lipid-based formulation
LipoCIP	Liposomal ciprofloxacin

LUV	Large unilamellar vesicles
MLV	Multilamellar vesicles
NaCl	Sodium chloride
NaN <sub>3</sub>	Sodium azide
NaOH	Sodium hydroxide
NaTDC	Sodium taurodeoxycholate hydrate
NH <sub>3</sub>	Ammonia
NMR	Nuclear magnetic resonance
PDI	Polydispersity index
PEG	Polyethylene glycol
PLA <sub>2</sub>	Phospholipase A2
RFA	Radiofrequency ablation
SAXS	Small angle X-ray scattering
TEA	Triethanolamine
TEM	Transmission electron microscopy
T <sub>m</sub>	Phase transition temperature
TPT	Topotecan
UV-vis	Ultraviolet–visible electronic absorption spectroscopy
VCR	Vincristine
WAXS	Wide angle X-ray scattering
XRD	X-ray powder diffraction

## **Chapter 1: Introduction**

## Statement of problem

The use of nanoparticles such as liposomes provides many benefits as drug delivery carriers, these include the ability to encapsulate actives of various physiochemical properties which in turn alter the pharmacokinetics behaviour, reduce systemic toxicity and improve therapeutic efficacy. Since the commercial success of Doxil many decades ago, extensive research and development have focused on developing various novel liposomal formulations with different purpose and indications. However as mentioned in the introduction, the physical states of the drug (in solution or in a solid state) inside the liposome directly affect the drug dissolution and release characteristics but are overlooked in previous literatures and poorly understood. Moreover, the lipid components of the liposomes may act as a lipid formulation and provide a means of solubilising drug during digestion.

Recently, Cipolla et al. reported a freeze-thawing method of liposomal ciprofloxacin where *in situ* crystallisation of ciprofloxacin enabled formation of intraliposomal drug ciprofloxacin nanocrystals. This enables alteration of the drug's physical state inside the liposome. Due to the size of the nanocrystals, it would provide a rapid dissolution rate compared to regular drug particles. Together with the lipid-based formulation properties of the liposomes, this provides a new avenue to explore the benefits and potential of liposomal drug nanocrystals especially in the context of oral drug delivery. Thus, this thesis focuses on inducing drug crystallization within lipid vesicles of various compositions with the aim to control the drug crystal dimensions and the digestion study of the formulations. This would enable designing towards oral drug delivery applications of liposomal drug nanocrystals.

## Hypotheses

It is envisaged that liposomal ciprofloxacin nanocrystals generated from the additional freeze-thawing step can provide an avenue to study the solid state characteristics of drug inside liposomes and explored for its potential in controlling the liposome shape and oral drug delivery applications.

1. That characterisation of the solid state properties of the ciprofloxacin inside the liposome after nanocrystallisation, specifically the form of the crystal precipitated is crucial for exploring their potential in oral drug delivery applications.
2. That the growth of the nanocrystals inside the liposomes can be controlled and manipulated through formulation and process variables.
3. That the solid state properties of the ciprofloxacin with and without nanocrystallisation would affect the *in vitro* drug release from the liposomes.
4. That the solid state properties of the ciprofloxacin with and without nanocrystallisation during *in vitro* digestion would affect the *in vitro* drug release from the liposomes in simulated digestive conditions.

## Aims

The aim of this project is to use ciprofloxacin liposomes as a model system to address the above hypotheses:

1. Determine the solid state characteristics and the crystal form of the ciprofloxacin precipitated inside the liposome after freeze-thawing.
2. Determine the effect of pH and temperature on the precipitated drug nanocrystals inside the liposome.
3. Determine a suitable method to quantitatively analyse the shape and size distribution of ciprofloxacin nanocrystals inside the liposome.
4. Investigate the effect of the liposome composition, thawing temperature and the drug concentration on the shape and size distribution of ciprofloxacin nanocrystals inside the liposome.
5. Determine the effect on the solid state properties of ciprofloxacin liposomes with and without nanocrystallisation during *in vitro* digestion and interaction with digestive components.
6. Investigate the *in vitro* drug release behaviour for ciprofloxacin liposomes with and without nanocrystallisation.

## Drug nanocrystallisation within liposomes

Tang Li<sup>a</sup>, David Cipolla<sup>b</sup>, Thomas Rades<sup>c</sup>, Ben J Boyd<sup>a</sup>

<sup>a</sup> ARC Centre of Excellence in Convergent Bio-Nano Science and Technology and Drug Delivery, Disposition and Dynamics, Monash Institute of Pharmaceutical Sciences, Monash University, Parkville, VIC, Australia.

<sup>b</sup> Aradigm Corporation, Hayward, California 94545

<sup>c</sup> Faculty of Health and Medical Sciences, Department of Pharmacy, University of Copenhagen, Copenhagen, Denmark

Published online: 2<sup>nd</sup> September 2018

Citation: J. Controlled Release (2018) 288: 96-110

DOI: 10.1016/j.jconrel.2018.09.001

### Abstract

Liposomes are phospholipid bilayer vesicles that have been explored in pharmaceutical research as drug delivery systems for more than 50 years. Despite being important to their morphology and drug release pattern, the physical state of the drug within liposomes (liquid, solid, crystalline form) is often overlooked. This review focuses on precipitation of drug within liposomes, which can result in the formation of confined nanocrystals, and consequent changes in liposome morphology and drug release patterns. The type of drugs that form nanocrystals within liposomes, preparation and characterisation of liposomal drug nanocrystals, and the in vitro drug release behaviour from these systems are communicated, with a discussion of their potential as drug delivery systems.

#### KEYWORDS

Liposomes; precipitation; nanocrystal; solid state; polymorph

### 1.1 Introduction

Liposomes are spherical colloidal systems consisting of a phospholipid bilayer shell with an aqueous internal core. These systems are widely explored in pharmaceutical research to reduce the systemic toxicity of the free drug through encapsulation (1, 2) and enable effective drug delivery of lipophilic, hydrophilic and amphiphilic drugs (3, 4). Since

their discovery by Alec D Bangham 50 years ago (5), liposomes have found success as nano-sized delivery carriers in the pharmaceutical, food, agriculture and cosmetic industry (6-10). With respect to utilizing liposomes as vehicles for drug delivery, the success of the liposomal doxorubicin formulation (Doxil<sup>®</sup>) (11, 12) has led to the development of many other approved liposomal products. Some of the examples include Ambisome<sup>®</sup> (amphotericin B) (13, 14), DaunoXome<sup>®</sup> (daunorubicin) (15, 16), Visudyne<sup>®</sup> (verteporphin) (17), Exparel<sup>®</sup> (bupivacaine) (18), Marqibo<sup>®</sup> (vincristine) (19) and the combination product Vyxeos<sup>®</sup> (daunorubicin-cytarabine) (20).

Most research into liposomes focuses on the modification of the composition of the liposome bilayer and surface chemistry (21). This includes passive, long-circulating PEGylated liposomes (22-25), ligand targeted liposomes (26-28) and stimuli-responsive liposomes (29-32). On the other hand, despite studies that focus on the physical state of the doxorubicin sulfate crystals in Doxil<sup>®</sup> (33-35), the physical state of the encapsulated drug inside other liposomal formulations has often been overlooked. The physical state of encapsulated drug within the liposomes, whether it is in solution or forms an amorphous or crystalline precipitate, would affect the amount of free drug dissolved inside the liposome; hence affecting the rate of drug release from these drug delivery systems. The precipitation of confined nanocrystals also presents opportunities for alternative applications. For these reasons, this review explores the current status of liposomes in drug delivery from the perspective of drug precipitation and crystallisation inside liposomes, characterisation techniques for the physical state of drug within liposomes and the *in vitro* drug release behaviour from liposomal drug nanocrystals.

## 1.2 Liposomes as drug delivery systems

Liposomal systems have been well exploited in drug delivery research especially in cancer treatment and the liposomal doxorubicin HCl injection; Doxil<sup>®</sup> is the first FDA approved nanomedicine (11, 12). For liposomal products given via systemic administration, one of the major hurdles is opsonisation of the liposomes in plasma. This can be addressed by functionalising the liposome surface with a hydrophilic polymer chain, most commonly polyethylene glycol (PEG) (**Figure 1**), creating a hydrophilic surface that hinders the electrostatic and hydrophobic interactions with blood plasma opsonins, and therefore inhibits the uptake of the liposomes via the mononuclear phagocytic system. These “stealth” liposomes will thus extend the blood circulation time, which allows the

liposomes to passively accumulate inside organs and tissues (24). The physicochemical properties of the liposome including its size, lipid composition, surface charge, route of administration can also influence its immunological response (36, 37). It has also been reported that shape is important in phagocytosis of nanoparticles and immune response (38-41). The shape distortion of the liposome to non-spherical shape induced by *in situ* drug crystallisation can be seen as shape engineering of liposomes. The relationship between the shapes of the liposome and the immune system is still not yet understood, although one study reported an increased reactogenicity of Doxil<sup>®</sup> compares to placebo Doxil<sup>®</sup> and SPI-77 (liposomal cisplatin with no intraliposomal precipitate and identical lipid composition to Doxil<sup>®</sup>). The increased complement activation of Doxil<sup>®</sup> could be due to the low surface curvature of the oval Doxil<sup>®</sup> vesicles (42).

Active targeting of liposomes that are functionalized with antibodies to enhance interaction with target antigens on cells at the site of interest, has also gained interest especially for cancer therapy (43). These so-called 'immunoliposomes' bind to overexpressed receptors in the tumour cells, improving therapeutic efficacy and reducing systemic toxicity (28, 44). Both anti-epidermal growth factor receptor (EGFR) and anti-HER2 tyrosine kinase receptor antibodies have been successfully conjugated to liposomes and are under clinical investigations. An anti-EGFR immunoliposome containing doxorubicin is in phase II clinical trials (45, 46).

Liposomes are also used as stimuli-responsive drug delivery systems. The lipid composition can be designed to respond to changes in pH, redox state and enzymes or to external stimuli such as heat, magnetic fields, ultrasound and light (30). The stimuli will trigger the release of the encapsulated drugs allowing "on demand" drug release from the liposomes. ThermoDox<sup>®</sup> is a heat-sensitive liposomal doxorubicin that changes structure when heated to 40-45°C, releasing doxorubicin at the target tumour site. This formulation is in phase III clinical trials in combination with radiofrequency ablation (RFA) for the treatment of primary liver cancer (47-49).

Liposomes are capable to entrap both hydrophilic and hydrophobic drugs. Hydrophilic drugs are typically encapsulated in the liposomal aqueous core or near the lipid-water interface. Poorly water-soluble lipophilic pharmaceutical actives can be solubilised within the acyl hydrocarbon chains of the lipid bilayers (**Figure 1**). The encapsulation efficiency of hydrophobic actives is dictated by the partition coefficient of the drug, the acyl chain length of the phospholipids, the packing density of the bilayer as well as the lipid to drug ratio (4, 50, 51). Other advantages of drug encapsulation into

liposomes include improved solubility for hydrophobic drugs (52) and reduction of non-specific organ toxicity compared to the free drug (2, 53, 54).

Whilst most studies have focussed on the pharmacokinetic and therapeutic efficacy of liposomal drug delivery systems (55-57), the physical characteristics of the encapsulated drugs are not well understood. A review of the literature shows only a few liposomal drug delivery systems for which the physical state of the drug has been reported. Lipophilic drugs that are solubilised within the bilayer (e.g. verteporfin and paclitaxel) as well as drugs that form ionic complexes with the oppositely charged lipid (e.g. amphotericin B) do not precipitate in a crystalline form within the liposome. In contrast, hydrophilic drugs that are encapsulated within the aqueous core of the liposome can exhibit different physical states. This includes supersaturated solutions (e.g. cisplatin, ciprofloxacin), amorphous precipitates (e.g. vinorelbine, vincristine) and nanocrystals (e.g. doxorubicin, topotecan, idarubicin) (**Figure 1**) (Refer **Table 3** for references). The crystalline precipitate that forms within liposomes for some drugs is intriguing both from a lipid biophysics perspective as it can stretch or deform the bilayer, as well as by providing an additional means to control the drug release rate by the addition of a dissolution step, and as such is the main focus of this review.

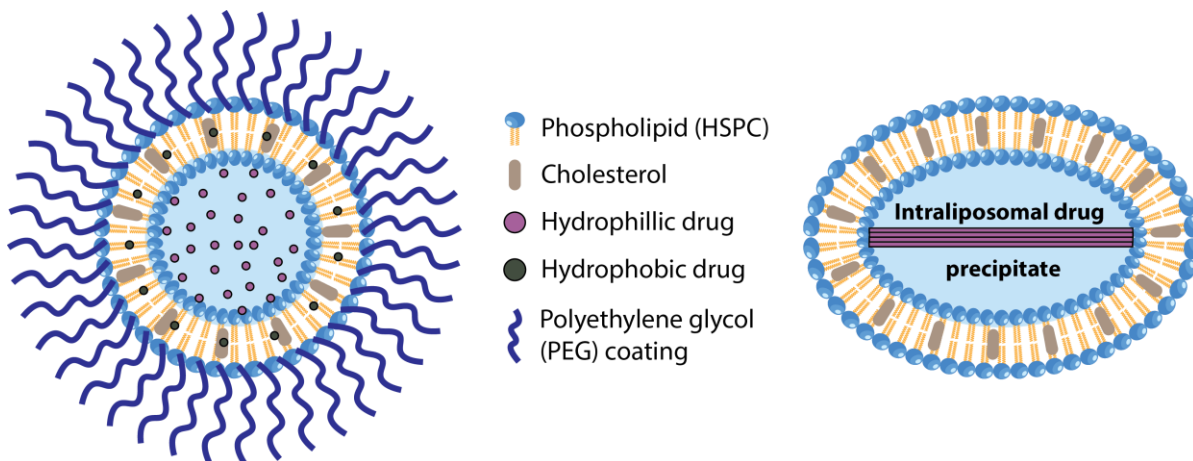


**Figure 1.** Left: a spherical vesicle with an aqueous core formed by a phospholipid and cholesterol bilayer. The liposome can also be functionalised with polyethylene glycol coating to avoid opsonisation. The liposome aqueous core can encapsulate hydrophilic drugs whereas hydrophobic drugs reside in the lipid bilayer. Right: schematic of a crystalline precipitate formed within a liposome. Depending on the shape and length of the drug precipitate, the bilayer may be stretched to accommodate the growth of the crystalline drug precipitate within the liposome.

### 1.3 Drug loading methods

Different drug loading methods can be used to enable drug encapsulation into liposomes but can also influence the physical state of the encapsulated drug and in some instances lead to precipitation as nanocrystals within the liposomes. Additional sample preparation methods (eg. freeze-thawing) can be also applied to modify the physical state of the encapsulated drug. These methods are discussed in this section and the relevance to the physical state is further discussed in section 5.

The simplest approach for drug encapsulation into liposomes is the passive loading method, where drugs are dissolved in the aqueous buffer used to hydrate the lipid bilayer. Thus, the concentration of drug in the aqueous core within the liposomes is similar to that in the aqueous phase exterior to the vesicles. This method is relatively easy and convenient in preparation and manufacturing. However it results in low encapsulation efficiency, high levels of non-encapsulated drug (which can be removed by dialysis, gel filtration and ultrafiltration) and high drug leakage for bilayer permeable drugs. The lipid bilayer is not permeable towards ions and charged molecules. When the drug is unprotonated, it can move in and out of the lipid bilayer of the liposome. The diffusion rate of the drug through the bilayer is dependent upon its partition coefficient. Due to the permeability of the bilayer to uncharged drug molecules, the passively-loaded drug molecules of weak acid and weak bases typically exhibit rapid leakage out of the liposomes. Passively-loaded liposomal ciprofloxacin has exhibited a 50% loss of encapsulated drug after 2 days at 25 °C (58), whereas ammonium sulfate-loaded liposomal ciprofloxacin (active loading) remained at around 99% encapsulation over 24 month period stored at 2-8 °C (59) .

The active loading approach (60) addresses the low encapsulation efficiency of passive loading by generating a transmembrane pH (or ion) gradient between the aqueous compartment inside of the preformed liposomes and the outside continuous aqueous medium. When the uncharged drug molecules diffuse through the lipid bilayer, they become protonated, which inhibits diffusion out of the liposome, thus enhancing the drug loading efficiency and the retention of drug inside the liposome. The loading efficiency is optimal when the drug is an amphipathic weak acid ( $pK_a > 3$ ) or weak base ( $pK_a \leq 11$ ) with a log D of -2.5 to 2.0 at pH 7 (61). **Table 1** compares the active and passive loading methods for liposomal drug delivery systems.

For amphipathic weak bases, an ammonium sulfate transmembrane gradient (62) is usually used. Firstly, the liposome is formed with an acidic ammonium sulfate buffer, then the transmembrane gradient is generated by replacement of the external buffer with a neutral pH buffer through dialysis or gel exclusion chromatography. When an uncharged ammonia molecule ( $\text{NH}_3$ ) escapes the liposome, one proton is generated and retained in the liposome, which results in a more acidic liposome core. The candidate drug (e.g. doxorubicin) is added to the liposome dispersion and loading is performed at a temperature above the phase transition temperature of the phospholipid used to make the liposome for a period of 30-60 minutes. During the drug loading process, the candidate drug diffuses into the liposome and becomes protonated due to the acidic liposomal core, and is then trapped within the liposome. The drug loaded into the liposome will transiently increase the internal pH, increasing the level of ammonia and therefore creating more protons, enabling more drug molecules to move into the liposome (**Figure 2**). After the majority of the drug is loaded into the liposome, non-encapsulated drug is usually removed by dialysis, diafiltration or gel chromatography.

A phosphate gradient method has also been applied to load doxorubicin into liposomes by Fritze *et al.* (63). In their study, a higher drug encapsulation efficiency (EE) was achieved using the phosphate gradient method compared to the ammonium sulfate or acetate gradient methods. The phosphate gradient loaded doxorubicin liposomes also showed a pH-dependent drug release profile that was not observed in the ammonium sulfate gradient loaded liposomes.

An EDTA gradient method has also been used to encapsulate idarubicin (64), topotecan (65) and doxorubicin (66). The EDTA gradient method enabled efficient drug accumulation and retention of idarubicin due to formation of crystals inside the liposomes providing slower drug release *in vivo* compared with other gradient loading methods (64). Liposomes produced by this method have demonstrated decreased cytotoxic activities compared with liposomes prepared by an ammonium sulfate gradient for doxorubicin and topotecan (65, 66). The calcium acetate gradient loading is applied to weakly acidic drugs (**Figure 2**). In this case calcium ions remain inside the liposome and the neutral acetate moves out of the liposome resulting in a high intraliposomal pH (67).

The ionophore loading method is another method that has been applied to many drugs. Nigericin or A23187 are common ionophores used for unilamellar liposomes. These ionophores facilitate outward transport of  $\text{K}^+$ ,  $\text{Mn}^{2+}$  and  $\text{Ca}^{2+}$  ions and shift protons into the liposome generating an acidic intraliposomal environment. This method has been used in

conjunction with a metal ion gradient for encapsulating e.g. ciprofloxacin, vincristine (68), doxorubicin (69), topotecan (70, 71), irinotecan (72) and mitoxantrone (73, 74). This drug loading method can generate high pH gradient, high drug loading and encapsulation efficiency and allows the encapsulation of different drugs by varying the selection of the ion gradient and ionophore. Depending on the ion used, the encapsulated drug molecules can also form ion-drug complexes within the liposome. The newly formed complex could alter the drug solubility and hence the drug release profile (60).

Although the active loading methods are very effective in encapsulating amenable drugs to achieve high and stable drug loading, the preparation methods are more complicated and time consuming compared to the passive loading method. Recently, microfluidic systems have been utilised to enable rapid and efficient remote loading of amphipathic drugs into liposomes. This method incorporates the liposome production, buffer exchange, and remote drug loading and mixing into a continuous process on a single microfluidic chip. This allows a multi-day sample preparation method to be performed in a few minutes (75). However, the limited experimental report on this method and its viability in industrial scale application is among one of the main drawback of the application of the microfluidic method of liposome preparation.

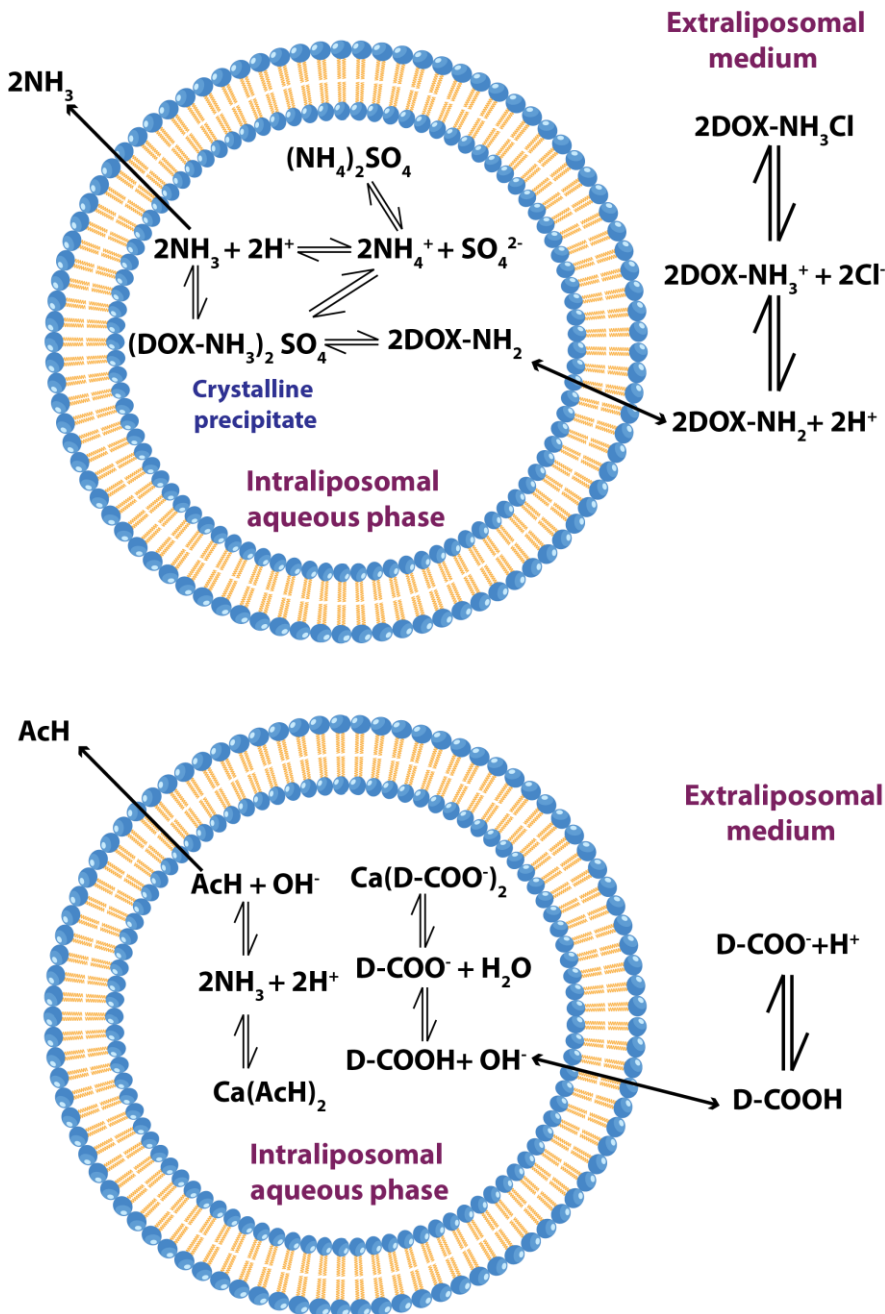


**Figure 2.** Top: Schematic of the active loading method of doxorubicin HCl into preformed liposomes using an ammonium sulfate gradient. Doxorubicin forms a crystalline precipitate due to the presence of sulfate anions inside the liposome. Bottom: Schematic of the active loading method of an amphipathic weak acid into preformed liposomes using a calcium acetate method (adapted with permission from (61)).

Freeze-thawing of MLVs is commonly applied before extrusion (**Table 1**) to break apart the closely-spaced lamellae of the liposomes. During the freeze-thawing process, ice formation of the inner water phase could break off or fragment the bilayers and the damaged bilayers would fuse to form new liposomes with decreasing in lamellarity. During the process, the trapped volume of the MLVs increases and improves the encapsulation efficiency (76-78). The extrusion of freeze-thawed MLVs results in more monodispersed

LUVs with a higher intraliposomal aqueous volume than LUVs prepared without freeze-thawing (79). Liposomes (both MLVs and LUVs) have also been used as a model membrane to study the effect of freezing and thawing on the biological cells. During the freeze-thawing process, a faster freezing rate ( $>10\text{ }^{\circ}\text{C min}^{-1}$ ) results in intraliposomal ice formation whereas a slow freezing rate ( $<2\text{ }^{\circ}\text{C min}^{-1}$ ) showed osmotic shrinkage of the liposome and no intraliposomal ice formation (80, 81). Recently, the use of a single freeze-thaw cycle was performed on the ammonium sulfate loaded ciprofloxacin liposomes (82). Freeze-thaw treatment resulted in ciprofloxacin precipitation inside the liposome. The precipitate was observed as a single rod-shaped ciprofloxacin nanocrystal within each liposome. The formations of intraliposomal ciprofloxacin nanocrystals have also stretched the liposome from a spherical vesicle to a rugby ball-shaped vesicle.

**Table 1.** Comparison of active and passive drug loading methods used for liposomal drug delivery systems.

Drug loading type	Method of Liposome Production	Advantages	Disadvantages	References
<b>Passive loading method</b> <ul style="list-style-type: none"> <li>• <b>Thin layer hydration (TLH)</b></li> <li>• <b>Reverse phase evaporation (REV)</b></li> <li>• <b>Dehydration-rehydration vesicles (DRV)</b></li> </ul>	<ul style="list-style-type: none"> <li>• Formation of dried lipid film</li> <li>• Lipophilic drug is dispersed with the lipid in organic solvent to form dried lipid film</li> <li>• Hydrophilic drug is solubilised in the aqueous buffer used to hydrate the dried lipid film to generate MLVs</li> <li>• Sonication/extrusion of the MLVs to make the LUVs</li> </ul>	<ul style="list-style-type: none"> <li>• Easy and convenient method</li> <li>• Can be used to encapsulate any water soluble drug</li> </ul>	<ul style="list-style-type: none"> <li>• Low drug encapsulation efficiency</li> <li>• High amount of non-encapsulated drug (can be removed by dialysis or diafiltration)</li> <li>• Rapid drug leakage of bilayer permeable drugs</li> </ul>	(3, 83, 84)
<b>Active loading method</b> <b>Examples</b> <ul style="list-style-type: none"> <li>• <b>Ammonium sulfate gradient, citric acid gradient (amphipathic weakly basic drugs)</b></li> <li>• <b>Calcium acetate gradient (amphipathic weakly acidic drugs)</b></li> <li>• <b>Ionophore loading (Nigericin/ A23187) with metal ion gradient (Mg<sup>2+</sup>, Mn<sup>2+</sup>, Cu<sup>2+</sup>)</b></li> <li>• <b>Phosphate gradient</b></li> <li>• <b>EDTA gradient</b></li> </ul>	<ul style="list-style-type: none"> <li>• Formation of dried lipid film</li> <li>• Active loading buffer used to hydrate the dried lipid film to generate MLVs</li> <li>• Sonication/extrusion of the MLVs to make LUVs</li> <li>• Generation of transmembrane pH gradient across the liposomal bilayer through buffer exchange</li> <li>• Drug solution is added, uncharged drug molecules diffuse through the lipid bilayer, become protonated and trapped inside the liposome</li> </ul>	<ul style="list-style-type: none"> <li>• High encapsulation efficiency</li> <li>• Minimal drug wastage (less non-encapsulated drug loss)</li> <li>• Better drug retention</li> </ul>	<ul style="list-style-type: none"> <li>• Drug needs to be water soluble and have a weakly basic or weakly acidic functional group</li> <li>• Time consuming and multi day preparations are required</li> </ul>	(60, 62, 67, 85, 86)

Abbreviations: MLVs, multilamellar vesicles; LUVs, unilamellar vesicles

## 1.4 Structural characterisation techniques for the state of drugs inside liposomes

The state of the drug loaded by the above methods is important in understanding behaviour, and there is a relative paucity of methods for studying this. **Table 2** summarises the advantages and disadvantages associated with the different techniques described in the following section. The physical state of the drug inside the liposome that each methods are capable of detecting are also incorporated within the table.

### 1.4.1 Cryogenic transmission electron microscopy (Cryo-TEM)/Cryogenic electron tomography

The most direct method to visualise the state of a drug inside a liposomal dispersion is using cryo-electron microscopy imaging techniques. In cryo-TEM investigations, the liposomal dispersion is loaded onto the microscopy grid as a thin aqueous film, which is then vitrified by plunging the sample-loaded grid into liquid ethane. The transmission micrograph is then taken at liquid nitrogen temperature to minimize the formation of ice crystals, which can compromise sample imaging. The transfer of the sample grid to the microscope is also performed under liquid nitrogen to prevent formation of crystalline ice (87, 88). The vitrified sample retains the structures present in their native form in contrast to conventional TEM where drying and staining of the samples disrupts the structures that exist in solution and produces artefacts. The cryo-TEM technique can analyse samples in the nanometer scale; it is best suited for nanoparticles in the size range from 4 to about 500 nm (89). Since the resolution of the electron microscope inversely correlates to the thickness of the object, smaller liposomes which form a thin film of sample (see above) gives a better signal to noise ratio in the image (90). This technique is ideal to determine the overall morphology of nanoprecipitates inside liposomes (**Figure 3A** and **Figures 4-6**) where such small sized particles (<500 nm) are not visible using light microscopic techniques such as polarised light microscopy (91). Cryogenic electron tomography (cryo-ET) acquires multiple cryo-TEM images (method as described above) at different tilt positions. These collected images are then used to generate a three dimensional field of view (a tomogram) of the sample. For liposome

with encapsulated drug nanocrystals, this technique provides information about the size and shape variations of the nanocrystals within the liposomes in three-dimensional space and has been used to characterize Doxil® (92) and liposomal ciprofloxacin nanocrystals (82). The advantage and application of the cryo-ET technique is similar to that of the cryo-TEM technique. Moreover it can provide additional details to the drug crystal morphology in three dimensional space that cannot be observed through 2D cryo-TEM images. Both cryo-TEM and cryo-ET can provide a direct visualization of the drug's solid state inside the liposome. Crystalline drug are displayed as electron dense band, however if the drug formed an amorphous gel or is dissolved inside the liposome, this cannot be easily distinguished in cryo-TEM or cryo-ET.

#### 1.4.2 Small/Wide angle X-ray scattering (SAXS/WAXS)

Small angle X-ray scattering, in the range of scattering angles  $0.001^\circ < 2\theta < 3^\circ$  is often used to assess the colloidal structure of dispersed formulations, and the structural attributes of liposomes, including their shape, size, bilayer thickness and lamellarity (93, 94).

Of specific relevance to this review, the same technique can be used to determine the structure of the drug precipitates from diffraction in the wider-angle scattering range ( $5^\circ < 2\theta < 90^\circ$ ), where diffraction from well-defined planes of symmetry within crystalline material enables determination of the solid state form against known crystalline forms (**Figure 3B**), or indeed detection of new polymorphic forms. Alternatively, an amorphous precipitate will present a halo in the diffractogram without defined peaks due to the disordered arrangement of drug molecules in an amorphous form. This scattering technique coupled to a synchrotron source provides high sensitivity and fast acquisition times and has been used to determine the solid state properties for doxorubicin sulfate (35, 95) and doxorubicin citrate nanocrystals inside liposomes (33).

#### 1.4.3 Differential scanning calorimetry (DSC)

Differential scanning calorimetry (DSC) is a thermal analytical technique that measures the specific heat capacity of phase transitions as a function of temperature (96). However, other techniques are required in combination with DSC technique if the system is undergoing different type of transitions. E.g. to distinguish between different transitions such as melting, polymorphic transitions or decomposition (97).

DSC has been used to determine the thermal behaviour of drug nanocrystals (98), the thermal behaviour and stability of lipid bilayers and liposomes (99, 100), and to characterise amorphous pharmaceutical solids (101) and drug polymorphism (102). Consequently, DSC can be applied to qualitatively indicate the thermotropic behaviour of the drug within the liposome and thus its physical state (i.e., amorphous or crystalline nature). For example, recently, studies using “high-sensitivity” DSC observed a two-phase transition for the Doxil® formulation (Figure 3C). The first transition overlapped with that for empty liposomes indicating the “melting” of the membrane lipid while the second transition indicated the melting of the intraliposomal doxorubicin sulfate nanocrystals (34, 103).

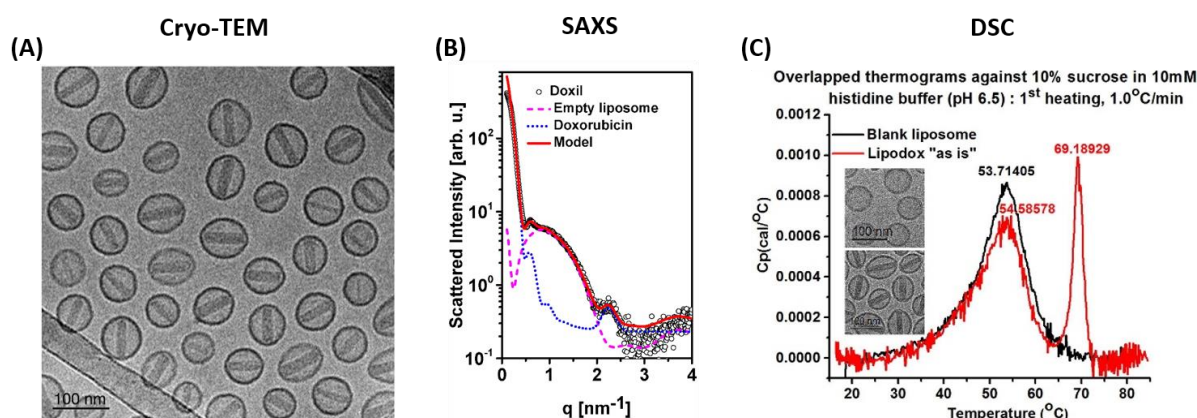


**Figure 3.** Solid state characterisation of intraliposomal doxorubicin precipitates. (A) Cryo-TEM image of Doxil®, which is ammonium sulfate loaded doxorubicin pegylated liposomes; a linear rod-shaped doxorubicin sulfate nanocrystal is observed inside each liposome (adapted with permission from (11)). (B) Background-subtracted radially-integrated scattering intensity from the Doxil® formulation. The peak identified at  $q = 2.25 \text{ nm}^{-1}$  for the fitted data (red curve) aligns with the (1,0,0) peak of the doxorubicin sulfate crystal, indicating that the doxorubicin inside the liposome was in a crystalline state (adapted with permission from (35)). (C) Thermotropic behaviour of Lipodox (FDA approved generic liposomal form of Doxil®) compared to empty liposomes using high sensitivity DSC. The first endotherm for both empty and doxorubicin loaded liposomes represents the membrane lipid phase transition. The second endotherm observed with Lipodox at  $\sim 70 \text{ }^\circ\text{C}$  represents melting of the intraliposomal doxorubicin-sulfate nanocrystals (adapted with permission from (34)).

#### 1.4.4 Other techniques

Other methods have also been used to study the encapsulated drug inside liposomes. Nuclear magnetic resonance (NMR) is a powerful analytical tool to evaluate both the lipid bilayer physical state and rate of motion as well as the

physical and chemical nature of the drug inside the liposome. It can also identify any drug to lipid interactions. The advantage of NMR compared to other fluorescent techniques is that the method is based on the use of intrinsic reporter moieties (104). A study used  $^{195}\text{Pt}$  NMR measurement to quantify the soluble cisplatin where any platinum in crystalline state would be undetected by  $^{195}\text{Pt}$  NMR due to line broadening. The study confirmed that the cisplatin in the liposome are in the soluble aqueous phase (104).  $^1\text{H}$ -NMR was used to study the state of ciprofloxacin located in the aqueous core of the ammonium sulfate gradient loaded liposome. Results demonstrated that ciprofloxacin was located in the aqueous core in a supersaturated state and did not precipitate inside the liposomes (105). Li *et al.* used  $^{13}\text{C}$ -NMR to assess the interaction of doxorubicin with the intraliposomal citrate ion. In citrate gradient loaded liposomes, the citrate resonance was shifted and broadened by loading of DOX indicating an interaction of DOX with citrate to form a 3:1 charge ratio precipitate (33). In another study, Arcon *et al.* used an extended X-ray absorption fine structure method and confirmed that the cisplatin within liposomes did not crystallize but rather formed a supersaturated solution in the liposome core containing 2000-3000 cisplatin molecules per liposome (106). Circular dichroism spectroscopy was also used to confirm the complexation changes of doxorubicin inside liposomes and monitor the electronic state of the drug for different gradient loaded liposomes (33, 107) (**Table 3**). Furthermore, electronic paramagnetic resonance spectroscopy (EPR) and UV-vis electronic absorption spectroscopy (UV-vis) were used to characterise the liposomal formulation Vyxeos<sup>TM</sup> (daunorubicin and cytarabine liposomes). EPR is a selective, sensitive spectroscopic technique based on magnetic resonance signals from unpaired electrons in an external magnetic field. Signal intensity is directly proportional to the concentration of paramagnetic species. The presence of the paramagnetic copper (II) ion in the copper gluconate/TEA buffer system used in liposomal cytarabine and daunorubicin formulation allows the use of EPR to investigate the coordination state of the buffer. With the use of different techniques, the interaction of copper gluconate/TEA with daunorubicin and cytarabine showed a 1:1 or 2:1 daunorubicin:copper complexation within the liposomes (108).

**Table 2.** The advantages and disadvantages associated with different characterisation techniques for the physical state analysis of encapsulated drugs inside liposome.

Characterisation techniques	Advantages	Disadvantages	References
<b>Cryogenic transmission electron microscopy (Cryo-TEM)</b> <b>Cryogenic electron tomography (Cryo-ET)</b>	<ul style="list-style-type: none"> <li>• Non-destructive (preserve liposome in its suspension form while imaging)</li> <li>• Direct visualisation of both the lipid membrane morphology and the structure of encapsulated drug</li> </ul>	<ul style="list-style-type: none"> <li>• Only liposome of certain sizes can be viewed</li> <li>• Cannot provide a clear picture of the whole sample distribution</li> <li>• Cannot be used for physical state/phase identification of drug in the liposome</li> <li>• Expensive and time consuming</li> <li>• Susceptible to electron beam radiation damage</li> </ul>	(82, 87, 90, 92)
<b>Small/Wide angle X-ray scattering (SAXS/WAXS)</b>	<ul style="list-style-type: none"> <li>• Direct physical state identification</li> <li>• Phase identification (crystal structure)</li> <li>• Rapid data acquisition</li> </ul>	<ul style="list-style-type: none"> <li>• Weak signal for liposomal suspension samples</li> <li>• The liposome signal and drug signal are combined</li> <li>• Limited access to synchrotron sourced SAXS/WAXS</li> <li>• Sample is susceptible to radiation damage</li> </ul>	(35, 95, 109)
<b>Differential scanning calorimetry (DSC)</b>	<ul style="list-style-type: none"> <li>• Indirect physical state identification</li> <li>• Provide thermotropic behaviour for crystalline drug in the liposome</li> <li>• Identify any drug interaction with phospholipid membrane</li> </ul>	<ul style="list-style-type: none"> <li>• Cannot be used for phase identification</li> <li>• Low sensitivity for liquid samples</li> <li>• Only crystals with highly ordered structures (high crystallinity) are detectable</li> </ul>	(34, 96, 100, 102, 103)
<b>Circular dichroism (CD)</b>	<ul style="list-style-type: none"> <li>• Rapid and non-destructive</li> <li>• Identify intermolecular interaction of the drug in the liposome (changes in physical state)</li> <li>• Monitor both the conformation and stability of drug in the liposome</li> </ul>	<ul style="list-style-type: none"> <li>• Only drugs with several chromophores or chiral centres can be studied</li> <li>• Background solution can contribute to the CD spectrum (350-200 nm)</li> <li>• Cannot be used for phase identification</li> </ul>	(33, 107, 110, 111)

<b>NMR</b>	<ul style="list-style-type: none"> <li>• Versatile technique based on the use of intrinsic reporter moieties (e.g. <math>^{13}\text{C}</math>, <math>^{31}\text{P}</math>, <math>^1\text{H}</math>, <math>^{15}\text{N}</math>, <math>^{195}\text{Pt}</math>)</li> <li>• Identify physical and chemical nature of the drug in the liposome</li> <li>• Identify any drug interaction with the phospholipid membrane</li> </ul>	<ul style="list-style-type: none"> <li>• Cannot be used for phase identification</li> <li>• Low sensitivity (Drug needs to be above a certain concentration for detection)</li> <li>• Time consuming</li> </ul>	(104, 112)
<b>Extended X-ray absorption fine structure (EXAFS)</b>	<ul style="list-style-type: none"> <li>• Study arrangement of atoms in materials without long range order</li> <li>• Can apply to both crystalline or amorphous materials, liquid or molecular gases</li> </ul>	<ul style="list-style-type: none"> <li>• Cannot be used for phase identification</li> <li>• Inability to distinguish between scattering atoms with little difference in atomic number (C, N, O or S, Cl or Mn, Fe)</li> </ul>	(106, 113)
<b>Electronic paramagnetic resonance spectroscopy (EPR)</b>	<ul style="list-style-type: none"> <li>• Detect unpaired electrons and provide structure and bonding information of paramagnetic species</li> <li>• Sensitive technique with low sample quantity requirement</li> <li>• High specificity</li> </ul>	<ul style="list-style-type: none"> <li>• Cannot be used for phase identification</li> <li>• Requires species to be paramagnetic hence might not be relevant in some systems</li> <li>• Low temperature for requirement</li> </ul>	(108)

**Table 3.** List of liposomal drug delivery systems that have been FDA approved, are currently under clinical investigation or were reported in literature with a focus on the physical state of the drug within the aqueous core of the liposome.

Liposome type	Drug (Formulation)	Drug loading method	Physical state of the encapsulated drug	Characterisation techniques	Comments	References
<b>FDA approved formulations</b>						
<b>Stealth liposome</b>	Doxorubicin (Doxil®/Caelyx®)	Ammonium sulfate gradient	Doxorubicin sulfate drug nanocrystals. Observed as rod shaped fibrous bundles.	<ul style="list-style-type: none"> <li>• Cryo-TEM</li> <li>• SAXS/XRD</li> <li>• DSC</li> </ul>	The doxorubicin sulfate nanocrystals showed a diffraction peak at $q=2.30 \text{ nm}^{-1}$ and melting point of $\sim 70^\circ\text{C}$ .	(11, 35, 85, 95, 114)
<b>Stealth liposome</b>	Irinotecan (Onivyde®)	TEA-sucrose octasulfate (TEA-SOS) gradient	Irinotecan form a gelated or precipitated state with sucrose octasulfate salt	NA		(115, 116)
<b>Conventional liposome</b>	Daunorubicin and cytarabine (Vyxeos™)	Copper gluconate, TEA buffer	Spherical internal structure inside the liposome identified as a second lamella	<ul style="list-style-type: none"> <li>• Cryo-TEM</li> <li>• Electron paramagnetic resonance spectroscopy</li> <li>• <math>^1\text{H-NMR}</math></li> <li>• UV-vis electronic absorption spectroscopy</li> </ul>	Copper interacts with both cytarabine and daunorubicin and assists in retaining both drugs inside the liposome.	(108, 117)

---

**Formulations under clinical investigation**


---

<b>Stealth liposome (Stimuli responsive)</b>	Doxorubicin <b>(ThermoDox®)</b> (Phase III)	Citrate gradient	Doxorubicin precipitated as fibrous bundles	<ul style="list-style-type: none"> <li>• Cryo-TEM</li> </ul>	Precipitate shape similar to Doxil®	(47, 118-120)
<b>Conventional liposome</b>	Ciprofloxacin <b>(Pulmaquin®/ Lipoquin®)</b> (Phase III/Phase II)	Ammonium sulfate gradient	No precipitation	<ul style="list-style-type: none"> <li>• Cryo-TEM/ET</li> <li>• <sup>1</sup>H-NMR</li> </ul>	Ciprofloxacin drug nanocrystals can be induced inside the liposome after freeze-thaw in the presence of a cryopreservative (e.g., sucrose)	(82, 121, 122)
<b>Stealth liposome (Glutathione)</b>	Doxorubicin <b>(2B3-101 or 2X-111)</b> (Phase II)	Ammonium sulfate gradient	Doxorubicin precipitated as fibrous bundles	<ul style="list-style-type: none"> <li>• Cryo-TEM</li> </ul>	Precipitate shape similar to Doxil®	(123, 124)
<b>Stealth liposome</b>	Cisplatin <b>(SPI-077)</b> (Phase II)	Passive loading	No precipitation	<ul style="list-style-type: none"> <li>• EXAFS</li> <li>• Cryo-TEM</li> <li>• <sup>31</sup>P-NMR</li> <li>• <sup>195</sup>Pt-NMR</li> </ul>	Cisplatin form a supersaturated solution inside the liposome	(57, 104, 106)
<b>Conventional liposome</b>	Topotecan <b>(INX-0076)</b> (Phase II)	Manganese sulfate gradient + ionophore A23187	Topotecan precipitated as thin linear structures	<ul style="list-style-type: none"> <li>• Cryo-TEM</li> </ul>	NA	(70)

<b>Conventional liposome</b>	Vinorelbine <b>(INX-0125)</b> (Phase I)	Magnesium sulfate gradient + ionophore A23187	Amorphous drug precipitate	<ul style="list-style-type: none"> <li>• Cryo-TEM</li> </ul>	Increased electron density observed for vinorelbine loaded liposomes	(125, 126)
<b>Experimental formulations</b>						
<b>Conventional liposome</b>	Vincristine/ Vinblastine/ Vinorelbine	Manganese sulfate gradient + ionophore A23187	Amorphous drug precipitate	<ul style="list-style-type: none"> <li>• Cryo-TEM</li> </ul>	Vincristine can form granular structures inside the liposome at higher drug to lipid ratio	(126, 127)
<b>Conventional liposome</b>	Doxorubicin	Citrate gradient	Doxorubicin precipitated as fibrous bundles	<ul style="list-style-type: none"> <li>• Cryo-TEM</li> <li>• Circular dichroism</li> <li>• <sup>13</sup>C-NMR</li> <li>• SAXS</li> </ul>	Linear, circular fiber bundles aligned longitudinally in hexagonal array	(33)
		Manganese sulfate gradient	No precipitation	<ul style="list-style-type: none"> <li>• Cryo-TEM</li> <li>• Circular dichroism</li> </ul>	Doxorubicin manganese complex	(107)
		Manganese sulfate gradient + ionophore A23187	Doxorubicin precipitated as fibrous bundles		Precipitate consisted of linear fibrous bundles	
		Manganese chloride gradient	No precipitation		NA	
		Manganese chloride gradient + ionophore A23187	No precipitation		NA	

		Phosphate gradient	Doxorubicin precipitated as linear bundles	• Cryo-TEM	NA	(63)	
		Magnesium sulfate gradient + ionophore A23187	Doxorubicin precipitated as linear bundles	• Cryo-TEM	Doxorubicin can form triangular or even rectangular precipitate structures at higher drug to lipid ratios	(128)	
<b>Conventional liposome</b>	Topotecan	Copper sulfate gradient + ionophore A23187	Topotecan precipitated as needle-like crystals	• Cryo-TEM	NA	(71, 129)	
		Ammonium sulfate gradient	Topotecan precipitated as thin needle-like crystals				
		Manganese sulfate gradient + ionophore A23187				Visually all topotecan precipitates are similar in morphology and size regardless of the D/L ratio and loading method	(70)
		Citrate gradient			• Cryo-TEM		
		Manganese chloride gradient + ionophore A23187					
<b>Stealth liposome</b>	Idarubicin	EDTA gradient	Idarubicin precipitated as elongated bundles	• Cryo-TEM	Precipitate bundles were mostly bent or circular-shaped structures	(64)	
<b>Stealth liposome</b>	Epirubicin	EDTA gradient	Epirubicin precipitated	• Cryo-TEM	Precipitate structures	(130)	

<b>Stealth liposome</b>	Ciprofloxacin	Magnesium sulfate gradient + ionophore A23187	No precipitation	• Cryo-TEM	were either circular or button-shaped	NA	(131)
		Calcium hydroxybenzensulfonate gradient + ionophore A23187	Ciprofloxacin precipitated		Ciprofloxacin precipitate formed between the lamellae of bilamellar liposomes.		
<b>Stealth liposome</b>	Mitoxantrone	Ammonium sulfate loading	Mitoxantrone precipitated as linear nanocrystals	• Cryo-TEM	NA	(132)	

---

## 1.5 Precipitation of drug within liposomes

Depending on the physiochemical properties and chemical structures of the drug, the active loading method used, and the process parameters applied, the encapsulated drug may exist as a crystalline precipitate, amorphous precipitate, or in a supersaturated or sub-saturated solution. The specific physical states of the drug within the liposome will impact on both the stability of the encapsulated drug and the apparent drug release rate from the liposomes. **Table 3** lists the liposomal formulation that has been FDA approved, under clinical investigation or experimental formulations with a focus on the physical state of the drug inside the liposome. In the following section, different classes of drugs that have been reported to form precipitates within liposomes will be discussed.

### 1.5.1 Doxorubicin

Lasic *et al.* first reported the physical state of doxorubicin (DOX) in the core of PEGylated liposomes loaded by the ammonium sulfate gradient method. Drug was observed as an electron opaque band within the liposomes and the authors concluded that the DOX sulfate precipitated as crystalline one-dimensional rods, which did not interact with the bilayer (refer to **Figure 4B**). The material within the liposome displayed a single sharp X-ray reflection at 27 Å which correlated with that of doxorubicin precipitated from ammonium sulfate solution, confirming the precipitate to be DOX-sulfate nanocrystals (114).

In another study by Li *et al.*, the physical state of DOX in citrate containing liposomes exhibited more curved and circular fibrous bundles (refer to **Figure 4C**) compared to the DOX-sulfate nanocrystals where only straight rods were observed. This indicated that DOX-citrate nanocrystals are more flexible. X-ray diffraction results showed that the DOX-citrate nanocrystals exhibited an interfiber spacing of 30-35 Å (33). In a more recent study by Schilt *et al.* (35), solution X-ray scattering was performed *in situ* on Doxil® and other DOX-containing liposomal generic formulations. The authors reaffirmed the crystalline state of the DOX-sulfate precipitate within the liposomes identifying a strong diffraction peak at  $q=2.30 \text{ nm}^{-1}$  (**Figure 3A**). The aggregation and ultimate crystallisation of DOX inside sulfate and citrate containing liposomes is also related to the self-aggregation of DOX through  $\pi$ - $\pi$  interactions between the planar anthracycline rings in DOX (**Figure 4C**). Drug complexation with anions present inside the liposome in the case of DOX-sulfate

nanocrystals showed tighter packing than DOX-citrate nanocrystals attributed to the sulfate ion being a smaller anion compared to the citrate ion (refer to **Figure 4**) (33).

Manganese chloride and manganese sulfate-loaded DOX liposomes with and without ionophore were also characterised with cryo-TEM to study the state of DOX inside the liposome. Manganese chloride gradient-loaded DOX liposomes did not show any drug precipitation regardless of ionophore addition. However, the manganese sulfate gradient loaded DOX liposomes with ionophore exhibited linear bundle-like nanocrystal structures similar to those of the citrate loaded DOX liposomes. The presence of the ionophore A23187 generated a >2.5 pH units gradient with an acidic core compared to little or no transmembrane pH gradient across the liposome in the absence of the ionophore. This allowed DOX to ionise and interact with the sulfate anion and precipitate within the liposome (107). Other gradient loaded DOX liposomes such as the phosphate gradient (63) and magnesium sulfate gradient (with ionophore) liposomes (128) also enabled DOX precipitation inside the liposome (refer to **Table 3**).

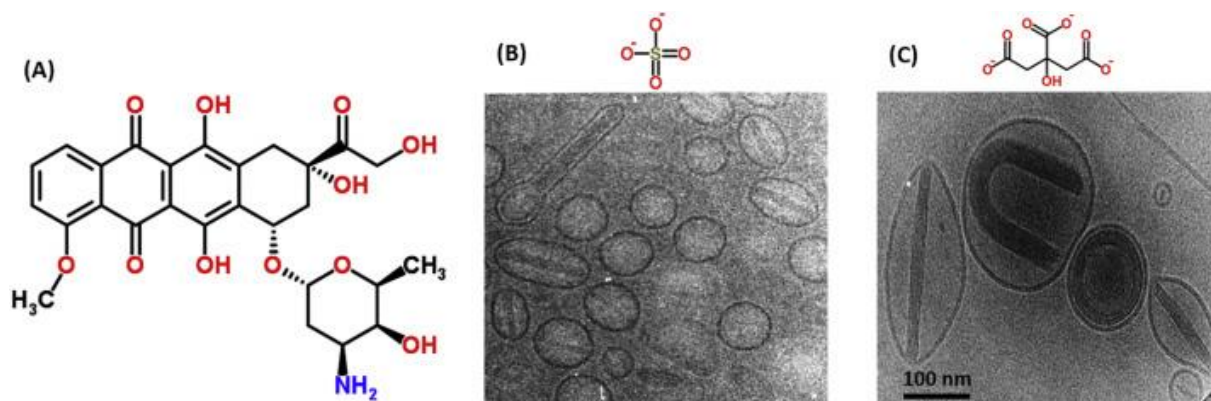


**Figure 4.** Dependence of the form of doxorubicin precipitates under confinement in liposomes on the counterion (A) Chemical structure of doxorubicin. (B) Cryo-TEM image of doxorubicin HCl loaded into liposomes using an ammonium sulfate gradient ([adapted with permission from \(114\)](#)) showing linear rod like nanocrystals (C) Cryo-TEM image of doxorubicin HCl loaded into liposomes using a citrate gradient showing circular and U-shaped nanocrystals ([adapted with permission from \(33\)](#)).

Overall, it is clear that the counter ions used to actively load the DOX into the liposomes result in differences in the structure of the precipitates, most likely due to the formation of salts with different crystal habits and rigidity.

### 1.5.2 Vincristine, vinorelbine and vinblastine

Liposomal vincristine sulfate (trade name: Marqibo®) has been approved for the treatment of lymphoblastic leukemia. Vincristine (VCR) is a vinca alkaloid with low aqueous solubility at physiological pH but with high permeability, making it ideal to be encapsulated into liposomes to reduce the acute toxicity of the free drug (133). Johnston *et al.* compared the physical states of magnesium sulfate gradient (with ionophore) loaded vincristine liposomes at different drug to lipid (D/L) ratios (**Figure 5**). At the highest D/L ratio of 1.03, the cryo-TEM image showed the liposomes with dense granular structures within their aqueous core (**Figure 5F**). These structures are very different to the linear crystal rods formed in DOX sulfate liposomes (127). In this study, the higher the D/L ratio, the better the drug retention (i.e., the lower the vincristine release rate). However a higher drug retention does not always correlate to the most optimal therapeutic efficacy; in the above study, the optimal therapeutic efficacy was achieved with liposomes formed at a D/L ratio of 0.1. Since for D/L ratio of 0.6, the drug retention is long that drug release is sufficiently slow and antitumor activity is compromised.

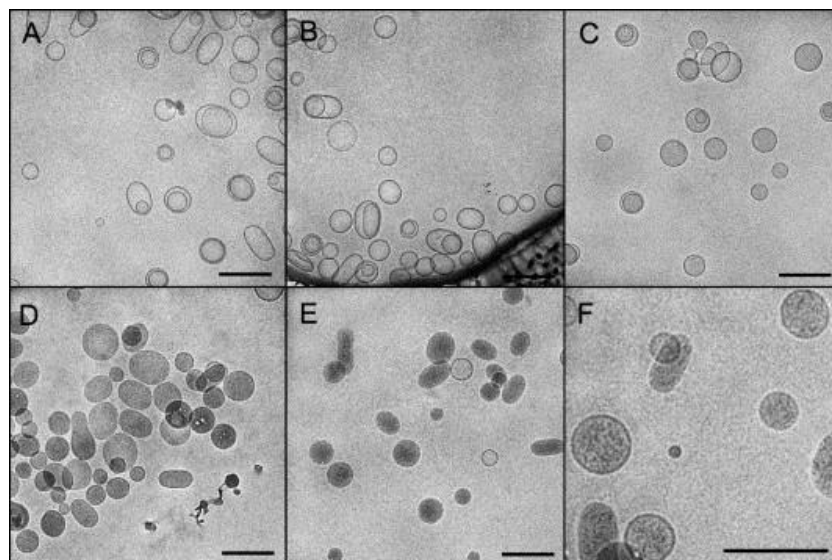


**Figure 5.** Cryo-TEM images of liposomal formulations of vincristine. The drugs were loaded into the liposomes using the ionophore A23187/MgSO<sub>4</sub> loading method at different D/L ratios. (A) Liposome in the absence of drug, and at a D/L ratio of 0.06 (B), 0.27 (C), 0.6 (D) and 1.03 (E). (F) Enlarged section of (E) showing granulated structures within the liposomes. The size bar represents 200 nm in each image (adapted with permission from (127)).

In another study, other vinca alkaloids, including vinorelbine and vinblastine were also investigated as liposomal formulations in comparison to vincristine (126). None of the vinca alkaloids, i.e., vinorelbine, vinblastine or vincristine showed crystalline precipitates

within magnesium sulfate (with ionophore) loaded liposomes (Figure 6). The more electron-dense appearance in the cryo-EM micrographs compared with drug-free liposomes indicated that the drug had precipitated in an amorphous rather than crystalline form within the liposome.

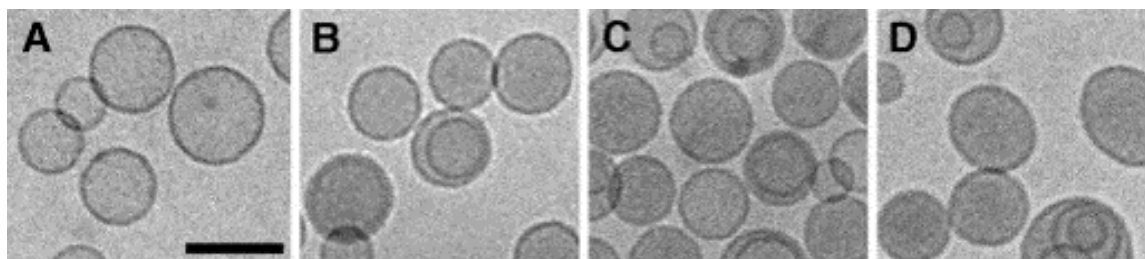


**Figure 6.** Cryo-TEM images of liposomal formulations of different vinca alkaloids. The drugs were loaded into the liposomes using the ionophore A23187/MgSO<sub>4</sub> loading method at a D/L ratio of 0.3. (A) Liposomes in the absence of drug, (B) liposomal vinblastine, (C) liposomal vinorelbine and (D) liposomal vincristine. The size bar represents 100 nm for all of the images (adapted with permission from (126)).

### 1.5.3 Topotecan

Topotecan (TPT), a camptothecin analogue, is a topoisomerase I inhibitor for the management of ovarian cancer. Its closed  $\alpha$ -lactone ring is therapeutically important for tumour cell targeting; however the stability of this molecule presents a challenge as it has a tendency to undergo hydrolysis at neutral physiological pH (134, 135). Encapsulation of TPT into liposomes can increase drug stability and enhance its therapeutic index (136, 137). Four different active loading methods were employed; namely ammonium sulfate, citrate, manganese sulfate (with ionophore), and manganese chloride (with ionophore). All methods induced the formation of intraliposomal linear nanocrystals at a low D/L ratio of 0.1 (70) (refer to Figure 7). The crystalline TPT precipitates also altered the vesicle morphology to a more stretched elliptical shape compared to the empty spherical liposomes.

Co-encapsulation of anticancer drugs, such as VCR and TPT, increases their therapeutic efficacy because the combination acts on different targets in the cancer cell and affects different phases in the cell cycle. TPT converts DNA topoisomerase I into a cellular toxin, leading to arrest in the S phase or G<sub>2</sub>-M phase, whereas, VCR causes depolymerisation of microtubules, leading to mitotic arrest (138). In the case of VCR and TPT, both drugs are amphiphilic weak bases and apparently do not interact with each other after co-encapsulation into ammonium sulfate gradient loaded liposomes (109). Analyses by SAXS showed that TPT crystallizes in the shape of longitudinal rods while

VCR did not precipitate. The author suggested since the intraliposomal VCR concentration significantly exceeds its maximal aqueous solubility, and that it probably formed a supersaturated amorphous gel-like phase inside the liposome (109).

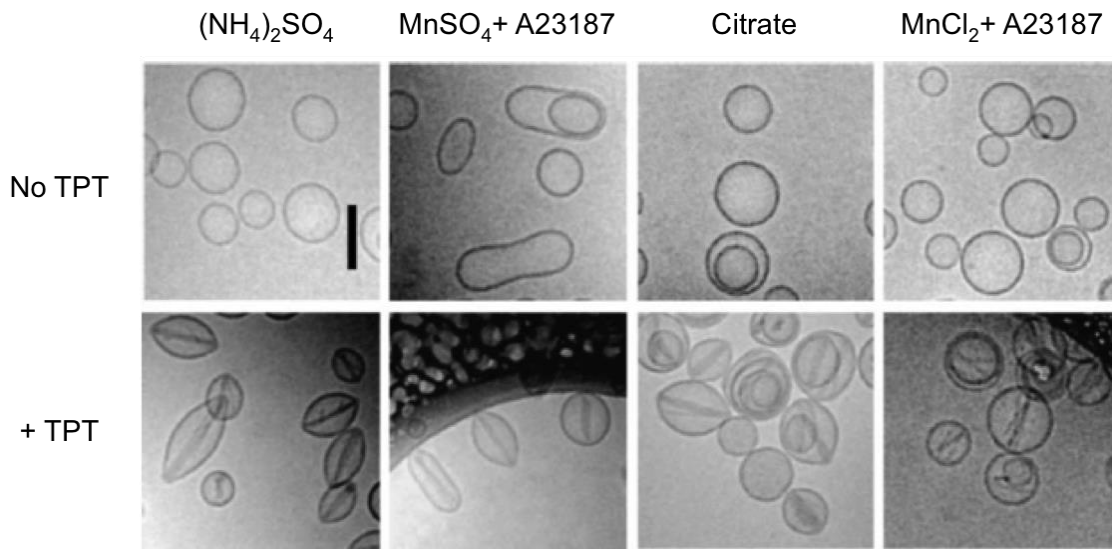


**Figure 7.** Cryo-TEM images of liposomes before and after active drug loading with topotecan (TPT). Top row: Empty liposomes before TPT loading. Bottom row: loaded topotecan at 0.1 w/w drug to lipid ratio. The type of active loading method is annotated above the images (adapted with permission from (70)). All loading methods resulted in formation of linear crystalline precipitates for TPT liposomes. Scale bar is equivalent to 100 nm for all the images.

#### 1.5.4 Other drugs

Ciprofloxacin is a fluoroquinolone broad-spectrum antibiotic and is a weakly basic drug with poor aqueous solubility at neutral pH (105). Actively loading liposomes with ciprofloxacin using an ammonium sulfate gradient can provide a high intraliposomal drug concentration; however the drug does not precipitate as nanocrystals (85). This led to acceptable long-term stability of 6 months in an early research liposomal ciprofloxacin batch (85) and 2 years in the GMP batches (e.g., with Lipoquin®) with no decrease in encapsulated drug (121). However, the drug leakage rate after dilution in plasma was faster for liposomal ciprofloxacin than for the liposomal formulation containing doxorubicin in a nanocrystalline state (85). Thus, attenuation of the ciprofloxacin release rate may be possible if it could be converted into a nanocrystalline state. Recently, an additional freeze-thawing step was introduced to the ammonium sulfate loaded ciprofloxacin liposomes that generated a linear rod-like ciprofloxacin precipitate inside the liposomes. The precipitate was visually similar to DOX sulfate crystals as observed in Doxil® (82). In another study with ciprofloxacin, hydroxybenzenesulfonate (HBS) was used in the loading of

ciprofloxacin into liposomes, and resulted in the formation of intravesicular ciprofloxacin-HBS non-soluble ion pair complexes (131). The negatively charged sulfonic group of HBS and the positive charge on the protonated amine in ciprofloxacin lead to the formation of insoluble ion pairs. Other drugs that have also precipitated inside liposomes include EDTA loaded idarubicin (64) and epirubicin (130). Both idarubicin and epirubicin formed circular button shaped bundles inside the liposome. For idarubicin, the EDTA loading method enabled efficient drug accumulation inside the liposome. The formation of a low solubility idarubicin EDTA precipitate inside the liposome leads to increased *in vivo* stability for the otherwise fast-leaking hydrophobic drug (64).

As discussed previously, the type of active loading buffer can influence the structure of the nanocrystal formed (i.e. in the case of doxorubicin). It should also be noted that among different drugs, slight differences in structure of the nanocrystal precipitate are also observed (**Table 3**). For example topotecan is reported to precipitate in thin needle like precipitate, whereas doxorubicin is precipitated in a more linear bundle like structure and epirubicin having some linear structures but mostly circular or button like structures. The difference in the doxorubicin nanocrystals to topotecan nanocrystals could be due to the chemical structure of the drug molecule itself. Topotecan is comprised of a planar pentacyclic ring structure, whereas doxorubicin contains a tetracenequinone ring structure with a sugar attached by glycosidic linkage. The difference in the molecular structure would affect the crystal packing which changes the nanocrystal structure formed. In the case of epirubicin (EDTA loaded liposomes), where the molecular structure is identical to doxorubicin, the difference in the nanocrystal structure formed inside the liposome could be due to the difference in the active loading buffer used.

## 1.6 Drug release from nanocrystallised drug within liposomes

The mechanism of drug release from liposomal drug delivery systems is dependent on the delivery route of the liposomes. When the liposomes are staying intact during the drug delivery process, the mechanism of drug release is fundamentally passive drug permeation and diffusion. Drug release from liposomal carriers is a complex process affected by the physiochemical properties of the liposome and the physical state of the encapsulated drug, as well as external factors such as the release medium selection, temperature and pH. The physiochemical properties that dictate drug release from liposomes include the bilayer permeability of the drug, the drug ionisation constant, drug

binding behaviour with the lipid bilayer, self-association of the drug and the presence of intraliposomal precipitate. The size and the cross sectional area of the molecule are also important in dictating the permeability and diffusion of the drug across the lipid bilayer (139, 140). Other parameters to be considered in the case of actively loaded liposomes are the concentration and type of the loading buffer, the D/L ratio, intraliposomal pH, volume, as well as external factors such as the presence of other permeable ions in the external buffer.

Dialysis is commonly used to study the drug release kinetics from liposomal formulations, however the drug release properties observed using the dialysis model often show poor correlation between *in vitro* and *in vivo* results. The liposomes dispersion is placed inside a dialysis bag, which is then sealed and placed into the release medium reservoir to generate sink conditions and drive drug release. However this method has serious, often unrecognised limitations in the ability to measure the release rate and kinetics from liposomal formulations. The barrier nature of the dialysis membrane itself can retard the apparent drug release rate, meaning that although drug is released from the liposome, it is not recognised as such until it reaches the receptor medium (141, 142) The drug could also reversibly or irreversibly bind to the dialysis membrane or the liposome after release from the carrier, which reduces the apparent release rate and concentration gradient across the membrane (143, 144). Another conventional method to evaluate drug release from liposomal formulations is the “sample and separate” method. The liposomal formulations are diluted into the release medium under sink condition and aliquots are removed from the release medium at different time intervals. The amount of drug release is determined after separation of the dispersed liposomal formulation (e.g. by ultracentrifugation or ultrafiltration) from the release medium (145-147). The limiting factor for this method is the efficiency and accuracy of the sample separation method that is used. The force and time applied for centrifugation to separate the liposomes from the free drug can potentially induce unwanted drug release and affect the apparent drug release (141, 148). It is important to note that despite Doxil® having been on the market for two decades now, there is still no pharmacopoeial method for the measurement of drug release from liposomes, although recent FDA sponsored work towards a continuous flow USP-4 method has been reported (149).

Several mechanistic models have been developed to predict drug release for Doxil® (143, 150) and liposomal topotecan (151, 152). These models explain the physiochemical properties important in dictating the drug release behaviour as well as gaining insight into

the *in vivo* - *in vitro* correlation to better predict the drug release behaviour *in vivo*. Csuha *et al.* determined the key parameters for mechanism-based models to help predict doxorubicin release from actively loaded liposomes (150). These parameters included drug pKa, permeability coefficients, drug self-association and relevant equilibrium constants, solubility product of the DOX-sulfate nanocrystals, and partition coefficients of DOX. The amount of drug loaded, and the concentration of the sulfate ion dictate how much drug is precipitated within the liposome. The solubility product constant ( $K_{sp}$ ) for DOX-sulfate nanocrystals of Doxil<sup>®</sup> was reported to be  $2.9 \times 10^{-7} \text{ M}^3$  at 37°C. The solubility of DOX decreases with increasing ammonium sulfate concentration, and the solubility product of the DOX-sulfate nanocrystals is temperature dependent. The authors assumed that only the unionised monomeric form of DOX can cross the liposomal membrane. Therefore the concentration of DOX in the monomeric form rather than the self-associated dimeric and oligomeric form will be the driving force for drug release.

It has also been reported that the precipitation of DOX-sulfate salt as nanocrystals inside the liposomes lowers the fraction of drug in solution (143). This reduces the driving force for release and retards DOX release from Doxil<sup>®</sup>. The solubility product of the precipitate is the rate limiting factor to control drug release rather than the dissolution rate. Since more than 90% of the total entrapped drug is precipitated as drug nanocrystals, the driving force for drug release remains constant, resulting in zero order release kinetics. Also the study observed that when there is no external ammonia in the release media, the internal pH is acidic, which protonates the DOX and the ionised drug is then membrane impermeable, resulting in an extremely slow release profile. However when ammonia is added externally, the reservoir pH is elevated and the influx of ammonia will raise the intraliposomal pH and accelerate drug release. This zero order release kinetics model is also consistent with the data reported for liposomes containing precipitated vincristine with the drug efflux rate being proportional to the soluble drug concentration (127).

A more recent study by Russell *et al.* assessed the kinetics of doxorubicin leakage from the Doxil<sup>®</sup> formulation (153), namely that the release of doxorubicin from Doxil<sup>®</sup> undergoes three processes, first the dissolution of the solid DOX-sulfate nanocrystals, then the protonation/deprotonation of the soluble DOX and finally passive transport of neutral DOX across the lipid bilayer to the external medium. They proposed that the dissolution of the DOX-sulfate nanocrystals followed first order kinetics with a rate constant of  $1.0 \times 10^{-9} \text{ cm s}^{-1}$ . The DOX leakage for transport across the lipid bilayer was also modelled by first order kinetics with a rate constant of  $1-3 \times 10^{-12} \text{ cm s}^{-1}$  depending on the

pH, with a more acidic pH resulting in a higher rate constant. The dissolution rate of the DOX-sulfate nanocrystal is three orders of magnitude faster than the leakage rate constant of DOX across the lipid bilayer. Hence, the kinetics of DOX leakage from the liposome are dominated by the rate constant for transport across the liposome bilayer and the pKa (153).

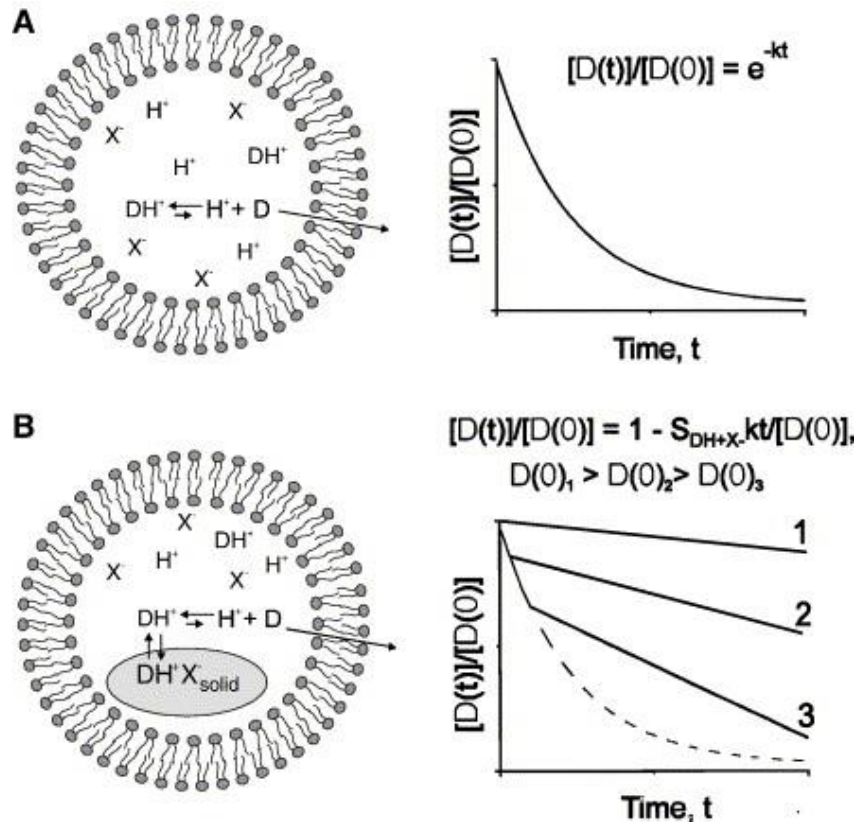


**Figure 8.** Schematics of different drug release kinetics. A Drug is present inside the liposome only in a solubilised form. The drug release rate follows first order kinetics. B Drug precipitation/crystallisation has occurred within the liposome core. The drug release rate follows zero order kinetics. Curve 1 represents if drug is predominately in the precipitated form, and the efflux rate of drug is slower than the dissolution of the precipitate. Curve 2 and 3 represent liposome containing saturated drug suspension in equilibrium with a precipitate, a biphasic drug release profile (adapted with permission from (131)).

As described earlier, Zhigaltsev *et al.* prepared HBS loaded liposomal vinorelbine and liposomal ciprofloxacin. The drug and HBS formed non-soluble ion pair complexes that precipitated inside the liposomes leading to improved drug retention (131). The *in vitro* release studies showed that when the precipitates had formed, release was governed by zero order kinetics, but in the absence of intraliposomal precipitation the release followed first order kinetics (**Figure 8**). Also they suggested that if the dissolution rate of the drug is

slower than the membrane diffusion rate of the unionised species, a biphasic release with a rapid initial loss of drug followed by slower linear zero order release will be observed. However if the membrane diffusion rate is slower than the dissolution of the precipitate, only a zero order release rate is observed.

The formation of ciprofloxacin nanocrystals inside the liposomes after using the freeze-thaw method was briefly discussed in section 5.4. In another study, addition of polysorbate 20 or Brij 30 during the preparation of liposomal ciprofloxacin before the freeze-thaw method was applied reduced the extent of ciprofloxacin nanocrystal growth inside the liposomes and hence allowed modification of the drug release profile (122). It was also noted that the samples that had nanocrystals formed inside the liposomes post the freeze-thaw process showed slower drug release compared to liposomal ciprofloxacin in the absence of nanocrystals, regardless whether surfactant was added or not. This study suggests the potential possibilities of controlling the size of nanocrystal formation within the liposomes, which may be useful in developing future liposomal drugs with tailored drug release profiles.

## 1.7 Future applications of nanocrystallised liposomes and conclusions

Nanocrystalline precipitates formed within liposomes provide many potential benefits for liposomal drug formulation including higher drug retention, better formulation stability, and more efficient drug loading. However, the solid state properties of the precipitates have not been studied in a detailed and systemic way (as shown in **Table 3**). To date, only DOX-sulfate and DOX-citrate precipitates in liposomal DOX have been fully characterised and confirmed to show the precipitates are in a crystalline form. This greatly limits the investigation into the mechanism of drug crystallisation within liposomes as well as the assessment of additional benefits in drug delivery applications. From **Table 3**, some observations can be drawn from the drugs that form “nanocrystal like” fibrous bundles/precipitate inside the liposomes. Firstly, these liposomal formulations are prepared using an active loading method (as described in section 3) so the drug needs to be an amphiphilic base or acid. Also the selection of ion for the active loading method is crucial in generating insoluble drug-ion complexes, which promote precipitation. Secondly, these actively loaded liposomal formulations have achieved high drug loading efficiency

and high drug retention properties. The high intraliposomal drug concentration means that more ionized drug molecules are able to form insoluble complexes with the ions inside the liposome. Lastly, these drugs have many aromatic rings in their structures that can form stacks through aromatic pi-pi interactions.

For drugs that did not precipitate inside the liposome after active loading, the freeze-thawing method which induced crystallisation of ciprofloxacin within liposomes (82, 122) could potentially be applied to enable crystallisation inside the liposome. This method may be easily incorporated in the process to form drug nanocrystals inside the liposome. Although there is no definitive mechanistic understanding of the formation of drug precipitate within the liposome, the expansion and study of a wider range of compounds exhibiting this phenomenon would generate increased interest and experimental studies to support theoretical modeling of possible mechanisms.

One possible future application for the liposomal drug nanocrystals may be in oral drug delivery. Traditionally, nanocrystals range from 10-1000 nm in particle size (154). The smaller particle size of these nanocrystals would increase the apparent surface area, which, together with the enhanced solubility by virtue of the lipids being present, will increase the dissolution rate of the poorly water soluble drugs predicted from the Noyes-Whitney equation (155). Hence, the nanocrystals present inside the liposome would provide a source for enhanced dissolution rate due to their small size. Liposomes, at least in theory, are inherently a lipid-based formulation (LBF) (156). During the digestion of LBF, bile salts can interact with liposomes forming mixed micelles (157, 158) and lipases and phospholipases have the ability to hydrolyse the phospholipid in the liposomes (159, 160). In the case of liposomes with encapsulated nanocrystals, if the crystallised drug is weakly basic in nature, the hydrolysis of phospholipid into free fatty acid by the nature of the digestion process would interact with the oppositely charged weakly basic drug to form an amorphous drug salt (161). This formation of the amorphous drug salt during digestion of liposomal drug nanocrystals could increase the drug dissolution rate in the GI tract, and enable enhanced absorption by providing an increased pool of non-crystalline drug.

Another possible future application for liposomal drug nanocrystals is their use as a new formulation approach for current drugs formulated as nanosuspensions. Nanosuspensions are being developed for drugs whose low solubility in lipid or water precludes their solubilisation into conventional carrier systems for IV administration. Preparing intravenous nanosuspensions of drugs, such as Abraxane® for paclitaxel (162), requires a complex manufacturing process with dedicated facilities and onerous quality

control. In the nanocrystal examples provided above, the confinement of the liposome appears to exclude external crystallization or growth through Ostwald ripening, leading to potentially greater size stability and thus increased safety for such products, while enabling the administration of a meaningful dose.

Liposomes, including conventional liposomes (163), highly deformable liposomes (transfersomes) (164, 165) and niosomes (166) have been explored to improve drug delivery through the skin (167, 168). The phospholipid of the liposomal bilayer acts as a penetration enhancer by loosening the lipid structure of the stratum corneum and this impaired barrier function of the skin subsequently increases skin partitioning of the drug (169, 170). There are currently three nanocrystalline-based products for topical drug delivery on the market and a few under clinical trials (171). Drug nanocrystals with their larger surface area compared to for example micronized drug particles, increase the drugs's dissolution rate and even saturation solubility (172, 173). The increased saturation solubility helps to maintain the concentration gradient between the suspension and the target cell which improves drug absorption by diffusion (171). Currently, drug nanocrystal suspensions are formulated in gels or creams for ease of application (174, 175). Liposomal drug nanocrystals however, can be beneficial in these cases as the liposomal bilayer acts as the stabiliser for the drug nanocrystals as noted above. This may reduce the requirement for additional formulation development. The liposomal bilayer may also act as a penetration enhancer for the encapsulated drug nanocrystals.

In conclusion, this review has explored the importance of the physical state of the drug encapsulated within liposomes and the role this state plays with respect to drug dissolution and release. The ability to modify the drug's physical state inside a liposome may provide an opportunity to modify the pharmacokinetics of the drug to optimise the safety and efficacy of treatment with liposomal products.

## **Conflict of Interest**

At the time of preparation of this manuscript, David Cipolla was an employee of Aradigm Corporation, developing liposomal ciprofloxacin.

## References

1. Batist G, Ramakrishnan G, Rao CS, Chandrasekharan A, Gutheil J, Guthrie T, et al. Reduced cardiotoxicity and preserved antitumor efficacy of liposome-encapsulated doxorubicin and cyclophosphamide compared with conventional doxorubicin and cyclophosphamide in a randomized, multicenter trial of metastatic breast cancer. *J Clin Oncol*. 2001;19(5):1444-54.
2. O'Brien MER, Wigler N, Inbar M, Rosso R, Grischke E, Santoro A, et al. Reduced cardiotoxicity and comparable efficacy in a phase III trial of pegylated liposomal doxorubicin HCl (CAELYX™/Doxil®) versus conventional doxorubicin for first-line treatment of metastatic breast cancer. *Annals of Oncology*. 2004;15(3):440-9.
3. Eloy JO, Claro de Souza M, Petrilli R, Barcellos JPA, Lee RJ, Marchetti JM. Liposomes as carriers of hydrophilic small molecule drugs: Strategies to enhance encapsulation and delivery. *Colloids and Surfaces B: Biointerfaces*. 2014;123:345-63.
4. Fahr A, Hoogevest Pv, May S, Bergstrand N, S. Leigh ML. Transfer of lipophilic drugs between liposomal membranes and biological interfaces: Consequences for drug delivery. *European Journal of Pharmaceutical Sciences*. 2005;26(3):251-65.
5. Bangham AD. Physical structure and behavior of lipids and lipid enzymes. In: Paoletti R, Kritchevsky D, editors. *Advances in Lipid Research*. 1: Elsevier; 1963. p. 65-104.
6. Allen TM, Cullis PR. Liposomal drug delivery systems: From concept to clinical applications. *Advanced Drug Delivery Reviews*. 2013;65(1):36-48.
7. Zylberberg C, Matosevic S. Pharmaceutical liposomal drug delivery: a review of new delivery systems and a look at the regulatory landscape. *Drug Delivery*. 2016;23(9):3319-29.
8. Taylor TM, Weiss J, Davidson PM, Bruce BD. Liposomal nanocapsules in food science and agriculture. *Critical Reviews in Food Science and Nutrition*. 2005;45(7-8):587-605.
9. Reza Mozafari M, Johnson C, Hatziantoniou S, Demetzos C. Nanoliposomes and their applications in food nanotechnology. *Journal of Liposome Research*. 2008;18(4):309-27.
10. Rahimpour Y, Hamishehkar H. Liposomes in cosmeceutics. *Expert opinion on drug delivery*. 2012;9(4):443-55.
11. Barenholz Y. Doxil® — The first FDA-approved nano-drug: Lessons learned. *Journal of Controlled Release*. 2012;160(2):117-34.

12. James ND, Coker RJ, Tomlinson D, Harris JRW, Gompels M, Pinching AJ, et al. Liposomal doxorubicin (Doxil): An effective new treatment for Kaposi's sarcoma in AIDS. *Clinical Oncology*. 1994;6(5):294-6.
13. Adler-Moore J, Proffitt RT. AmBisome: liposomal formulation, structure, mechanism of action and pre-clinical experience. *Journal of Antimicrobial Chemotherapy*. 2002;49(suppl\_1):21-30.
14. Boswell GW, Buell D, Bekersky I. AmBisome (Liposomal Amphotericin B): A comparative review. *The Journal of Clinical Pharmacology*. 1998;38(7):583-92.
15. Forssen EA. The design and development of DaunoXome® for solid tumor targeting in vivo. *Advanced Drug Delivery Reviews*. 1997;24(2):133-50.
16. Rosenthal E, Poizot-Martin I, Saint-Marc T, Spano JP, Cacoub P, Group DNXS. Phase IV study of liposomal daunorubicin (DaunoXome) in AIDS-related Kaposi sarcoma. *Am J Clin Oncol*. 2002;25(1):57-9.
17. Treatment of age-related macular degeneration with photodynamic therapy study G. Photodynamic therapy of subfoveal choroidal neovascularization in age-related macular degeneration with verteporfin: One-year results of 2 randomized clinical trials—tap report 1. *Archives of Ophthalmology*. 1999;117(10):1329-45.
18. McAlvin JB, Padera RF, Shankarappa SA, Reznor G, Kwon AH, Chiang HH, et al. Multivesicular liposomal bupivacaine at the sciatic nerve. *Biomaterials*. 2014;35(15):4557-64.
19. Silverman JA, Deitcher SR. Marqibo® (vincristine sulfate liposome injection) improves the pharmacokinetics and pharmacodynamics of vincristine. *Cancer Chemotherapy and Pharmacology*. 2013;71(3):555-64.
20. Franco MS, Oliveira MC. Liposomes co-encapsulating anticancer drugs in synergistic ratios as an approach to promote increased efficacy and greater safety. *Anticancer Agents Med Chem*. 2018.
21. Torchilin VP. Recent advances with liposomes as pharmaceutical carriers. *Nature Reviews Drug Discovery*. 2005;4:145.
22. Nag OK, Awasthi V. Surface engineering of liposomes for stealth behavior. *pharmaceutics*. 2013;5(4):542-69.
23. Čeh B, Winterhalter M, Frederik PM, Vallner JJ, Lasic DD. Stealth® liposomes: from theory to product. *Advanced Drug Delivery Reviews*. 1997;24(2):165-77.

24. Immordino ML, Dosio F, Cattel L. Stealth liposomes: review of the basic science, rationale, and clinical applications, existing and potential. *International Journal of Nanomedicine*. 2006;1(3):297-315.
25. Moghimi SM, Szebeni J. Stealth liposomes and long circulating nanoparticles: critical issues in pharmacokinetics, opsonization and protein-binding properties. *Progress in Lipid Research*. 2003;42(6):463-78.
26. Forssen E, Willis M. Ligand-targeted liposomes. *Advanced Drug Delivery Reviews*. 1998;29(3):249-71.
27. Noble CO, Kirpotin DB, Hayes ME, Mamot C, Hong K, Park JW, et al. Development of ligand-targeted liposomes for cancer therapy. *Expert Opinion on Therapeutic Targets*. 2004;8(4):335-53.
28. Noble GT, Stefanick JF, Ashley JD, Kiziltepe T, Bilgicer B. Ligand-targeted liposome design: challenges and fundamental considerations. *Trends in Biotechnology*. 2014;32(1):32-45.
29. Kneidl B, Peller M, Winter G, Lindner LH, Hossann M. Thermosensitive liposomal drug delivery systems: state of the art review. *International Journal of Nanomedicine*. 2014;9:4387-98.
30. Boyd BJ, Fong W-K. Stimuli-responsive lipid-based self-assembled systems. *Self-Assembled Supramolecular Architectures*: John Wiley & Sons, Inc.; 2012. p. 257-88.
31. Jain A, Jain SK. Stimuli-responsive smart liposomes in cancer targeting. *Current drug targets*. 2018;19(3):259-70.
32. Movahedi F, Hu RG, Becker DL, Xu C. Stimuli-responsive liposomes for the delivery of nucleic acid therapeutics. *Nanomedicine: Nanotechnology, Biology and Medicine*. 2015;11(6):1575-84.
33. Li X, Hirsh DJ, Cabral-Lilly D, Zirkel A, Gruner SM, Janoff AS, et al. Doxorubicin physical state in solution and inside liposomes loaded via a pH gradient. *Biochimica et Biophysica Acta (BBA) - Biomembranes*. 1998;1415(1):23-40.
34. Wei X, Cohen R, Barenholz Y. Insights into composition/structure/function relationships of Doxil® gained from “high-sensitivity” differential scanning calorimetry. *European Journal of Pharmaceutics and Biopharmaceutics*. 2016;104:260-70.
35. Schilt Y, Berman T, Wei X, Barenholz Y, Raviv U. Using solution X-ray scattering to determine the high-resolution structure and morphology of PEGylated liposomal doxorubicin nanodrugs. *Biochimica et Biophysica Acta (BBA) - General Subjects*. 2016;1860 (1, Part A):108-19.

36. Landesman-Milo D, Peer D. Altering the immune response with lipid-based nanoparticles. *Journal of controlled release : official journal of the Controlled Release Society*. 2012;161(2):600-8.
37. Watson DS, Endsley AN, Huang L. Design considerations for liposomal vaccines: Influence of formulation parameters on antibody and cell-mediated immune responses to liposome associated antigens. *Vaccine*. 2012;30(13):2256-72.
38. Doshi N, Mitragotri S. Macrophages recognize size and shape of their targets. *PLOS ONE*. 2010;5(4):e10051.
39. Champion JA, Mitragotri S. Shape induced inhibition of phagocytosis of polymer particles. *Pharmaceutical Research*. 2009;26(1):244-9.
40. Champion JA, Mitragotri S. Role of target geometry in phagocytosis. *Proceedings of the National Academy of Sciences of the United States of America*. 2006;103(13):4930.
41. Gratton SEA, Ropp PA, Pohlhaus PD, Luft JC, Madden VJ, Napier ME, et al. The effect of particle design on cellular internalization pathways. *Proceedings of the National Academy of Sciences*. 2008;105(33):11613.
42. Szebeni J, Bedőcs P, Rozsnyay Z, Weiszhar Z, Urbanics R, Rosivall L, et al. Liposome-induced complement activation and related cardiopulmonary distress in pigs: factors promoting reactogenicity of Doxil and AmBisome. *Nanomedicine: Nanotechnology, Biology and Medicine*. 2012;8(2):176-84.
43. Maruyama K, Ishida O, Takizawa T, Moribe K. Possibility of active targeting to tumor tissues with liposomes. *Advanced Drug Delivery Reviews*. 1999;40(1):89-102.
44. Eloy JO, Petrilli R, Trevizan LNF, Chorilli M. Immunoliposomes: A review on functionalization strategies and targets for drug delivery. *Colloids and Surfaces B: Biointerfaces*. 2017;159:454-67.
45. Mamot C, Drummond DC, Greiser U, Hong K, Kirpotin DB, Marks JD, et al. Epidermal growth factor receptor (EGFR)-targeted immunoliposomes mediate specific and efficient drug delivery to EGFR- and EGFRvIII-overexpressing tumor cells. *Cancer Research*. 2003;63(12):3154.
46. Mamot C, Ritschard R, Wicki A, Stehle G, Dieterle T, Bubendorf L, et al. Tolerability, safety, pharmacokinetics, and efficacy of doxorubicin-loaded anti-EGFR immunoliposomes in advanced solid tumours: a phase 1 dose-escalation study. *The Lancet Oncology*. 2012;13(12):1234-41.
47. Needham D, Park J-Y, Wright AM, Tong J. Materials characterization of the low temperature sensitive liposome (LTSL): effects of the lipid composition (lysolipid and

- DSPE-PEG2000) on the thermal transition and release of doxorubicin. *Faraday Discussions*. 2013;161(0):515-34.
48. Lencioni R, Cioni D. RFA plus lyso-thermosensitive liposomal doxorubicin: in search of the optimal approach to cure intermediate-size hepatocellular carcinoma. *Hepatic Oncology*. 2016;3(3):193-200.
49. Poon RT, Borys N. Lyso-thermosensitive liposomal doxorubicin: an adjuvant to increase the cure rate of radiofrequency ablation in liver cancer. *Future Oncology*. 2011;7(8):937-45.
50. Mohammed AR, Weston N, Coombes AGA, Fitzgerald M, Perrie Y. Liposome formulation of poorly water soluble drugs: optimisation of drug loading and ESEM analysis of stability. *International Journal of Pharmaceutics*. 2004;285(1):23-34.
51. Ali MH, Moghaddam B, Kirby DJ, Mohammed AR, Perrie Y. The role of lipid geometry in designing liposomes for the solubilisation of poorly water soluble drugs. *International Journal of Pharmaceutics*. 2013;453(1):225-32.
52. Yang T, Cui FD, Choi MK, Lin H, Chung SJ, Shim CK, et al. Liposome formulation of paclitaxel with enhanced solubility and stability. *Drug delivery*. 2007;14(5):301-8.
53. Tremblay C, Barza M, Szoka F, Lahav M, Baum J. Reduced toxicity of liposome-associated amphotericin B injected intravitreally in rabbits. *Investigative ophthalmology & visual science*. 1985;26(5):711-8.
54. Mehta RT. Liposome encapsulation of clofazimine reduces toxicity in vitro and in vivo and improves therapeutic efficacy in the beige mouse model of disseminated *Mycobacterium avium-M. intracellulare* complex infection. *Antimicrobial agents and chemotherapy*. 1996;40(8):1893-902.
55. Gabizon A, Tzemach D, Mak L, Bronstein M, Horowitz AT. Dose dependency of pharmacokinetics and therapeutic efficacy of pegylated liposomal doxorubicin (DOXIL) in murine models. *Journal of drug targeting*. 2002;10(7):539-48.
56. Papahadjopoulos D, Allen TM, Gabizon A, Mayhew E, Matthay K, Huang SK, et al. Sterically stabilized liposomes: improvements in pharmacokinetics and antitumor therapeutic efficacy. *Proceedings of the National Academy of Sciences*. 1991;88(24):11460-4.
57. Newman MS, Colbern GT, Working PK, Engbers C, Amantea MA. Comparative pharmacokinetics, tissue distribution, and therapeutic effectiveness of cisplatin encapsulated in long-circulating, pegylated liposomes (SPI-077) in tumor-bearing mice. *Cancer Chemotherapy and Pharmacology*. 1999;43(1):1-7.

58. M.J. Hope KFW. Liposomal formulation of ciprofloxacin. In: Shek PN, editor. *Liposomes in Biomedical Applications*. New York: Harwood Academic Publishers; 1995. p. 121-34.
59. Cipolla D, Wu H, Gonda I, Chan HK. Aerosol performance and long-term stability of surfactant-associated liposomal ciprofloxacin formulations with modified encapsulation and release properties. *AAPS PharmSciTech*. 2014;15(5):1218-27.
60. Gubernator J. Active methods of drug loading into liposomes: recent strategies for stable drug entrapment and increased in vivo activity. *Expert opinion on drug delivery*. 2011;8(5):565-80.
61. Zucker D, Marcus D, Barenholz Y, Goldblum A. Liposome drugs' loading efficiency: A working model based on loading conditions and drug's physicochemical properties. *Journal of Controlled Release*. 2009;139(1):73-80.
62. Haran G, Cohen R, Bar LK, Barenholz Y. Transmembrane ammonium sulfate gradients in liposomes produce efficient and stable entrapment of amphipathic weak bases. *Biochimica et biophysica acta*. 1993;1151(2):201-15.
63. Fritze A, Hens F, Kimpfler A, Schubert R, Peschka-Süss R. Remote loading of doxorubicin into liposomes driven by a transmembrane phosphate gradient. *Biochimica et Biophysica Acta (BBA) - Biomembranes*. 2006;1758(10):1633-40.
64. Gubernator J, Chwastek G, Korycińska M, Stasiuk M, Grynkiewicz G, Lewrick F, et al. The encapsulation of idarubicin within liposomes using the novel EDTA ion gradient method ensures improved drug retention in vitro and in vivo. *Journal of Controlled Release*. 2010;146(1):68-75.
65. Yang Y, Ma Y, Wang S. A novel method to load topotecan into liposomes driven by a transmembrane NH<sub>4</sub>EDTA gradient. *European Journal of Pharmaceutics and Biopharmaceutics*. 2012;80(2):332-9.
66. Song Y, Huang Z, Song Y, Tian Q, Liu X, She Z, et al. The application of EDTA in drug delivery systems: doxorubicin liposomes loaded via NH<sub>4</sub>EDTA gradient. *International Journal of Nanomedicine*. 2014;9:3611-21.
67. Clerc S, Barenholz Y. Loading of amphipathic weak acids into liposomes in response to transmembrane calcium acetate gradients. *Biochimica et Biophysica Acta (BBA) - Biomembranes*. 1995;1240(2):257-65.
68. Fenske DB, Wong KF, Maurer E, Maurer N, Leenhouts JM, Boman N, et al. Ionophore-mediated uptake of ciprofloxacin and vincristine into large unilamellar vesicles

- exhibiting transmembrane ion gradients. *Biochimica et Biophysica Acta (BBA) - Biomembranes*. 1998;1414(1):188-204.
69. Cheung BCL, Sun THT, Leenhouts JM, Cullis PR. Loading of doxorubicin into liposomes by forming Mn<sup>2+</sup>-drug complexes. *Biochimica et Biophysica Acta (BBA) - Biomembranes*. 1998;1414(1):205-16.
70. Abraham SA, Edwards K, Karlsson G, Hudon N, Mayer LD, Bally MB. An evaluation of transmembrane ion gradient-mediated encapsulation of topotecan within liposomes. *Journal of Controlled Release*. 2004;96(3):449-61.
71. Taggar AS, Alnajim J, Anantha M, Thomas A, Webb M, Ramsay E, et al. Copper-topotecan complexation mediates drug accumulation into liposomes. *Journal of controlled release : official journal of the Controlled Release Society*. 2006;114(1):78-88.
72. Ramsay E, Alnajim J, Anantha M, Zastre J, Yan H, Webb M, et al. A novel liposomal irinotecan formulation with significant anti-tumour activity: Use of the divalent cation ionophore A23187 and copper-containing liposomes to improve drug retention. *European Journal of Pharmaceutics and Biopharmaceutics*. 2008;68(3):607-17.
73. Li C, Cui J, Li Y, Wang C, Li Y, Zhang L, et al. Copper ion-mediated liposomal encapsulation of mitoxantrone: The role of anions in drug loading, retention and release. *European Journal of Pharmaceutical Sciences*. 2008;34(4):333-44.
74. Cui J, Li C, Wang L, Wang C, Yang H, Li Y, et al. Ni<sup>2+</sup>-mediated mitoxantrone encapsulation: Improved efficacy of fast release formulation. *International Journal of Pharmaceutics*. 2009;368(1):24-30.
75. Hood RR, Vreeland WN, DeVoe DL. Microfluidic remote loading for rapid single-step liposomal drug preparation. *Lab on a Chip*. 2014;14(17):3359-67.
76. Castile JD, Taylor KMG. Factors affecting the size distribution of liposomes produced by freeze-thaw extrusion. *International Journal of Pharmaceutics*. 1999;188(1):87-95.
77. Hope MJ, Bally MB, Webb G, Cullis PR. Production of large unilamellar vesicles by a rapid extrusion procedure. Characterization of size distribution, trapped volume and ability to maintain a membrane potential. *Biochimica et Biophysica Acta (BBA) - Biomembranes*. 1985;812(1):55-65.
78. Mayer LD, Hope MJ, Cullis PR, Janoff AS. Solute distributions and trapping efficiencies observed in freeze-thawed multilamellar vesicles. *Biochimica et Biophysica Acta (BBA) - Biomembranes*. 1985;817(1):193-6.

79. Mayer LD, Hope MJ, Cullis PR. Vesicles of variable sizes produced by a rapid extrusion procedure. *Biochimica et Biophysica Acta (BBA) - Biomembranes*. 1986;858(1):161-8.
80. Ozer Y, Talsma H, Crommelin DJA, Hincal AA. Influence of freezing and freeze-drying on the stability of liposomes dispersed in aqueous media. *Acta Pharmaceutica Technologica*. 1988;34(3):129-39.
81. Callow RA, McGrath JJ. Thermodynamic modeling and cryomicroscopy of cell-size, unilamellar, and paucilamellar liposomes. *Cryobiology*. 1985;22(3):251-67.
82. Cipolla D, Wu H, Salentinig S, Boyd B, Rades T, Vanhecke D, et al. Formation of drug nanocrystals under nanoconfinement afforded by liposomes. *RSC Advances*. 2016;6(8):6223-33.
83. Mayer LD, Bally MB, Hope MJ, Cullis PR. Techniques for encapsulating bioactive agents into liposomes. *Chemistry and Physics of Lipids*. 1986;40(2):333-45.
84. Cullis PR, Mayer LD, Bally MB, Madden TD, Hope MJ. Generating and loading of liposomal systems for drug-delivery applications. *Advanced Drug Delivery Reviews*. 1989;3(3):267-82.
85. Lasic DD, Čeh B, Stuart MCA, Guo L, Frederik PM, Barenholz Y. Transmembrane gradient driven phase transitions within vesicles: lessons for drug delivery. *Biochimica et Biophysica Acta (BBA) - Biomembranes*. 1995;1239(2):145-56.
86. Barenholz Y. Amphipathic weak base loading into preformed liposomes having a transmembrane ammonium ion gradient: from the bench to approved Doxil. 2006. 1-25
87. Lepault J, Pattus F, Martin N. Cryo-electron microscopy of artificial biological membranes. *Biochimica et Biophysica Acta (BBA) - Biomembranes*. 1985;820(2):315-8.
88. Grassucci RA, Taylor DJ, Frank J. Preparation of macromolecular complexes for cryo-electron microscopy. *Nature protocols*. 2007;2(12):3239-46.
89. Almgren M, Edwards K, Karlsson G. Cryo transmission electron microscopy of liposomes and related structures. *Colloids and Surfaces A: Physicochemical and Engineering Aspects*. 2000;174(1):3-21.
90. Frederik PM, Hubert DHW. Cryoelectron microscopy of liposomes. *Methods in Enzymology*. 391: Academic Press; 2005. p. 431-48.
91. Placzek M, Kosela M. Microscopic methods in analysis of submicron phospholipid dispersions. *Acta pharmaceutica*. 2016;66(1):1-22.
92. Lengyel J, Milne JLS, Subramaniam S. Electron tomography in nanoparticle imaging and analysis. *Nanomedicine*. 2008;3(1):125-31.

93. Pabst G, Rappolt M, Amenitsch H, Laggner P. Structural information from multilamellar liposomes at full hydration: full q-range fitting with high quality x-ray data. *Physical review E, Statistical physics, plasmas, fluids, and related interdisciplinary topics*. 2000;62(3 Pt B):4000-9.
94. Rappolt M. Bilayer thickness estimations with “poor” diffraction data. *Journal of Applied Physics*. 2010;107(8):084701.
95. Wibroe PP, Ahmadvand D, Oghabian MA, Yaghmur A, Moghimi SM. An integrated assessment of morphology, size, and complement activation of the PEGylated liposomal doxorubicin products Doxil®, Caelyx®, DOXOrubicin, and SinaDoxosome. *Journal of Controlled Release*. 2016;221:1-8.
96. Chiu MH, Prenner EJ. Differential scanning calorimetry: An invaluable tool for a detailed thermodynamic characterization of macromolecules and their interactions. *Journal of Pharmacy and Bioallied Sciences*. 2011;3(1):39-59.
97. Bunjes H, Unruh T. Characterization of lipid nanoparticles by differential scanning calorimetry, X-ray and neutron scattering. *Advanced Drug Delivery Reviews*. 2007;59(6):379-402.
98. Chogale MM, Ghodake VN, Patravale VB. Performance parameters and characterizations of nanocrystals: A brief review. *Pharmaceutics*. 2016;8(3):26.
99. Biltonen RL, Lichtenberg D. The use of differential scanning calorimetry as a tool to characterize liposome preparations. *Chemistry and Physics of Lipids*. 1993;64(1):129-42.
100. Demetzos C. Differential Scanning Calorimetry (DSC): A tool to study the thermal behavior of lipid bilayers and liposomal stability. *Journal of Liposome Research*. 2008;18(3):159-73.
101. Yu L. Amorphous pharmaceutical solids: preparation, characterization and stabilization. *Advanced Drug Delivery Reviews*. 2001;48(1):27-42.
102. Giron D. Thermal analysis and calorimetric methods in the characterisation of polymorphs and solvates. *Thermochimica Acta*. 1995;248:1-59.
103. Wei X, Shamrakov D, Nudelman S, Peretz-Damari S, Nativ-Roth E, Regev O, et al. Cardinal role of intraliposome doxorubicin-sulfate nanorod crystal in doxil properties and performance. *ACS Omega*. 2018;3(3):2508-17.
104. Peleg-Shulman T, Gibson D, Cohen R, Abra R, Barenholz Y. Characterization of sterically stabilized cisplatin liposomes by nuclear magnetic resonance. *Biochimica et Biophysica Acta (BBA) - Biomembranes*. 2001;1510(1):278-91.

105. Maurer N, Wong KF, Hope MJ, Cullis PR. Anomalous solubility behavior of the antibiotic ciprofloxacin encapsulated in liposomes: a <sup>1</sup>H-NMR study. *Biochimica et Biophysica Acta (BBA) - Biomembranes*. 1998;1374(1):9-20.
106. Arčon I, Kodre A, Abra RM, Huang A, Vallner JJ, Lasič DD. EXAFS study of liposome-encapsulated cisplatin. *Colloids and Surfaces B: Biointerfaces*. 2004;33(3):199-204.
107. Abraham SA, Edwards K, Karlsson G, MacIntosh S, Mayer LD, McKenzie C, et al. Formation of transition metal–doxorubicin complexes inside liposomes. *Biochimica et Biophysica Acta (BBA) - Biomembranes*. 2002;1565(1):41-54.
108. Dicko A, Kwak S, Frazier AA, Mayer LD, Liboiron BD. Biophysical characterization of a liposomal formulation of cytarabine and daunorubicin. *International Journal of Pharmaceutics*. 2010;391(1):248-59.
109. Zucker D, Andriyanov AV, Steiner A, Raviv U, Barenholz Y. Characterization of PEGylated nanoliposomes co-remotely loaded with topotecan and vincristine: relating structure and pharmacokinetics to therapeutic efficacy. *Journal of Controlled Release*. 2012;160(2):281-9.
110. Straubinger RM, Balasubramanian SV. Preparation and characterization of taxane-containing liposomes. *Methods in Enzymology*. 391: Academic Press; 2005. p. 97-117.
111. Siligardi G, Hussain R, Patching SG, Phillips-Jones MK. Ligand- and drug-binding studies of membrane proteins revealed through circular dichroism spectroscopy. *Biochimica et Biophysica Acta (BBA) - Biomembranes*. 2014;1838(1, Part A):34-42.
112. Rezhdo O, Speciner L, Carrier RL. Lipid-associated Oral Delivery: Mechanisms and Analysis of Oral Absorption Enhancement. *Journal of controlled release : official journal of the Controlled Release Society*. 2016;240:544-60.
113. Yano J, Yachandra VK. X-ray absorption spectroscopy. *Photosynthesis Research*. 2009;102(2-3):241-54.
114. Lasic DD, Frederik PM, Stuart MCA, Barenholz Y, McIntosh TJ. Gelation of liposome interior A novel method for drug encapsulation. *FEBS Letters*. 1992;312(2):255-8.
115. AusPAR attachment 1: Product information for Irinotecan (as sucrosfate). In: Health Do, editor.: *Therapeutic Goods Administration*; 2017.
116. Drummond DC, Noble CO, Guo Z, Hong K, Park JW, Kirpotin DB. Development of a highly active nanoliposomal irinotecan using a novel intraliposomal stabilization strategy. *Cancer Res*. 2006;66(6):3271-7.

117. Tardi P, Johnstone S, Harasym N, Xie S, Harasym T, Zisman N, et al. In vivo maintenance of synergistic cytarabine:daunorubicin ratios greatly enhances therapeutic efficacy. *Leukemia Research*. 2009;33(1):129-39.
118. Landon CD, Park J-Y, Needham D, Dewhirst MW. Nanoscale drug delivery and hyperthermia: The materials design and preclinical and clinical testing of low temperature-sensitive liposomes used in combination with mild hyperthermia in the treatment of local cancer. *The open nanomedicine journal*. 2011;3:38-64.
119. Chiu GNC, Abraham SA, Ickenstein LM, Ng R, Karlsson G, Edwards K, et al. Encapsulation of doxorubicin into thermosensitive liposomes via complexation with the transition metal manganese. *Journal of Controlled Release*. 2005;104(2):271-88.
120. Andriyanov AV, Koren E, Barenholz Y, Goldberg SN. Therapeutic efficacy of combining PEGylated liposomal doxorubicin and radiofrequency (RF) ablation: Comparison between slow-drug-releasing, non-thermosensitive and fast-drug-releasing, thermosensitive nano-liposomes. *PLOS ONE*. 2014;9(5):e92555.
121. Cipolla D, Blanchard J, Gonda I. Development of liposomal ciprofloxacin to treat lung infections. *Pharmaceutics*. 2016;8(1):6.
122. Cipolla D, Wu H, Eastman S, Redelmeier T, Gonda I, Chan HK. Tuning ciprofloxacin release profiles from liposomally encapsulated nanocrystalline drug. *Pharmaceutical Research*. 2016;33(11):2748-62.
123. Gaillard PJ, Appeldoorn CCM, Dorland R, van Kregten J, Manca F, Vugts DJ, et al. Pharmacokinetics, brain delivery, and efficacy in brain tumor-bearing mice of glutathione pegylated liposomal doxorubicin (2B3-101). *PLoS ONE*. 2014;9:e82331.
124. Rip J, Chen L, Hartman R, van den Heuvel A, Reijerkerk A, van Kregten J, et al. Glutathione PEGylated liposomes: pharmacokinetics and delivery of cargo across the blood–brain barrier in rats. *Journal of Drug Targeting*. 2014;22(5):460-7.
125. Semple SC, Leone R, Wang J, Leng EC, Klimuk SK, Eisenhardt ML, et al. Optimization and characterization of a sphingomyelin/cholesterol liposome formulation of vinorelbine with promising antitumor activity. *Journal of Pharmaceutical Sciences*. 2005;94(5):1024-38.
126. Zhigaltsev IV, Maurer N, Akhong Q-F, Leone R, Leng E, Wang J, et al. Liposome-encapsulated vincristine, vinblastine and vinorelbine: A comparative study of drug loading and retention. *Journal of Controlled Release*. 2005;104(1):103-11.
127. Johnston MJW, Semple SC, Klimuk SK, Edwards K, Eisenhardt ML, Leng EC, et al. Therapeutically optimized rates of drug release can be achieved by varying the drug-to-

- lipid ratio in liposomal vincristine formulations. *Biochimica et Biophysica Acta (BBA) - Biomembranes*. 2006;1758(1):55-64.
128. Johnston MJ, Edwards K, Karlsson G, Cullis PR. Influence of drug-to-lipid ratio on drug release properties and liposome integrity in liposomal doxorubicin formulations. *Journal of liposome research*. 2008;18(2):145-57.
129. Chernov L, Deyell RJ, Anantha M, Dos Santos N, Gilabert-Oriol R, Bally MB. Optimization of liposomal topotecan for use in treating neuroblastoma. *Cancer Medicine*. 2017;6(6):1240-54.
130. Gubernator J, Lipka D, Korycińska M, Kempieńska K, Milczarek M, Wietrzyk J, et al. Efficient human breast cancer xenograft regression after a single treatment with a novel liposomal formulation of epirubicin prepared using the EDTA ion gradient method. *PLOS ONE*. 2014;9(3):e91487.
131. Zhigaltsev IV, Maurer N, Edwards K, Karlsson G, Cullis PR. Formation of drug-arylsulfonate complexes inside liposomes: A novel approach to improve drug retention. *Journal of Controlled Release*. 2006;110(2):378-86.
132. Pedrosa LRC, ten Hagen TLM, Süß R, van Hell A, Eggermont AMM, Verheij M, et al. Short-chain glycosphingolipids promote intracellular mitoxantrone delivery from novel nanoliposomes into breast cancer cells. *Pharmaceutical Research*. 2015;32(4):1354-67.
133. Mayer LD, Bally MB, Loughrey H, Masin D, Cullis PR. Liposomal vincristine preparations which exhibit decreased drug toxicity and increased activity against murine L1210 and P388 tumors. *Cancer Research*. 1990;50(3):575.
134. Hertzberg RP, Caranfa MJ, Hecht SM. On the mechanism of topoisomerase I inhibition by camptothecin: evidence for binding to an enzyme-DNA complex. *Biochemistry*. 1989;28(11):4629-38.
135. Fassberg J, Stella VJ. A kinetic and mechanistic study of the hydrolysis of camptothecin and some analogues. *Journal of Pharmaceutical Sciences*. 1992;81(7):676-84.
136. Burke TG, Gao X. Stabilization of topotecan in low pH liposomes composed of distearoylphosphatidylcholine. *Journal of Pharmaceutical Sciences*. 1994;83(7):967-9.
137. Tardi P, Choice E, Masin D, Redelmeier T, Bally M, Madden TD. Liposomal encapsulation of topotecan enhances anticancer efficacy in murine and human xenograft models. *Cancer Research*. 2000;60(13):3389.

138. Zucker D, Barenholz Y. Optimization of vincristine–topotecan combination — Paving the way for improved chemotherapy regimens by nanoliposomes. *Journal of Controlled Release*. 2010;146(3):326-33.
139. Xiang TX, Anderson BD. Influence of chain ordering on the selectivity of dipalmitoylphosphatidylcholine bilayer membranes for permeant size and shape. *Biophysical Journal*. 1998;75(6):2658-71.
140. Mitragotri S, Johnson ME, Blankschtein D, Langer R. An analysis of the size selectivity of solute partitioning, diffusion, and permeation across lipid bilayers. *Biophysical Journal*. 1999;77(3):1268-83.
141. Shen J, Burgess DJ. In vitro dissolution testing strategies for nanoparticulate drug delivery systems: Recent developments and challenges. *Drug delivery and translational research*. 2013;3(5):409-15.
142. Bhardwaj U, Burgess DJ. A novel USP apparatus 4 based release testing method for dispersed systems. *International Journal of Pharmaceutics*. 2010;388(1):287-94.
143. Fugit KD, Xiang TX, Choi DH, Kangarlou S, Cshai E, Bummer PM, et al. Mechanistic model and analysis of doxorubicin release from liposomal formulations. *Journal of Controlled Release*. 2015;217:82-91.
144. Moreno-Bautista G, Tam KC. Evaluation of dialysis membrane process for quantifying the in vitro drug-release from colloidal drug carriers. *Colloids and Surfaces A: Physicochemical and Engineering Aspects*. 2011;389(1):299-303.
145. Xiao C, Qi X, Maitani Y, Nagai T. Sustained release of cisplatin from multivesicular liposomes: Potentiation of antitumor efficacy against S180 murine carcinoma. *Journal of Pharmaceutical Sciences*. 2004;93(7):1718-24.
146. Cipolla D, Wu H, Eastman S, Redelmeier T, Gonda I, Chan HK. Development and characterization of an in vitro release assay for liposomal ciprofloxacin for inhalation. *Journal of Pharmaceutical Sciences*. 2014;103(1):314-27.
147. D'Souza S. A review of in vitro drug release test methods for nano-sized dosage forms. *Advances in Pharmaceutics*. 2014;2014:12.
148. Wallace SJ, Li J, Nation RL, Boyd BJ. Drug release from nanomedicines: selection of appropriate encapsulation and release methodology. *Drug Delivery and Translational Research*. 2012;2(4):284-92.
149. Yuan W, Kuai R, Dai Z, Yuan Y, Zheng N, Jiang W, et al. Development of a flow-through USP-4 apparatus drug release assay to evaluate doxorubicin liposomes. *The AAPS Journal*. 2017;19(1):150-60.

150. Csuhai E, Kangarlou S, Xiang TX, Ponta A, Bummer P, Choi D, et al. Determination of key parameters for a mechanism-based model to predict doxorubicin release from actively loaded liposomes. *Journal of Pharmaceutical Sciences*. 2015;104(3):1087-98.
151. Fugit KD, Anderson BD. The role of pH and ring-opening hydrolysis kinetics on liposomal release of topotecan. *Journal of Controlled Release*. 2014;174:88-97.
152. Fugit KD, Jyoti A, Upreti M, Anderson BD. Insights into accelerated liposomal release of topotecan in plasma monitored by a non-invasive fluorescence spectroscopic method. *Journal of Controlled Release*. 2015;197:10-9.
153. Russell LM, Hultz M, Searson PC. Leakage kinetics of the liposomal chemotherapeutic agent Doxil: The role of dissolution, protonation, and passive transport, and implications for mechanism of action. *Journal of Controlled Release*. 2018;269:171-6.
154. Junghanns JU, Müller RH. Nanocrystal technology, drug delivery and clinical applications. *International Journal of Nanomedicine*. 2008;3(3):295-310.
155. Noyes AA, Whitney WR. The rate of solution of solid substances in their own solutions. *Journal of the American Chemical Society*. 1897;19(12):930-4.
156. Porter CJ, Trevaskis NL, Charman WN. Lipids and lipid-based formulations: optimizing the oral delivery of lipophilic drugs. *Nature reviews Drug discovery*. 2007;6(3):231-48.
157. Schubert R, Beyer K, Wolburg H, Schmidt KH. Structural changes in membranes of large unilamellar vesicles after binding of sodium cholate. *Biochemistry*. 1986;25(18):5263-9.
158. Hildebrand A, Beyer K, Neubert R, Garidel P, Blume A. Solubilization of negatively charged DPPC/DPPG liposomes by bile salts. *Journal of Colloid and Interface Science*. 2004;279(2):559-71.
159. Anderson M, Omri A. The Effect of Different Lipid Components on the In Vitro Stability and Release Kinetics of Liposome Formulations. *Drug Delivery*. 2004;11(1):33-9.
160. Nacka F, Cansell M, Entressangles B. In vitro behavior of marine lipid-based liposomes. Influence of pH, temperature, bile salts, and phospholipase A2. *Lipids*. 2001;36(1):35-42.
161. Khan J, Rades T, Boyd BJ. Lipid-based formulations can enable the model poorly water-soluble weakly basic drug cinnarizine to precipitate in an amorphous-salt form during in vitro digestion. *Molecular Pharmaceutics*. 2016;13(11):3783-93.
162. Hennenfent KL, Govindan R. Novel formulations of taxanes: a review. Old wine in a new bottle? *Annals of Oncology*. 2006;17(5):735-49.

163. Egbaria K, Weiner N. Liposomes as a topical drug delivery system. *Advanced Drug Delivery Reviews*. 1990;5(3):287-300.
164. Benson HAE. Transfersomes for transdermal drug delivery. *Expert Opinion on Drug Delivery*. 2006;3(6):727-37.
165. Cevc G. Transfersomes, liposomes and other lipid suspensions on the skin: permeation enhancement, vesicle penetration, and transdermal drug delivery. *Critical reviews in therapeutic drug carrier systems*. 1996;13(3-4):257-388.
166. Choi MJ, Maibach HI. Liposomes and niosomes as topical drug delivery systems. *Skin pharmacology and physiology*. 2005;18(5):209-19.
167. El Maghraby GM, Barry BW, Williams AC. Liposomes and skin: From drug delivery to model membranes. *European Journal of Pharmaceutical Sciences*. 2008;34(4):203-22.
168. Elsayed MMA, Abdallah OY, Naggar VF, Khalafallah NM. Lipid vesicles for skin delivery of drugs: Reviewing three decades of research. *International Journal of Pharmaceutics*. 2007;332(1):1-16.
169. Kirjavainen M, Monkkonen J, Saukkosaari M, Valjakka-Koskela R, Kiesvaara J, Urtti A. Phospholipids affect stratum corneum lipid bilayer fluidity and drug partitioning into the bilayers. *Journal of controlled release : official journal of the Controlled Release Society*. 1999;58(2):207-14.
170. Kirjavainen M, Urtti A, Jääskeläinen I, Marjukka Suhonen T, Paronen P, Valjakka-Koskela R, et al. Interaction of liposomes with human skin in vitro — The influence of lipid composition and structure. *Biochimica et Biophysica Acta (BBA) - Lipids and Lipid Metabolism*. 1996;1304(3):179-89.
171. Patel V, Sharma OP, Mehta T. Nanocrystal: a novel approach to overcome skin barriers for improved topical drug delivery. *Expert opinion on drug delivery*. 2018;15(4):351-68.
172. Hecq J, Deleers M, Fanara D, Vranckx H, Amighi K. Preparation and characterization of nanocrystals for solubility and dissolution rate enhancement of nifedipine. *International Journal of Pharmaceutics*. 2005;299(1):167-77.
173. Van Eerdenbrugh B, Vermant J, Martens JA, Froyen L, Humbeeck JV, Van den Mooter G, et al. Solubility increases associated with crystalline drug nanoparticles: methodologies and significance. *Molecular Pharmaceutics*. 2010;7(5):1858-70.
174. Bhol KC, Schechter PJ. Topical nanocrystalline silver cream suppresses inflammatory cytokines and induces apoptosis of inflammatory cells in a murine model of allergic contact dermatitis. *The British journal of dermatology*. 2005;152(6):1235-42.

175. Mitri K, Shegokar R, Gohla S, Anselmi C, Muller RH. Lutein nanocrystals as antioxidant formulation for oral and dermal delivery. *International journal of pharmaceutics*. 2011;420(1):141-6.



**Chapter 2: Solid state characterisation of ciprofloxacin  
liposome nanocrystals**

## Solid state characterisation of ciprofloxacin liposome nanocrystals

Tang Li,<sup>a,b</sup> Stephen Mudie,<sup>c</sup> David Cipolla,<sup>d</sup> Thomas Rades,<sup>e</sup> Ben J. Boyd<sup>a,b</sup>

<sup>a</sup> Drug Delivery, Disposition and Dynamics, Monash Institute of Pharmaceutical Sciences, Monash University (Parkville Campus), 381 Royal Parade, Parkville, Victoria 3052, Australia

<sup>b</sup> ARC Centre of Excellence in Convergent Bio-Nano Science and Technology, Monash Institute of Pharmaceutical Sciences, Monash University, Parkville Campus, 381 Royal Parade, Parkville, Victoria 3052, Australia

<sup>c</sup> SAXS/WAXS beamline, Australian Synchrotron, Clayton, Victoria, Australia

<sup>d</sup> Insmmed Inc., 10 FINDERNE AVE., BUILDING 10, BRIDGEWATER, NEW JERSEY 08807-3365, UNITED STATES

<sup>e</sup> Department of Pharmacy, University of Copenhagen, Copenhagen 2100, Denmark

Published online: 29<sup>th</sup> November 2018

Citation: Mol. Pharmaceutics (2019) 166: 184-194

DOI: 10.1021/acs.molpharmaceut.8b00940

### Abstract

Liposomes have been widely researched as drug delivery systems; however the solid state form of drug inside the liposome, whether it is in solution or in a solid state, is often not studied. The solid state properties of the drug inside the liposomes are important, as they dictate the drug release behaviour when the liposomes come into contact with physiological fluid. Recently, a new approach of making liposomal ciprofloxacin nanocrystals was proposed by the use of an additional freeze-thawing step in the liposomal preparation method. This paper aims to determine the solid state properties of ciprofloxacin inside the liposomes after this additional freeze-thawing cycle using cryo-TEM, small angle X-ray scattering (SAXS) and cross polarised light microscopy (CPLM). Ciprofloxacin precipitated in the ciprofloxacin hydrate crystal form with a unit cell dimension of 16.7 Å. The nanocrystals also showed a phase transition at 93 °C, which represents dehydration of the hydrate crystals to the anhydrate form of ciprofloxacin, verified by temperature-dependent SAXS measurements. Furthermore, the dependence of the solid state form of the nanocrystals on pH was investigated *in situ* and it was shown

that the liposomal ciprofloxacin nanocrystals retained their crystalline form at pH 6-10. Understanding the solid state attributes of nanocrystals inside liposomes provides improved understanding of drug dissolution and release as well as opening avenues to new applications where the nano-sized crystals can provide a dissolution benefit.

#### KEYWORDS

Ciprofloxacin; small angle X-ray scattering; liposomes; nanocrystals; solid state; cryo-TEM

## 2.1 Introduction

Liposomes are lipid-based colloidal systems, comprised of one or more lipid bilayers with an internal aqueous core. Liposomal formulations have achieved tremendous success as drug delivery carriers because of their biocompatibility and versatility in encapsulating drugs with different physicochemical properties (1, 2). The first FDA approved nanomedicine was Doxil<sup>®</sup>, a PEGylated liposomal formulation of doxorubicin for the treatment of AIDS-related Kaposi's sarcoma, in 1995 (3, 4). Liposomal formulations of other drugs such as daunorubicin (5, 6), cytarabine (7), co-encapsulated daunorubicin and cytarabine (8, 9), vincristine (10), irinotecan (11-14), amphotericin B (15-17), verteporfin (18), morphine sulfate (19, 20) and bupivacaine (21) have also been approved for the treatment of various indications, with a number of other drugs such as ciprofloxacin (22), cisplatin (23) and paclitaxel (24) under clinical investigations. For cancer therapies, the liposomal formulations allowed for an increased delivery of drug to the tumour sites and reduced systemic toxicity resulting in less severe side effects compared to the free drug (25-28). For analgesic treatment, multivesicular liposomes (DepoFoam<sup>™</sup> technology) enable sustained drug delivery leading to extended periods of pain management with prolonged drug half-life and reduced systemic drug toxicity (29, 30).

The Doxil<sup>®</sup> formulation is a liposomal doxorubicin hydrochloride injection, where the drug has been actively loaded into liposomes using a transmembrane ammonium sulfate gradient (31). The sulfate anion inside the liposome is believed to cause the formation of doxorubicin sulfate nanocrystals (32, 33). The presence of the intraliposomal doxorubicin sulfate nanocrystals enables high drug loading and improved drug retention, thus increasing formulation stability (3). Another method has reported that aging asulacrine liposomes in the presence of glucose forms a "coffee bean"-like drug precipitate inside the liposome. The precipitate formation results in a 1.9 fold longer half-life *in vivo* compared to non-precipitated liposomal asulacrine (34). This highlights the relevance of the drug solid

state inside the liposome and its retention within the liposome and pharmacokinetics properties. Ciprofloxacin has been loaded into liposomes using the ammonium sulfate gradient method (35), but in contrast to doxorubicin the drug does not precipitate spontaneously inside the liposome. The drug is reported to be in the soluble form despite the intraliposomal ciprofloxacin concentration exceeding its solubility in the external phase by orders of magnitude (36). The absence of nanocrystals and the high non-crystalline drug concentration inside the liposome results in fast drug release in plasma (36, 37). Inspired by the potential to alter the pharmacokinetics of release, an approach to induce ciprofloxacin drug crystallisation within liposomes for pulmonary delivery was developed (38). *In situ* nanocrystallisation of ciprofloxacin within the interior of the liposome was achieved by an additional freeze-thawing cycle after ammonium sulfate loading of ciprofloxacin into the liposomes (38, 39). This process step allowed the conversion of the soluble drug into drug nanocrystals with the ice crystals inside the vesicles proposed to serve as nucleation sites for drug crystallisation. The formation of nanocrystals within liposomes also resulted in the deformation of the spherical vesicles to more ellipsoid-shaped particles to accommodate the growth of the drug nanocrystals inside the aqueous core of the liposomes (Figure 1).

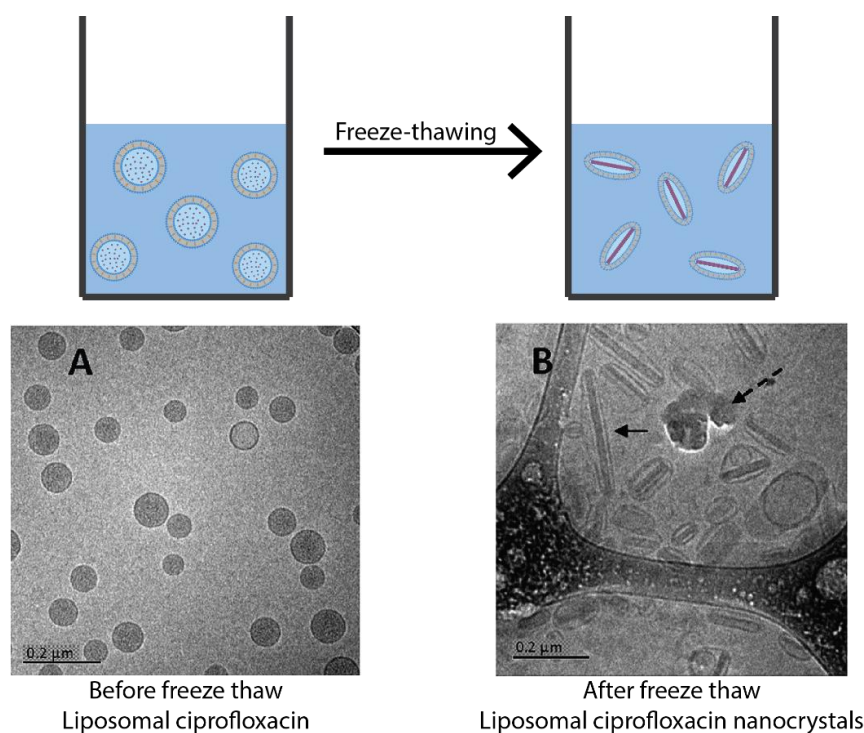


**Figure 1.** Schematics and cryo-TEM images of formation of liposomal ciprofloxacin nanocrystals from liposomal ciprofloxacin using the freeze-thawing preparation method. The cryo-TEM images

are adapted from (38) (The dashed arrow shown in panel B is an artefact produced during sample preparation).

The cryo-transmission electron microscopy (cryo-TEM) images of ciprofloxacin liposomes after freeze-thawing confirmed the presence of ciprofloxacin nanocrystals inside the liposomes (38). Small angle X-ray scattering (SAXS) was used to study the elongation of the liposome after freeze-thawing (38). SAXS has previously been used to study the solid state of doxorubicin sulfate nanocrystals encapsulated in liposomes (32, 33). Although the solid state of the ciprofloxacin precipitates is important in understanding drug solubility, dissolution and release rate, the solid state form of ciprofloxacin nanocrystals inside liposomes has not been investigated.

The liposomal nanocrystals would have a higher apparent surface area, where same volumes of nanocrystals are distributed in large number of smaller vesicles, therefore a larger total area. The liposomal bilayer encapsulating the drug nanocrystals consists of digestible phospholipids, meaning that such a formulation could be considered to be a type of lipid-based formulation. The fatty acids produced on digestion of the phospholipids are widely known to enhance drug absorption of poorly water-soluble drugs through solubilisation enhancement (40). In consideration of the high proportion of drugs in discovery programs that exhibit dissolution-rate-limited bioavailability, these properties could also be considered as advantageous for oral drug delivery applications.

Consequently, in this study we determined the solid state properties of the ciprofloxacin nanocrystals within the liposomes using cryo-TEM and SAXS. The thermotropic behaviour of the nanocrystals within the liposomal dispersion was also investigated using temperature-dependent SAXS. Previously, high sensitivity DSC was used to study the thermotropic behaviour of doxorubicin sulfate nanocrystals in the Doxil<sup>®</sup> formulation (41, 42). Although DSC can identify the thermotropic transitions of the nanocrystals, the crystal form during the transition cannot be elucidated. Hence, in this study, we used temperature-dependent SAXS to identify the crystal structure and the melting point of the ciprofloxacin nanocrystals within the liposomes. Furthermore, the solid state properties of the ciprofloxacin nanocrystals at different external pHs were investigated using pH-dependent SAXS measurements. This attribute will be important to understand for the potential application of liposomal nanocrystals in oral drug delivery since different pH environments exist throughout the gastrointestinal (GI) tract.

## 2.2 Hypotheses and aims

Hypotheses: That liposomal ciprofloxacin nanocrystals precipitated in a known crystalline form of the parent drug ciprofloxacin and that understanding the effect of pH on the solid state of the ciprofloxacin inside the liposome is relevant for its application in oral drug delivery.

In order to investigate these hypotheses, the following aims will be achieved:

1. To prepare liposomal ciprofloxacin nanocrystals using freeze-thawing and examine the presence of nanocrystals and confirm the nature of the solid state using cryo-TEM imaging and SAXS/WAXS.
2. To investigate the thermotropic behaviour and pH-dependent solid-state characteristics using SAXS/WAXS.

## 2.3 Experimental section

### 2.3.1 Materials

Ciprofloxacin liposomes (50 mg/mL) were kindly gifted by Aradigm Corporation (Hayward, CA, USA). Tris maleate (reagent grade), Triton X-100, ammonium sulfate (>99.0%), cholesterol (>99%) and sucrose (>99.5%) were purchased from Sigma Aldrich (St. Louis, MO, USA). Calcium chloride (>99%) and sodium hydroxide pellets (reagent grade) were obtained from Ajax Finechem (Seven Hills, NSW, Australia). Sodium chloride (>99%), ciprofloxacin hydrochloride monohydrate and ciprofloxacin were purchased from Chem Supply (Gillman, SA, Australia). Sodium azide was purchased from Merck Schuchardt OHG (Eduard-Buchner-Straße, Hohenbrunn, Germany). Hydrochloric acid 36% (analytical grade) was purchased from Biolab Aust Ltd (Clayton, VIC, Australia). Phospholipid (hydrogenated soy phosphatidylcholine (HSPC), >98%) was obtained from Lipoid GmbH (Ludwigshafen, Germany). The water used was sourced from a Millipore water purification system using a Quantum™ EX Ultrapure Organex cartridge (Millipore, Australia). Sodium hydroxide and hydrochloric acid were prepared as 1 M stock solutions and were used as pH adjustment solutions.

### 2.3.2 Sample preparation

Empty liposomes were prepared by dissolving hydrogenated soy phosphatidylcholine (HSPC) and cholesterol in a 7:3 (weight ratio) in chloroform. The mixtures were then dried

with nitrogen gas for 3 h, and residual solvent was removed by placing the sample under vacuum at 50 °C overnight. The dried lipid film was subsequently hydrated with 500 mM ammonium sulfate pH 3.0 solution to form a 10% w/w lipid dispersion and incubated at 70 °C in an oven for 30 min to heat the lipids above their transition temperature, followed by vortex-mixing to form a coarse dispersion (multilamellar liposomes). The lipid dispersion was then extruded 20 times through a 0.1 µm polycarbonate membrane filter (Nucleopore®, Whatman, USA) using an extruder (Avanti Polar Lipids Inc, Alabaster, USA) at 60 °C to generate unilamellar vesicles.

Ciprofloxacin liposomes gifted by Aradigm Corporation (Hayward, CA, USA) at 50 mg/mL were diluted 4-fold with 180 mg/mL sucrose in Tris buffer (50 mM Tris maleate, 5 mM CaCl<sub>2</sub>·2H<sub>2</sub>O, 150 mM NaCl, 6 mM sodium azide and adjusted to pH 6.0) to produce ciprofloxacin liposome dispersions containing drug at a concentration of 12.5 mg/mL. The prepared dispersions were transferred in 1 mL aliquots to 2 mL HPLC glass vials for the freeze-thawing cycle. The formulations were first snap frozen in liquid nitrogen and then stored in the -80 °C freezer for at least 2 days. The samples were then thawed in water at room temperature prior to conducting SAXS measurements. All experiments conducted on the liposomal ciprofloxacin nanocrystals were performed within 24 h after thawing. The choice of sucrose as the cryoprotectant at the above concentration for preparation of samples has been reported to provide best stability and least loss of encapsulated drug after the freeze-thaw process (38, 39).

In order to obtain higher signals for the solid state characterisation of drug inside the liposomal nanocrystal dispersion, higher concentrations of liposomal nanocrystal formulations were prepared by freeze-drying the freeze-thawed 12.5 mg/mL liposomal ciprofloxacin preparation and reconstitution in a smaller volume of buffer to formulate at 25 mg/mL. The liposomes were frozen in liquid nitrogen in 2 mL aliquots in 4 mL glass vials. The frozen samples were then placed in the freeze drier (VirTis Wizard 2.0 lyophiliser, SP scientific, NY, USA) pre-cooled to -40 °C shelf temperature. Primary drying was performed at a pressure of <12 mTorr, condenser temperature of -93 °C and shelf temperature of -40 °C for 48 hour followed by secondary drying at a pressure of <12 mTorr and shelf temperature of 25 °C for 12 h. The lyophilised liposome powders were redispersed in Tris buffer at a concentration of 25 mg/mL, i.e., double the concentration of the original preparation. These samples were used in both temperature-dependent and pH-dependent SAXS measurements to overcome the dilute nature of the flow through experiment and the

high background interference of the hot stage setup. Pellets were prepared by placing 200  $\mu\text{L}$  of the liposomal ciprofloxacin nanocrystal dispersion in a glass HPLC insert (6 x 31 mm, conical point, 250  $\mu\text{L}$  purchased from Sigma Aldrich) held within an Eppendorf tube and subjected to centrifugation at 7378 g for 1 min (Sigma 1-14 microfuge, Sigma Laborzentrifugen GmbH, Germany).

### 2.3.3 Cryogenic transmission electron microscopy (Cryo-TEM)

Samples were prepared for cryo-TEM using a laboratory-built humidity-controlled vitrification system, with humidity kept close to 80% for all experiments, and ambient temperature of 22 °C.

Copper grids (200 mesh) coated with perforated carbon film (Lacey carbon film: ProSciTech, Qld, Australia) were glow discharged in nitrogen gas to ensure a hydrophilic supporting substrate. An aliquot (4  $\mu\text{L}$ ) of the sample was pipetted onto each grid and allowed to adsorb for 30 s. Grids were blotted manually using Whatman 541 filter paper, for approximately 2 s. The blotting time was optimised for each sample. Grids were then plunged into liquid ethane cooled by liquid nitrogen. Frozen grids were stored in liquid nitrogen until required.

The samples were examined using a Gatan 626 cryoholder (Gatan, Pleasanton, CA, USA) and Tecnai 12 Transmission Electron Microscope (FEI, Eindhoven, The Netherlands) at an operating voltage of 120 kV. Low dose procedures were followed at all times using an electron dose of 8-10 electrons/ $\text{\AA}^2$  for imaging. Images were recorded using a FEI Eagle 4k x 4k CCD camera at magnifications ranging from 15 000x to 50 000x.

### 2.3.4 Solid state characterisation of the ciprofloxacin liposome nanocrystals in dispersion

Solid state characterisation was performed at the SAXS/WAXS beamline at the Australian Synchrotron. The X-ray beam had a wavelength of 0.954  $\text{\AA}$  (13.0 keV) and was calibrated using silver behenate to give a camera to detector distance of 571.9 mm, and a  $q$ -range of the magnitude of the scattering vector from 0.03 to 1.9  $\text{\AA}^{-1}$ . A 1-s acquisition period was used and the two-dimensional scattering patterns were acquired using a Pilatus 1 M detector with a pixel size of 172  $\mu\text{m}$ . The scattering patterns were then integrated into the one-dimensional scattering function  $I(q)$  vs.  $q$  using the ScatterBrain Analysis software. Identification of the drug solid state was determined from the positions of the diffraction peaks in the scattering function and compared to the published diffractograms of different crystalline forms of ciprofloxacin.

For all other static SAXS measurements, 200  $\mu\text{L}$  of the liposomal samples was transferred into the HPLC glass inserts. The samples were also centrifuged as described above to form a drug pellet from the dispersion. The glass inserts were then placed in a custom designed 3D printed holder that was inserted in a 96-well plate holder mounted in the X-ray beam.

### 2.3.5 Temperature-dependent SAXS measurements of the solid state of drug nanocrystals

Freeze-dried liposomal powders ( $\sim 10$  mg) were packed onto 22 x 22 mm glass cover slips (Scientific laboratory supplies Ltd, Nottingham, UK); the powder was hydrated with 2  $\mu\text{L}$  of Tris buffer, and the slides were sealed together with Kapton tape and taped onto an FP82HT hot stage (Mettler Toledo, VIC, Australia). The hot stage was vertically mounted onto a stage holder aligned with the X-ray beam and connected to a Mettler Toledo FP90 central processor. Heating scans were conducted from 30 to 170  $^{\circ}\text{C}$  at 10  $^{\circ}\text{C}/\text{min}$ . Scattering patterns were acquired using an automatic in-built scanner that acquires SAXS data simultaneously with an 11 s delay, which results in an approximately 2.5  $^{\circ}\text{C}$  temperature difference per scan.

### 2.3.6 pH-dependent SAXS measurements of the solid state of drug nanocrystals

The change in solid state of the liposomal ciprofloxacin nanocrystals with changes in pH was determined *in situ* using SAXS and was compared to the non-freeze-thawed ciprofloxacin liposomes.

Figure 2 depicts the setup of the flow-through pH titration configuration coupled with SAXS measurements. A thermostatted glass vessel (37  $^{\circ}\text{C}$ ) was connected to a magnetic stirrer with a mixing speed of 100 rpm and a glass pH electrode (iUnitrode) (Metrohm AG, Herisau, Switzerland). Tiamo 2.0 software was used to monitor the pH and temperature. A 15 mL aliquot of the liposomal dispersion was added to the glass beaker. A peristaltic pump was used to cycle the contents of the vessel through a 1.5-mm diameter quartz capillary aligned with the X-ray beam at approximately 10 mL/min. Before commencing the titration, the pH of the sample was adjusted to pH 1.0 using HCl (1 M) solution. NaOH (0.6 M) was loaded into a 10 mL syringe and delivered to the sample via a cannula using a remotely controlled syringe driver. Scattering patterns were acquired at increasing pH during the titration experiment.

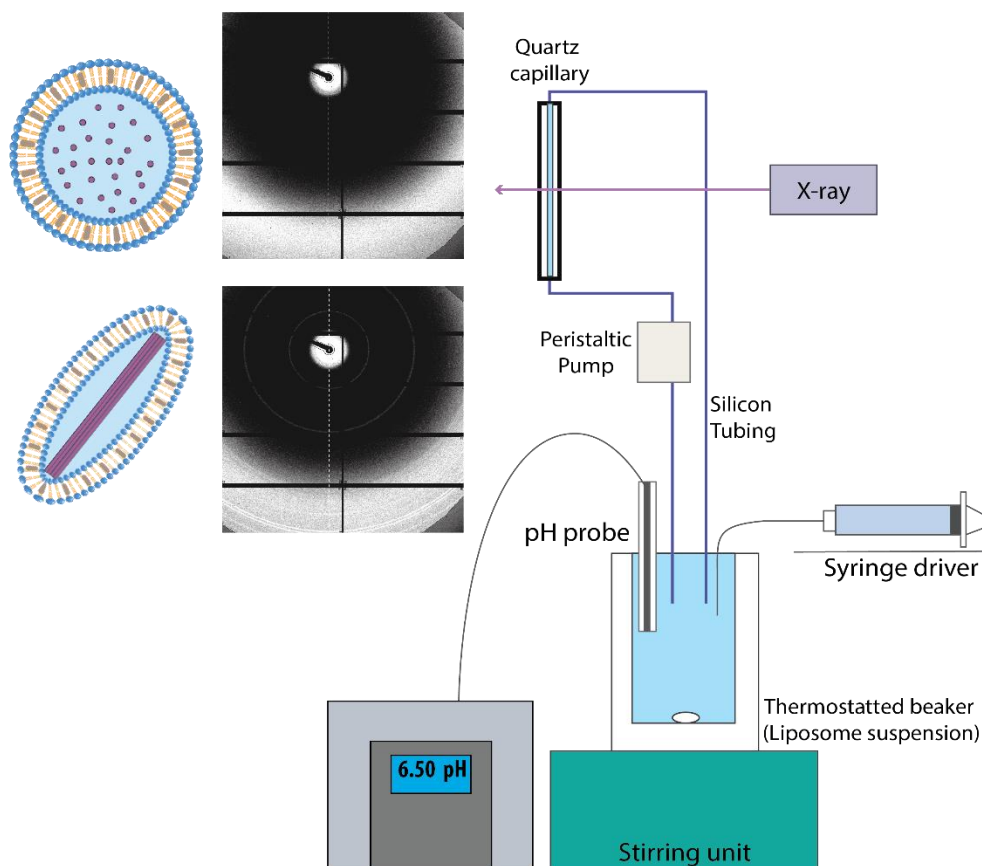


**Figure 2.** Experimental configuration for pH-dependent solid state determination using SAXS. Samples were magnetically stirred in a thermostatted beaker at 37 °C. The peristaltic pump circulated the aqueous sample through the quartz capillary in line with the X-ray beam. The pH probe recorded the pH of the sample and a NaOH (0.6 M) solution was delivered into the sample using a syringe driver to increase the pH. SAXS measurements were acquired at increasing pH with an equilibration time of 5 min at each measurement level. Images are representative SAXS detector views of liposomes containing drug in solution (top left), or as nanocrystals (bottom left).

## 2.4 Results and Discussion

### 2.4.1 Morphology of liposomal nanocrystals

Cryo-TEM images were captured to confirm the formation of ciprofloxacin nanocrystals inside the liposomes before and after the freeze-thawing cycle for the commercial ciprofloxacin liposomes (Figure 3a, b respectively). The rod-like drug crystals were only observed within the aqueous core of the ciprofloxacin liposome after the freeze-thawing cycle and not in the surrounding medium (Figure 3b), with the majority of the nanocrystals present as one crystal per liposome, consistent with previous studies (38,

39). The nanocrystals were located in the centre of the liposome with both ends touching the internal edge of the bilayer. The size of the nanocrystals was on average 140 nm in length and 30 nm in width. Due to the high aspect ratio of the nanocrystals formed, the growth of the ciprofloxacin crystal stretched the liposomes longitudinally forming “rugby ball”-shaped particles. This suggests that the liposomal bilayer, containing hydrogenated soy phosphatidylcholine and cholesterol in a 7:3 weight ratio, was capable of stretching and deforming its shape in order to accommodate the growth of the drug nanocrystals within the aqueous core.

The growth of nanocrystals inside liposomes is not a new phenomenon; other drugs such as doxorubicin (32, 33, 41) and topotecan (43) have been reported to precipitate as nanocrystals inside the liposome (44). Apart from drug crystallisation inducing liposome deformation, rod-shaped microtubules formed through tubulin polymerisation inside the aqueous core of giant liposomes have also been reported (45). The microtubules transformed the spherical liposomes first into rugby ball-shaped and then bipolar-shaped liposomes. The transformation in shape did not alter the overall surface area of the liposome; however, the volume was decreased. One proposed mechanism for the ability of the liposomes to form tubular structures is the translocation of lipid molecules from the spherical portion to the tubular portion of the liposome rather than an elastic expansion of the membrane. Elongation of the microtubule inside the liposome provides a mechanical force resulting in increased bending energy in the membrane which increases curvature (45). It has also been proposed that the liposome can transform into the rugby ball-shapes when the internal pressure is higher than the extra-liposomal pressure (46).

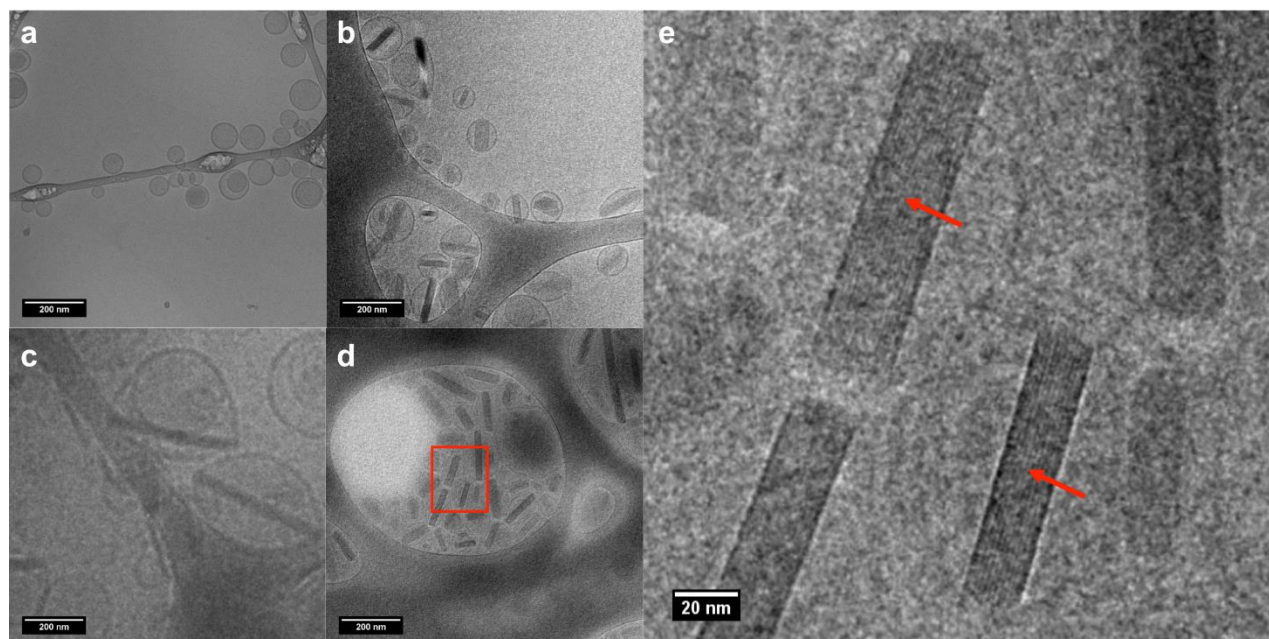


**Figure 3.** Cryo-TEM images of ciprofloxacin liposome dispersions, a) Ciprofloxacin liposomes before freeze-thawing. b) Ciprofloxacin liposome after freeze-thawing, ciprofloxacin formed high aspect ratio rod-like nanocrystals inside the liposome. c) Freeze-dried ciprofloxacin liposome nanocrystals redispersed in Tris buffer. d) Redispersed pelletized ciprofloxacin liposome nanocrystals (to increase the concentration of particles). e) Magnified nanocrystals, with the red arrows indicating the crystal lattice structure of the ciprofloxacin nanocrystals.

The freeze-dried liposomal ciprofloxacin nanocrystals that were redispersed in Tris buffer (Figure 3c) appeared similar in shape and size to the freeze-thawed liposomes. Liposomal ciprofloxacin nanocrystals were also centrifuged in a glass insert to concentrate the nanocrystals for SAXS studies (described in the next section) to improve the detection sensitivity over non-centrifuged dispersions. The cryo-TEM images acquired for the reconstituted liposome pellet (Figure 3d) confirm that the centrifugation step did not alter the formulation integrity and that the drug nanocrystals were still encapsulated by the liposomal bilayer. The sizes and morphologies of the nanocrystals and the liposomal vesicles after centrifugation appear the same as for the non-centrifuged liposomal nanocrystal dispersions. The section in the red box within Figure 3d is magnified and displayed as Figure 3e. Distinct crystal lattice planes embedded in the drug nanocrystals were observed. The interplanar distance of the lattice planes was measured to be approximately 16.67 Å. The presence of crystal lattice planes confirms that the ciprofloxacin forms a crystalline precipitate within the liposome after the freeze-thawing

process. To study the thermal behaviour of the ciprofloxacin nanocrystals and their pH-dependent solid state properties, reconstituted lyophilised liposomes were therefore used to improve sensitivity.

#### 2.4.2 Solid state characterisation of liposomal ciprofloxacin nanocrystals

To identify the crystal structure of the liposomal ciprofloxacin nanocrystals, static SAXS measurements were performed. Figure 4 shows the stacked SAXS scattering profiles for the liposomal ciprofloxacin nanocrystals after freeze-thawing. In Figure 4b, the scattering profile of the sample in dispersion without centrifugation showed several weak crystalline peaks with an identifiable peak at  $q = 0.46 \text{ \AA}^{-1}$  (equivalent to  $2\theta = 6.42^\circ$  at an X-ray wavelength of  $1.54 \text{ \AA}$ ). In order to improve the detection sensitivity allowing better resolution of the diffraction patterns, the scattering profile of the pellet from the centrifuged dispersion was acquired (Figure 4c). As mentioned in the previous section, this additional centrifugation step concentrated the sample and enabled determination of both the scattering from the liposome bilayers at  $q = 0.39$  and  $0.83 \text{ \AA}^{-1}$  and a better-resolved drug diffraction peak at  $q = 0.46 \text{ \AA}^{-1}$ .

The lyophilised liposomal ciprofloxacin nanocrystals were reconstituted in Tris buffer to double the concentration of the drug nanocrystals to  $25 \text{ mg/mL}$ . The scattering profiles shown in Figure 4d for the dispersion and Figure 4e for the pellets confirm that the nanocrystals are in the same crystalline form as in the non-lyophilised samples. The higher concentration of drug nanocrystals increased the intensity of the scattering profiles compared to that of  $12.5 \text{ mg/mL}$  non-lyophilised sample.

The acquired scattering profiles for the liposomal ciprofloxacin nanocrystals were compared to a range of published ciprofloxacin crystal structures in the Cambridge Crystallographic Data Centre. All the scattering profiles were identical to the diffraction profile of the ciprofloxacin hydrate form (CCDC-822709 (47)). Revisiting the interplanar distance of  $\sim 16.67 \text{ \AA}$  calculated from the cryo-TEM image in Figure 3e, the results correlated closely to the  $c = 16.55 \text{ \AA}$  unit cell dimension reported for the ciprofloxacin hydrate (47). The ciprofloxacin hydrate crystal exhibits a triclinic crystal system with the  $P1$  space group. The structure of the hydrate consists of three 1D supramolecular chains formed by the hydrogen bonding interactions of the zwitterionic functional groups of ciprofloxacin. There are 29 water clusters distributed in a globular type fashion along the  $[100]$  direction trapped inside the void within the supramolecular framework (47).

The mechanism of precipitation for ciprofloxacin inside the liposome upon freeze-thawing is not yet established. During the cryo-TEM study, the liposomes are snap frozen and kept at a temperature below  $-170\text{ }^{\circ}\text{C}$ . The ciprofloxacin liposomes that were not freeze-thawed did not show any ciprofloxacin crystals inside the liposome during cryo-TEM imaging. This suggests that the crystal formation (and growth) occurs during the thawing of the frozen liposome. A previous study showed that ciprofloxacin loading using an ammonium sulfate active loading approach, resulted in high drug accumulation inside the liposomes with the ciprofloxacin concentration inside the liposomes exceeding  $250\text{ mM}$  (excessively beyond its saturation solubility) (36). Therefore the ciprofloxacin inside the liposome is already in a supersaturated state. During the freezing of the ciprofloxacin liposomes, as the temperature decreases, ciprofloxacin inside the liposomes will become more supersaturated. The classical nucleation theory could potentially explain the phenomenon. Also the intraliposomal water should crystallise around  $-45\text{ }^{\circ}\text{C}$  (38, 39), and the presence of ice crystals could be serving as a seed crystal for the nucleation of the drug crystals. During the warming of the frozen liposomes, the intraliposomal water starts to melt and rearrange itself into water clusters bound inside the voids of the ciprofloxacin stacks forming the ciprofloxacin hydrate crystals. Another reason why freeze-thawing could have induced the precipitation, apart from the effect of ice nucleation, is that the extraliposomal ice formed at around  $-20\text{ }^{\circ}\text{C}$  could generate osmotic forces that induce water evacuation from the liposomes (48, 49). This would further increase the supersaturation of ciprofloxacin inside the liposome making it more prone to nucleation. The prenucleation cluster theory could also be a possible mechanism in this case, where the drug dissolved forms stable prenucleation clusters, which are thermodynamically stable solutes. The clusters would aggregate to form amorphous intermediates, and eventually solidify to form nanocrystals (50).

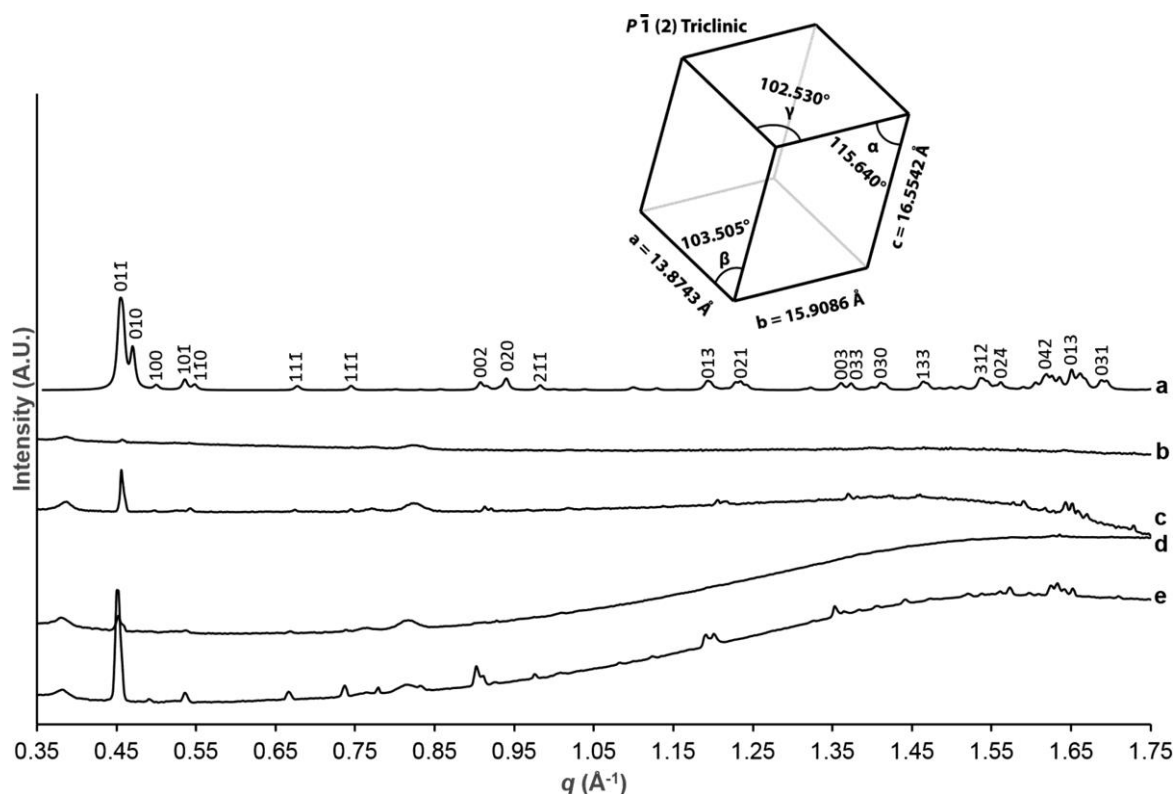


**Figure 4.** Stacked scattering pattern of a) Ciprofloxacin hydrate (Cambridge Crystallographic Data Centre reference- CCDC-822709). b) Liposomal ciprofloxacin nanocrystal dispersion at 12.5 mg/mL. c) Centrifuged pelleted liposome dispersion. d) Lyophilised liposomal ciprofloxacin nanocrystals redispersed in Tris buffer at 25 mg/mL. e) Lyophilised liposomal ciprofloxacin nanocrystals redispersed and pelletized in Tris buffer at 25 mg/mL. All liposomal ciprofloxacin nanocrystals were in a crystalline state and precipitated as the ciprofloxacin hydrate form with a signature peak at  $0.46 \text{ \AA}^{-1}$ . The illustration inset displays the unit cell dimension of the crystal of ciprofloxacin hydrate exhibiting a triclinic crystal system with space group  $P\bar{1}$ .

### 2.4.3 Temperature-dependent structure of ciprofloxacin hydrate nanocrystals within liposomes

The temperature-dependent structure of the ciprofloxacin hydrate nanocrystals within the ciprofloxacin liposomes formed after freeze-thawing were studied in the temperature-dependent SAXS. Stacked scattering profiles (Figure 5) were plotted from 30 to 110 °C at a heating rate of 10 °C/min. The temperature and heating rate were controlled by a hot stage for the lyophilised ciprofloxacin liposome samples hydrated with Tris buffer. SAXS profiles were acquired at fixed increasing temperatures. The ciprofloxacin hydrate crystalline peaks were observed from 30 to 93 °C. At 96 °C, the signature peak at  $q = 0.46$

$\text{\AA}^{-1}$  disappeared, and the samples were observed to be completely melted at 100 °C (Figure 5a). This melting point observed through the temperature-dependent SAXS study agrees well with the literature where the transformation from the hydrate to anhydrate form of ciprofloxacin was observed at 95 °C using variable temperature powder X-ray diffractometry (47). In another study, the dehydration of ciprofloxacin hydrate had an onset at  $91.8 \pm 0.1$  °C determined by DSC (51). The scattering from the crystallised liposomal drug nanocrystals showed liposomal peaks were present until 110 °C. The anhydrate ciprofloxacin base peaks inside the liposome are not observed on the hot stage SAXS. Hence the experiment was only conducted up to 110 °C to confirm the initial existence of ciprofloxacin hydrate crystals. Separate experiments for the melting of ciprofloxacin reference material were also conducted on temperature-dependent SAXS, CPLM, and DSC (supplementary data), and the ciprofloxacin anhydrate form showed a melting point in the range of 260 – 273.3 °C depending on the technique used. This agrees well with the literature value for ciprofloxacin melting at 268.3 °C (52). The temperature-dependent SAXS for ciprofloxacin anhydrate showed relatively low intensity peaks even for pure crystalline drug powder (Figure S3). Given that the nanocrystals inside the liposomes are in a dispersion and are nanosized, it is possible that the crystals are present but not detected due to sensitivity limitations. With the freeze-dried liposomal ciprofloxacin nanocrystals, It should also be noted that a CPLM study showed that the freeze-dried liposomes started to melt at 170 °C and decomposed above 180 °C. This means that even if the ciprofloxacin anhydrate form was detectable, the melting of the anhydrate may not be observable, as the liposome would have decomposed before the melting of ciprofloxacin.

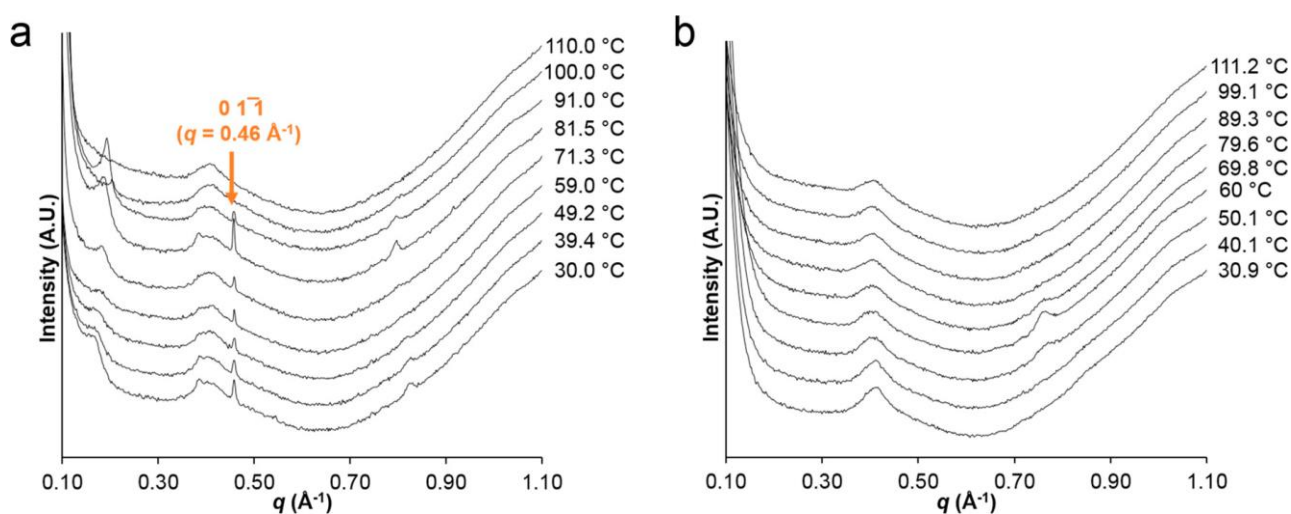


**Figure 5.** a) Temperature-dependent SAXS scattering profiles of liposomal ciprofloxacin nanocrystals. The peak indicating ciprofloxacin hydrate at  $q = 0.46 \text{ \AA}^{-1}$  (diffraction from plane  $0\ 1\bar{1}$ ) was observed from 30 to 93 °C. b) Temperature-dependent SAXS scattering profiles of control, non-crystallised ciprofloxacin liposomes. (The hump observed in both ciprofloxacin liposome nanocrystals and non-freeze-thaw ciprofloxacin liposomes at  $q = 0.40 \text{ \AA}^{-1}$  is background scattering from the Kapton tape on the glass coverslip).

The control formulation, i.e., the non-freeze-thawed ciprofloxacin liposome formulation, did not show any crystallinity in the scattering profiles throughout the same temperature scan (Figure 5b), which agrees well with the cryo-TEM results where no nanocrystals were observed and the ciprofloxacin was apparently dissolved in solution.

#### 2.4.4 Effect of pH on the solid state of the ciprofloxacin nanocrystals upon dissolution

The pH-dependent solid state analysis of the ciprofloxacin liposomes with and without nanocrystals was monitored on increasing pH using the flow-through SAXS setup (Figure 2). This setup allows the determination of the solid state of ciprofloxacin inside the liposomes *in situ* across a range of pH conditions. Small incremental changes in pH could be applied, as the nanocrystals did not need to be isolated as would be the case with regular X-ray diffraction measurements. This is useful to screen for any potential changes to the ciprofloxacin solid state inside the liposome, including any changes in polymorphic form under different pH conditions.

The low detection sensitivity of crystalline drug peaks in liposomal dispersions (as seen, e.g., in Figure 4b), together with the dilution effect upon titration with NaOH, meant that higher starting concentrations of ciprofloxacin liposome nanocrystals (25 mg/mL, e.g., equivalent concentration to the profile in Figure 4d) had to be used for the pH titration study with concurrent X-ray diffraction measurement in flow-through at 37 °C.

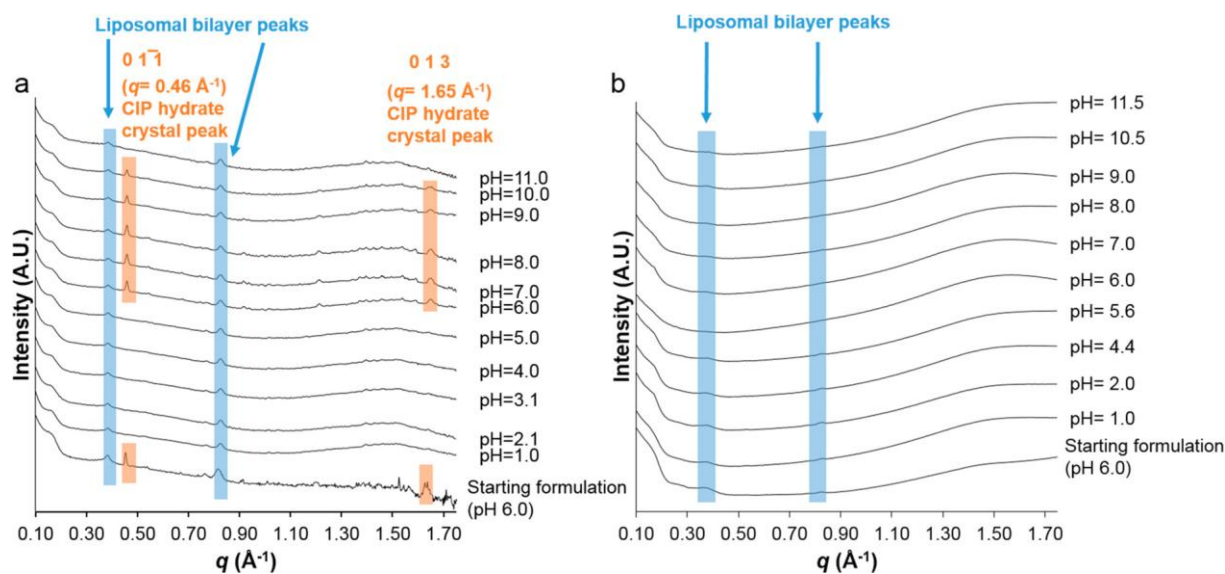


**Figure 6.** a) Effect of pH on the solid state characteristics of the liposomal ciprofloxacin nanocrystals from pH 1-11 determined using *in situ* pH-dependent SAXS measurements. Crystalline diffraction from the nanocrystals was observed at pH 6-10, apparent from the diffraction peaks at  $q = 0.46 \text{ \AA}^{-1}$  and  $1.65 \text{ \AA}^{-1}$  (annotated in orange, diffraction from plane  $0\ 1\bar{1}$  and  $0\ 1\ 3$ ). b) Effect of pH on the solid state of the ciprofloxacin liposome formulation without the freeze-thawing cycle from *in situ* pH-dependent SAXS measurements. Only lamellar peaks for the liposomal vesicles were identified, and there was no crystallinity observed throughout the pH range 1.0-11.5.

The diffraction profiles of the liposomal ciprofloxacin nanocrystals did not show any peaks attributable to drug between pH 1-5; however, the resolution of the scattering technique does not preclude the presence of smaller crystals still being present. At this pH range, only the lamellar peaks of the liposome bilayers were observed at  $q = 0.39$  and  $0.83 \text{ \AA}^{-1}$ . From pH 6-10, the lamellar peaks of the liposomes remained unchanged. However, crystalline peaks at  $q = 0.46$  and  $1.65 \text{ \AA}^{-1}$  were identified for the ciprofloxacin drug nanocrystals. These peaks correlate well with the diffraction profiles in Figure 4 and confirm that the ciprofloxacin drug nanocrystals were in the ciprofloxacin hydrate form within the liposomes. Above pH 10, the ciprofloxacin nanocrystals appeared to be amorphous or dissolved, as no crystalline drug peaks were observed. Throughout the experiment, there was no indication of other ciprofloxacin polymorphic forms present at the various pH conditions.

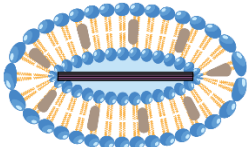
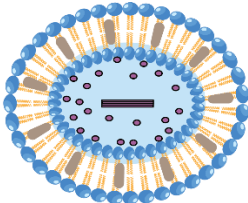
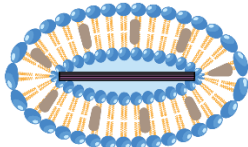
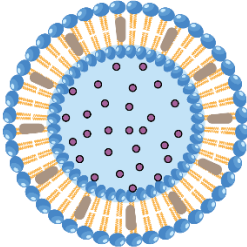
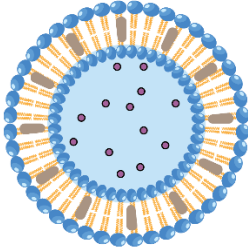
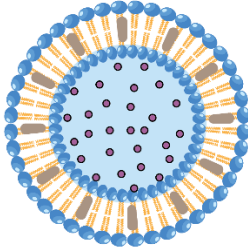
The presence of an intact bilayer supports the concept although ion exchange can happen through the bilayer, it is apparent that drug is not released. If there was a sufficiently high external drug concentration due to release, it would be expected that drug

would precipitate and form larger crystals, which would show highly ordered crystalline structures with an increase in the crystalline peak intensity. This was not observed in this study, suggesting the ciprofloxacin liposomes are capable of retaining encapsulated drug even in extreme pH conditions.

The non-freeze-thawed ciprofloxacin liposomes were also assessed for solid state changes at different pH using SAXS (Figure 6b). There was an absence of crystalline drug diffraction peaks throughout the pH range of 1.0-11.5, indicating that ciprofloxacin did not precipitate inside the liposomes, which agrees well with the cryo-TEM results (Figure 3) and previous literature (36). This result also suggests that the non-freeze-thawed ciprofloxacin was encapsulated within the liposomes throughout different pH conditions (similar to liposomal ciprofloxacin nanocrystals), since any significant drug leakage from the liposome would result in drug precipitation outside the liposome, and drug precipitation would be detected as crystalline peaks in the scattering profiles. Changes in the extraliposomal pH conditions did not alter the solid state of the dissolved drug within the liposome, even at neutral pH, where ciprofloxacin is believed to be uncharged with low solubility.

The ciprofloxacin molecular structure contains two ionisable functional groups with a piperazinyl secondary amine ( $pK_a = 8.74$ ) and a carboxylic acid ( $pK_a = 6.09$ ) (53). These physicochemical properties render it to be more water-soluble at  $pH < 6.09$  (35) and  $> 8.74$ . When the extraliposomal pH environment was below pH 6, only the piperazinyl amine would be ionised, increasing the water solubility of ciprofloxacin (52). From the stacked scattering profiles of liposomal ciprofloxacin nanocrystals, the crystalline peaks for the ciprofloxacin hydrate nanocrystals are not observed at pH 1-5, illustrated schematically in Figure 7. This can be explained by the increased solubility of ciprofloxacin at lower pH, which reduces the crystalline fraction of ciprofloxacin inside the liposomes. However, there could be still smaller nanocrystals inside the liposome, the concentration and size of which could be below the detection limit of the scattering technique. Ciprofloxacin inside the liposomal ciprofloxacin nanocrystal formulations was expected to be in a supersaturated state with respect to the outside when the pH is  $> 6$ . For the non-freeze-thawed ciprofloxacin liposome, the drug inside the liposome is in a supersaturated state with no indication of crystal formation. When the pH is  $< 6$ , the increase in solubility would reduce the supersaturation ratio, and when  $pH > 6$ , the supersaturation ratio is returned to the

original starting state. Hence, there is no change of solid state observed attributable to ciprofloxacin inside the control liposome formulation.

	Starting formulation	pH $\leq$ 5 (e.g. stomach)	pH 6-10 (e.g. small intestine)
Liposomal Ciprofloxacin Nanocrystals			
Liposomal Ciprofloxacin			

**Figure 7.** Schematic representation of the solid state form of liposomal ciprofloxacin at different pH for (top row) liposomal ciprofloxacin nanocrystals formed after freeze-thawing and (bottom row) non-crystallised liposomal ciprofloxacin. The freeze-thawed liposomal ciprofloxacin showed intraliposomal ciprofloxacin hydrate nanocrystals at pH 6-10, and solubility of the ciprofloxacin in the nanocrystals increased at pH 5 and below. For non-freeze-thawed liposomal ciprofloxacin, drug nanocrystals were not observed throughout the range of pH studied.

#### 2.4.5 Implications for the use of ciprofloxacin liposomal nanocrystals *in vivo*

For *in vivo* application of the liposomal ciprofloxacin nanocrystals, understanding the solid state of the ciprofloxacin nanocrystals inside the liposome *in situ* in different environments is important. When these drug delivery systems are exposed to body fluids, the changes in the solid state of the drug nanocrystals inside the liposomes at different pHs would affect the amount of free drug dissolved inside the liposome, which in turn would affect the rate and kinetics of drug release. A previous report suggested that drug release from liposomes bearing intraliposomal precipitates follows zero order kinetics, whereas solubilised drug inside the liposome follows first order kinetics (54). The formation of drug nanocrystals results in lower soluble drug concentrations within the liposomes,

which would be expected to reduce the rate of drug release across the lipid membrane barrier, and it may become zero order if the crystals dissolve at a faster rate than the drug being transported across the membrane, keeping the soluble concentration constant (55). As mentioned in the introduction, the liposomal nanocrystals have the advantage of the nano-sized drug particles with high surface area, as well as the potential benefits of a lipid-based formulation. These properties have the potential to improve the dissolution and solubilisation behaviour of the encapsulated drug. For oral applications of the liposomal drug nanocrystals, the rate-limiting step for drug absorption of most poorly soluble drugs is the dissolution rate of the crystals, for which in turn the intrinsic drug solubility is an important factor (56). As discussed above, the solubility of ciprofloxacin is greatly pH-dependent, and the pH of the GI fluids varies with the location within the GI tract and the pre and postprandial state. The fasted stomach fluids have a pH of 1-2 (56), and in the fed state, stomach pH can range from 2.7-6.4 (57), whereas the upper small intestine has a pH of 5-6.5, which in the fasted state is a higher pH than the fed state (56). Therefore, *in situ* analysis of the solid state of liposomal drug nanocrystals at different pHs using SAXS can be used to anticipate the dissolution rate from the liposomal carrier when the formulation is ingested orally. In the case of liposomal ciprofloxacin (Figure 7), the liposome with crystallised ciprofloxacin would potentially exhibit first order drug release kinetics in the stomach, since the drug is mostly dissolved with the possibility of smaller nanocrystals inside the liposomes. When the liposomes transit to the upper small intestine with the pH increasing to approximately 6.5, the drug nanocrystals are stable at this pH inside the liposome, which may present a dissolution profile with zero order drug release kinetics. For liposomal ciprofloxacin prepared without the freeze-thawing, there was no change in the solid state of the drug inside the liposome; hence the drug release kinetics would be unchanged throughout the GI tract.

## 2.5 Conclusion

Liposomal ciprofloxacin nanocrystals prepared using a freeze-thawing cycle resulted in precipitation inside the liposome as ciprofloxacin hydrate nanocrystals with a unit cell dimension of approximately 16.67 Å. The ciprofloxacin hydrate nanocrystals have a thermal transition point of 93 °C, which correlates to an apparent transformation from the hydrate form to the anhydrate form. Ciprofloxacin hydrate nanocrystals were only observed within the liposomes at an external pH of 6-10 for the freeze-thawed

ciprofloxacin liposomes and no pH induced polymorphic transformations were observed. This study also identified SAXS as a useful technique to study the solid state of nanocrystals in liposomes and dispersions. It is also a versatile platform to study the temperature- and pH-dependent behaviour of drug nanocrystals and liposome formulations in dispersion. It is important to understand how the drug in the nanoparticle formulation behaves under different pH conditions, as identification of potential changes in solid state properties are crucial in understanding changes in solubility and absorption of the drug *in vivo*.

## Conflict of Interest

At the time of these studies David Cipolla was an employee of Aradigm Corp. who supplied the liposomes studies in this manuscript.

## Acknowledgments

This study is funded under the Australian Research Council Centre of Excellence in Convergent Bio-Nano Science and Technology. SAXS studies were conducted on the SAXS/WAXS beamline at the Australian Synchrotron, Victoria, Australia. BB is the recipient of an ARC Future Fellowship. Cryo-TEM studies were conducted with assistance of Dr. Lynne Waddington at the CSIRO Materials Science and Engineering.

## Supporting information

### Methods

#### S.1 Temperature-dependent Cross Polarised Light Microscopy (CPLM)

Freeze dried liposomal ciprofloxacin nanocrystals powder (~10 mg) and hydrated ciprofloxacin powder (~10 mg) were packed onto glass microscope slides 25 x 75 mm (Sail brands, China) and covered with 22 x 22 mm glass cover slips (Scientific laboratory supplies Ltd, Nottingham, UK). The microscope slides containing the powdered samples were then inserted into the FP82HT hot stage connected to a Mettler Toledo FP90 central processor (Mettler Toledo, VIC, Australia). The hot stage was then placed onto the Nikon ECLIPSE Ni-U upright microscope (Nikon, Tokyo, Japan) fitted with cross polarizing filters. Images were taken with the DS-U3 digital camera unit (Nikon, Tokyo, Japan) connected to the microscope and operated using NIS-Elements F version 4.00.00 software. Heating scans were conducted from 30°C to 250°C (or until decomposition occurred) at 10°C/min. At every 20°C increase, heating scans were paused and an equilibration time of 5 minutes was allowed before images were taken on the microscope. This method is used to visualise the thermotropic behaviour of the freeze dried liposomal ciprofloxacin nanocrystals as well as the reference material ciprofloxacin hydrate crystals.

## **S.2 Differential Scanning Calorimetry (DSC)**

Additional thermotropic studies of the liposomal ciprofloxacin nanocrystals as well as the reference drugs were investigated by DSC using a DSC-8500 apparatus (Perkin Elmer, MA, USA). Freeze dried liposomal nanocrystals, liposomal control powders and drug powders (~2.5 mg) were accurately weighed into the 50  $\mu$ L aluminium pans covered with the aluminium pin hole lids (TA Instrument, DE, USA) and hermetically sealed. Two empty pans were prepared as a blank and a reference. Equilibration of the DSC at 30°C was performed before each sample run. The thermograms were obtained at 30°C for a minute and at the range of 30-350°C with a heating rate of 10°C/min. Nitrogen gas was flushed at 20 mL/min. Thermograms were analysed and exported using the Pyris software (version 11.1.1.0497).

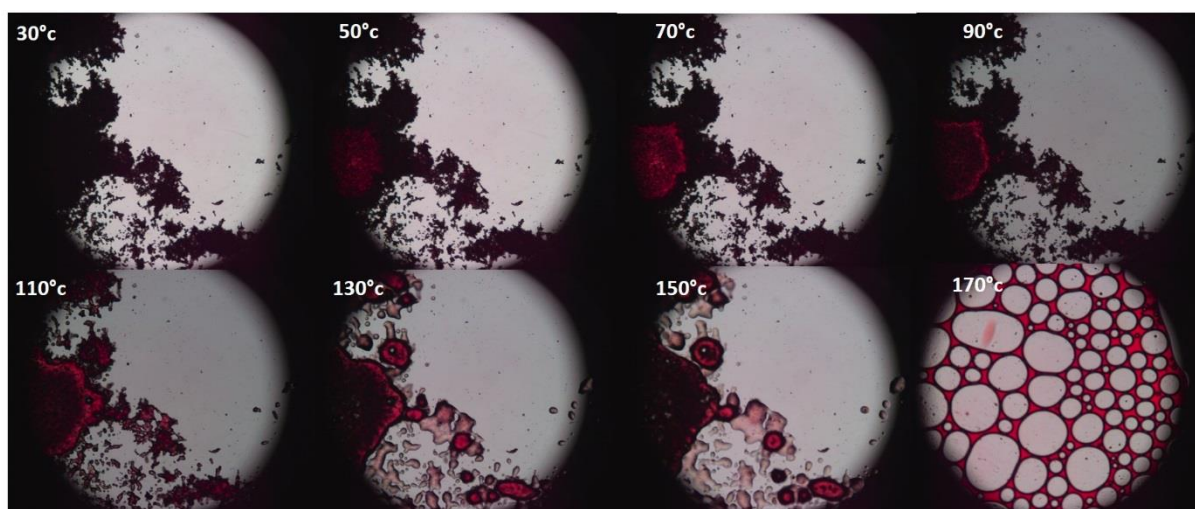


**Figure S1.** Temperature-dependent cross polarised light microscopy (CPLM) images of freeze-dried liposomal ciprofloxacin nanocrystals at increasing temperature at a heating rate of 10 °C/min.

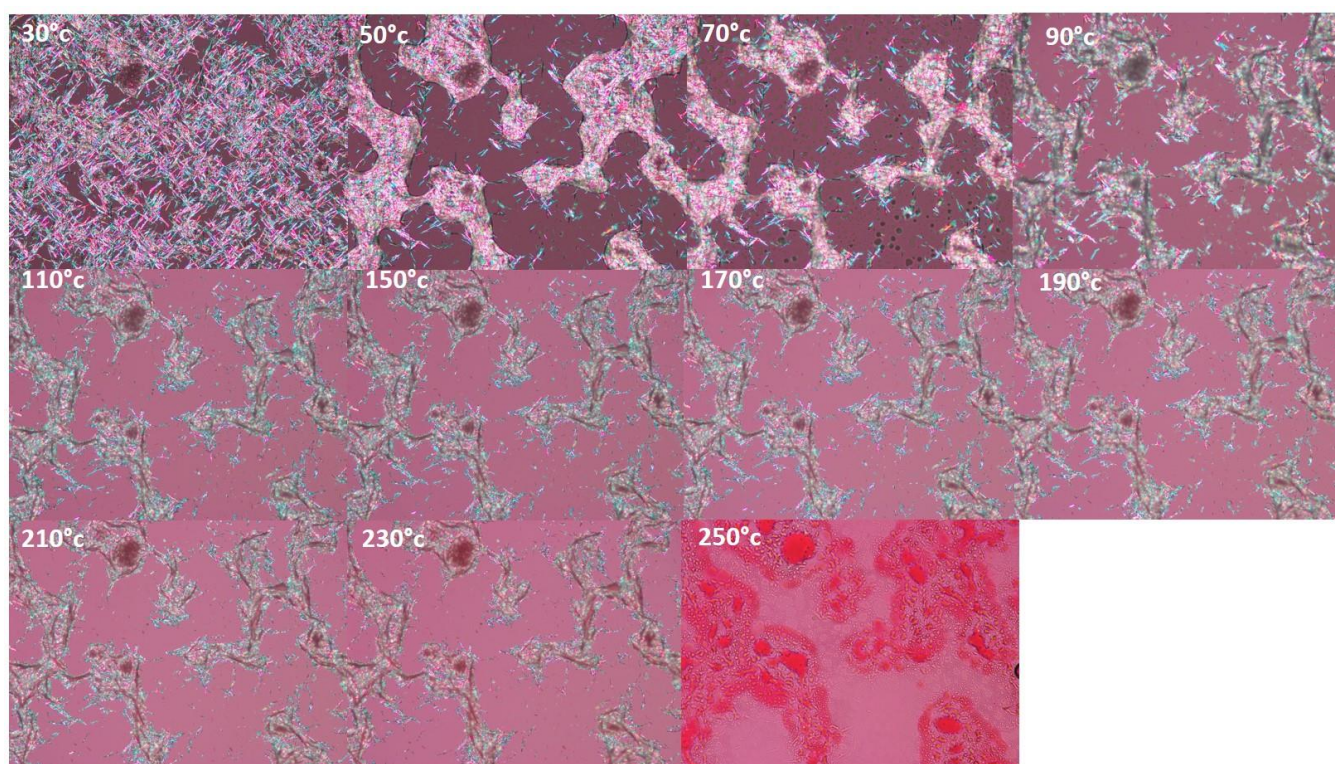


**Figure S2.** Temperature-dependent cross polarised light microscopy (CPLM) images of ciprofloxacin hydrate crystals at increasing temperature at a heating rate of 10 °C/min.

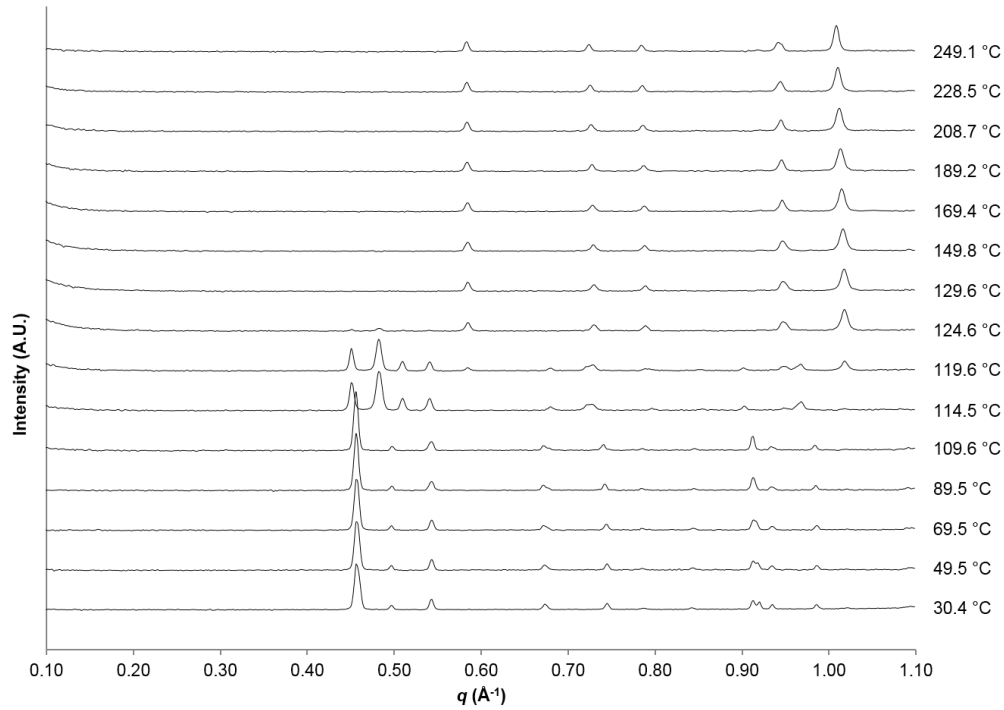


**Figure S3.** Temperature-dependent SAXS scattering profiles of ciprofloxacin hydrate crystals stacked at increasing temperature at 10 °C/min.

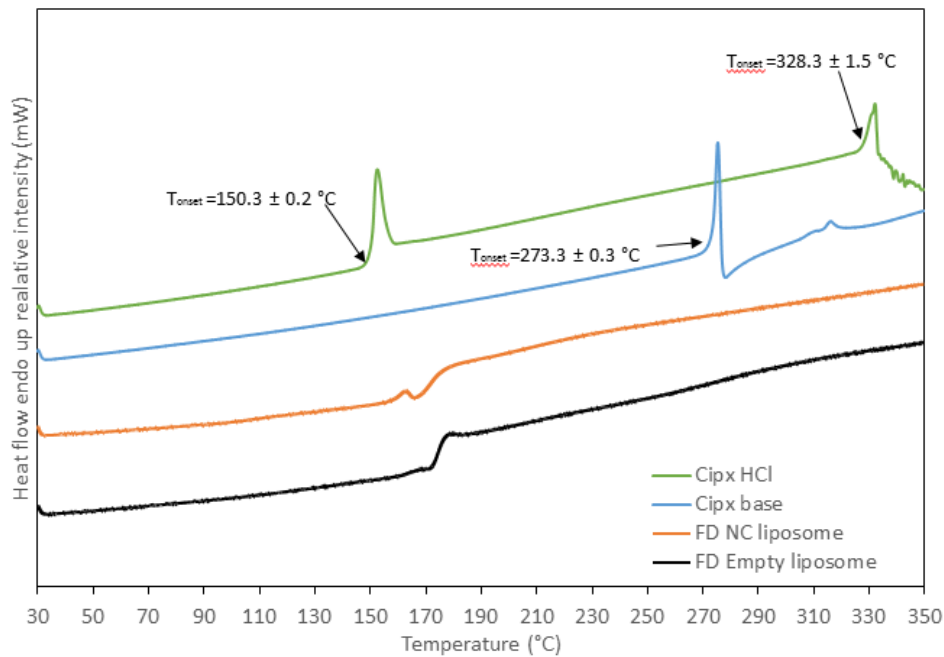


**Figure S4.** Differential scanning calorimetry (DSC) thermographs of ciprofloxacin hydrochloride, ciprofloxacin base (anhydrate), freeze-dried liposomal ciprofloxacin nanocrystals (FD NC liposome) and freeze dried empty liposome (FD empty liposome).

## References

1. Allen TM, Cullis PR. Liposomal drug delivery systems: From concept to clinical applications. *Advanced Drug Delivery Reviews*. 2013;65(1):36-48.
2. Sharma A, Sharma US. Liposomes in drug delivery: Progress and limitations. *International Journal of Pharmaceutics*. 1997;154(2):123-40.
3. Barenholz Y. Doxil® — The first FDA-approved nano-drug: Lessons learned. *Journal of Controlled Release*. 2012;160(2):117-34.
4. James ND, Coker RJ, Tomlinson D, Harris JRW, Gompels M, Pinching AJ, et al. Liposomal doxorubicin (Doxil): An effective new treatment for Kaposi's sarcoma in AIDS. *Clinical Oncology*. 1994;6(5):294-6.
5. Forssen EA. The design and development of DaunoXome® for solid tumor targeting in vivo. *Advanced Drug Delivery Reviews*. 1997;24(2):133-50.
6. Rosenthal E, Poizot-Martin I, Saint-Marc T, Spano JP, Cacoub P, Group DNXS. Phase IV study of liposomal daunorubicin (DaunoXome) in AIDS-related Kaposi sarcoma. *Am J Clin Oncol*. 2002;25(1):57-9.
7. Benesch M, Urban C. Liposomal cytarabine for leukemic and lymphomatous meningitis: recent developments. *Expert Opinion on Pharmacotherapy*. 2008;9(2):301-9.
8. Crain ML. Daunorubicin & Cytarabine Liposome (Vyxeos™). *Oncology Times*. 2018;40(10):30.
9. Chen EC, Fathi AT, Brunner AM. Reformulating acute myeloid leukemia: liposomal cytarabine and daunorubicin (CPX-351) as an emerging therapy for secondary AML. *OncoTargets and therapy*. 2018;11:3425-34.
10. Silverman JA, Deitcher SR. Marqibo® (vincristine sulfate liposome injection) improves the pharmacokinetics and pharmacodynamics of vincristine. *Cancer Chemotherapy and Pharmacology*. 2013;71(3):555-64.
11. Drummond DC, Noble CO, Guo Z, Hong K, Park JW, Kirpotin DB. Development of a highly active nanoliposomal irinotecan using a novel intraliposomal stabilization strategy. *Cancer Res*. 2006;66(6):3271-7.
12. Kang MH, Wang J, Makena MR, Lee JS, Paz N, Hall CP, et al. Activity of MM-398, nanoliposomal irinotecan (nal-IRI), in Ewing's family tumor xenografts is associated with high exposure of tumor to drug and high SLFN11 expression. *Clinical cancer research : an official journal of the American Association for Cancer Research*. 2015;21(5):1139-50.

13. Passero FC, Grapsa D, Syrigos KN, Saif MW. The safety and efficacy of Onivyde (irinotecan liposome injection) for the treatment of metastatic pancreatic cancer following gemcitabine-based therapy. *Expert Review of Anticancer Therapy*. 2016;16(7):697-703.
14. Zhang H. Onivyde for the therapy of multiple solid tumors. *OncoTargets and therapy*. 2016;9:3001-7.
15. Boswell GW, Buell D, Bekersky I. AmBisome (Liposomal Amphotericin B): A Comparative Review. *The Journal of Clinical Pharmacology*. 1998;38(7):583-92.
16. Meyerhoff A. U.S. Food and Drug Administration Approval of AmBisome (Liposomal Amphotericin B) for Treatment of Visceral Leishmaniasis. *Clinical Infectious Diseases*. 1999;28(1):42-8.
17. Mills W, Chopra R, Linch DC, Goldstone AH. Liposomal amphotericin B in the treatment of fungal infections in neutropenic patients: a single-centre experience of 133 episodes in 116 patients. *British Journal of Haematology*. 1994;86(4):754-60.
18. Treatment of Age-related Macular Degeneration With Photodynamic Therapy Study G. Photodynamic therapy of subfoveal choroidal neovascularization in age-related macular degeneration with verteporfin: One-year results of 2 randomized clinical trials—tap report 1. *Archives of Ophthalmology*. 1999;117(10):1329-45.
19. Gambling D, Hughes T, Martin G, Horton W, Manvelian G. A Comparison of Depodur™, a Novel, Single-Dose Extended-Release Epidural Morphine, with Standard Epidural Morphine for Pain Relief After Lower Abdominal Surgery. *Anesthesia & Analgesia*. 2005;100(4):1065-74.
20. Nagle PC, Gerancher JC. DepoDur® (extended-release epidural morphine): a review of an old drug in a new vehicle. *Techniques in Regional Anesthesia and Pain Management*. 2007;11(1):9-18.
21. Surdam JW, Licini DJ, Baynes NT, Arce BR. The Use of Exparel (Liposomal Bupivacaine) to Manage Postoperative Pain in Unilateral Total Knee Arthroplasty Patients. *The Journal of Arthroplasty*.30(2):325-9.
22. Cipolla D, Blanchard J, Gonda I. Development of Liposomal Ciprofloxacin to Treat Lung Infections. *Pharmaceutics*. 2016;8(1):6.
23. Boulikas T. Clinical overview on Lipoplatin: a successful liposomal formulation of cisplatin. *Expert opinion on investigational drugs*. 2009;18(8):1197-218.
24. Koudelka S, Turanek J. Liposomal paclitaxel formulations. *Journal of controlled release : official journal of the Controlled Release Society*. 2012;163(3):322-34.

25. Gabizon A, Chemla M, Tzemach D, Horowitz AT, Goren D. Liposome longevity and stability in circulation: effects on the in vivo delivery to tumors and therapeutic efficacy of encapsulated anthracyclines. *Journal of drug targeting*. 1996;3(5):391-8.
26. Gabizon A, Shmeeda H, Barenholz Y. Pharmacokinetics of pegylated liposomal Doxorubicin: review of animal and human studies. *Clinical pharmacokinetics*. 2003;42(5):419-36.
27. Gabizon AA, Lyass O, Berry GJ, Wildgust M. Cardiac Safety of Pegylated Liposomal Doxorubicin (Doxil®/Caelyx®) Demonstrated by Endomyocardial Biopsy in Patients with Advanced Malignancies. *Cancer Investigation*. 2004;22(5):663-9.
28. O'Brien MER, Wigler N, Inbar M, Rosso R, Grischke E, Santoro A, et al. Reduced cardiotoxicity and comparable efficacy in a phase III trial of pegylated liposomal doxorubicin HCl (CAELYX™/Doxil®) versus conventional doxorubicin for first-line treatment of metastatic breast cancer. *Annals of Oncology*. 2004;15(3):440-9.
29. Kim BST, Murdande MSS, Gruber MDA, Kim MDS. Sustained-release Morphine for Epidural Analgesia in Rats. *Anesthesiology*. 1996;85(2):331-8.
30. Mantripragada S. A lipid based depot (DepoFoam® technology) for sustained release drug delivery. *Progress in Lipid Research*. 2002;41(5):392-406.
31. Haran G, Cohen R, Bar LK, Barenholz Y. Transmembrane ammonium sulfate gradients in liposomes produce efficient and stable entrapment of amphipathic weak bases. *Biochimica et biophysica acta*. 1993;1151(2):201-15.
32. Li X, Hirsh DJ, Cabral-Lilly D, Zirkel A, Gruner SM, Janoff AS, et al. Doxorubicin physical state in solution and inside liposomes loaded via a pH gradient. *Biochimica et Biophysica Acta (BBA) - Biomembranes*. 1998;1415(1):23-40.
33. Schilt Y, Berman T, Wei X, Barenholz Y, Raviv U. Using solution X-ray scattering to determine the high-resolution structure and morphology of PEGylated liposomal doxorubicin nanodrugs. *Biochimica et Biophysica Acta (BBA) - General Subjects*. 2016;1860(1, Part A):108-19.
34. Zhang W, Falconer JR, Baguley BC, Shaw JP, Kanamala M, Xu H, et al. Improving drug retention in liposomes by aging with the aid of glucose. *International Journal of Pharmaceutics*. 2016;505(1):194-203.
35. Webb MS, Boman NL, Wiseman DJ, Saxon D, Sutton K, Wong KF, et al. Antibacterial Efficacy against an In Vivo *Salmonella typhimurium* Infection Model and Pharmacokinetics of a Liposomal Ciprofloxacin Formulation. *Antimicrobial agents and chemotherapy*. 1998;42(1):45-52.

36. Maurer N, Wong KF, Hope MJ, Cullis PR. Anomalous solubility behavior of the antibiotic ciprofloxacin encapsulated in liposomes: a <sup>1</sup>H-NMR study. *Biochimica et Biophysica Acta (BBA) - Biomembranes*. 1998;1374(1):9-20.
37. Lasic DD, Čeh B, Stuart MCA, Guo L, Frederik PM, Barenholz Y. Transmembrane gradient driven phase transitions within vesicles: lessons for drug delivery. *Biochimica et Biophysica Acta (BBA) - Biomembranes*. 1995;1239(2):145-56.
38. Cipolla D, Wu H, Salentinig S, Boyd B, Rades T, Vanhecke D, et al. Formation of drug nanocrystals under nanoconfinement afforded by liposomes. *RSC Advances*. 2016;6(8):6223-33.
39. Cipolla D, Wu H, Eastman S, Redelmeier T, Gonda I, Chan H-K. Tuning Ciprofloxacin Release Profiles from Liposomally Encapsulated Nanocrystalline Drug. *Pharmaceutical Research*. 2016;33(11):2748-62.
40. Porter CJ, Trevaskis NL, Charman WN. Lipids and lipid-based formulations: optimizing the oral delivery of lipophilic drugs. *Nature reviews Drug discovery*. 2007;6(3):231-48.
41. Wei X, Cohen R, Barenholz Y. Insights into composition/structure/function relationships of Doxil® gained from “high-sensitivity” differential scanning calorimetry. *European Journal of Pharmaceutics and Biopharmaceutics*. 2016;104:260-70.
42. Wei X, Shamrakov D, Nudelman S, Peretz-Damari S, Nativ-Roth E, Regev O, et al. Cardinal Role of Intraliposome Doxorubicin-Sulfate Nanorod Crystal in Doxil Properties and Performance. *ACS Omega*. 2018;3(3):2508-17.
43. Abraham SA, Edwards K, Karlsson G, Hudon N, Mayer LD, Bally MB. An evaluation of transmembrane ion gradient-mediated encapsulation of topotecan within liposomes. *Journal of Controlled Release*. 2004;96(3):449-61.
44. Li T, Cipolla D, Rades T, Boyd BJ. Drug nanocrystallisation within liposomes. *Journal of Controlled Release*. 2018;288:96-110.
45. Hotani H, Miyamoto H. Dynamic features of microtubules as visualized by dark-field microscopy. *Advances in Biophysics*. 1990;26:135-56.
46. Umeda T, Nakajima H, Hotani H. Theoretical Analysis of Shape Transformations of Liposomes Caused by Microtubule Assembly. *Journal of the Physical Society of Japan*. 1998;67(2):682-8.
47. Mafra L, Santos SM, Siegel R, Alves I, Paz FA, Dudenko D, et al. Packing interactions in hydrated and anhydrous forms of the antibiotic Ciprofloxacin: a solid-state

- NMR, X-ray diffraction, and computer simulation study. *J Am Chem Soc.* 2012;134(1):71-4.
48. Izutsu KI, Yomota C, Kawanishi T. Stabilization of liposomes in frozen solutions through control of osmotic flow and internal solution freezing by trehalose. *Journal of Pharmaceutical Sciences.* 2011;100(7):2935-44.
49. Wessman P, Edwards K, Mahlin D. Structural effects caused by spray- and freeze-drying of liposomes and bilayer disks. *Journal of Pharmaceutical Sciences.* 2009;99(4):2032-48.
50. Gebauer D, Kellermeier M, Gale JD, Bergström L, Cölfen H. Pre-nucleation clusters as solute precursors in crystallisation. *Chemical Society Reviews.* 2014;43(7):2348-71.
51. Paluch KJ, McCabe T, Müller-Bunz H, Corrigan OI, Healy AM, Tajber L. Formation and Physicochemical Properties of Crystalline and Amorphous Salts with Different Stoichiometries Formed between Ciprofloxacin and Succinic Acid. *Molecular Pharmaceutics.* 2013;10(10):3640-54.
52. Yu X, Zipp GL, Davidson III GWR. The Effect of Temperature and pH on the Solubility of Quinolone Compounds: Estimation of Heat of Fusion. *Pharmaceutical Research.* 1994;11(4):522-7.
53. Torniainen K, Tammilehto S, Ulvi V. The effect of pH, buffer type and drug concentration on the photodegradation of ciprofloxacin. *International Journal of Pharmaceutics.* 1996;132(1):53-61.
54. Zhigaltsev IV, Maurer N, Edwards K, Karlsson G, Cullis PR. Formation of drug-arylsulfonate complexes inside liposomes: A novel approach to improve drug retention. *Journal of Controlled Release.* 2006;110(2):378-86.
55. Fugit KD, Xiang T-X, Choi DH, Kangarlou S, Csuhai E, Bummer PM, et al. Mechanistic model and analysis of doxorubicin release from liposomal formulations. *Journal of Controlled Release.* 2015;217:82-91.
56. Hörter D, Dressman JB. Influence of physicochemical properties on dissolution of drugs in the gastrointestinal tract. *Journal of Pharmaceutical Sciences.* 1997;86(1):1-14. The article was originally published in *Advanced Drug Delivery Reviews* 25 (1997) 3–14. *Advanced Drug Delivery Reviews.* 2001;46(1):75-87.
57. Mudie DM, Amidon GL, Amidon GE. Physiological parameters for oral delivery and in vitro testing. *Mol Pharm.* 2010;7(5):1388-405.



## **Chapter 3: Engineering the dimension of nanocrystals inside liposomes**

Chapter 3 overall addresses the possibility to tune the dimensions of the formed nanocrystals inside the liposomes using composition and process variables. The first section describes new methodology developed to enable high throughput investigations of these variables and has been published in Molecular Pharmaceutics, while the second part describes the use of these methodologies to further explore the 'engineering' of these nanocrystals.

### **Chapter 3 A: Direct comparison of standard TEM and cryogenic TEM in imaging nanocrystals inside liposomes**

## **Direct comparison of standard transmission electron microscopy (TEM) and cryogenic-TEM in imaging nanocrystals inside liposomes**

Tang Li<sup>a</sup>, Cameron J. Nowell<sup>b</sup>, David Cipolla<sup>c</sup>, Thomas Rades<sup>d</sup>, Ben J. Boyd<sup>a</sup>

<sup>a</sup> ARC Centre of Excellence in Convergent Bio-Nano Science and Technology and Drug Delivery, Disposition and Dynamics, Monash Institute of Pharmaceutical Sciences, Monash University, Parkville, VIC, Australia

<sup>b</sup> Drug Discovery Biology, Monash Institute of Pharmaceutical Sciences, Monash University, Australia

<sup>c</sup> Insmed Inc., 10 Funderne Ave., Building 10, Bridgewater, NJ, USA

<sup>d</sup> Faculty of Health and Medical Sciences, Department of Pharmacy, University of Copenhagen, Copenhagen, Denmark

Accepted manuscript as a brief article in *Molecular Pharmaceutics*.

### **Abstract**

The use of electron microscopy techniques in the understanding of shape and size of nanoparticles are commonly applied to drug nanotechnology but the type of microscopy and suitability for the particles of interest can have a significant impact on the result. The size and shape of the nanoparticles are crucial in clinical applications however direct comparison of the results from standard TEM and cryo-TEM have rarely been reported. As a useful case for comparison, liposomal drug nanocrystals are studied here. In this study, the effect of thawing temperature on the size and shape of the ciprofloxacin nanocrystals was determined. A quantitative standard TEM assay was developed to allow high throughput particle size analysis. These results were compared to size and shape information obtained using the cryo-TEM method. The results showed broad agreement between the two TEM methods, and that ciprofloxacin nanocrystals formed shorter and thinner crystals inside the liposomes at higher thawing temperatures. The results provide confidence in the use of standard TEM to determine the size and shape distribution of solid nanoparticles (in this case encapsulated inside liposomes) from aqueous media without fear of sample preparation altering the conclusions.

### **KEYWORDS**

Liposomes; nanocrystals; cryo-TEM; TEM; nanoparticle size analysis; DLS

### 3A.1 Introduction

Nano-sized drug delivery particles have received much recent literature interest due to their potential benefits in improving clinical outcomes, with a focus on cancer (1). Liposomes are one class of lipid-based nanocarrier that have been used to encapsulate a variety of drug molecules for the treatment of different indications (2, 3). The liposomal formulation of doxorubicin sulfate nanocrystals, Doxil<sup>®</sup>, was the first FDA approved nanomedicine on the market (4-6). Iconic cryo-TEM images of Doxil<sup>®</sup> liposomes containing a precipitated doxorubicin sulfate nanocrystal (**Figure 1a**) have driven more recent interest in other liposomal nanocrystal formulations (7). Recently *in situ* crystallisation of ciprofloxacin inside liposomes was reported (**Figure 1b**), induced by a freeze-thawing step after drug loading (8). The formation of ciprofloxacin nanocrystals inside the liposomes was shown to attenuate the *in vitro* drug release rate which may prove beneficial *in vivo* (9). The ability to engineer the shape and size of the ciprofloxacin nanocrystals within liposomes therefore provides an exciting opportunity for tailored release liposomal formulations. The size distribution and shape of nanocarriers is important as it can also affect their immunological interactions and pharmacokinetics (10-13). Therefore it is crucial to effectively characterise and analyse these physical parameters of drug nanocarriers to design toward more effective formulations.

Transmission electron microscopy (TEM) is commonly used to visualise the shape and size of solid particles, but is also used, often inappropriately, for self-assembled nanocarriers, (14, 15). Standard TEM requires a drop of liquid sample to be dried onto the TEM grid and images are acquired as electrons are transmitted through the sample. The process of drying could potentially affect structural integrity of the nanocarrier, particularly with complex samples and where self-assembled lipids are present (16, 17). Negative staining is commonly used in standard TEM to increase contrast for lipid based nanoparticles but could also produce artefacts in the image (17-20) especially where water provides a significant contribution to the shape and structure of the particles.

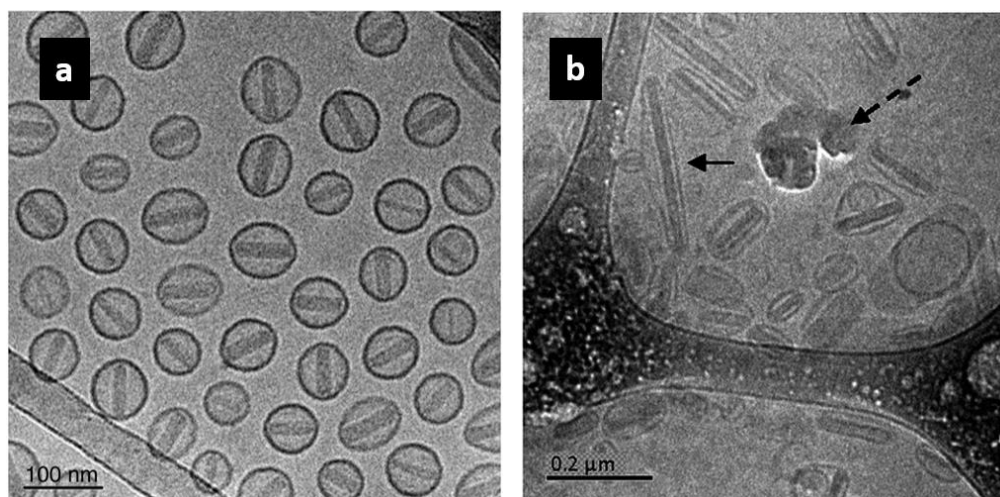


**Figure 1.** Cryo-TEM image of a) commercial Doxil (pegylated liposome with doxorubicin sulfate remotely loaded (reprinted with permission from (4)). b) GMP liposomal ciprofloxacin after freeze-thaw (liposomal ciprofloxacin nanocrystals) (reprinted with permission from (8)). The dotted arrow in b indicates ice artefacts during cryo-TEM imaging.

Therefore researchers often turn to cryogenic TEM (cryo-TEM), in which the liquid sample is vitrified by plunge freezing to form a thin layer of sample onto the TEM grid, allowing preservation of the shape and internal structure of particles containing aqueous compartments; e.g. liposomes (21-26). However this technique is very expensive and time consuming compared to standard TEM (**Table 1**) and requires highly skilled microscopists so that ice contamination (**Figure 1b**) and defects are minimised (16). Other disadvantages of cryo-TEM include that this technique may be biased towards small particles due to the preparation technique requiring an ultra-thin film of sample (27). Due to these shortcomings, cryo-TEM is not amenable as a quantitative method for nanocarrier particle size distribution analysis. Standard TEM on the contrary is a faster and more economical technique for number-based distribution analysis of particle shape and size (16, 28) (**Table 1**). Although both the standard TEM and cryo-TEM are commonly used as a qualitative measure to analyse the physical parameters of nanocarriers in drug research, the two methods are rarely compared head to head in particle shape and size analysis. Liposomal nanocrystals provide an interesting opportunity for comparison of the two methods on the same sample, as cryo-TEM is also often used to study liposome lamellarity and morphology but the nanocrystals are also clear (**Figure 1**). In contrast, in standard TEM the liposome bilayer is collapsed under dehydration, but the nanocrystalline particles are expected to also be clear.

**Table 1.** Direct comparison between the standard TEM and cryo-TEM techniques for their cost, time and technical aspects.

	<b>Standard TEM</b>	<b>Cryo-TEM</b>
<b>Hours/sample (Sample loading and imaging)</b>	0.5	2-3
<b>Cost/sample (AUD)</b>	\$22.5	\$214 - \$321
<b>Number of particles analysed per image</b>	>500	60-200
<b>Can be imaged in native state</b>	No	Yes
<b>Soft materials in suspension (liposomes)</b>	<ul style="list-style-type: none"> <li>• Need negative staining</li> <li>• Dehydration during sample fixing may produce artefacts</li> </ul>	<ul style="list-style-type: none"> <li>• Staining is not required</li> <li>• Risk of ice crystal formation during sample loading</li> </ul>
<b>Dry/hard particles (drug nanocrystals)</b>	<ul style="list-style-type: none"> <li>• Staining is not required</li> <li>• High contrast for nanocrystals</li> <li>• Quantitatively analyse size and shape distribution of nanocrystals</li> </ul>	<ul style="list-style-type: none"> <li>• Qualitative method to visualise nanocrystals inside liposome</li> <li>• Bias toward smaller particles</li> </ul>

### 3A.2 Hypotheses and aims

Hypotheses: That standard TEM can be used as a high throughput quantitative method to analyse the liposomal drug nanocrystals size distribution. That the dimensions of the liposomal drug nanocrystals can be altered by the thawing rate.

In order to investigate these hypotheses, the following aims will be achieved:

1. To develop a high throughput standard TEM assay to quantitatively assess the shape and size distribution of the ciprofloxacin nanocrystals inside liposomes.

2. To establish a comparison between cryo-TEM and the developed standard TEM quantitative assay (where no negative staining is applied) for the analysis of the shape and size distribution of ciprofloxacin nanocrystals inside liposomes.
3. To investigate the effect of thawing temperature on the dimension and aspect ratios of ciprofloxacin nanocrystals grown under the constraints of the liposomal bilayers.

### 3A.3 Experimental section

#### 3A.3.1 Materials

Ciprofloxacin liposomes (50 mg/mL) were kindly gifted by Aradigm Corporation (Hayward, CA, USA). Tris maleate (reagent grade) and sucrose (>99.5%) were purchased from Sigma Aldrich (St. Louis, MO, USA). Calcium chloride (>99%) and sodium hydroxide pellets (reagent grade) were obtained from Ajax Finechem (Seven Hills, NSW, Australia). Sodium chloride (>99%) was purchased from Chem Supply (Gillman, SA, Australia). Sodium azide was purchased from Merck Schuchardt OHG (Eduard-Buchner-StraÙe, Hohenbrunn, Germany). Hydrochloric acid 36% (analytical grade) was purchased from Biolab Aust Ltd (Clayton, VIC, Australia). The water used was sourced from a Millipore water purification system using a Quantum™ EX Ultrapure Organex cartridge (Millipore, Australia).

#### 3A.3.2 Sample preparation for thawing temperature effect study

GMP ciprofloxacin liposomes were gifted by Aradigm Corporation (Hayward, CA, USA). It contains 50 mg/mL ciprofloxacin (as the hydrochloride salt), which is equivalent to 45 mg/mL ciprofloxacin. The lipids are comprised of cholesterol (at 26.3 mg/mL) and hydrogenated soy phosphatidylcholine (HSPC) (at 60 mg/mL). The liposomal dispersion has a pH of 6.0. The details of the development and manufacturing method of the liposomal ciprofloxacin were reported by Cipolla et al. (29). The liposomal dispersion were diluted four-fold with 180 mg/mL sucrose and Tris buffer (50 mM Tris maleate, 5 mM CaCl<sub>2</sub>·2H<sub>2</sub>O, 150 mM NaCl, 6 mM sodium azide and adjusted to pH 6.0). The prepared dispersions were injected into rectangular borosilicate glass capillaries 0.40 x 8.00 mm ID (VitroCom, Mountain Lakes, NJ, USA) enclosed with Blu-Tak for the freeze-thawing cycle. The formulations were first snap frozen in liquid nitrogen for 5 minutes and then thawed at 4°C, 20°C and 50°C. After thawing was completed, the samples were withdrawn from the capillaries and stored in glass vials and stored at ambient temperature (20°C) before

standard TEM or cryo-TEM analysis. The use of the rectangular borosilicate glass capillaries for the freeze-thawing experiment is to provide a high surface area for effective snap freezing in liquid nitrogen. The freeze-thawing cycles were performed one day prior to any EM analysis.

### 3A.3.3 Standard transmission electron microscopy (standard TEM)

Continuous carbon only TEM grids on 400 or 200 mesh (ProSciTech Pty.Ltd, Australia) were plasma cleaned for 2 minutes in oxygen/argon gas using the Solarus Plasma Cleaner (Gatan, Inc. CA, USA). An aliquot (2  $\mu$ L) of the sample was pipetted onto each grid and 1 minute adsorption time was allowed. Grids were blotted manually using Whatman 541 filter paper to absorb the excess liquid on the grids. The grids were then left to air dry at room temperature for 10 minutes. No negative staining protocol was applied to the grid preparation for every sample. The samples were examined using a Tecnai single tilt holder and FEI Tecnai G2 T20 microscope (200 kV) (FEI, Oregon, USA) and images were recorded at a magnification of 13000x, with an objective aperture 1, defocus of -20  $\mu$ m and 2 seconds exposure.

### 3A.3.4 Cryogenic transmission electron microscopy (cryo-TEM)

Cryo-TEM samples were prepared within a laboratory-built humidity-controlled vitrification system (humidity at 80% and temperature at 22°C). Lacey carbon films 200 mesh (ProSciTech, Qld, Australia) were glow discharged in nitrogen gas to provide a hydrophilic substrate for sample loading. An aliquot (4  $\mu$ L) of the sample was pipetted onto each grid and allowed to adsorb for 30 seconds before being blotted manually using Whatman 541 filter paper for 2 seconds. Grids were then plunged into liquid ethane cooled by liquid nitrogen and stored in liquid nitrogen until imaging. The samples were loaded onto the Gatan 626 cryoholder (Gatan, Pleasanton, CA, USA) and were examined using the Tecnai 12 Transmission Electron Microscope (FEI, Eindhoven, The Netherlands) at an operating voltage of 120 kV. Low dose procedures were performed using an electron dose of 8-10 electrons/ $\text{\AA}^2$  for imaging. Images were recorded using a FEI Eagle 4kx4k CCD camera at magnifications ranging from 15 000x to 50 000x.

### 3A.3.5 Microscopy image data analysis and visualisation

Microscopy images captured from standard TEM and cryo-TEM were analysed using Fiji software (30). For standard TEM, the selected nanocrystals within each image (well segmented from other nanocrystals) were manually highlighted with the wand tool and the ROI manager function and the length and width measurement (nm) of each nanocrystal

was then automatically generated through an in-house developed macro script. The aspect ratios were then calculated as a ratio of length to width. For cryo-TEM images, due to the limited liposomal nanocrystals observed per image, the length and width measurements of the nanocrystals were performed manually using Fiji. The measurement results were then imported into R studio software for data visualisation. Boxplots comparing the length, width and aspect ratio were generated for each method and formulation. The polydispersity was calculated as standard deviation/mean (16). The one-way analysis of variance (ANOVA) was used to determine whether there were any statistically significant differences between the means of the different thawed samples for both standard TEM and cryo-TEM.

### 3A.3.6 Dynamic light scattering measurement (DLS)

DLS measurements were conducted using Zetasizer Nano ZS (Malvern Instruments, Worcestershire, UK). Liposomal ciprofloxacin nanocrystal samples thawed at different temperatures were diluted 100 fold with milliQ water and transferred to low volume polystyrene cuvettes (Sigma, Castle Hill, Australia). The zeta average size (nm) and PDI of the liposomal nanocrystals were measured at 25 °C using the parameters of 173° backscatter angle, viscosity 0.8872 cP, refractive index 1.33, equilibration time 120 seconds. Three measurements were conducted per sample.

## 3A.4 Results and discussion

Liposomal ciprofloxacin nanocrystals were imaged using the negative staining method to validate the hypothesis that the negative staining would produce artefacts, which could affect the drug nanocrystals visualisation. A sample image of the negatively stained liposomal ciprofloxacin nanocrystals can be found in the supplementary information (Figure S1). The image shows the quality of the imaging has been negatively impacted by the negative staining method. The image does not allow one to visually distinguish the liposome or the nanocrystals at a good resolution. Hence standard TEM without negative staining was performed and examples of standard TEM images of liposomal ciprofloxacin nanocrystals are shown in **Figure 2 a-f**. Each image was acquired at 13 000x SA magnification and as seen in the figures, the use of objective aperture and strong defocus were required in standard TEM imaging to enhance the contrast of the nanocrystals against the background. Generally, 20-30 images were acquired per sample and around 20-50 nanocrystals were counted for size measurement per image. This yields

more than 500 nanocrystals measured per sample for the standard TEM technique. Another observation from the standard TEM images was that the liposomes cannot be visualised in the images although light grey circular shades are observed in **Figure 2 d, e**. The nanocrystals showed an electron dense band, which has much higher contrast against the background making the liposomes out of focus, and not well resolved. Consistent with previous reports for liposomal doxorubicin nanocrystals, when standard TEM was performed without staining, the liposome structures are altered by the drying process and the lipids interacted with the carbon film to form a supported lipid bilayer (17). The nanocrystals also tended to aggregate in clusters as shown in the standard TEM images; this is due to the “coffee-ring effect” as the capillary flow carries particles towards the periphery of the drying droplet which accumulate near the drop perimeter (31).

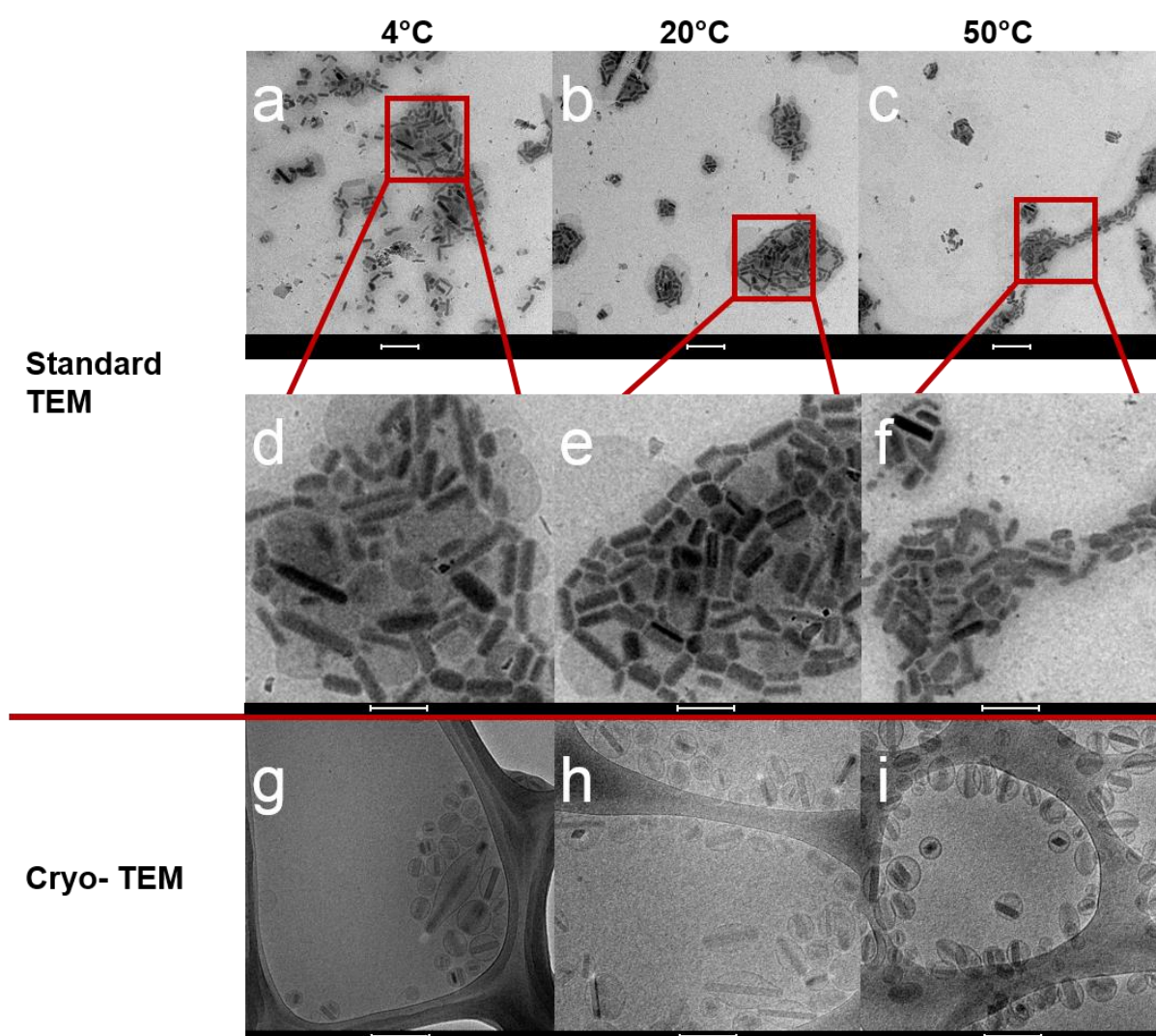


**Figure 2.** Comparison of standard TEM images and cryo-TEM images of liposomal ciprofloxacin nanocrystals with lipid bilayer composition of HSPC and cholesterol and thawed at different temperatures. Standard TEM images are presented in panel d-f and are enlarged from a-c to fit the

scale of the cryo-TEM images (g-i) for direct comparison. The liposomes are thawed at 4 °C, 20 °C and 50 °C. The scale bars in a-c represent 500 nm, and the scale bars in d-i represent 200 nm.

**Figure 2 d-f** show the magnified section of the standard TEM images from Figure 2 a-c. At higher magnification the nanocrystals, although bundled in clusters, were still well segmented which enabled high throughput nanocrystal analysis to be performed.

Cryo-TEM allows visualisation of both the liposomal bilayer and the drug nanocrystals. It provides a benchmark check for the shape and size analysis from standard TEM. It is also the only technique available to determine whether the nanocrystals are encapsulated inside the liposome rather than dispersed in the bulk aqueous phase outside the liposome. However, its low throughput and cost as mentioned **Table 1** are major limitations to routine quantitative use. On average, only 200 liposomal nanocrystals were analysed for the different thawing temperature samples. In other preliminary data, when the sample quality or the sample preparation was not optimised, the quantity of nanocrystals viewed using cryo-TEM would often be as low as 60 nanocrystals.

By comparing the two techniques side by side in **Figure 2 d-i** at the same magnification, visually, the drug nanocrystals exhibited the same rod-shaped morphology and size distributions. This confirms that the drug nanocrystals observed in standard TEM images are drug nanocrystals encapsulated inside the liposome and that the standard TEM sample preparation used did not affect the sample integrity of the liposomal ciprofloxacin nanocrystals. Also, from the comparison it is visually evident that at higher thawing temperatures (e.g. 50 °C), the nanocrystals were smaller and appear to have a shorter length compared to samples that were thawed at lower temperature (4 °C). The growth of the ciprofloxacin nanocrystals during the freeze thawing process is believed to have occurred during the thawing step (8). In this study, with the lower thawing temperature, longer crystals are observed. Although the purpose of this study is to compare the electron microscopy techniques side by side using an appropriate system, mechanistically, when thawed at lower temperatures, it is believed that because the thawing rate is slower compared to thawing at higher temperatures, crystal growth may be favoured over nucleation. More extensive studies are underway to elaborate the mechanism behind differences in the aspect ratio of liposomal drug nanocrystals, not only due to thawing temperature, but also lipid composition and bilayer rigidity using the TEM approach described here.

**Figure 3** shows the size distribution measured for each technique for the samples thawed at different temperatures. The length measurements of the liposomal nanocrystals showed good agreement between the standard TEM and the cryo-TEM techniques. The size distribution for the length measurement for the two techniques also agreed well with each other, although with cryo-TEM, the 20 °C sample showed a larger distribution and a higher median than the 50 °C sample. This is due to a number of outlier particles biasing the distribution, as the number of particles measured was less than half of the standard TEM method, hence the standard TEM was much more powerful in quantitative analysis. Post-hoc test for the length measurement by standard TEM method showed that there is significance between different thawing temperatures ( $p < 0.0005$ ).

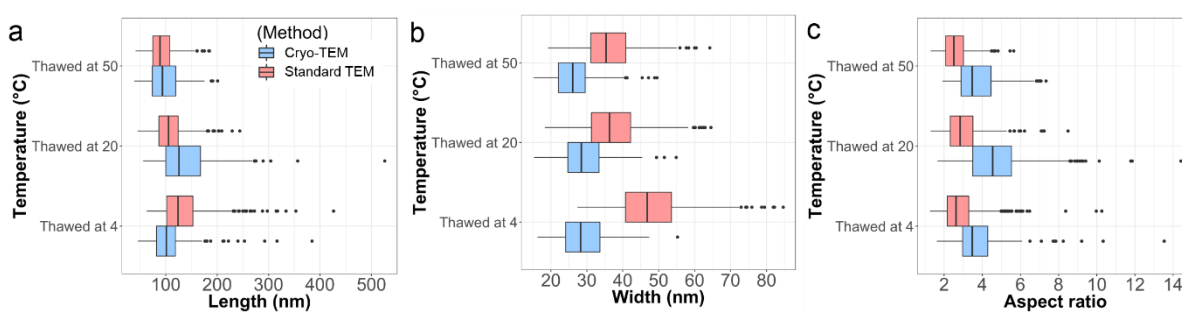


**Figure 3.** Size distributions ciprofloxacin nanocrystals derived from cryo-TEM and standard TEM images. The liposomal ciprofloxacin nanocrystals were thawed at 4 °C, 20 °C and 50 °C. The length (Panel a) and width (Panel b) of the ciprofloxacin nanocrystals were measured from standard TEM images using the Image J software and the aspect ratios (Panel c) were calculated from the ratio of length to width. (Image J of 200 cryo-TEM images and 500 TEM images)

For width measurements, with the standard TEM method, the samples thawed at 4 °C have significantly wider crystals than those thawed at 20 °C and 50 °C ( $p < 0.0005$ ). There is no significant difference in width of the nanocrystals for the 20 °C and 50 °C samples. For the cryo-TEM method, the nanocrystal width showed no significant difference between the 4 °C and 20 °C samples, but the 50 °C samples had significantly thinner crystals than the other samples. The difference in width is not as obvious visually as the length, as the nanocrystals tend to grow in length rather than width. Overall both standard TEM and cryo-TEM methods showed the same trend that samples thawed at 50 °C producing shorter and thinner crystals with a smaller size distribution compared to samples thawed at 4 °C or 20 °C. **Table 2** shows that overall, the standard TEM method gave a lower polydispersity output for the nanocrystal length and width measurement than the

cryo-TEM method, mostly attributable to the greater number of samples for standard TEM. One thing to be cautious of the results for the nanocrystals for either the standard TEM or cryo-TEM method is that both techniques require the imaged samples to be diluted before imaging, and since the nanocrystals are small particles, it is possible that the dilution could induce dissolution, affecting the measurement. However, in this case, when the nanocrystals are encapsulated inside the liposomes, the internal aqueous phase acts as a non-sink condition and the lipid bilayer acts as a barrier against the dissolution of the nanocrystals. Additionally, in this study both techniques required dilution of the sample, supporting the overall conclusions in comparison between the two techniques.

**Table 2.** Summary of the standard TEM and cryo-TEM measurements of liposomal nanocrystal size distributions (nm) at different thawing temperatures.

		Thawing temperatures					
		4°C		20°C		50°C	
		Analysis methods					
		Standard TEM	Cryo-TEM	Standard TEM	Cryo-TEM	Standard TEM	Cryo-TEM
<b>Length</b>	Median	134.57	108.00	107.94	141.97	93.12	97.94
	Mean	123.84	101.11	105.42	125.74	88.82	93.55
	Polydispersity	0.35	0.41	0.28	0.43	0.27	0.33
<b>Width</b>	Median	47.83	29.06	37.18	29.30	36.53	26.43
	Mean	46.80	28.28	36.31	28.48	35.35	26.07
	Polydispersity	0.21	0.23	0.22	0.22	0.21	0.24
<b>Aspect</b>	Median	2.90	3.78	3.00	4.93	2.60	3.78
<b>Ratio (AR)</b>	Mean	2.62	3.47	2.84	4.54	2.51	3.47

Dynamic light scattering was also performed on the liposomal ciprofloxacin nanocrystals thawed at different temperatures (**Figure 4**). The size distributions obtained from DLS were similar to the length measurements from the standard TEM methods. As the polydispersity of the sample increased for the samples that were thawed at lower temperature (e.g. 4°C), the DLS measurements showed a slightly shorter length compared to standard TEM methods. For a non-spherical particle, in this case the liposomal ciprofloxacin nanocrystals where the crystals have stretched the liposome to a non-spherical shape, DLS analysis provides the diameter of a sphere that has the same average translational diffusion coefficient as the particle being measured (through the

Stokes-Einstein equation) (32). The z-average diameter (hydrodynamic diameter) reported from the DLS results is an intensity-weighted mean diameter based on a spherical particle model, it is very sensitive to aggregates and large contaminants due to intensity weighting. Also the liposomal ciprofloxacin nanocrystals is a combination of two nanoparticles, one as a rectangular rod (drug nanocrystal) and one as an ellipsoidal particle (stretched liposome). This further complicates the understanding of the translational diffusion coefficient measured from DLS. This is because it is hard to distinguish or assume as to whether the translational diffusion coefficient is attributed to the vesicle or to the nanocrystal or a mixture of both. From cryo-TEM imaging, the nanocrystal length is close to equivalent to the stretched liposome length along the major axis (for the ellipsoidal shape) since both ends of the crystal touch the liposomal bilayer. Assuming the length is the same for the nanocrystal and the liposome, in order to work out the actual length of the nanocrystal rather than the hydrodynamic diameter, we would also need to assume that both the drug nanocrystal and the liposome have the same translational and rotational diffusion coefficient (measured by DLS and dynamic depolarized light scattering (DDLS) respectively). Furthermore, one would require the information on the shape of the nanocrystal and the aspect ratio of the nanocrystal in order to calculate the length and width of the nanocrystal (32-35). In addition to DLS there are other techniques that can be used to determine particle size such as small angle X-ray scattering (SAXS) (36, 37). These methods do not provide a visualisation of the nanoparticles specifically, and do not provide contrast between the liposome and the nanocrystals. With DLS, dissimilar vesicles have been demonstrated to produce similarity in the intensity-weighted distribution; hence the information from DLS alone is insufficient for the determination of vesicle size distribution and shape (38). Hence, to fully work out the nanocrystal dimension, DLS alone is not possible and an imaging technique such as TEM or cryo-TEM is essential in understanding the shape and aspect ratio of the nanocrystal inside the liposome.

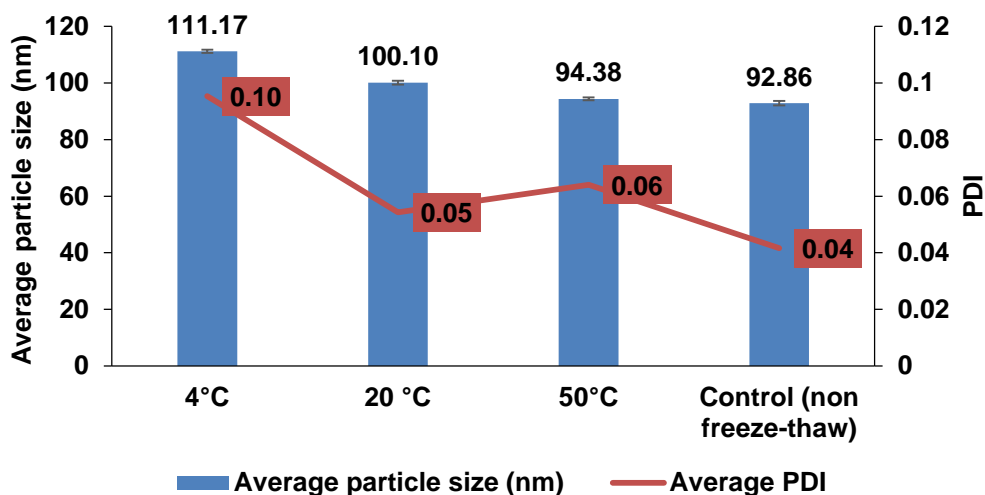


**Figure 4.** DLS measurements of liposomal ciprofloxacin nanocrystals thawed at different temperatures compared to the control. The polydispersity index (PDI) is also shown.

### 3A.5 Conclusion

Standard TEM is a powerful tool for high throughput particle analysis and can be used as a quantitative assay to analyse the size and shape of liposomal nanocrystals *in situ* inside the liposome. The existence of the nanocrystals encapsulated inside the liposome still require verification by cryo-TEM and only work for some systems. It is an easier, faster and less expensive technique compared to cryo-TEM and it also provides a better overview of the particle size distribution due to the greater number of nanocrystals that can be analysed. General agreement between standard and cryo-TEM methods provides confidence in the use of standard TEM for size and shape distributions of solid drug nanoparticles from aqueous systems even with the required drying step in TEM.

The size and shape of the liposomal nanocrystals could also be controlled by the thawing temperature, where the higher the thawing temperature, the smaller and shorter the drug nanocrystals. The size distribution and trends observed in both techniques are also closely aligned which makes the standard TEM technique a potential assay in visualising and differentiating nanocrystal particle shape and size distribution for other liposomal nanocrystal formulations.

## Acknowledgements

This study was funded under the Australian Research Council Centre of Excellence in Convergent Bio-Nano Science and Technology. BB is the recipient of an ARC Future Fellowship. Cryo-TEM studies were conducted with assistance of Dr. Lynne Waddington at the CSIRO Materials Science and Engineering. The authors acknowledge use of the facilities and assistance of Dr. Tim Williams at the Monash Centre for Electron Microscopy for room temperature TEM studies.

## Conflict of Interest

At the time of these studies David Cipolla was an employee of Aradigm Corp. who supplied the liposomes studied in this manuscript.

## Supporting information

### TEM preparation for the negative staining liposomal ciprofloxacin nanocrystals

A 200 mesh TEM grid was glow discharged with a PELCO easiGlow discharger at 0.22 mBar for 30 seconds prior to sample loading. A 5  $\mu$ L aliquot of liposome dispersion was dropped on top of a glass slide, followed by placing the grid face down on top of the sample. Samples were allowed to absorb onto the grid for 10 mins, followed by removal of excess samples with filter paper. 3  $\mu$ L of 2% uranyl acetate solution was dropped on top of a glass slide and contact with the grid for 10 seconds, followed by removal of extra uranyl acetate solution with a filter paper. Grids were then left to dry for 10 mins before imaging with TEM.

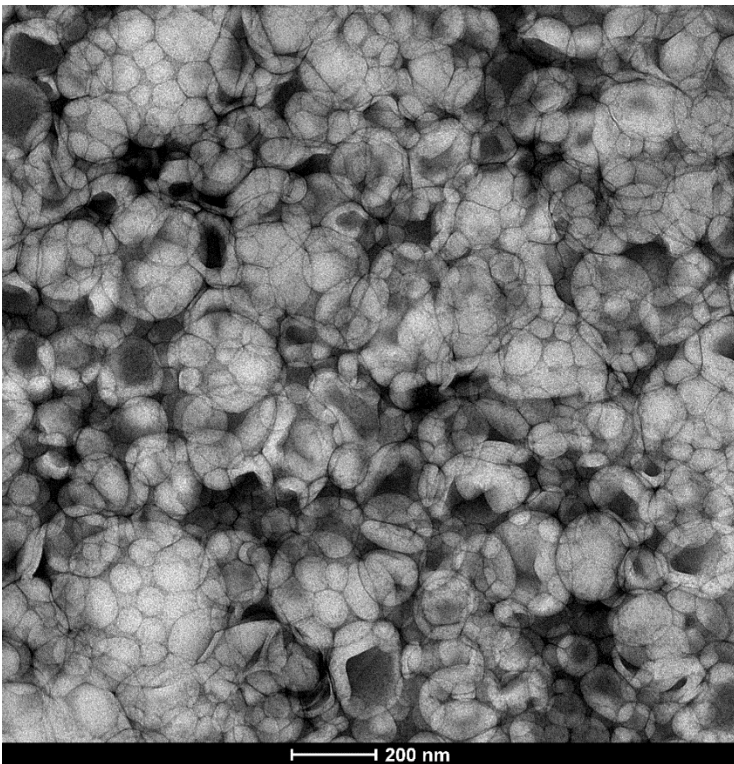


Figure S1. Negatively stained (2% uranyl acetate) liposomal ciprofloxacin nanocrystals imaged using standard TEM

**Scattering plot of the length and width size distribution comparing the two TEM methods**

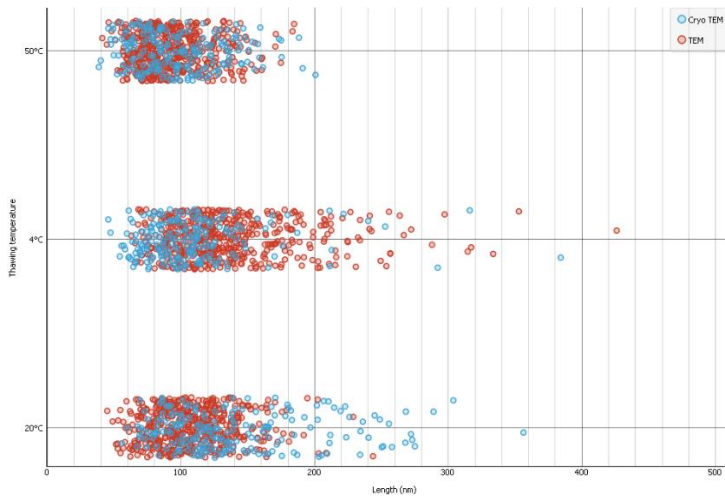


Figure S2. Length measurements comparing TEM and cryo-TEM for different samples presented as individual particle distribution using Orange 3 data visualisation software

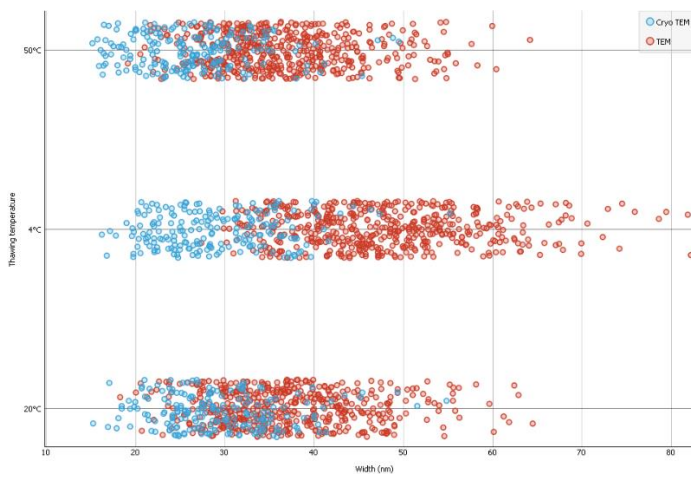


Figure S3. Width measurements comparing TEM and cryo-TEM for different samples presented as individual particle distribution using Orange 3 data visualisation software

## References

1. Wilczewska AZ, Niemirowicz K, Markiewicz KH, Car H. Nanoparticles as drug delivery systems. *Pharmacological Reports*. 2012;64(5):1020-37.
2. Allen TM, Cullis PR. Liposomal drug delivery systems: From concept to clinical applications. *Advanced Drug Delivery Reviews*. 2013;65(1):36-48.
3. Sercombe L, Veerati T, Moheimani F, Wu SY, Sood AK, Hua S. Advances and challenges of liposome assisted drug delivery. *Frontiers in Pharmacology*. 2015;6:286.
4. Barenholz Y. Doxil® — The first FDA-approved nano-drug: Lessons learned. *Journal of Controlled Release*. 2012;160(2):117-34.
5. James ND, Coker RJ, Tomlinson D, Harris JRW, Gompels M, Pinching AJ, et al. Liposomal doxorubicin (Doxil): An effective new treatment for Kaposi's sarcoma in AIDS. *Clinical Oncology*. 1994;6(5):294-6.
6. Li X, Hirsh DJ, Cabral-Lilly D, Zirkel A, Gruner SM, Janoff AS, et al. Doxorubicin physical state in solution and inside liposomes loaded via a pH gradient. *Biochimica et Biophysica Acta (BBA) - Biomembranes*. 1998;1415(1):23-40.
7. Li T, Cipolla D, Rades T, Boyd BJ. Drug nanocrystallisation within liposomes. *Journal of Controlled Release*. 2018;288:96-110.
8. Cipolla D, Wu H, Salentinig S, Boyd B, Rades T, Vanhecke D, et al. Formation of drug nanocrystals under nanoconfinement afforded by liposomes. *RSC Advances*. 2016;6(8):6223-33.
9. Cipolla D, Wu H, Eastman S, Redelmeier T, Gonda I, Chan HK. Tuning ciprofloxacin release profiles from liposomally encapsulated nanocrystalline drug. *Pharmaceutical Research*. 2016;33(11):2748-62.
10. Toy R, Peiris PM, Ghaghada KB, Karathanasis E. Shaping cancer nanomedicine: the effect of particle shape on the in vivo journey of nanoparticles. *Nanomedicine*. 2014;9(1):121-34.
11. Champion JA, Mitragotri S. Role of target geometry in phagocytosis. *Proceedings of the National Academy of Sciences of the United States of America*. 2006;103(13):4930.
12. Doshi N, Mitragotri S. Macrophages recognize size and shape of their targets. *PLOS ONE*. 2010;5(4):e10051.
13. Gratton SEA, Ropp PA, Pohlhaus PD, Luft JC, Madden VJ, Napier ME, et al. The effect of particle design on cellular internalization pathways. *Proceedings of the National Academy of Sciences*. 2008;105(33):11613.

14. Pyrz WD, Buttrey DJ. Particle size determination using TEM: A discussion of image acquisition and analysis for the novice microscopist. *Langmuir*. 2008;24(20):11350-60.
15. Tiede K, Boxall ABA, Tear SP, Lewis J, David H, Hassellöv M. Detection and characterization of engineered nanoparticles in food and the environment. *Food Additives & Contaminants: Part A*. 2008;25(7):795-821.
16. Michen B, Geers C, Vanhecke D, Endes C, Rothen-Rutishauser B, Balog S, et al. Avoiding drying-artifacts in transmission electron microscopy: Characterizing the size and colloidal state of nanoparticles. *Scientific Reports*. 2015;5:9793.
17. Franken LE, Boekema EJ, Stuart MCA. Transmission electron microscopy as a tool for the characterization of soft materials: Application and interpretation. *Advanced science (Weinheim, Baden-Wurttemberg, Germany)*. 2017;4(5):1600476.
18. Friedrich H, Frederik PM, de With G, Sommerdijk NAJM. Imaging of self-assembled structures: Interpretation of TEM and cryo-TEM Images. *Angewandte Chemie International Edition*. 2010;49(43):7850-8.
19. Thompson RF, Walker M, Siebert CA, Muench SP, Ranson NA. An introduction to sample preparation and imaging by cryo-electron microscopy for structural biology. *Methods*. 2016;100:3-15.
20. Ohi M, Li Y, Cheng Y, Walz T. Negative staining and image classification – powerful tools in modern electron microscopy. *Biological Procedures Online*. 2004;6:23-34.
21. Almgren M, Edwards K, Karlsson G. Cryo transmission electron microscopy of liposomes and related structures. *Colloids and Surfaces A: Physicochemical and Engineering Aspects*. 2000;174(1):3-21.
22. Frederik PM, Hubert DHW. Cryoelectron microscopy of liposomes. *Methods in Enzymology*. 391: Academic Press; 2005. p. 431-48.
23. Milne JL, Borgnia MJ, Bartesaghi A, Tran EE, Earl LA, Schauder DM, et al. Cryo-electron microscopy-a primer for the non-microscopist. *The FEBS journal*. 2013;280(1):28-45.
24. Nogales E, Scheres SHW. Cryo-EM: A unique tool for the visualization of macromolecular complexity. *Molecular cell*. 2015;58(4):677-89.
25. Patterson JP, Xu Y, Moradi M-A, Sommerdijk NAJM, Friedrich H. CryoTEM as an advanced analytical tool for materials chemists. *Accounts of Chemical Research*. 2017;50(7):1495-501.

26. Kuntsche J, Horst JC, Bunjes H. Cryogenic transmission electron microscopy (cryo-TEM) for studying the morphology of colloidal drug delivery systems. *International Journal of Pharmaceutics*. 2011;417(1):120-37.
27. Mittal V, Matsko NB. *Analytical imaging techniques for soft matter characterization*: Springer Berlin Heidelberg; 2012.
28. Rice SB, Chan C, Brown SC, Eschbach P, Han L, Ensor DS, et al. Particle size distributions by transmission electron microscopy: an interlaboratory comparison case study. *Metrologia*. 2013;50(6):663-78.
29. Cipolla D, Blanchard J, Gonda I. Development of liposomal ciprofloxacin to treat lung infections. *Pharmaceutics*. 2016;8(1):6.
30. Schindelin J, Arganda-Carreras I, Frise E, Kaynig V, Longair M, Pietzsch T, et al. Fiji: an open-source platform for biological-image analysis. *Nature Methods*. 2012;9:676.
31. Deegan RD, Bakajin O, Dupont TF, Huber G, Nagel SR, Witten TA. Capillary flow as the cause of ring stains from dried liquid drops. *Nature*. 1997;389:827.
32. Boluk Y, Danumah C. Analysis of cellulose nanocrystal rod lengths by dynamic light scattering and electron microscopy. *Journal of Nanoparticle Research*. 2013;16(1):2174.
33. Mao Y, Liu K, Zhan C, Geng L, Chu B, Hsiao BS. Characterization of nanocellulose using small-angle neutron, X-ray, and dynamic light scattering techniques. *The Journal of Physical Chemistry B*. 2017;121(6):1340-51.
34. Garcia de la Torre JG, Bloomfield VA. Hydrodynamic properties of complex, rigid, biological macromolecules: theory and applications. *Quarterly reviews of biophysics*. 1981;14(1):81-139.
35. Broersma S. Rotational diffusion constant of a cylindrical particle. *The Journal of Chemical Physics*. 1960;32(6):1626-31.
36. Di Cola E, Grillo I, Ristori S. Small angle X-ray and neutron scattering: Powerful tools for studying the structure of drug-loaded liposomes. *Pharmaceutics*. 2016;8(2):10.
37. Wibroe PP, Ahmadvand D, Oghabian MA, Yaghmur A, Moghimi SM. An integrated assessment of morphology, size, and complement activation of the PEGylated liposomal doxorubicin products Doxil®, Caelyx®, DOXOrubicin, and SinaDoxosome. *Journal of Controlled Release*. 2016;221:1-8.
38. Pencer J, Hallett FR. Effects of vesicle size and shape on static and dynamic light scattering measurements. *Langmuir*. 2003;19(18):7488-97.





**Chapter 3 B: Controlling the size and shape of liposomal ciprofloxacin nanocrystals by varying the lipid bilayer rigidity and drug to lipid ratio**

## Controlling the size and shape of liposomal ciprofloxacin nanocrystals by varying the lipid bilayer rigidity and drug to lipid ratio

Tang Li<sup>a,b</sup>, Andrew J. Clulow<sup>b</sup>, Cameron J. Nowell<sup>c</sup>, Adrian Hawley<sup>d</sup>, David Cipolla<sup>e</sup>, Thomas Rades<sup>f</sup>, Ben J. Boyd<sup>a,b</sup>

<sup>a</sup> ARC Centre of Excellence in Convergent Bio-Nano Science and Technology, Monash Institute of Pharmaceutical Sciences, 381 Royal Parade, Parkville, Victoria 3052, Australia

<sup>b</sup> Drug Delivery, Disposition and Dynamics, Monash Institute of Pharmaceutical Sciences, 381 Royal Parade, Parkville, Victoria 3028, Australia

<sup>c</sup> Drug Discovery Biology, Monash Institute of Pharmaceutical Sciences, 381 Royal Parade, Parkville, Victoria 3028, Australia

<sup>d</sup> SAXS/WAXS beamline, Australian Synchrotron, ANSTO, 800 Blackburn Road, Clayton, Victoria 3169, Australia

<sup>e</sup> Insmad Inc., 10 FINDERNE AVE., BUILDING 10, BRIDGEWATER, NJ, USA

<sup>f</sup> Department of Pharmacy, Faculty of Health and Medical Sciences, University of Copenhagen, Universitetsparken 2, 2100 Copenhagen, Denmark

This manuscript was submitted to the Journal of Controlled Release.

### Abstract

Drug nanocrystals precipitated inside liposomes are of increasing interest in liposomal drug delivery. For the liposomal nanocrystal formulations, the size and shape of the drug nanocrystals can influence the apparent drug release properties, providing opportunities for developing tailored liposomal drug release systems. Small angle X-ray scattering and quantitative TEM can be used to analyse the size distributions of the nanoparticles. In this study, by controlling the liposomal bilayer rigidity through the use of different membrane phospholipids with varying cholesterol content, the impact of bilayer rigidity on the size distribution of ciprofloxacin nanocrystals was investigated using standard TEM and SAXS as orthogonal techniques. The results show that the phospholipid gel-to-liquid crystalline phase transition temperature has a direct effect on the nanocrystal size distribution, where shorter and thinner nanocrystals were formed in liposomes made from HSPC and DPPC phospholipids with higher phase transition temperatures than DMPC and DOPC with lower transition temperatures. The addition of cholesterol which increases the rigidity of the liposomal bilayer was also shown to restrict the growth of the ciprofloxacin nanocrystals. Moreover, increasing the drug loading of the

liposomes made from HSPC and DPPC phospholipid produced longer and wider nanocrystals. The findings open new opportunities to tailor nanocrystal size distributions, as well as the aspect ratio of the enclosing liposomes with potential to alter drug release and *in vivo* behaviour.

### 3B.1 Introduction

Nanoparticles such as liposomes have been widely used and researched as drug delivery carriers (1, 2). These lipid-based vesicles can encapsulate drugs of various physiochemical properties (3, 4) and reduce toxicity (5, 6). Although research has been focussed on the pharmacokinetics and drug release from different liposomal formulations, the physical state of the encapsulated active pharmaceutical ingredient is often overlooked, especially when the drug is precipitated as nanocrystals. The physical state of the drug inside the liposome is important as it can affect the stability of the encapsulated active as well as the apparent drug release rate from the liposomes (7). Doxil, the first FDA approved liposomal formulation forms doxorubicin sulfate nanocrystals inside the liposome upon active drug loading (8-10). Despite having been on the market for more than 20 years, the physical state of the encapsulated doxorubicin has only garnered more attention in recent years (11-13). Ciprofloxacin liposomes have shown promise in treating lung infections via inhalation delivery and the benefit of using liposomal inhaled antibiotics is the sustained drug release from liposome allows reduction of dosing frequency (14). A method to induce *in situ* nanocrystallisation of ciprofloxacin inside liposomes, where the nanocrystal growth is apparently limited by stretching of the liposome bilayer was also recently reported (15). It was shown that addition of surfactant can influence the shape and size of the ciprofloxacin nanocrystals inside liposomes and affect the *in vitro* drug release rate (16). The ability to control not only the physical state of the drug inside the liposome but also the shape and size of the drug nanocrystals within the liposomes provides great potential for development of tailored release liposomal delivery carriers.

It is crucial to effectively characterise and analyse the physical parameters of these nanoscale drug delivery systems, in this case the shape and size distribution of the drug nanocrystals inside the liposomes. Recently, we have developed a quantitative standard transmission electron microscopy (standard TEM) method to analyse large numbers of drug nanocrystals inside the liposome. The nanocrystal size distribution results were compared to cryogenic transmission electron microscopy (cryo-TEM), which allowed

visualisation of the nanocrystals and the liposome in its innate form (17-21). Standard TEM revealed similar crystal size distribution to cryo-TEM in the initial assessment of liposomal ciprofloxacin nanocrystals. TEM analysis provides more statistically powerful results with lower cost and faster data acquisition compared to the cryo-TEM method. The use of standard TEM enabled high throughput determination of the effect of different formulation parameters in controlling the growth of ciprofloxacin nanocrystals inside the liposomes (22).

Small angle X-ray scattering (SAXS) is another powerful technique that provides structural information on nanomaterials such as liposomes in the 1 to 300 nm size range (23-25). The use of SAXS together with wide angle X-ray scattering (WAXS) to examine the PEGylated liposomal doxorubicin allowed both accurate modelling of the scattering curve and determination of the crystalline state of doxorubicin (11). In addition, one study also showed good agreement between SAXS and TEM results in determining the size distribution of CoPt<sub>3</sub> nanocrystals (26). The benefits of SAXS include its fast acquisition time and ease in measurement of native samples. However, when analysing nanoparticles with broad size distributions or heterogeneous and complicated inner structures, it would require previous knowledge of the morphology of the sample (23).

## 3B.2 Hypotheses and aims

Hypotheses:

That the dimensions of the liposomal drug nanocrystals can be altered by formulation parameters, namely the lipid composition (to control bilayer rigidity) and the drug to lipid concentration. And that increasing the bilayer rigidity will limit the growth of the nanocrystals inside the liposome.

In order to investigate these hypotheses, the following aims will be achieved:

1. To prepare liposomal ciprofloxacin nanocrystals containing phospholipids with varying phase transition temperatures (27) and altering cholesterol content within the lipid bilayer (28, 29) in order to modify the liposomal bilayer rigidity.
2. Determine the effect on the shape and size distribution of nanocrystals formed under the constraint of liposomes with different rigidity using standard TEM and SAXS.

3. To investigate the influence of the amount of drug loaded with respect to the phospholipid concentration, known as the drug to lipid (D/L) ratio on the size distribution of the ciprofloxacin nanocrystals within different liposomal formulations.

## 3B.3 Materials and Methods

### 3B.3.1 Materials

Hydrogenated soy phosphatidylcholine (HSPC), 1,2-dipalmitoyl-sn-glycero-3-phosphocholine (DPPC) and 1,2-dimyristoyl-sn-glycero-3-phosphocholine (DMPC) were obtained from Lipoid GmbH (Ludwigshafen, Germany). 1,2-Dioleoyl-sn-glycero-3-PC (DOPC) was purchased from Cayman Chemical Company (Michigan, USA). Tris maleate (reagent grade), ammonium sulfate (>99%), cholesterol (>99%), L-histidine ( $\geq 99\%$ ) and sucrose (>99.5%) were purchased from Sigma Aldrich (St. Louis, MO, USA). Calcium chloride (>99%) and sodium hydroxide pellets (reagent grade) were obtained from Ajax Finechem (Seven Hills, NSW, Australia). Sodium chloride (>99%), ciprofloxacin hydrochloride monohydrate were purchased from Chem Supply (Gillman, SA, Australia). Sodium azide was purchased from Merck Schuchardt OHG (Eduard-Buchner-StraÙe, Hohenbrunn, Germany). Hydrochloric acid 36% (analytical grade) was purchased from Biolab Aust Ltd (Clayton, VIC, Australia). The water used was sourced from a Millipore water purification system using a Quantum™ EX Ultrapure Organex cartridge (Millipore, Australia).

### 3B.3.2 Sample preparation

Liposomes of different phospholipid composition (see **Table 1**) were prepared by dissolving DOPC/DMPC/DPPC/HSPC and cholesterol at a 1.0 : 0.87 molar ratio in chloroform. Liposomes of different cholesterol contents were prepared by dissolving DOPC and cholesterol at 1.0 : 0.0, 1.0 : 0.25, 1.0 : 0.50, and 1.0 : 0.87 molar ratio (which represents 0, 11, 20 and 30 wt % cholesterol) in chloroform (also **Table 1**). The lipid mixtures were then dried with nitrogen gas for 3 hours and residual solvent was extracted by placing the mixture under vacuum at 50 °C overnight. The dried lipid film was hydrated with 500 mM ammonium sulfate pH 3.0 solution to obtain a 10% w/w lipid dispersion and incubated at 60 °C for 30 minutes before vortex mixing to form a coarse dispersion (multilamellar liposomes). The lipid dispersions were then extruded 20 times through 0.1 µm polycarbonate membrane filters (Nucleopore®, Whatman, USA) using an extruder

Chapter 3B: Controlling the size and shape of liposomal ciprofloxacin nanocrystals by varying the lipid bilayer rigidity and drug to lipid ratio

(Avanti Polar Lipids Inc, Alabaster, USA) to generate unilamellar vesicles. To perform active drug loading, the external medium of each formulation was dialfiltrated with 10 volumes of 5 mM histidine buffer (pH 6.0) containing 145 mM NaCl and 6 mM NaN<sub>3</sub> using a 10 mL Amicon<sup>®</sup> stirred ultrafiltration cell (Merck, Australia) through Ultracel<sup>®</sup> 30 kDa regenerated cellulose ultrafiltration discs, diameter 25 mm (EMD Millipore Corporation, Billerica, MA, USA). The dialfiltrated liposomes were analysed for the lipid concentration using the Wako Phospholipid C assay kit (FUJIFILM Wako Diagnostics U.S.A). Ciprofloxacin solutions at the required drug to lipid (D/L) molar ratios were prepared in water and were used for drug loading by mixing the pre-prepared drug solution and dialfiltrated liposome solution at 1:1 v/v ratio (**Table 1**). The liposome and drug mixtures were then vortex mixed and stored at 60°C oven for an hour to complete drug loading.

**Table 1.** Table of liposomal ciprofloxacin nanocrystal formulations prepared for this study

<b>Effect Studied</b>	<b>Lipid composition (phospholipid : cholesterol mol ratio)</b>	<b>D/L mol ratio</b>
<b>Effect of Lipid composition</b>	DOPC : Chol (1.0 : 0.87)	0.6
	DMPC : Chol (1.0 : 0.87)	0.6
	DPPC : Chol (1.0 : 0.87)	0.6
	HSPC : Chol (1.0 : 0.87)	0.6
<b>Effect of Cholesterol Content</b>	DOPC : Chol (1.0 : 0.0) = 0 wt% cholesterol	0.6
	DOPC : Chol (1.0 : 0.25) = 11 wt% cholesterol	0.6
	DOPC : Chol (1.0 : 0.50) = 20 wt% cholesterol	0.6
	DOPC : Chol (1.0 : 0.87) = 30 wt% cholesterol	0.6
<b>Effect of Drug to Lipid ratio</b>	DOPC : Chol (1.0 : 0.87)	0.3
		0.9
	DPPC : Chol (1.0 : 0.87)	0.3
		0.9
	HSPC : Chol (1.0 : 0.87)	0.3
		0.9

To generate liposomal ciprofloxacin nanocrystals, the drug-loaded liposomes were diluted 4-fold with 50 mM Tris maleate buffer (pH 6.0 containing 5 mM CaCl<sub>2</sub>.2H<sub>2</sub>O, 150 mM NaCl and 6 mM NaN<sub>3</sub>) containing 180 mg/mL sucrose. The prepared dispersions were

injected into rectangular borosilicate glass capillaries 0.40 x 8.00 mm ID (VitreCom, Mountain Lakes, NJ, USA) enclosed with Blu-Tak for the freeze-thawing cycle. The formulations were first snap frozen in liquid nitrogen for 5 minutes and then thawed at 20°C. After thawing was completed, the samples were withdrawn from the capillaries and stored in glass vials before standard TEM or SAXS analysis. The use of the rectangular borosilicate glass capillaries for the freeze-thawing process provided a high surface area for effective snap freezing in liquid nitrogen. The drug loaded liposomes were stored at 4°C and freeze-thawing processes were performed one day prior to analytical measurements.

### 3B.3.3 Cryogenic transmission electron microscopy (cryo-TEM)

Copper grids (200 mesh) with Lacey formvar/carbon film (ProSciTech, Qld, Australia) were glow discharged at 30 mA, 0.38 mBar in nitrogen gas for 45 seconds using the Pelco easiGlow glow discharge cleaning system (Ted Pella, Inc. CA, USA) to ensure a hydrophilic supporting substrate. The treated grids were then fixed onto the FEI Vitrobot setting at 100% humidity and temperature of 4°C for sample loading. An aliquot (2 µL) of each sample was pipetted onto a grid and the blotting conditions were set at blot force setting at -2, blot time at 2.5 s, blot total setting at 1, wait time and drain time 0 s. The Vitrobot then plunged the sample-loaded grids into liquid ethane cooled by liquid nitrogen. Frozen grids were stored in liquid nitrogen until required.

The samples were examined using a Gatan cryoholder (Gatan, Pleasanton, CA, USA) and FEI Tecnai 12 Transmission Electron Microscope (FEI, Oregon, USA) at an operating voltage of 120 kV. At all times low dose procedures were followed.

### 3B.3.4 Standard transmission electron microscopy (standard TEM)

Continuous carbon-only TEM grids on 400 or 200 mesh (ProSciTech Pty.Ltd, Australia) were plasma cleaned for 2 minutes in oxygen/argon gas using the Solarus Plasma Cleaner (Gatan, Inc. CA, USA). An aliquot (2 µL) of the sample was pipetted onto each grid and 1 minute adsorption time was allowed. Grids were blotted manually using Whatman 541 filter paper to absorb the excess liquid on the grids. The grids were then left to air dry at room temperature for 10 minutes. The samples were examined using a Tecnai single tilt holder and FEI Tecnai G2 T20 microscope (200 kV) (FEI, Oregon, USA) and

images were recorded at magnification of 13000x, objective aperture 1, defocus of -20  $\mu\text{m}$  and 2 seconds exposure.

### 3B.3.5 Small angle x-ray scattering (SAXS) measurements and analysis

SAXS measurements were performed at the Small and Wide Angle X-ray Scattering (SAXS/WAXS) beamline of the Australian Synchrotron (30). The autoloader sample environment developed at the Australian Synchrotron was used for all measurements at the ambient temperature of the SAXS/WAXS experimental hutch, which is typically approximately 27 °C. Liposome samples were loaded into 96-well plates covered with a silicone mat to prevent evaporation. The samples were drawn one at a time into a quartz capillary held stationary in the beam and up to 32 scattering measurements were performed as the solution was drawn into and then ejected from the capillary back into the sample well. The capillary was then washed with water and 2% Helmanex® detergent solution. The capillary was filled with water and the background scattering from the water-filled capillary was recorded to monitor capillary contamination due to beam damage prior to the next sample being measured, which was observed to be negligible by comparing the water/capillary shots from earlier in the series of measurements. The average of the water/capillary scattering profiles recorded throughout the course of the measurements was used as a background that was subtracted from the scattering profiles of the liposomal samples. X-ray scattering was recorded at two sample-to-detector distances: 7159 mm with a photon energy of 12 keV (wavelength  $\lambda = 1.033 \text{ \AA}$ ) and scattering at higher-Q values was recorded with a sample-detector distance of 956 mm with a photon energy of 12 keV, respectively. 2D scattering patterns were radially integrated into plots of scattered X-ray intensity  $I(Q)$  versus the scattering vector  $Q [= (4\pi/\lambda)\sin\theta$ , where  $2\theta$  is the scattering angle] using the in-house developed software package ScatterBrain. The scattering function was plotted on an absolute scale with units of  $\text{cm}^{-1}$  using the scattering from water as a standard. The scattering profiles of drug-loaded but not freeze-thawed (w/o nanocrystal) liposomes and drug-loaded freeze-thawed (with nanocrystal) liposomes from the same batch of sample were recorded for comparison.

The low- and high-Q data were stitched together using the IRENA data analysis suite (Version 2.61) in the IgorPro 7 environment, which was also used to determine the size distributions of the ciprofloxacin nanocrystals using the inbuilt Size Distribution macros (31). The Maximum Entropy method was used to generate a size distribution from the recorded SAXS data by solving the equation

$$I(Q) = |\Delta\rho|^2 \sum_{r_{\min}}^{r_{\max}} |F(Q, r)|^2 V^2(r) NP(r) \Delta r$$

where  $\Delta\rho$  is the scattering length density contrast between the particle and the medium (set to an arbitrary value of 1 for the modelling herein as the size distributions were subsequently normalised),  $r_{\max}$  and  $r_{\min}$  are the maximum and minimum particle dimensions modelled by the software,  $\Delta r$  is the bin size of the size distribution histogram,  $F(Q, r)$  is the particle form factor,  $V(r)$  is the particle volume,  $N$  is the total number of particles and  $P(r)$  is the probability that a particle will be present with the associated dimension  $r$ .

In the modelling associated with this work the form factor used was the Unified rod model first described by Beaucage (32, 33), The form factor is given by

$$|F(Q)|^2 = \exp\left\{-\frac{Q^2 R_{g2}^2}{3}\right\} + \frac{\pi}{lQ_2^*} \exp\left\{-\frac{Q^2 R_{g1}^2}{3}\right\} + \frac{2r}{3l} \exp\left\{-\frac{Q^2 R_{g1}^2}{3}\right\} + \frac{4(l+r)}{(r^3 l^2) Q_1^{*4}}$$

where  $r$  is the radius of the rod cross section,  $l$  is the rod length,

$$R_{g1} = \sqrt{3} \frac{r}{2}, \quad R_{g2} = \sqrt{\frac{r^2}{2} + \frac{l^2}{12}} \quad \text{and} \quad Q_n^* = \frac{Q}{\text{erf}\left\{\left(\frac{QR_{gn}}{\sqrt{6}}\right)\right\}^3} \quad \text{where } n = 1 \text{ or } 2.$$

The output given by the fitting software was in the form of a volume distribution function of rod cross-sectional diameters for a pre-defined aspect ratio (length/diameter). Aspect ratios between 2.0 and 5.0 were tested in 0.5 intervals to determine which gave the best fit to the recorded data. As the maximum entropy method only converges when the  $X^2$  value for the fit equals the number of points fitted, all fit curves were of the same quality in terms of the  $X^2$  value and this final quality check was performed by visually comparing the fit curves produced with the recorded data. As described in the IRENA manual, an error multiplier was required to allow the maximum entropy-fitting algorithm to converge and these were between 2 and 4 in most cases. The maximum and minimum diameters modelled were set to 1500 and 50 Å, respectively, with 100 logarithmic bins between these limits used to generate volume distribution functions. These functions were normalised to make the area under the histogram curve equal to 1. The volume distribution functions were subsequently converted to number distribution functions for comparison with the size distribution analysis of the TEM images. This was done by dividing each point in the histogram by the diameter cubed and renormalising the resulting number distribution functions. The normalised number distributions were plotted as cumulative distributions to

ascertain the median particle diameter and the first and third quartile diameters. The corresponding rod lengths were determined by multiplying the diameters by the optimum aspect ratios determined from the fitting process.

### 3B.3.6 Particle size analysis from RT-TEM images

Standard TEM images were analysed with Fiji (Fiji is just Image J) (34) to determine the size distribution of the nanocrystals. The selected nanocrystals within each image were manually highlighted with the wand tool and the ROI manager function. The length and width measurements (nm) of highlighted nanocrystals were then automatically generated through an in-house developed macro script (Available for download in the supplementary information). This script allows the large number of selected nanocrystals to be highlighted on the TEM image and automatic generation of the lengths and widths of the selected crystals. The length and width results were then exported to an Excel spreadsheet and the aspect ratios were then calculated as a ratio of length to width. The measurement results were then visualised in r studio, where boxplots comparing the lengths, widths (cross-sectional diameters) and aspect ratios of different samples were generated. One-way analyses of variance (ANOVA) were used to determine whether there were any statistically significant differences between different samples in terms of the lengths, widths and aspect ratios of the nanocrystals formed inside the liposome.

## 3B.4 Results and Discussion

### 3B.4.1 Effect of lipid composition on the size and shape of the ciprofloxacin nanocrystals

Standard TEM and cryo-TEM images of liposomal ciprofloxacin nanocrystals grown in liposomes comprising the different phospholipids are shown in **Figure 1** (phospholipid to cholesterol mol ratio = 1.0 : 0.87). Three saturated phospholipids (DMPC, DPPC and HSPC) were chosen where DMPC has two C14:0 acyl chains ( $T_m = 23^\circ\text{C}$  (35)), DPPC has two C16:0 acyl chains ( $T_m = 42.37^\circ\text{C}$  (36)) and HSPC has a mixture of C16:0 and C18:0 acyl chains with a mol ratio of 12:88 ( $T_m = 53.72^\circ\text{C}$  (36)). In addition, the unsaturated phospholipid DOPC with two C18:1 acyl chains ( $T_m = -16.5^\circ\text{C}$  (37)) was also used. The differences in the hydrocarbon chain lengths of the phospholipids contribute to the differences in their transition temperatures. The longer the hydrocarbon chains, the stronger the Van der Waal interactions, therefore more energy is required to disrupt the

## Chapter 3B: Controlling the size and shape of liposomal ciprofloxacin nanocrystals by varying the lipid bilayer rigidity and drug to lipid ratio

ordered packing, hence a higher transition temperature (35, 38, 39). The degree of unsaturation also affects the transition temperature since kinks in the hydrocarbon chains introduced by *cis*-double bonds prevent the tight packing in the gel state which reduce the lipid's transition temperature (35). The cryo-TEM images confirm that the ciprofloxacin nanocrystals were formed inside the liposomes rather than outside. In this study, a minimum of 500 nanocrystals was measured using the standard TEM technique and only 500 quantitative results per sample were used for data analysis.

The standard TEM and cryo-TEM images (**Figure 1**) showed that as the transition temperature of the phospholipid was increased, the size of the ciprofloxacin nanocrystals decreased. The boxplots in **Figure 1 panel i-k** show the quantitative analysis for the ciprofloxacin nanocrystals formed inside liposomes composed of the different phospholipids.

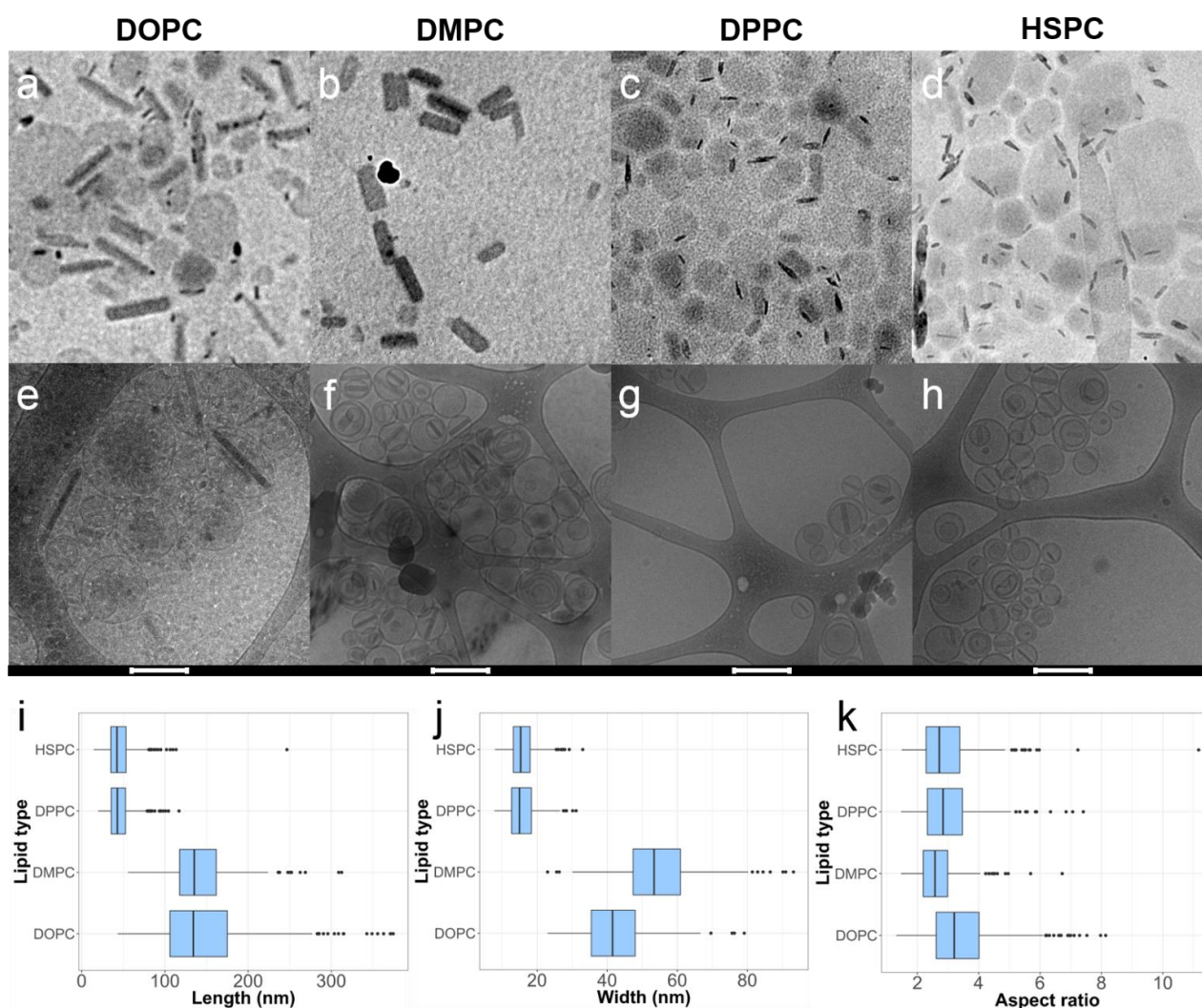


**Figure 1.** Standard TEM (a-d) and cryo-TEM (e-h) images of liposomal ciprofloxacin nanocrystals made from different lipid compositions. DOPC:Chol (1.0 : 0.87) liposomes with ciprofloxacin nanocrystals (a,e), DMPC:Chol (1.0 : 0.87) liposomes with ciprofloxacin nanocrystals (b,f),

### Chapter 3B: Controlling the size and shape of liposomal ciprofloxacin nanocrystals by varying the lipid bilayer rigidity and drug to lipid ratio

DPPC:Chol (1.0 : 0.87) liposomes with ciprofloxacin nanocrystals (c,g), and HSPC:Chol (1.0 : 0.87) liposomes with ciprofloxacin nanocrystals (d,h). Boxplots of standard TEM results showing nanocrystal particle length (i), width (j) and aspect ratio (k) distributions for different lipid composition. The outliers are presented as scattered black dots where the results are outside one-and-a-half times the interquartile range. The scale bars for the standard TEM and cryo-TEM images represents 200 nm in length.

The length measurements for the nanocrystals showed DOPC and DMPC liposomes produced significantly longer nanocrystals ( $p < 0.001$ ) compared to DPPC and HSPC liposomes. There were no significant differences to the length measurements between HSPC and DPPC ( $p = 0.9997$ ) and between DOPC and DMPC ( $p = 0.2544$ ). For the nanocrystal width, there was no significant difference between HSPC and DPPC ( $P = 0.9983$ ), but DMPC and DOPC liposomes have significantly wider ( $p < 0.001$ ) nanocrystals than DPPC and HSPC liposomes. From the ANOVA results, the aspect ratios of the nanocrystals showed statistically significant differences ( $p < 0.001$ ) between the different liposomes apart from that between the HSPC and DPPC liposomes ( $p = 0.8995$ ). Although looking at the raw values (Table S1), the medians of the aspect ratio for the different samples are in the close range of 2.57-3.20. It is also evident that DOPC liposomes generated nanocrystals with higher aspect ratios.

The difference in the lengths and widths of the nanocrystals formed in the different liposomes appear to be influenced by the lipid transition temperature from the rigid gel phase to the more fluidic liquid crystalline phase. The membrane elastic modulus (rigidity of the membrane) is much higher at or below the phase transition temperature than that above the phase transition temperature for saturated phospholipids (27, 40). Reviewing the sample preparation method for generating ciprofloxacin nanocrystals inside the liposomes, it is important to remember that the intraliposomal crystallisation is hypothesised to have occurred during the thawing process of the freeze-thaw procedure (15, 41). Since the liposomal ciprofloxacin formulations were thawed at ambient temperature ( $20^{\circ}\text{C} \pm 2^{\circ}\text{C}$ ), this temperature is roughly the same as the transition temperature of DMPC and is well above the transition temperature of DOPC. This means that at this thawing temperature, liposomes containing these phospholipids are in a more fluid state with lower membrane elastic modulus compared to DPPC and HSPC. On the other hand, the lipids with the higher phase transition temperatures (DPPC and HSPC) are in a more rigid gel state at ambient temperature with low membrane fluidity. The high

elastic modulus (rigidity) of the membrane was hypothesised to impart greater restrictions on the growth of the ciprofloxacin nanocrystals inside the liposome. Hence, the observation that shorter and thinner crystals were formed inside the HSPC and DPPC liposomes compared to those formed inside the DOPC and DMPC liposomes supports this hypothesis.

As an orthogonal technique to microscopy, SAXS was also conducted on the ciprofloxacin nanocrystals inside the liposomes. The detailed SAXS results can be found in the online supporting information. The SAXS profiles of liposomes were measured before and after freeze-thawing to observe the differences between the nanocrystallised and non-crystallised ciprofloxacin liposomes from the same preparation batch. There was little difference in the high-Q scattering features after freeze-thawing liposomes comprising DMPC, DPPC and HSPC, the lipids with higher transition temperatures. This indicated that the structure of the liposome bilayers were not significantly altered by the freeze-thawing/crystallisation process and subsequent liposome stretching by the growing ciprofloxacin nanocrystals. There was also an increase in the scattered X-ray intensity at low-Q resulting from the formation of the drug nanocrystals. It was deemed that the additional scattered intensity at low-Q as shown by the difference in scattering between the nanocrystallised and non-crystallised ciprofloxacin liposomes (electronic supporting information) came from the drug nanocrystals in the DMPC, DPPC and HSPC liposomes.

The size distributions of the ciprofloxacin nanocrystals were then estimated from the difference profiles using the IRENA analysis software assuming rod-like particles with a fixed aspect ratio and the results obtained from standard TEM and SAXS are compared in **Figure 3** (For the numerical values presented in **Figure 3** please see electronic supporting information, Table S1). It should be noted that given that the aspect ratio in the SAXS data modelling must be fixed at the beginning of the modelling procedure, a number of aspect ratios between 2.0 and 4.0 were used for modelling and the one that gave the best visual fit to the data was chosen to provide the final size distribution. Furthermore, the IRENA software provides the size distribution as a volume distribution and this was converted to a number distribution for comparison with the TEM data as described in the Experimental section. The length and width distributions for the DPPC and HSPC liposomes generally showed good agreement between the standard TEM technique and the SAXS measurements, with the SAXS measurements yielding slightly narrower size distributions compared to the results obtained from standard TEM. However, the size distributions produced by the TEM and SAXS analyses were not in agreement for the DMPC

liposomes, for which the standard TEM results showed a much greater lengths and widths compared to the corresponding SAXS results. The potential reasons behind this disparity will be discussed after further comparisons have been drawn between SAXS and TEM size distributions in the following sections.

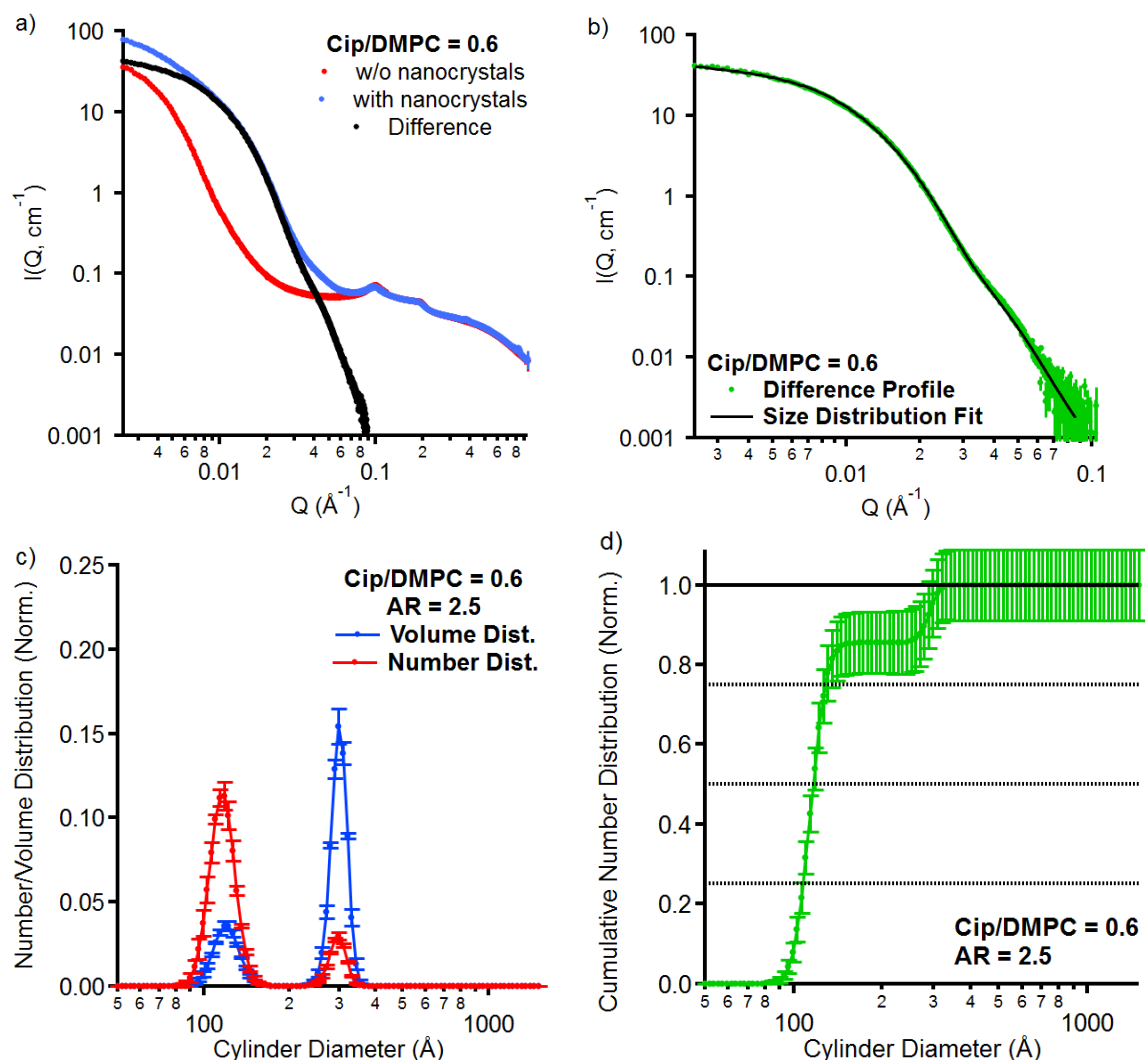


**Figure 2.** Process of analysis of the SAXS data collected. a) SAXS profiles of liposomes with (blue) and without (w/o, red) ciprofloxacin nanocrystals and the difference between them due to the presence of the nanocrystals (black). b) Size distribution fitting of the difference profiles. c) Volume (blue) and number (red) distributions of cylinder diameter generated using the IRENA size distribution fitting algorithm and normalised so that the area under curve = 1.0, AR = modelled aspect ratio. d) The corresponding cumulative number distribution used to determine the upper/lower quartile and median cylinder diameters (intercepts with dotted horizontal lines).

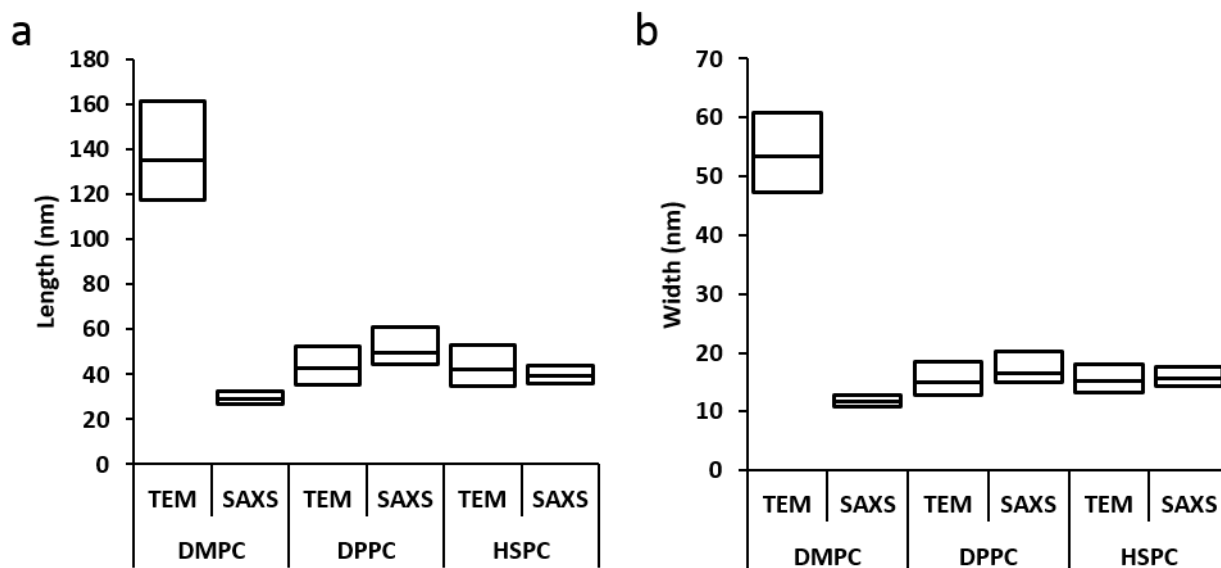


**Figure 3.** Box plots comparing the size distribution of the length (a) and width (b) measurements of the ciprofloxacin nanocrystals formed inside liposomes made from DMPC: Chol, DPPC/Chol and HSPC/Chol (PL/Chol = 1.0 : 0.87) obtained from standard TEM (TEM) and SAXS techniques.

### 3B.4.2 Effect of cholesterol content on the size and shape of the ciprofloxacin nanocrystals

To explore the effect of cholesterol content within the liposomal bilayer on the growth of the ciprofloxacin nanocrystals, the phospholipid with the lowest phase transition temperature (DOPC) was chosen as a model system as these were likely to have the most deformable outer bilayers of the phospholipids studied. The TEM images presented in **Figure 1** revealed that for liposomes composed of phospholipids with lower phase transition temperatures (e.g. DOPC and DMPC), the ciprofloxacin nanocrystals grew further in both length and width directions. This resulted in significantly longer and wider nanocrystals compared to liposomes made from phospholipids with higher phase transition temperatures (DPPC, HSPC). It has been reported that the addition of cholesterol can reduce the passive permeability of neutral solutes through lipid bilayers (42) and that cholesterol can also reduce the mobility of the phospholipid chains in the gel state (43, 44). Crucially, increasing the cholesterol content in phospholipid bilayers is also reported to increase the elastic modulus, thereby making the bilayer more rigid (28, 29). Hence by reducing the amount of cholesterol in the liposome bilayer from DOPC : Chol mol ratio of 1.0 : 0.87 (this is equivalent to the DOPC: Chol liposomes studied in Section 3.1.) to 1.0 : 0.0 mol ratio, this would reduce the elastic modulus (rigidity) of the lipid bilayer.

**Figure 4 (panel a-d)** shows the standard TEM images of ciprofloxacin nanocrystals grown inside DOPC liposomes with different cholesterol contents. Visually the nanocrystals look much longer and wider for the DOPC liposomes without cholesterol in the liposome bilayers. In the absence of cholesterol, there were far fewer nanocrystals present in each TEM grid and the crystal size was much larger compared to formulations that contained cholesterol. This resulted in the analysis of fewer crystals (100 nanocrystals compared to more than 500 nanocrystals for other samples) but the number of crystals analysed was still statistically significant. It was hypothesised that this was due to the fragility of the soft DOPC liposomes without cholesterol and that during the freeze-thaw process, the growth of nanocrystals ruptured the liposomal membrane producing large crystals dispersed in the bulk aqueous phase. This hypothesis was supported by the SAXS profiles measured for the DOPC/Chol liposomes (**Figure 5**). The peaks observed around  $Q = 0.1\text{--}0.2 \text{ \AA}^{-1}$  result from scattering from the liposome bilayer membrane. In all samples with DOPC/Chol bilayers, there was an observed decrease of the intensity of these features after nanocrystal growth, which indicates that the bilayer structure was being disrupted. This was not the case with the DMPC-, DPPC- and HSPC-based liposomes, whose bilayer structures appeared to be robust to nanocrystal growth. The decrease in intensity of the DOPC bilayer features was most pronounced in the case where there was no cholesterol in the phospholipid bilayer, with an almost complete loss of the intensity of this feature. Furthermore, the low  $Q$  feature corresponding to the larger structural features in the system (the liposome shell and the nanocrystals) moved to lower  $Q$  after freeze-thawing when no DOPC was present in the bilayer, which suggests that the nanocrystals formed were much larger than the original liposome size. All of these pieces of evidence are consistent with the bursting of DOPC bilayer membranes in the absence of cholesterol when the nanocrystals grow. Because of the extreme distortion of the bilayer membranes by the growth of the nanocrystals inside DOPC-based liposomes, subtraction of the scattering patterns of non-crystallised liposomes from those of the nanocrystallised liposomes would likely not be a meaningful background subtraction and so the full size distribution analysis of the SAXS data was not attempted with this system.

Quantitative measurements of the size distributions from the TEM images are presented as boxplots in **Figure 4 (panels e-g)**. The results showed that DOPC liposomes with no cholesterol afforded significantly longer nanocrystals than those that contain cholesterol ( $p < 0.0001$ ). With DOPC : Chol mol ratio of 1.0 : 0.25, the nanocrystal lengths were significantly longer than those at DOPC : Chol 1.0 : 0.50 mol ratio ( $p < 0.0001$ ) and at

### Chapter 3B: Controlling the size and shape of liposomal ciprofloxacin nanocrystals by varying the lipid bilayer rigidity and drug to lipid ratio

DOPC : Chol 1.0 : 0.87 mol ratio ( $p < 0.0001$ ). DOPC liposomes with 0.50 mol ratio of cholesterol also produced significantly longer nanocrystals than liposomes with 0.87 mol ratio of cholesterol ( $p < 0.01$ ). This is consistent with the hypothesis that decreasing the cholesterol content in the bilayer results in ciprofloxacin nanocrystals that can stretch the bilayer further to grow longer. In addition, with increasing cholesterol content the polydispersity of the nanocrystal lengths was also reduced (see electronic supporting information, Table S2).

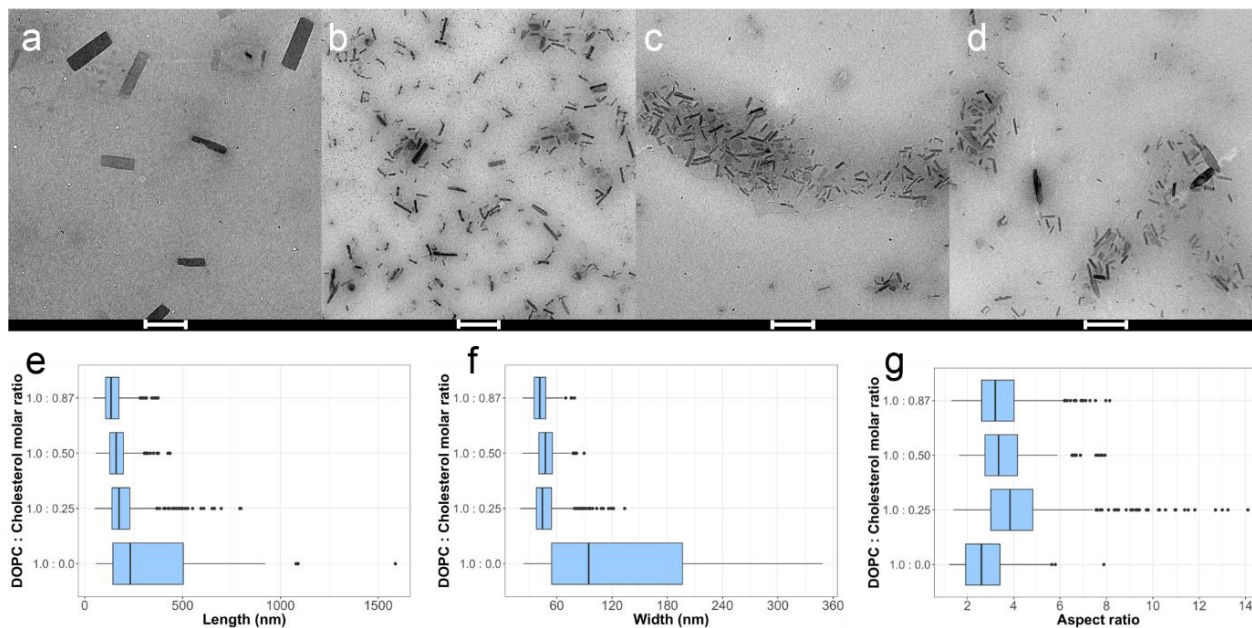


**Figure 4.** Standard TEM (a-d) of liposomal ciprofloxacin nanocrystals prepared using DOPC liposomes with increasing mol ratio of cholesterol. The formulations included (a) DOPC with no cholesterol (1.0 : 0.0), (b) Liposomal ciprofloxacin with DOPC : Chol at 1.0 : 0.25 mol ratio bilayer composition, (c) DOPC : Chol at 1.0 : 0.50 mol ratio and (d) DOPC : Chol at 1.0 : 0.87 mol ratio. Boxplots of standard TEM results showing nanocrystal particle length (e), width (f) and aspect ratio (g) distributions for DOPC liposomes with increasing mol ratio of cholesterol. The scale bars for the standard TEM represents 200 nm in length.

Chapter 3B: Controlling the size and shape of liposomal ciprofloxacin nanocrystals by varying the lipid bilayer rigidity and drug to lipid ratio

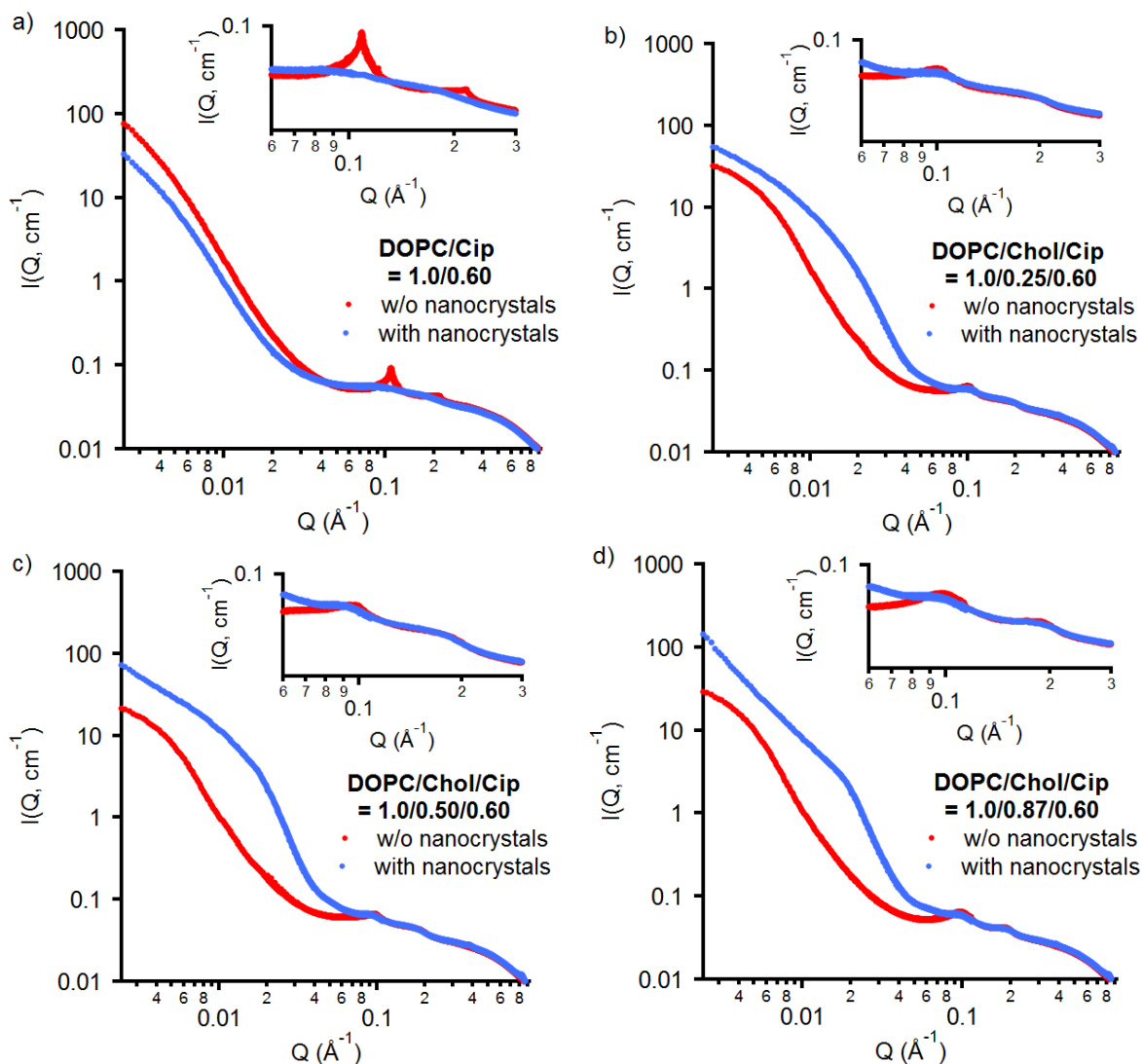


**Figure 5.** SAXS profiles of DOPC-based liposomes loaded with ciprofloxacin (DOPC/Ciprofloxacin = 1.0:0.60) and increasing amounts of cholesterol. Non-crystallised liposomes (red profiles) were actively loaded with ciprofloxacin prior to freeze-thawing and nanocrystallised liposomes (blue profiles) were freeze-thawed to initiate crystallisation. Insets highlight the changes in scattering intensity occurring in the high Q scattering feature associated with the bilayer membrane surrounding the liposomes.

Considering the width measurements, the DOPC liposomes with no cholesterol produced significantly wider nanocrystals compared to those that contained cholesterol ( $p < 0.0001$ ). Liposomes with DOPC : Chol 1.0 : 0.87 mol ratio resulted in significantly thinner nanocrystals compared to liposomes with DOPC : Chol 1.0 : 0.25 mol ratio ( $p < 0.01$ ) and DOPC : Chol 1.0 : 0.50 mol ratio ( $p < 0.01$ ). However, there were no statistical differences observed between the widths of nanocrystals grown in DOPC liposomes with mol ratio of 0.25 and 0.50 ( $p = 0.99996$ ). This shows that the addition of cholesterol can

restrict the growth of the nanocrystals and that at higher cholesterol contents, growth restrictions are observed in both the direction of length and width. Again, these results are in good agreement with the membrane rigidity hypothesis proposed. Increasing the cholesterol content in the lipid bilayers results in an increase of the membrane rigidity (or elastic modulus) and restricts the ciprofloxacin nanocrystal growth during the freeze-thaw process.

### 3B.4.3 Effect of drug to lipid ratio on the size and shape of the ciprofloxacin nanocrystals

For liposomal ciprofloxacin formulations prepared using different phospholipids, the drug to lipid ratio was also modified to investigate the effect of drug concentration on the growth of the nanocrystals inside the liposomes. The quantitative size distributions provided by standard TEM analysis are presented as boxplots in **Figure 6**. Significant disruption of the DOPC-based bilayer membranes was again evident in the SAXS profiles of these samples (as described in the previous section) and as such a full size analysis was not possible using the SAXS profiles as the non-crystallised liposome profile no longer represented a suitable background for subtraction of the scattering intensity from the liposomes themselves (Figure S8 in the electronic supporting information). For DOPC liposomes with a low D/L ratio of 0.3, the length of the nanocrystals was significantly shorter than formulations with a D/L ratio of 0.6 ( $p < 0.01$ ) and 0.9 ( $p < 0.05$ ). At the higher D/L ratio (0.6 and 0.9), there were no statistical differences in the observed nanocrystal lengths. When comparing the nanocrystal widths, the DOPC liposomes with D/L ratio of 0.6 afforded significantly thinner nanocrystals than D/L ratio of 0.9 ( $p < 0.05$ ). However, the liposomes with a D/L ratio of 0.3 resulted in a significantly wider nanocrystals compared to that at higher D/L ratios ( $p < 0.0001$ ).

The same batch of DMPC liposomes with a D/L ratio of 0.9 was not studied due to sample showing obvious bulk external precipitation upon drug loading. However the difference in both length and width between DMPC liposomes with D/L ratios of 0.3 and 0.6 was clear and statistically significant. At the lower D/L ratio of 0.3, the observed nanocrystals were significantly shorter and thinner compared to those at higher D/L ratio of 0.6 ( $p < 0.001$ ). For DPPC liposomes, the nanocrystals formed at highest D/L ratio of 0.9 were significantly longer and wider than those formed at lower D/L ratios of 0.6 and 0.3 ( $p < 0.0001$ ). No significant differences in the widths of the nanocrystals were observed

### Chapter 3B: Controlling the size and shape of liposomal ciprofloxacin nanocrystals by varying the lipid bilayer rigidity and drug to lipid ratio

between the lower D/L ratios of 0.6 and 0.3 ( $p=0.6638$ ), however, liposomes with a D/L ratio of 0.3 contained slightly longer nanocrystals than liposomes with D/L of 0.6 ( $p<0.01$ ).

Finally, HSPC liposomes with D/L ratios of 0.3 and 0.6 produced nanocrystals with no significant differences in their lengths ( $p=0.4223$ ). Liposomes with a D/L ratio of 0.9 produced significantly longer nanocrystals compared to liposomes with D/L ratio of 0.3 and 0.6 ( $p<0.0001$ ). Liposomes at all D/L ratios produced nanocrystals that had significant differences in width ( $p<0.001$ ) with a general trend for increasing nanocrystal width with increasing ciprofloxacin/HSPC ratio.

Comparing these results, the effect of increasing the D/L ratio increased the extent of nanocrystal growth in both length and width directions for the more intrinsically rigid phospholipids (DPPC and HSPC). This trend was not observed with the more flexible bilayers made from DOPC. This could be that for the softer lipid, the nanocrystals have already grown to form longer and wider nanocrystals due to low rigidity of the membrane. The growth of the nanocrystals within the DOPC liposomes had apparently plateaued and was independent of the drug concentration within the liposomes.

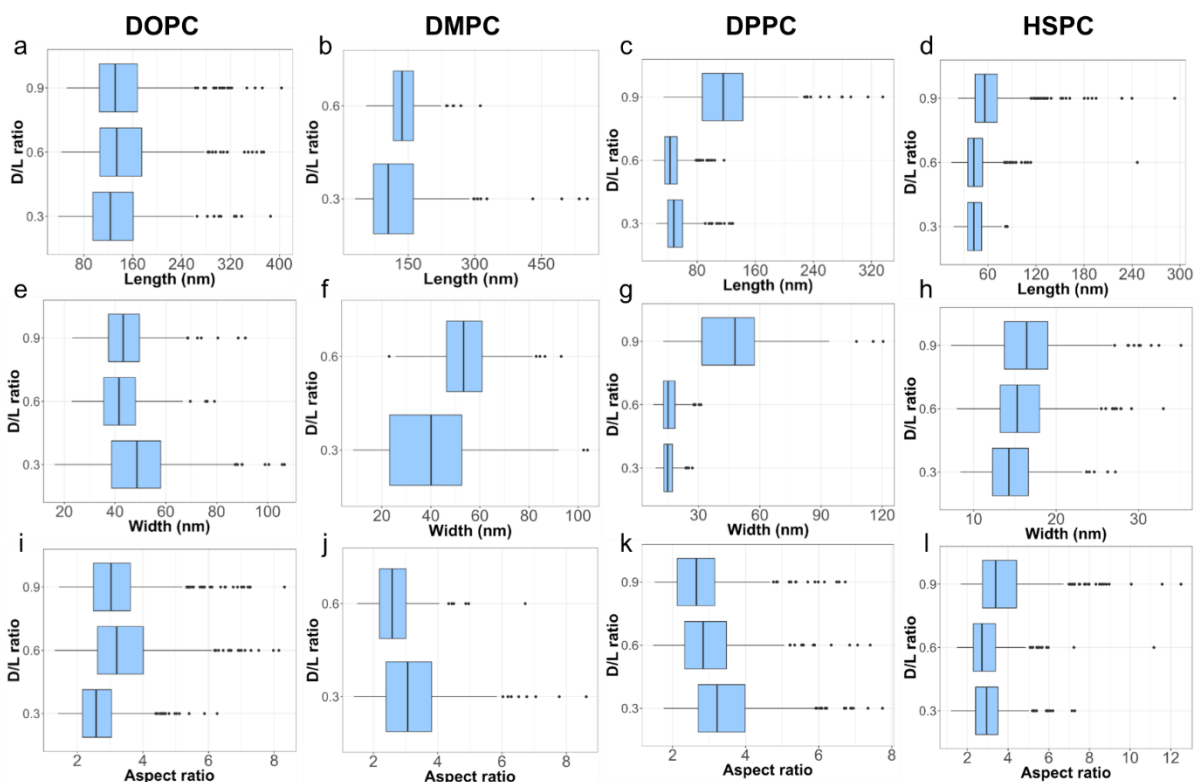


**Figure 6.** Boxplots of standard TEM results showing nanocrystal particle length (a-d), width (e-h) and aspect ratio (i-l) distributions for different liposomal ciprofloxacin nanocrystal formulations with different D/L ratios. Liposomes composed of DOPC: Chol (1.0 : 0.87) liposomal ciprofloxacin prepared at different D/L ratio (a, e, i), DMPC: Chol (1.0 : 0.87) liposomal ciprofloxacin prepared at different D/L ratio (b, f, j), DPPC: Chol (1.0 : 0.87) liposomal ciprofloxacin prepared at different D/L

Chapter 3B: Controlling the size and shape of liposomal ciprofloxacin nanocrystals by varying the lipid bilayer rigidity and drug to lipid ratio

ratio (c, g, k) and HSPC: Chol (1.0 : 0.87) liposomal ciprofloxacin prepared at different D/L ratio (d, h, l).

Size distributions were also calculated from the SAXS profiles for DMPC-, DPPC- and HSPC-based liposomes with different D/L ratios and the results are presented as boxplots for comparison with the standard TEM results in **Figure 6** (see electronic supporting information Table S3 for the numerical data). As previously observed in **Figure 3**, DMPC liposomes with different D/L ratios again showed different results in both the lengths and widths derived from the standard TEM and SAXS analyses (**Figure 7 a and d**). For DPPC liposomes (**Figure 7 b and e**), at lower D/L ratio of 0.3 and 0.6, both length and width measurements showed good agreement between standard TEM and SAXS methods but different lengths and widths were observed for DPPC liposomes with highest D/L ratio of 0.9. This could be due to the presence of longer and wider crystals (size similar to the DMPC liposomes). For HSPC liposomes (**Figure 7 c and f**), results obtained from the two methods again showed good agreement for the lower D/L ratio of 0.3 and 0.6 for length and width measurements, with the differences between the two methods for HSPC liposomes with D/L ratio of 0.9 not being as dramatic as that observed in the DPPC formulations.

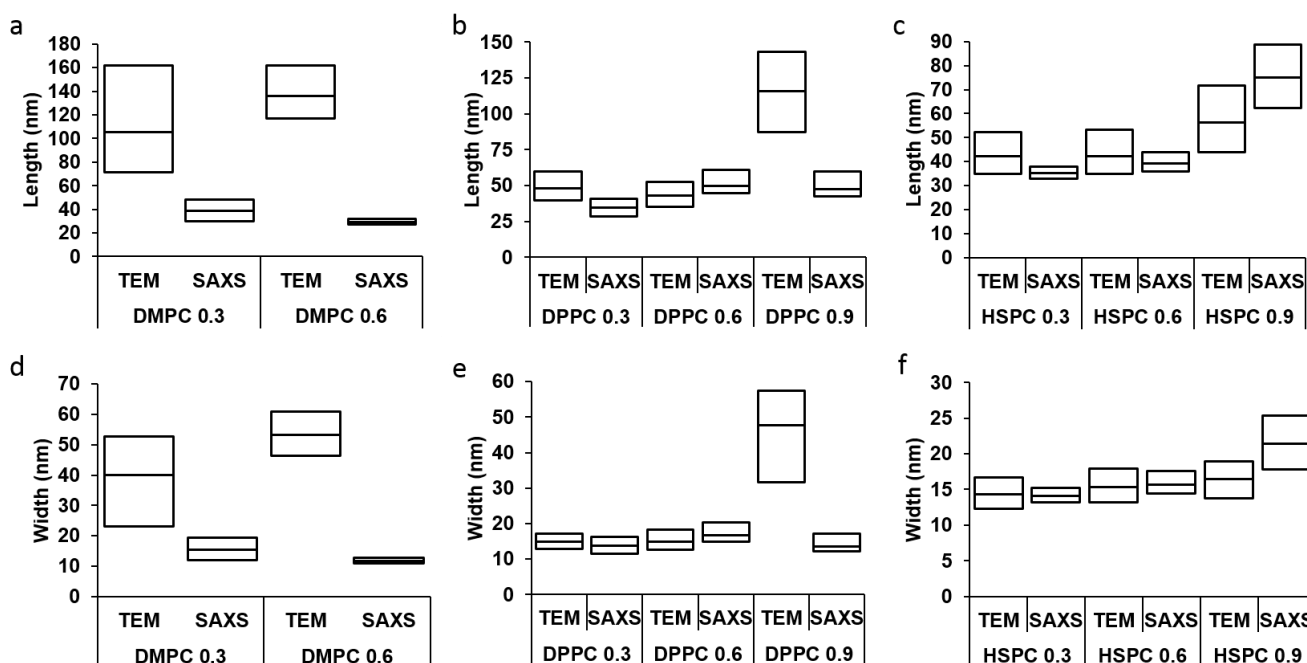


**Figure 7.** Box plots comparing the size distribution of the length (a-c) and width (d-f) measurements of the ciprofloxacin nanocrystals formed inside liposomes obtained from standard TEM (TEM) and SAXS techniques. The liposomes were prepared using DMPC (a, d), DPPC (b, e), HSPC cholesterol (1.0 : 0.87) liposomes (c, f) at different D/L ratio.

### 3B.4.4 Comparing the results from standard TEM and SAXS size distribution analyses

When comparing the size distributions obtained by the two different analyses the commonality between the samples that produced substantially different results in the TEM and SAXS analyses were where when the particles observed by TEM were larger with median widths in excess of 40 nm and median lengths in excess of 100 nm. These larger particles were more polydisperse in the TEM measurements, showing smaller nanocrystals with narrower size distributions typically affording smaller differences in the size distributions yielded from SAXS and TEM. The tendency of the SAXS technique to ineffectively resolve the larger crystals may be due to the limitation in the lowest  $Q$  data point recorded, with the radius of gyration of the largest object observable being limited to  $\sim Q_{\min}^{-1}$ . In these experiments,  $Q_{\min} = 0.0024 \text{ \AA}^{-1}$  and the largest observable radius of gyration is on the order of 41.7 nm. Given that the radius of gyration of a rod is given by

$$R_g = \sqrt{\frac{l^2}{12} + \frac{r^2}{2}}, \text{ where } R_g \text{ is the radius of gyration, } l \text{ is the rod length and } r \text{ is the rod radius.}$$

The largest rod that could be observed using SAXS with an aspect ratio of 3.0 would have a length of around 134 nm and a width (diameter) of around 45 nm. As such, only surface (Porod) scattering from the larger crystals observed by TEM would be observed within the range of scattering vectors measured in this work. This may partially explain why the nanocrystal widths/length for samples observed to have larger crystals in TEM (the DMPC liposomes and the DPPC liposomes with the highest D/L ratio) were not faithfully reproduced by the SAXS data analysis. Moreover, the polydispersity of the larger nanocrystal sizes in these samples will also complicate the SAXS analysis by smearing out the scattering features observed. Furthermore, it is important to note that when looking at the TEM data, there is an apparent correlation between length of the nanocrystals and aspect ratio, with no such inverse correlation observed between the nanocrystal width and the corresponding aspect ratio (see electronic supporting information, Figure S9). This indicates that it is the crystal length that directly determines the aspect ratio of the particles in these systems, with the particle widths being essentially randomly distributed throughout particles with different aspect ratios. The SAXS data modelling requires a constant aspect ratio for all particles, not a greater one for longer particles. This might explain why the modelling doesn't effectively model the scattering from longer particles as it is trying to model them with widths greater than are observed in the system to maintain a constant aspect ratio.

The benefits of synchrotron SAXS analysis compared to standard TEM analysis include rapid data acquisition, which provides an indication of the whole particle ensemble in the dispersion. There are also a number of publically-available data modelling algorithms currently available to users but those used herein seem to be most effective when particle growth is highly constrained by rigid liposome bilayers to give smaller particles with narrower size distributions. The analysis of nanocrystal sizes is also only possible if a suitable background signal can be subtracted to remove the contribution to scattering from the liposome shells. This was possible with the more rigid phospholipids whose structures were relatively unperturbed by the nanocrystal growth process but in the case of DOPC, which is significantly distorted by nanocrystal growth, SAXS was not an appropriate method for determining nanocrystal size as the non-crystallised liposomes did not provide a suitable background for subtraction. SAXS measurements would therefore be insufficient for uniquely determining the size distributions in some cases and complimentary imaging techniques would be required to provide the size and shape of the drug nanocrystals. The TEM analysis performed in this work is a statistically rigorous type of image analysis but it is understandable more manual and time consuming than the automated SAXS analysis.

#### 3B.4.5 Difference in the size of the liposomal ciprofloxacin nanocrystals and applications

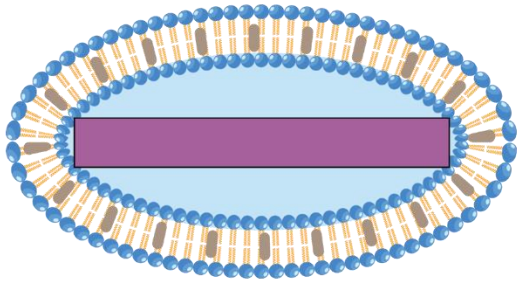
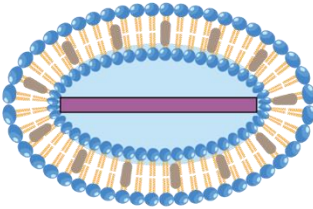
For the liposomes with longer nanocrystals such as the DOPC and DMPC liposomes relative to the DPPC and HSPC liposomes, the width of the particles are also larger. It seemed that the overall nanocrystal size is larger in the DOPC and DMPC liposomes than the DPPC and HSPC liposomes. This might indicate that the DOPC and DMPC liposomes contained a higher proportion of drug in the crystallised form and that for the DPPC and HSPC liposomes, more drug was present in the dissolved form. The crystal growth appeared to be driven by the longitudinal direction, forming rectangular rod-like particles with relatively similar median aspect ratios at around 2.5-3.2. The higher elasticity of the DOPC and DMPC liposomes resulted in the enablement of the crystal to grow in the longitudinal direction to a fuller extent relative to more rigid DPPC and HSPC liposomes. Hence the aspect ratio is relatively similar, the crystal tends to be larger with the effect mostly due to the longer length of the nanocrystal. The shorter nanocrystals resulting from the restriction by the liposome bilayer resulted in less drug contributing to the crystal growth inside the liposome and more drug being in the dissolved form. For the cholesterol modified DOPC liposomes, the same concept applies, however it was observed that the

## Chapter 3B: Controlling the size and shape of liposomal ciprofloxacin nanocrystals by varying the lipid bilayer rigidity and drug to lipid ratio

greater crystal growth resulted when DOPC : Chol was at 0.25 and 0.5 molar ratio. Inclusion of the highest amount of cholesterol restricted the size growth longitudinally which resulted in smaller crystals and more portion of dissolved drug inside the liposome. When cholesterol was completely omitted from the bilayer composition, the lipid was apparently less stable to the freeze-thawing process and resulted in a drug leakage, hence a reduced amount of drug was available inside the liposomes to form nanocrystals. Generally, the higher the D/L ratio, the more drug was available inside the liposome for forming nanocrystals, hence the larger the nanocrystal. This was true for DMPC and HSPC liposomes. It is difficult to predict from the current data, whether for different D/L ratio of the same phospholipid-based liposome, the ratio between the crystal form versus the dissolved form is unchanged or not.

A previous study has suggested that the shape and size of the nanoparticle strongly influence the uptake into cells (45). Rod-like hydrogel particles with high aspect ratio nanoparticles are internalized by HeLa cells more rapidly and efficiently and the extent of the internalization is also dependent on the particle size (46). It is also reported that the particle shape plays a dominant role in phagocytosis (47). Rod shaped micelles also showed a ten-fold longer circulation lifetime than spherical micelles (48). Thus, the liposomal ciprofloxacin nanocrystals with different nanocrystal sizes stretching the bilayer to form non-spherical liposomes with different dimension could provide benefits in controlling cellular interactions and recognition *in vivo*.

### 3B.5 Conclusion

<ul style="list-style-type: none"><li>• DOPC, DMPC liposomes (Lower <math>T_m</math>)</li><li>• Absence or low cholesterol (DOPC liposomes)</li><li>• High D/L ratio (HSPC, DPPC liposomes)</li></ul>  <p><b>Wider and longer nanocrystals</b></p>	<ul style="list-style-type: none"><li>• DPPC, HSPC liposomes (Higher <math>T_m</math>)</li><li>• High cholesterol (DOPC liposomes)</li><li>• Low D/L ratio (HSPC, DPPC liposomes)</li></ul>  <p><b>Thinner and shorter nanocrystals</b></p>
---	---

**Figure 8.** Schematic summarising the key findings in this study, how different parameters affect the encapsulated ciprofloxacin drug nanocrystal dimensions inside the liposome.

In the present study, quantitative standard TEM and SAXS methods were used to determine the sizes of ciprofloxacin nanocrystals formed within phospholipid liposomes. The effect of liposomal bilayer rigidity on the size distributions of the ciprofloxacin nanocrystals was evaluated and four primary conclusions could be drawn from the findings (**Figure 8**). Firstly, it was found that the phase transition temperature of the phospholipid utilised in liposome preparation can affect the growth of the ciprofloxacin nanocrystals inside the liposome, with less flexible (more rigid) bilayers restricting nanocrystal growth. This is likely due to the fluidity and the physical state of the liposomal bilayer membrane when the liposomes are thawed after freezing (the crystal growth phase). It was observed that liposomes made from the highest transition temperature phospholipids HSPC and DPPC produced shorter and thinner nanocrystals compared to those produced inside DOPC and DMPC liposomes with lower transition temperatures. Secondly, the amount of cholesterol in the bilayers, which influences the membrane rigidity, can also be used to control the resulting nanocrystal size distribution. Increasing the cholesterol content of DOPC liposomes reduced the membrane fluidity which restricted the growth of ciprofloxacin nanocrystals in both the length and width directions. Thirdly, increasing the D/L ratio can produce longer and wider nanocrystals for liposomes made from more rigid phospholipids (HSPC, DPPC). However, this effect is not obvious when using more fluid lipids such as DOPC. Lastly, quantitative standard TEM is a useful tool in evaluating the size distribution and shape of nanocrystals formed inside liposomes. SAXS can also be used as a complimentary method in analysing the nanocrystal size distributions but due caution must be applied when analysing samples containing larger nanocrystals with broader size distributions and in cases where it appears that significant disruption of the liposome shape has occurred.

## Acknowledgements

This study was funded under the Australian Research Council Centre of Excellence in Convergent Bio-Nano Science and Technology. This work was partly funded by the Australian Research Council Discovery Program (DP160102906). Cryo-TEM studies were conducted with assistance of Dr. Lynne Waddington at the CSIRO Materials Science and Engineering. The authors acknowledge use of the facilities and assistance of Dr. Tim Williams at the Monash Centre for Electron Microscopy for room temperature TEM studies.

## Conflict of Interest

At the time of these studies, David Cipolla was an employee of Aradigm Corp.

## Electronic Supporting Information

The Electronic Supporting Information contains SAXS profiles, particle size distribution profiles, Scatter plots and tables. The in house developed image J macro script is also available for download from the ESI. Please cite this work if the provided macro script is used for particle size analysis of future work.

## Supporting Information

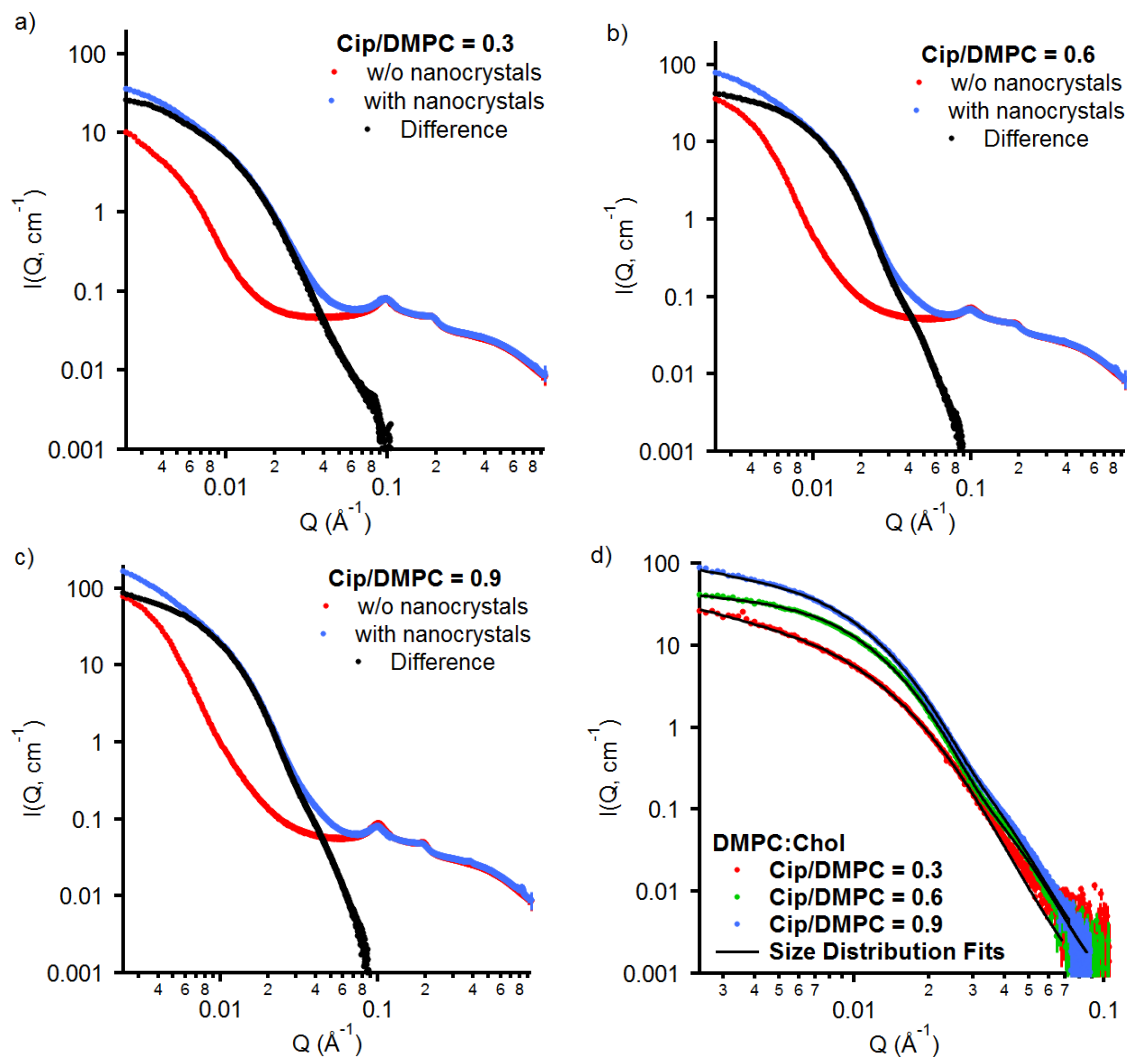


**Figure S1** a)–c) SAXS profiles for DMPC/Cholesterol-based (DMPC/Chol = 1.15:1 w/w) liposomes charged with ciprofloxacin. Liposomes without nanocrystals (w/o, red profiles) were actively loaded with ciprofloxacin prior to freeze-thawing, liposomes with nanocrystals (blue profiles) were freeze-thawed to initiate crystallisation and the difference profiles (black profiles) are the difference between the two. d) The size distribution fitting models of the difference profiles from a)–c).

Chapter 3B: Controlling the size and shape of liposomal ciprofloxacin nanocrystals by varying the lipid bilayer rigidity and drug to lipid ratio

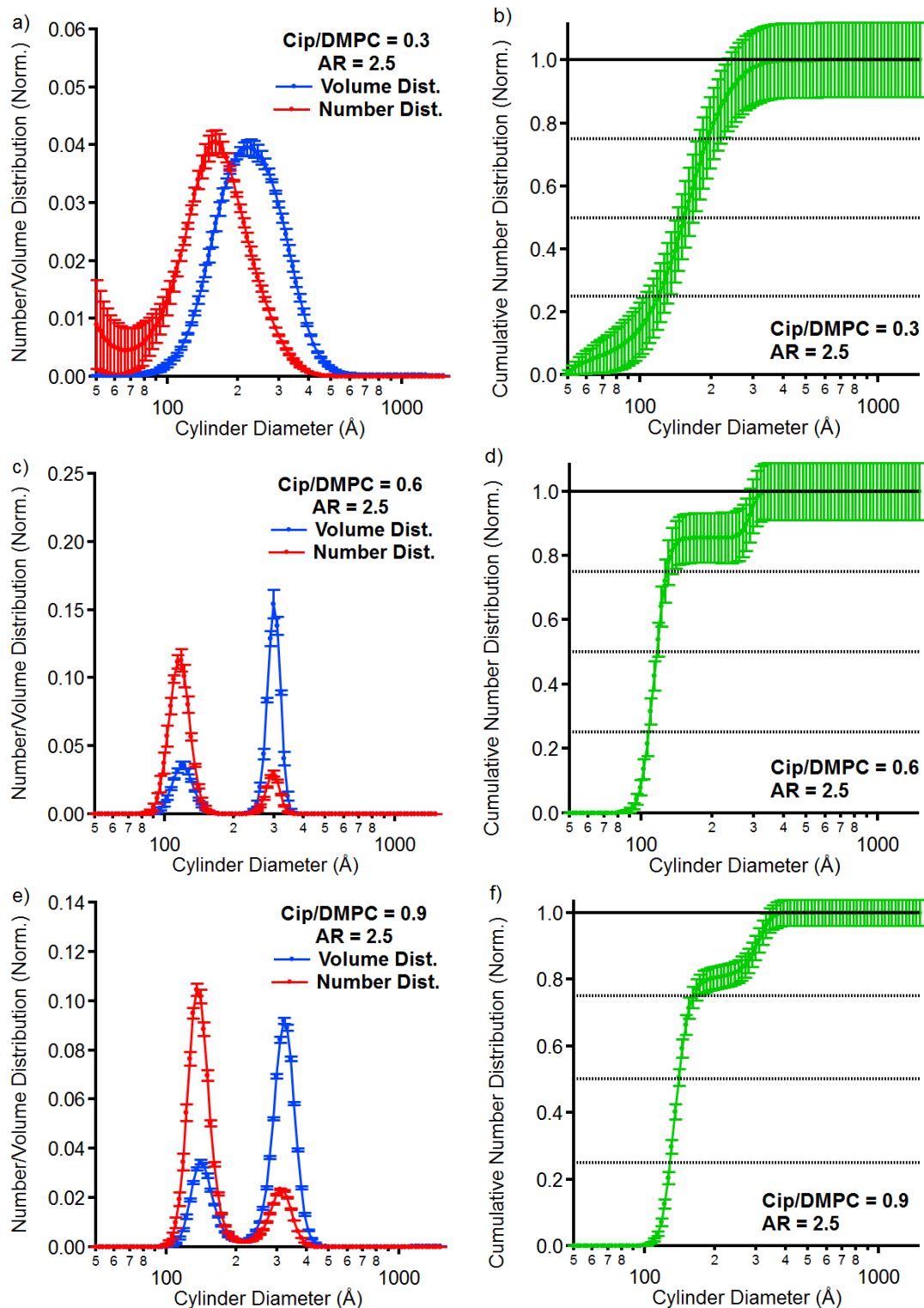


**Figure S2** Particle size distributions for ciprofloxacin crystals in DMPC/Cholesterol-based liposomes calculated from the SAXS data in Figure S3. a), c) and e) show the normalised volume and number distributions for drug/lipid ratios of 0.3, 0.6 and 0.9, respectively. b), d) and f) show the corresponding cumulative number distributions, which were used to determine the median particle sizes and upper and lower quartile diameters. AR = optimum aspect ratio used in the SAXS data modelling.

Chapter 3B: Controlling the size and shape of liposomal ciprofloxacin nanocrystals by varying the lipid bilayer rigidity and drug to lipid ratio

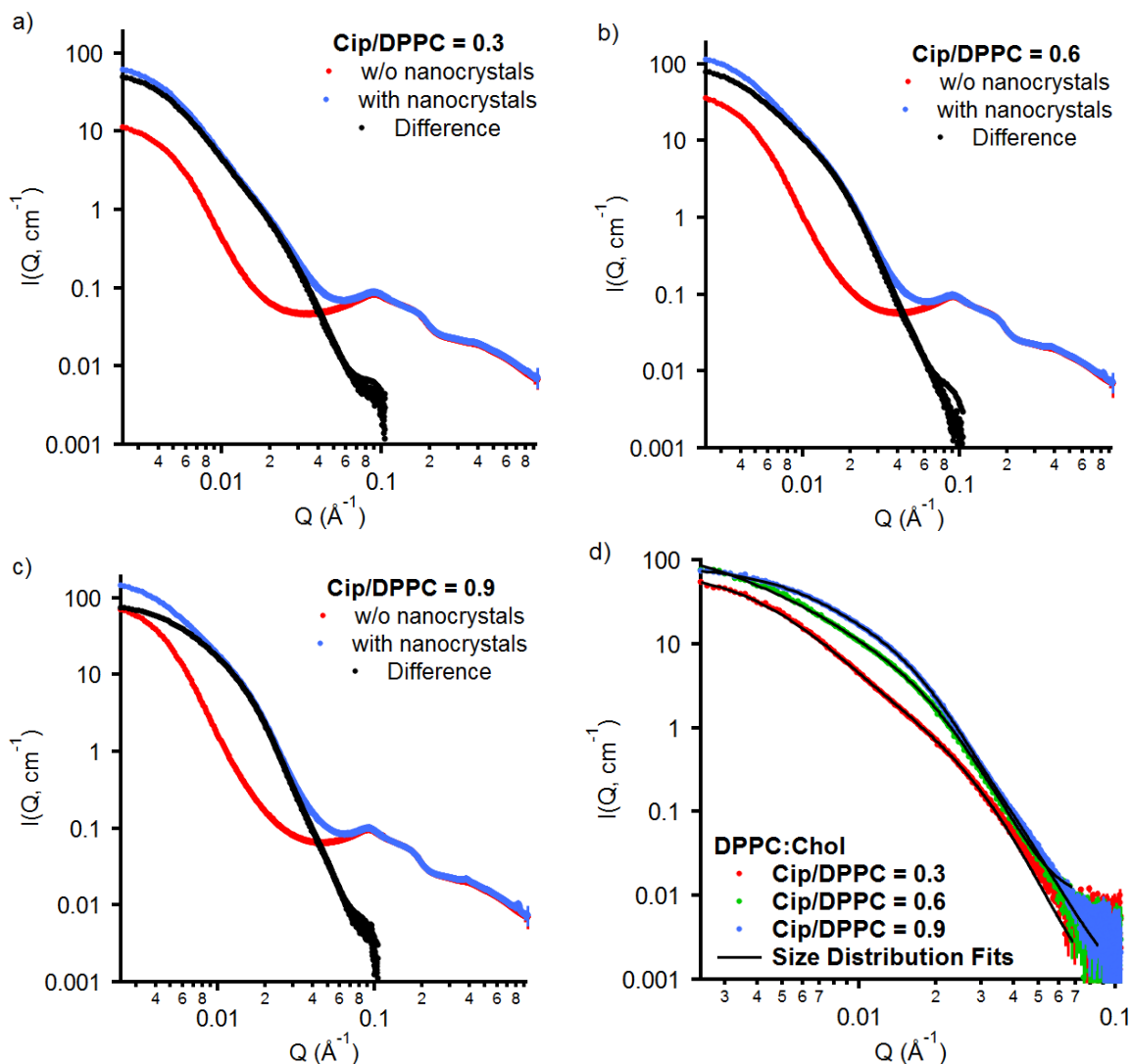


**Figure S3** a)–c) SAXS profiles for DPPC/Cholesterol-based (DPPC/Chol = 1.15:1 w/w) liposomes charged with ciprofloxacin. Liposomes without nanocrystals (w/o, red profiles) were actively loaded with ciprofloxacin prior to freeze-thawing, liposomes with nanocrystals (blue profiles) were freeze-thawed to initiate crystallisation and the difference profiles (black profiles) are the difference between the two. d) The size distribution fitting models of the difference profiles from a)–c).

Chapter 3B: Controlling the size and shape of liposomal ciprofloxacin nanocrystals by varying the lipid bilayer rigidity and drug to lipid ratio

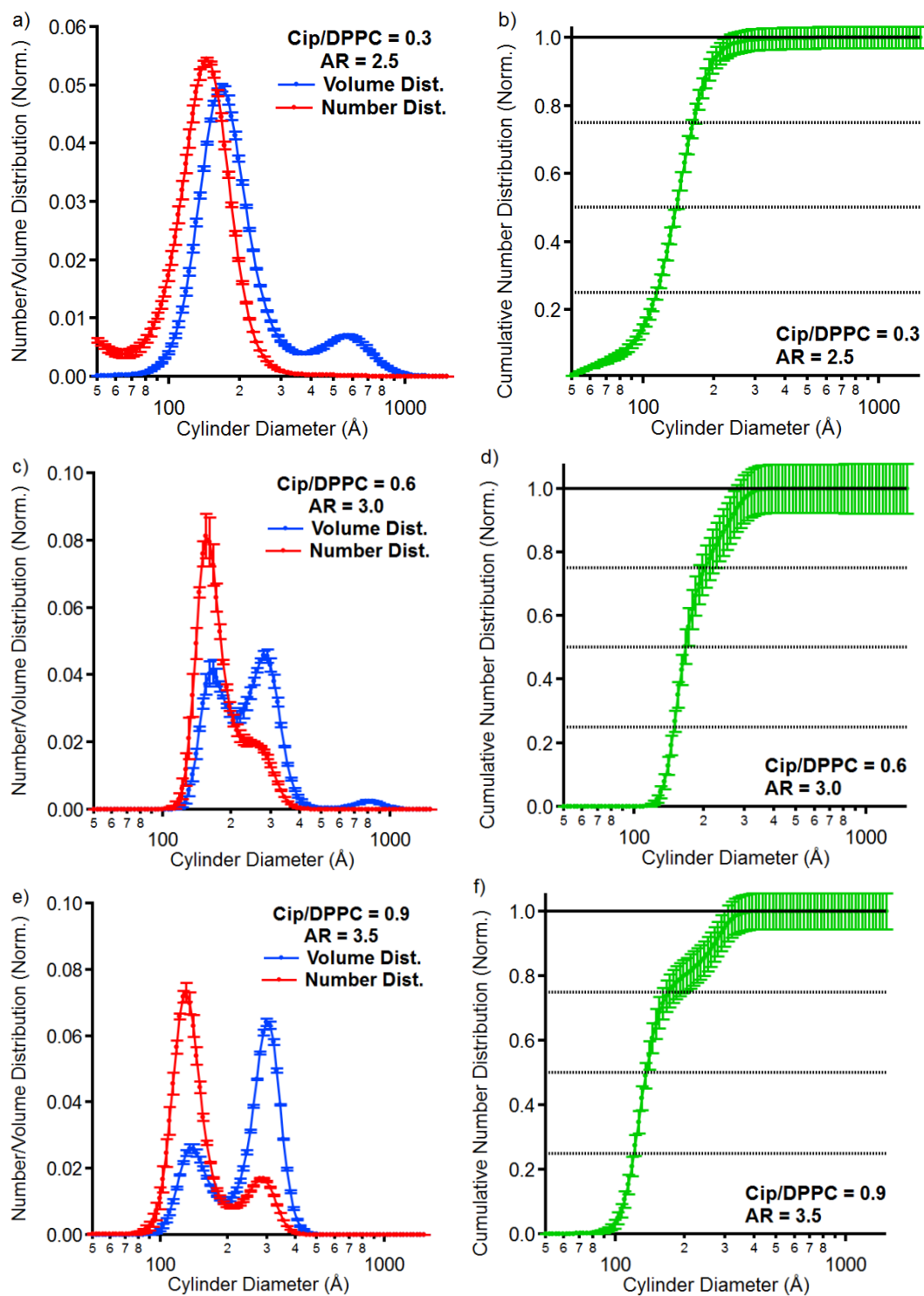


**Figure S4** Particle size distributions for ciprofloxacin crystals in DPPC/Cholesterol-based liposomes calculated from the SAXS data in Figure S3. a), c) and e) show the normalised volume and number distributions for drug/lipid ratios of 0.3, 0.6 and 0.9, respectively. b), d) and f) show the corresponding cumulative number distributions, which were used to determine the median particle sizes and upper and lower quartile diameters. AR = optimum aspect ratio used in the SAXS data modelling.

Chapter 3B: Controlling the size and shape of liposomal ciprofloxacin nanocrystals by varying the lipid bilayer rigidity and drug to lipid ratio

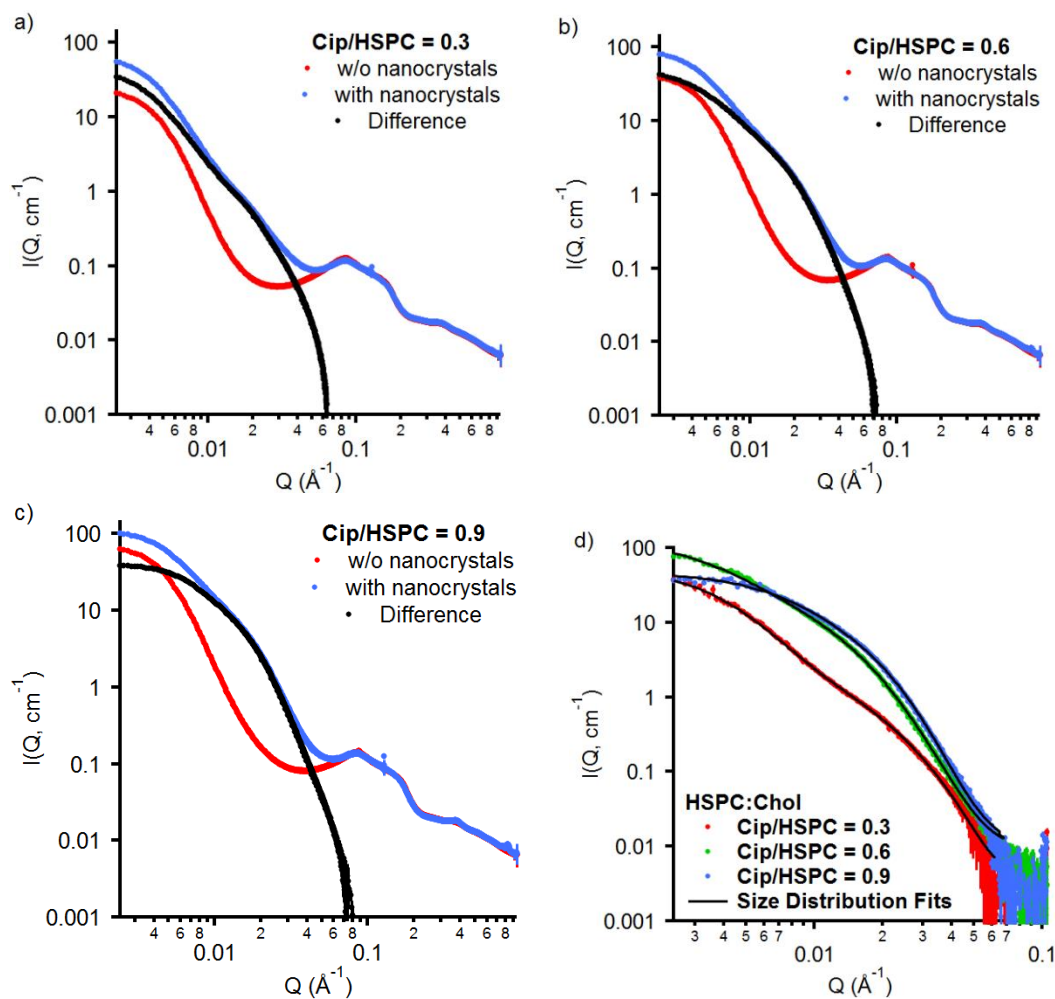


**Figure S5** a)–c) SAXS profiles for HSPC/Cholesterol-based (HSPC/Chol = 1.15:1 w/w) liposomes charged with ciprofloxacin. Liposomes without nanocrystals (w/o, red profiles) were actively loaded with ciprofloxacin prior to freeze-thawing, liposomes with nanocrystals (blue profiles) were freeze-thawed to initiate crystallisation and the difference profiles (black profiles) are the difference between the two. d) The size distribution fitting models of the difference profiles from a)–c).

Chapter 3B: Controlling the size and shape of liposomal ciprofloxacin nanocrystals by varying the lipid bilayer rigidity and drug to lipid ratio

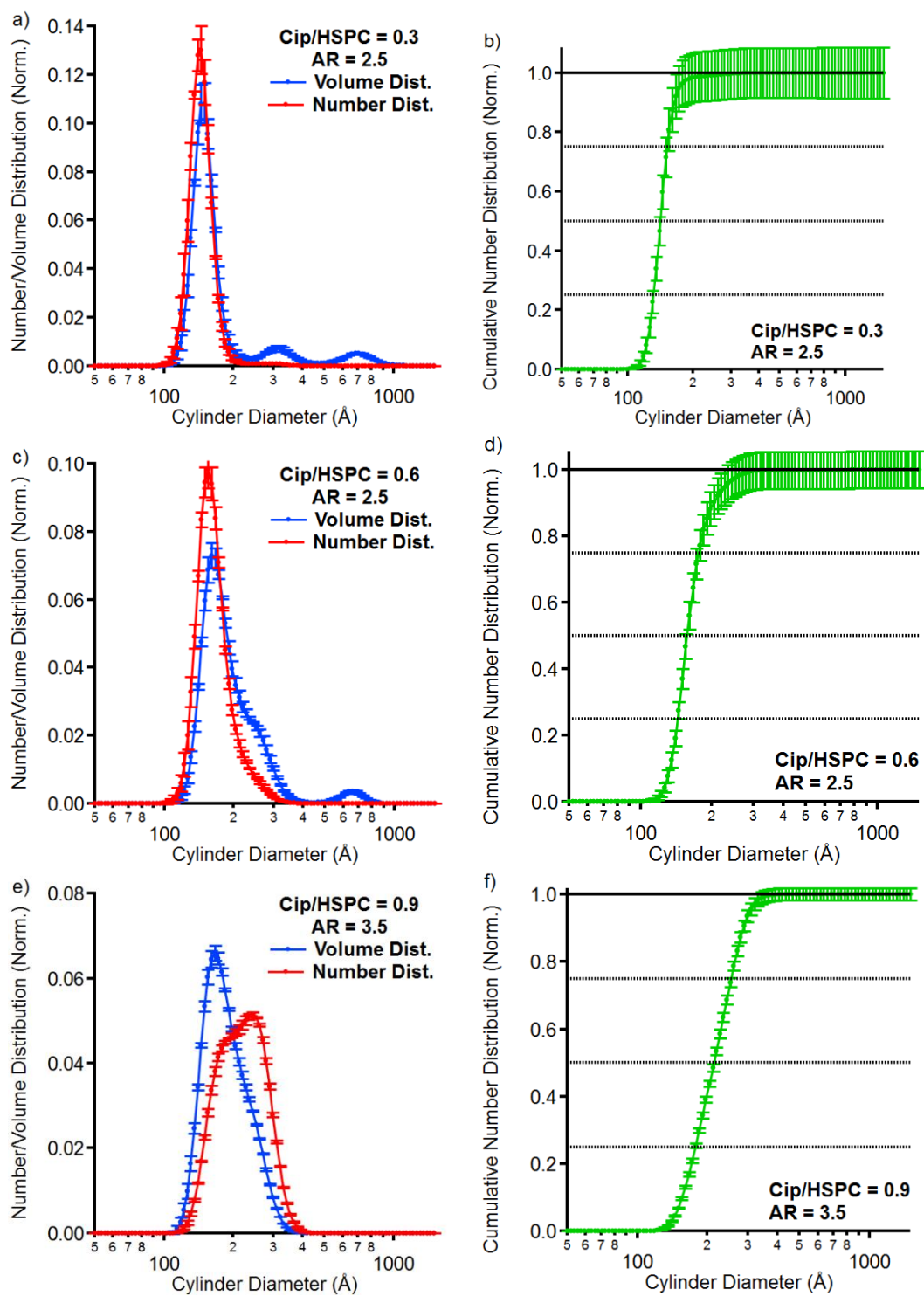


**Figure S6** Particle size distributions for ciprofloxacin crystals in HSPC/Cholesterol-based liposomes calculated from the SAXS data in Figure S3. a), c) and e) show the normalised volume and number distributions for drug/lipid ratios of 0.3, 0.6 and 0.9, respectively. b), d) and f) show the corresponding cumulative number distributions, which were used to determine the median particle sizes and upper and lower quartile diameters. AR = optimum aspect ratio used in the SAXS data modelling.

Chapter 3B: Controlling the size and shape of liposomal ciprofloxacin nanocrystals by varying the lipid bilayer rigidity and drug to lipid ratio

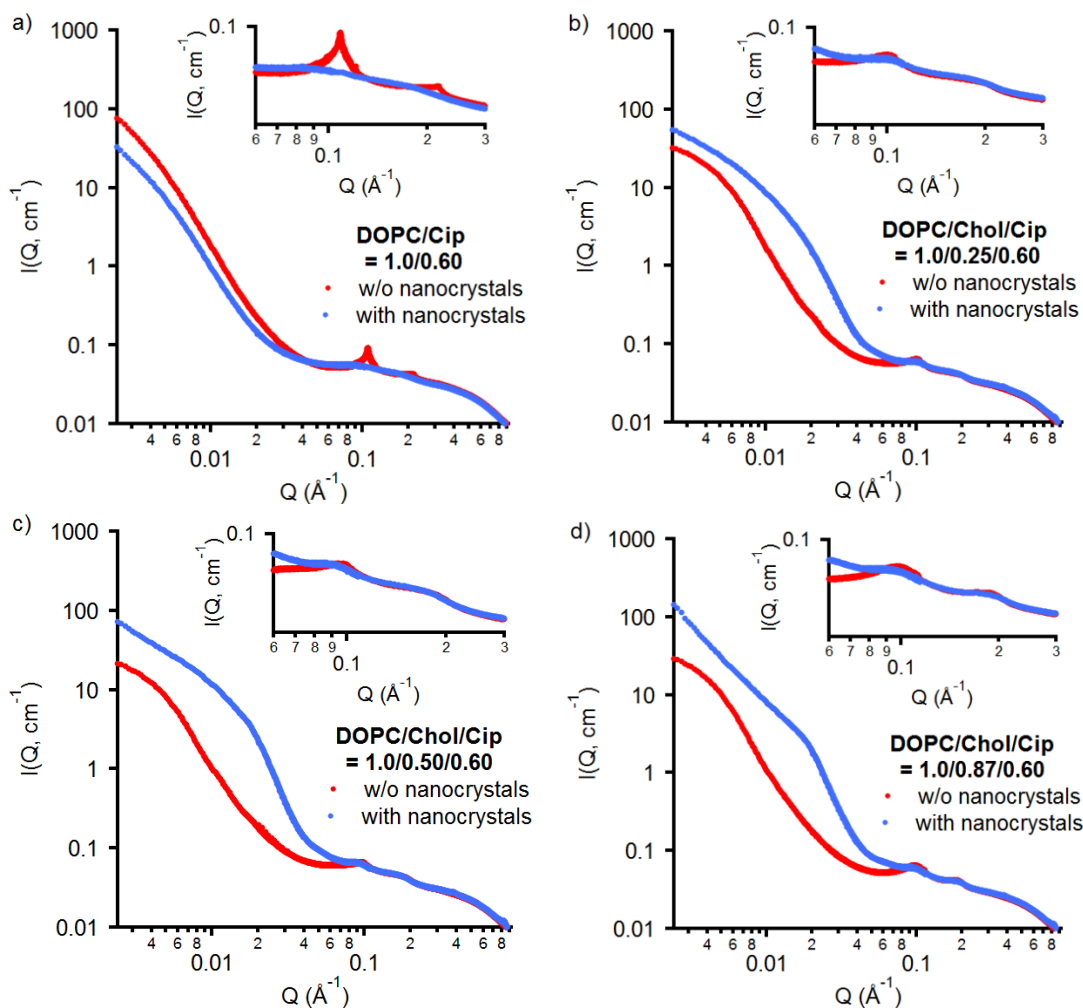


**Figure S7** SAXS profiles of DOPC-based liposomes charged with ciprofloxacin (DOPC/Ciprofloxacin = 1.0:0.6 w/w) and different amounts of cholesterol. Liposomes without nanocrystals (w/o, red profiles) were actively loaded with ciprofloxacin prior to freeze-thawing and liposomes with nanocrystals (blue profiles) were freeze-thawed to initiate crystallisation.

Chapter 3B: Controlling the size and shape of liposomal ciprofloxacin nanocrystals by varying the lipid bilayer rigidity and drug to lipid ratio

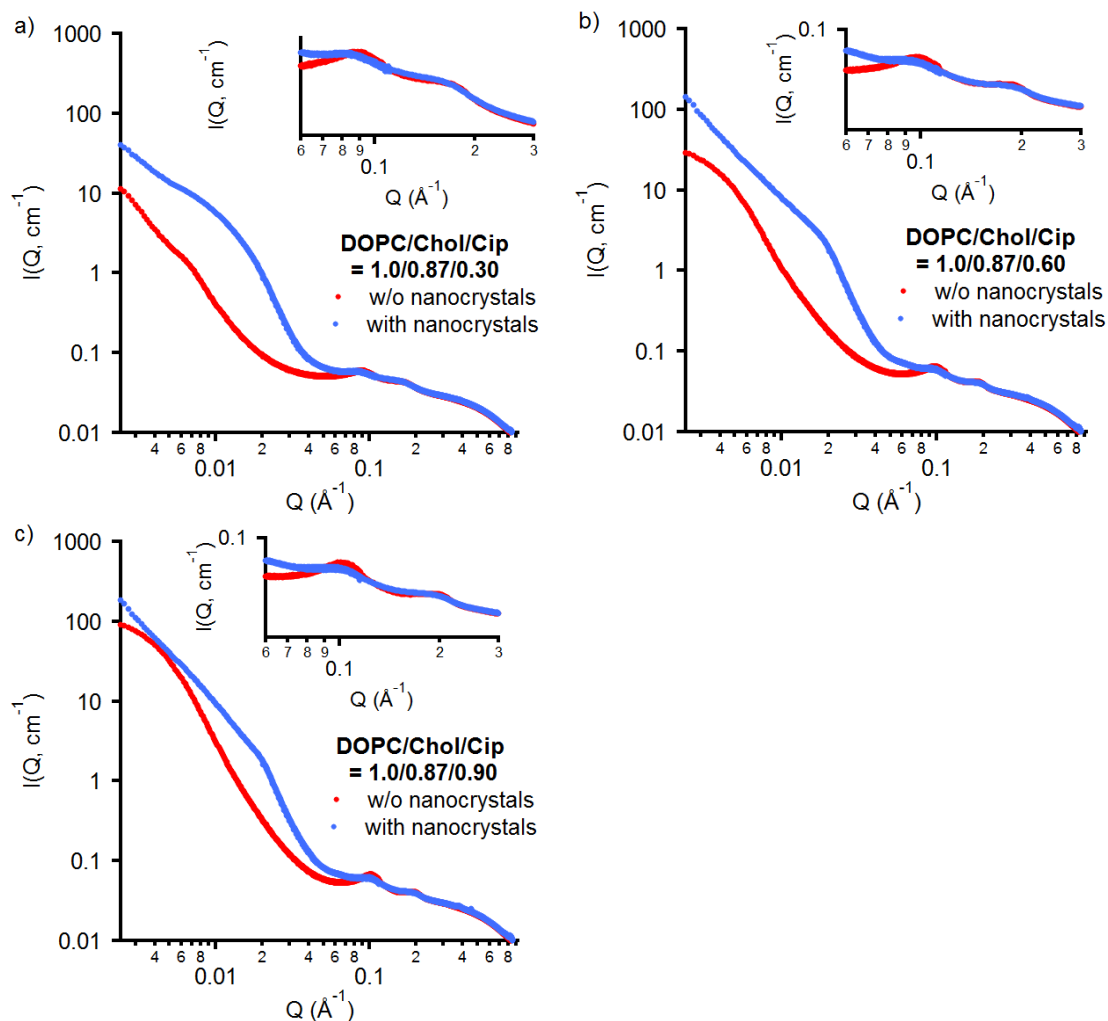


**Figure S8** SAXS profiles of DOPC-based liposomes charged with different amounts of ciprofloxacin with a constant DOPC/Cholesterol ratio of 1.15:1.0 w/w. Liposomes without nanocrystals (w/o, red profiles) were actively loaded with ciprofloxacin prior to freeze-thawing and liposomes with nanocrystals (blue profiles) were freeze-thawed to initiate crystallisation.

### Chapter 3B: Controlling the size and shape of liposomal ciprofloxacin nanocrystals by varying the lipid bilayer rigidity and drug to lipid ratio

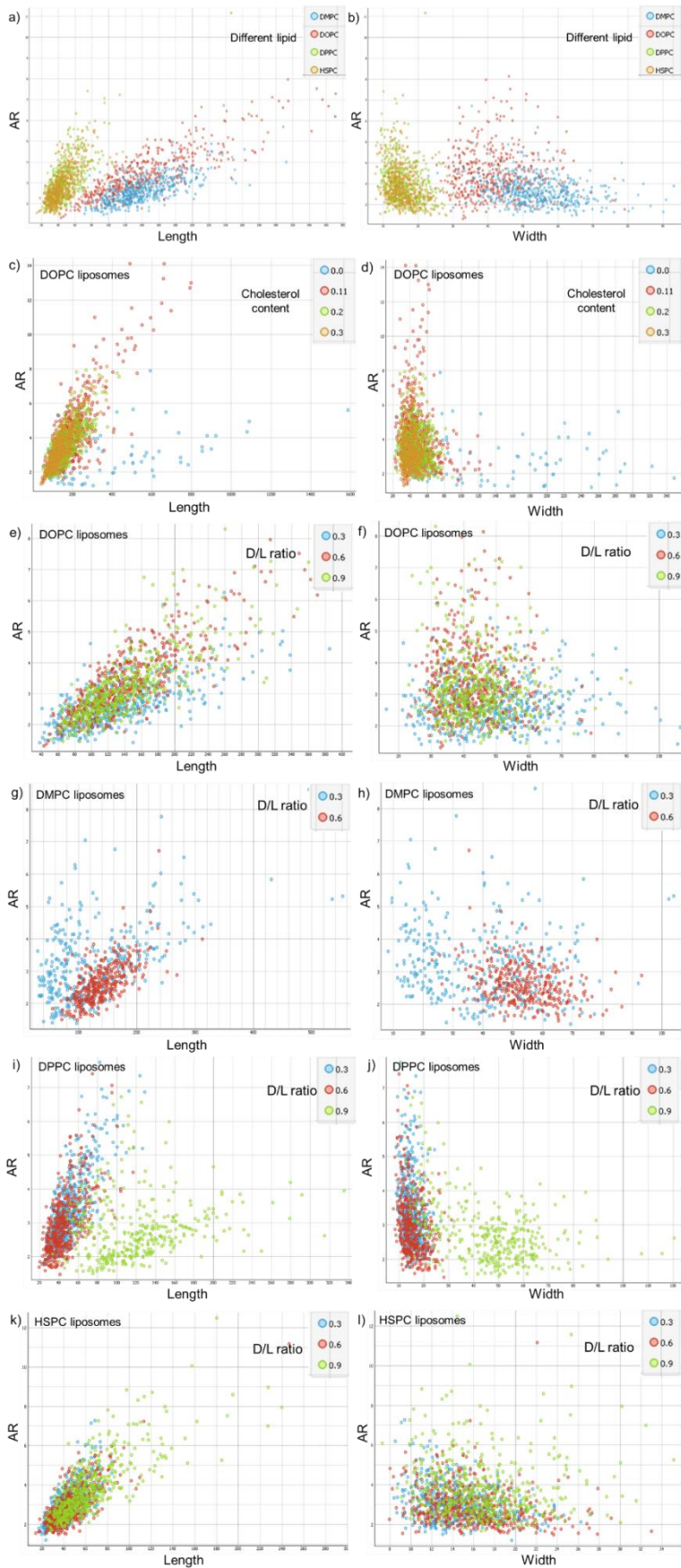


**Figure S9** Scatter plot showing data distribution comparing length and width against aspect ratio for different liposomal ciprofloxacin nanocrystal formulations obtained from standard TEM analysis. Panel a,b for liposomes made from different phospholipid. Panel c,d for DOPC liposomes with different cholesterol content. Panel e,f for DOPC liposomes with different D/L ratio. Panel g,h for DMPC liposomes with different D/L ratio. Panel i,j for DPPC liposomes with different D/L ratio. Panel k,l for HSPC liposomes with different D/L ratio.

Chapter 3B: Controlling the size and shape of liposomal ciprofloxacin nanocrystals by varying the lipid bilayer rigidity and drug to lipid ratio

**Table S1.** Numerical results obtained from standard TEM and SAXS method for liposomal ciprofloxacin nanocrystals made from different phospholipid. The results listed represents for the lower quartile, median and upper quartile values of the length, width and aspect ratio of liposomal ciprofloxacin nanocrystals.

Lipid composition		Standard TEM			SAXS		
		Length	Width	AR	Length	Width	AR
<b>DOPC: Chol</b> <b>(1.0 : 0.87)</b>	Lower quartile	106.11	35.43	2.61			
	Median	134.12	41.51	3.20			
	Upper quartile	174.99	48.01	4.01			
<b>DMPC: Chol</b> <b>(1.0 : 0.87)</b>	Lower quartile	117.65	47.38	2.19	27.00	10.80	2.50
	Median	135.19	53.38	2.57	29.25	11.70	2.50
	Upper quartile	161.61	60.89	2.99	32.25	12.90	2.50
<b>DPPC: Chol</b> <b>(1.0 : 0.87)</b>	Lower quartile	35.42	12.73	2.33	44.70	14.90	3.00
	Median	42.88	14.94	2.84	49.80	16.60	3.00
	Upper quartile	52.59	18.37	3.47	60.90	20.30	3.00
<b>HSPC: Chol</b> <b>(1.0 : 0.87)</b>	Lower quartile	34.97	13.21	2.29	36.00	14.40	2.50
	Median	42.38	15.28	2.72	39.25	15.70	2.50
	Upper quartile	53.23	17.98	3.38	44.00	17.60	2.50

Chapter 3B: Controlling the size and shape of liposomal ciprofloxacin nanocrystals by varying the lipid bilayer rigidity and drug to lipid ratio

**Table S2.** Numerical results obtained from standard TEM method for DOPC liposomal ciprofloxacin nanocrystals containing different PL to chol mol ratio. The results listed the median, mean, standard deviation (SD) and polydispersity of the length, width and aspect ratio measured and calculated from DOPC liposomal ciprofloxacin nanocrystals.

		<b>DOPC : Chol mol ratio</b>			
		<b>1.0 : 0.0</b>	<b>1.0 : 0.25</b>	<b>1.0 : 0.50</b>	<b>1.0 : 0.87</b>
<b>Length</b>	Median	232.07	174.85	160.09	134.12
	Mean	345.03	198.51	167.79	145.00
	SD	281.25	103.17	59.08	57.14
	Polydispersity	0.82	0.52	0.35	0.39
<b>Width</b>	Median	94.59	44.37	47.59	41.51
	Mean	124.37	48.08	48.16	42.48
	SD	83.77	16.00	11.07	9.25
	Polydispersity	0.67	0.33	0.23	0.22
<b>AR</b>	Median	2.60	3.84	3.34	3.20
	Mean	2.89	4.25	3.52	3.42
	SD	1.27	1.97	1.06	1.14

Chapter 3B: Controlling the size and shape of liposomal ciprofloxacin nanocrystals by varying the lipid bilayer rigidity and drug to lipid ratio

**Table S3.** Numerical results obtained from standard TEM and SAXS method for liposomal ciprofloxacin nanocrystals made from different phospholipid with different D/L ratio. The results listed represents for the lower quartile, median and upper quartile values of the length, width and aspect ratio of different liposomal ciprofloxacin nanocrystals formulations.

		Standard TEM			SAXS		
		Length	Width	AR	Length	Width	AR
<b>DOPC</b> <b>D/L=0.3</b>	Lower Quartile	94.72	38.64	2.16			
	Median	123.23	48.53	2.57			
	Upper Quartile	160.93	57.96	3.05			
<b>DOPC</b> <b>D/L=0.6</b>	Lower Quartile	106.11	35.43	2.61			
	Median	134.12	41.51	3.20			
	Upper Quartile	174.99	48.01	4.01			
<b>DOPC</b> <b>D/L=0.9</b>	Lower Quartile	105.46	37.41	2.49			
	Median	131.52	43.14	3.03			
	Upper Quartile	167.82	49.53	3.62			
<b>DMPC</b> <b>D/L=0.3</b>	Lower Quartile	71.69	23.17	2.39	30.00	12.00	2.50
	Median	105.25	40.06	3.07	38.50	15.40	2.50
	Upper Quartile	161.69	52.59	3.81	48.25	19.30	2.50
<b>DMPC</b> <b>D/L=0.6</b>	Lower Quartile	116.85	46.39	2.19	27.00	10.80	2.50
	Median	136.23	53.35	2.58	29.25	11.70	2.50
	Upper Quartile	162.06	60.87	3.01	32.25	12.90	2.50
<b>DPPC</b> <b>D/L=0.3</b>	Lower Quartile	39.66	12.94	2.70	28.50	11.40	2.50
	Median	48.01	14.82	3.21	34.50	13.80	2.50
	Upper Quartile	60.05	17.23	3.98	40.75	16.30	2.50
<b>DPPC</b> <b>D/L=0.6</b>	Lower Quartile	35.42	12.73	2.33	44.70	14.90	3.00
	Median	42.88	14.94	2.84	49.80	16.60	3.00
	Upper Quartile	52.59	18.37	3.47	60.90	20.30	3.00
<b>DPPC</b> <b>D/L=0.9</b>	Lower Quartile	87.05	31.56	2.12	42.35	12.10	3.50
	Median	115.79	47.79	2.65	47.60	13.60	3.50
	Upper Quartile	142.98	57.35	3.15	59.85	17.10	3.50
<b>HSPC</b> <b>D/L=0.3</b>	Lower Quartile	34.73	12.27	2.40	33.00	13.20	2.50
	Median	42.38	14.27	2.94	35.25	14.10	2.50
	Upper Quartile	52.14	16.63	3.51	38.00	15.20	2.50
<b>HSPC</b> <b>D/L=0.6</b>	Lower Quartile	34.97	13.21	2.29	36.00	14.40	2.50
	Median	42.38	15.28	2.72	39.25	15.70	2.50
	Upper Quartile	53.23	17.98	3.38	44.00	17.60	2.50
<b>HSPC</b> <b>D/L=0.9</b>	Lower Quartile	43.94	13.72	2.74	62.3	17.8	3.50
	Median	56.13	16.42	3.39	74.9	21.4	3.50
	Upper Quartile	71.77	18.99	4.42	88.9	25.4	3.50

## References

1. Allen TM, Cullis PR. Liposomal drug delivery systems: From concept to clinical applications. *Advanced Drug Delivery Reviews*. 2013;65(1):36-48.
2. Zylberberg C, Matosevic S. Pharmaceutical liposomal drug delivery: a review of new delivery systems and a look at the regulatory landscape. *Drug Delivery*. 2016;23(9):3319-29.
3. Eloy JO, Claro de Souza M, Petrilli R, Barcellos JPA, Lee RJ, Marchetti JM. Liposomes as carriers of hydrophilic small molecule drugs: Strategies to enhance encapsulation and delivery. *Colloids and Surfaces B: Biointerfaces*. 2014;123:345-63.
4. Fahr A, Hoogevest Pv, May S, Bergstrand N, S. Leigh ML. Transfer of lipophilic drugs between liposomal membranes and biological interfaces: Consequences for drug delivery. *European Journal of Pharmaceutical Sciences*. 2005;26(3):251-65.
5. Batist G, Ramakrishnan G, Rao CS, Chandrasekharan A, Gutheil J, Guthrie T, et al. Reduced cardiotoxicity and preserved antitumor efficacy of liposome-encapsulated doxorubicin and cyclophosphamide compared with conventional doxorubicin and cyclophosphamide in a randomized, multicenter trial of metastatic breast cancer. *J Clin Oncol*. 2001;19(5):1444-54.
6. O'Brien MER, Wigler N, Inbar M, Rosso R, Grischke E, Santoro A, et al. Reduced cardiotoxicity and comparable efficacy in a phase III trial of pegylated liposomal doxorubicin HCl (CAELYX/Doxil) versus conventional doxorubicin for first-line treatment of metastatic breast cancer. *Ann Oncol*. 2004;15(3):440-9.
7. Li T, Cipolla D, Rades T, Boyd BJ. Drug nanocrystallisation within liposomes. *Journal of Controlled Release*. 2018;288:96-110.
8. Li X, Hirsh DJ, Cabral-Lilly D, Zirkel A, Gruner SM, Janoff AS, et al. Doxorubicin physical state in solution and inside liposomes loaded via a pH gradient. *Biochimica et Biophysica Acta (BBA) - Biomembranes*. 1998;1415(1):23-40.
9. Barenholz Y. Doxil® — The first FDA-approved nano-drug: Lessons learned. *Journal of Controlled Release*. 2012;160(2):117-34.
10. Barenholz Y. Amphipathic weak base loading into preformed liposomes having a transmembrane ammonium ion gradient: from the bench to approved Doxil. 2006. 1-25
11. Schilt Y, Berman T, Wei X, Barenholz Y, Raviv U. Using solution X-ray scattering to determine the high-resolution structure and morphology of PEGylated liposomal

Chapter 3B: Controlling the size and shape of liposomal ciprofloxacin nanocrystals by varying the lipid bilayer rigidity and drug to lipid ratio

doxorubicin nanodrugs. *Biochimica Et Biophysica Acta-General Subjects*. 2016;1860(1):108-19.

12. Wei X, Cohen R, Barenholz Y. Insights into composition/structure/function relationships of Doxil® gained from “high-sensitivity” differential scanning calorimetry. *European Journal of Pharmaceutics and Biopharmaceutics*. 2016;104:260-70.

13. Wei X, Shamrakov D, Nudelman S, Peretz-Damari S, Nativ-Roth E, Regev O, et al. Cardinal role of intraliposome doxorubicin-sulfate nanorod crystal in doxil properties and performance. *ACS Omega*. 2018;3(3):2508-17.

14. Cipolla D, Blanchard J, Gonda I. Development of liposomal ciprofloxacin to treat lung infections. *Pharmaceutics*. 2016;8(1):6.

15. Cipolla D, Wu H, Salentinig S, Boyd B, Rades T, Vanhecke D, et al. Formation of drug nanocrystals under nanoconfinement afforded by liposomes. *RSC Advances*. 2016;6(8):6223-33.

16. Cipolla D, Wu H, Eastman S, Redelmeier T, Gonda I, Chan H-K. Tuning ciprofloxacin release profiles from liposomally encapsulated nanocrystalline drug. *Pharmaceutical Research*. 2016;33(11):2748-62.

17. Almgren M, Edwards K, Karlsson G. Cryo transmission electron microscopy of liposomes and related structures. *Colloids and Surfaces A: Physicochemical and Engineering Aspects*. 2000;174(1):3-21.

18. Frederik PM, Hubert DHW. Cryoelectron microscopy of liposomes. *Methods in enzymology*. 391: Academic Press; 2005. p. 431-48.

19. Friedrich H, Frederik PM, de With G, Sommerdijk NAJM. Imaging of self-assembled structures: interpretation of TEM and cryo-TEM Images. *Angewandte Chemie International Edition*. 2010;49(43):7850-8.

20. Kuntsche J, Horst JC, Bunjes H. Cryogenic transmission electron microscopy (cryo-TEM) for studying the morphology of colloidal drug delivery systems. *International Journal of Pharmaceutics*. 2011;417(1):120-37.

21. Thompson RF, Walker M, Siebert CA, Muench SP, Ranson NA. An introduction to sample preparation and imaging by cryo-electron microscopy for structural biology. *Methods*. 2016;100:3-15.

22. Li T, Nowell CJ, Cipolla D, Rades T, Boyd BJ. Direct comparison of standard transmission electron microscopy (TEM) and cryogenic-TEM in imaging nanocrystals inside liposomes. *Molecular Pharmaceutics*. 2019 (Just accepted).

23. Garcia-Diez R, Gollwitzer C, Krumrey M, Varga Z. Size Determination of a liposomal drug by small-angle X-ray scattering using continuous contrast variation. *Langmuir*. 2016;32(3):772-8.
24. Di Cola E, Grillo I, Ristori S. Small angle X-ray and neutron scattering: powerful tools for studying the structure of drug-loaded liposomes. *Pharmaceutics*. 2016;8(2):10.
25. Pabst G, Kučerka N, Nieh MP, Rheinstädter MC, Katsaras J. Applications of neutron and X-ray scattering to the study of biologically relevant model membranes. *Chemistry and Physics of Lipids*. 2010;163(6):460-79.
26. Borchert H, Shevchenko EV, Robert A, Mekis I, Kornowski A, Grübel G, et al. Determination of nanocrystal sizes: a comparison of TEM, SAXS, and XRD Studies of highly monodisperse CoPt<sub>3</sub> particles. *Langmuir*. 2005;21(5):1931-6.
27. Yi Z, Nagao M, Bossev DP. Bending elasticity of saturated and monounsaturated phospholipid membranes studied by the neutron spin echo technique. *J Phys Condens Matter*. 2009;21(15):155104.
28. Chen Z, Rand RP. The influence of cholesterol on phospholipid membrane curvature and bending elasticity. *Biophysical Journal*. 1997;73(1):267-76.
29. Méléard P, Gerbeaud C, Pott T, Fernandez-Puente L, Bivas I, Mitov MD, et al. Bending elasticities of model membranes: influences of temperature and sterol content. *Biophysical Journal*. 1997;72(6):2616-29.
30. Kirby NM, Mudie ST, Hawley AM, Cookson DJ, Mertens HDT, Cowieson N, et al. A low background intensity focusing small-angle X-ray scattering undulator beamline. *Journal of Applied Crystallography*. 2013;46(6):1670-80.
31. Ilavsky J, Jemian PR. Irena: tool suite for modeling and analysis of small-angle scattering. *Journal of Applied Crystallography*. 2009;42(2):347-53.
32. Beaucage G. Approximations leading to a unified exponential/power-law approach to small-angle scattering. *Journal of Applied Crystallography*. 1995;28(6):717-28.
33. Beaucage G. Small-angle scattering from polymeric mass fractals of arbitrary mass-fractal dimension. *Journal of Applied Crystallography*. 1996;29(2):134-46.
34. Schindelin J, Arganda-Carreras I, Frise E, Kaynig V, Longair M, Pietzsch T, et al. Fiji: an open-source platform for biological-image analysis. *Nature Methods*. 2012;9:676.
35. Chapman D, Williams RM, Ladbroke BD. Physical studies of phospholipids. VI. Thermotropic and lyotropic mesomorphism of some 1,2-diacyl-phosphatidylcholines (lecithins). *Chemistry and Physics of Lipids*. 1967;1(5):445-75.

Chapter 3B: Controlling the size and shape of liposomal ciprofloxacin nanocrystals by varying the lipid bilayer rigidity and drug to lipid ratio

36. Chen J, Cheng D, Li J, Wang Y, Guo JX, Chen ZP, et al. Influence of lipid composition on the phase transition temperature of liposomes composed of both DPPC and HSPC. *Drug Dev Ind Pharm.* 2013;39(2):197-204.
37. Ulrich AS, Sami M, Watts A. Hydration of DOPC bilayers by differential scanning calorimetry. *Biochimica et Biophysica Acta (BBA) - Biomembranes.* 1994;1191(1):225-30.
38. Li J, Wang X, Zhang T, Wang C, Huang Z, Luo X, et al. A review on phospholipids and their main applications in drug delivery systems. *Asian Journal of Pharmaceutical Sciences.* 2015;10(2):81-98.
39. Eze MO. Phase transitions in phospholipid bilayers: Lateral phase separations play vital roles in biomembranes. *Biochemical Education.* 1991;19(4):204-8.
40. Zook JM, Vreeland WN. Effects of temperature, acyl chain length, and flow-rate ratio on liposome formation and size in a microfluidic hydrodynamic focusing device. *Soft Matter.* 2010;6(6):1352-60.
41. Li T, Mudie S, Cipolla D, Rades T, Boyd BJ. Solid state characterization of ciprofloxacin liposome nanocrystals. *Molecular Pharmaceutics.* 2019;16(1):184-194.
42. Demel RA, Bruckdorfer KR, Van Deenen LLM. The effect of sterol structure on the permeability of liposomes to glucose, glycerol and Rb<sup>+</sup>. *Biochimica et Biophysica Acta (BBA) - Biomembranes.* 1972;255(1):321-30.
43. Taylor KMG, Morris RM. Thermal analysis of phase transition behaviour in liposomes. *Thermochimica Acta.* 1995;248:289-301.
44. Ladbrooke BD, Williams RM, Chapman D. Studies on lecithin-cholesterol-water interactions by differential scanning calorimetry and X-ray diffraction. *Biochimica et Biophysica Acta (BBA) - Biomembranes.* 1968;150(3):333-40.
45. Albanese A, Tang PS, Chan WC. The effect of nanoparticle size, shape, and surface chemistry on biological systems. *Annu Rev Biomed Eng.* 2012;14:1-16.
46. Gratton SE, Ropp PA, Pohlhaus PD, Luft JC, Madden VJ, Napier ME, et al. The effect of particle design on cellular internalization pathways. *Proc Natl Acad Sci U S A.* 2008;105(33):11613-8.
47. Champion JA, Mitragotri S. Role of target geometry in phagocytosis. *Proceedings of the National Academy of Sciences of the United States of America.* 2006;103(13):4930.
48. Geng Y, Dalhaimer P, Cai S, Tsai R, Tewari M, Minko T, et al. Shape effects of filaments versus spherical particles in flow and drug delivery. *Nat Nanotechnol.* 2007;2(4):249-55.



**Chapter 4: Exposure of nanocrystallised ciprofloxacin liposomes to digestive media induces solid-state transformation and altered *in vitro* drug release**

## Exposure of nanocrystallised ciprofloxacin liposomes to digestive media induces solid-state transformation and altered *in vitro* drug release

Tang Li,<sup>a,b</sup> Adrian Hawley,<sup>c</sup> Thomas Rades,<sup>d</sup> Ben J. Boyd<sup>a,b,\*</sup>

<sup>a</sup> Drug Delivery, Disposition and Dynamics, Monash Institute of Pharmaceutical Sciences, Monash University (Parkville Campus), 381 Royal Parade, Parkville, Victoria 3052, Australia

<sup>b</sup> ARC Centre of Excellence in Convergent Bio-Nano Science and Technology, Monash Institute of Pharmaceutical Sciences, Monash University, Parkville Campus, 381 Royal Parade, Parkville, Victoria 3052, Australia

<sup>c</sup> SAXS/WAXS beamline, Australian Synchrotron, Clayton, Victoria, Australia

<sup>d</sup> Department of Pharmacy, University of Copenhagen, Copenhagen 2100, Denmark

This manuscript was submitted to the Journal of Controlled Release.

### Abstract

Commercially available liposomal formulations are mostly limited to the intravenous route of administration. A recently reported approach to nanocrystallise encapsulated ciprofloxacin *in situ* within liposomes generated increasing interest to explore the solid state properties of these drug nanocrystals within confinement. The main advantages of the nanocrystallised drug liposomes are their high drug loading and the liposomes acting as a lipid-based formulation. To explore the potential application of the nanocrystallised drug liposomes in oral delivery applications, liposomal ciprofloxacin formulation was used as a model system. *Ex situ* digestion coupled SAXS study was used to analyse the solid state of the pellet phase formed during *in vitro* digestion of the liposomal ciprofloxacin nanocrystal formulations. Furthermore bile salt titration SAXS study was conducted to evaluate the effect of the drug solid state inside the liposome upon exposure to simulated digestive environment *in situ*. Results showed a complete polymorphic transformation of the ciprofloxacin hydrate (CIPH<sub>2</sub>O) nanocrystals to a new salt form at a NaTDC : CIP molar ratio of 0.6. The new salt crystal displayed two signature diffraction peaks at  $q = 0.35$  and  $0.62 \text{ \AA}^{-1}$ , and is identified as the ciprofloxacin bile salt crystal (CIPTDC), resulting

## Chapter 4: Exposure of nanocrystallised ciprofloxacin liposomes to digestive media induces solid state transformation and altered *In vitro* drug release

from the complexation of the nitrogen on the ciprofloxacin piperazine functional group with the sulfonate group of the bile salt (sodium taurodeoxycholate NaTDC). When isolated and dried the new CIPTDC salt crystal showed a melting point of 150-170 °C from temperature-dependent SAXS analysis and hot stage cross polarised microscopy (CPLM) measurements. The *in vitro* drug release from liposomal ciprofloxacin when drug nanocrystals were present showed controlled drug release behaviour under non-digestive conditions, while a 3.5-fold increase in the drug release was seen when the liposomal ciprofloxacin nanocrystals were exposed to the simulated digestive environment. In conclusion, the solid state of the drug inside the liposome is important in dictating the drug release behaviour from the liposomes. The identification of the solid state transformation during digestion in real time and the bile salt induced polymorphic transformation of ciprofloxacin from nanocrystallised ciprofloxacin liposome is important to understand how the drug is released *in vivo*, as well as for future formulation design.

### KEYWORDS

Ciprofloxacin; small angle X-ray scattering, sodium taurodeoxycholate, liposomal ciprofloxacin nanocrystals, oral drug delivery, bile salt, nanocrystals, *in vitro* drug release

## 4.1 Introduction

In oral drug delivery, poor solubility of the drug would greatly impact the oral absorption and bioavailability, limiting its therapeutic efficacy (1). There have been many approaches to address low drug solubility (2). Among a range of approaches lipid-based formulations (3) and nanocrystal technology (4) have gained increasing interest. Lipids have the capacity to enhance drug solubilisation in the gastrointestinal tract, which would ultimately increase drug bioavailability for drugs where solubility and dissolution rate limit absorption (3, 5). For nanocrystals, the increased dissolution velocity resulting from a higher surface area would also improve oral bioavailability and enhance drug absorption for such drugs (4, 6, 7).

One example of lipid-based formulations are liposomes; a phospholipid-based colloidal system, composing one or more lipid bilayers with an internal aqueous core. Liposomal formulations have achieved tremendous success in systemic drug delivery due to their biocompatibility, surface modification to increase circulation time and ability to reduce toxicity of encapsulated anti-cancer actives (8-10). When drug is encapsulated inside the aqueous core, various physical states of the drug can be identified, i.e. when drug dissolved in solution, or presented as amorphous or crystalline precipitate (11). Recently, liposomes where drug molecules are precipitated as nanocrystals have gained increased attention (Chapter 1). Induction of *in situ* nanocrystallisation of ciprofloxacin to form ciprofloxacin nanocrystals inside liposomes was achieved by an additional freeze-thawing step to the actively-loaded ciprofloxacin liposomes (12, 13). This allowed conversion of the soluble drug to precipitate as the ciprofloxacin hydrate (CIPH<sub>2</sub>O) drug nanocrystals with an average length of 200 nm (Chapter 2) (14). The formation of drug nanocrystals within liposomes also induced a deformation of the spherical vesicles to a football-shaped vesicle in order to accommodate for the growth of drug nanocrystals inside the liposome. The appearance of the nanocrystallised ciprofloxacin liposomes in cryo-TEM is very similar to the commercially available Doxil formulation (15), where doxorubicin have precipitated as doxorubicin sulfate nanocrystals after actively-loaded into the liposomes (16, 17).

Lipid based formulations (such as phospholipid composed liposomes) when ingested would be subject to lipolysis generating digestion products (fatty acids and lysophospholipids). These components, and particularly the fatty acids would be expected to provide enhancement of solubilisation of poorly water soluble drugs in the

gastrointestinal tract (3). The liposomal ciprofloxacin nanocrystals present an example of coexisting lipid-based formulation and drug nanocrystal technology. The lipid would protect the drug nanocrystals from degradation and aggregation which could improve formulation stability without the use of polymeric and surfactant stabilisers. Using vesicles as the carrier and stabiliser for the drug nanocrystals also provides high drug loading since active drug loading achieves more than 90% drug encapsulation in most cases and the post *in situ* nanocrystallisation would allow preservation of high drug concentration. Previous reports also identified a potential for the poorly water-soluble weakly basic drug cinnarizine to precipitate in an amorphous-salt form during *in vitro* digestion of the lipid-based formulation. The formation of the high energy amorphous-salt formed during digestion, could optimise the overall fraction of drug to be absorbed from a single dose (18).

Previously, the effect of pH on the solid state characteristics of ciprofloxacin inside the liposome was investigated. As pH was varied to represent different regions of the gastrointestinal tract (GIT), it was found that although pH could affect the fraction of crystallised drug versus dissolved drug, it did not affect the crystal form of the drug nanocrystals inside the liposome (Chapter 2). In the present study, the liposomes were exposed to *in vitro* digestion conditions, where bile components and pancreatic lipase are present to represent the intestinal environment. The solid state characteristics of the ciprofloxacin in the liposomes was studied during digestion using *ex situ* SAXS measurements. Serendipitously, it was found that upon digestion, a polymorphic transformation of the CIPH<sub>2</sub>O nanocrystals to a new salt crystal was identified. This triggered an additional study to determine the component responsible for this behaviour. Specifically, the effect of bile salt on this polymorphic transformation was investigated using an *in situ* bile salt titration approach coupled to SAXS studies. The mechanism of the transformation to the new crystal form and the characteristics of the new crystal were further analysed with cryo-TEM, cross-polarised light microscopy, FTIR and temperature-dependent SAXS. The study concluded with *in vitro* drug release experiments for the different liposomal ciprofloxacin formulations under simulated digestive and non-digestive environments.

## 4.2 Experimental section

### 4.2.1 Materials

Liposomal ciprofloxacin (50 mg/mL) was kindly gifted from Aradigm Corporation (Hayward, CA, USA). Tris maleate (reagent grade), ammonium sulfate (>99%), bile salt (sodium taurodeoxycholate hydrate NaTDC >95%), cholesterol (>99%), L-histidine ( $\geq 99\%$ ), triethanolamine ( $\geq 99\%$ ), 4-bromophenylboronic acid (4-BPBA, >95%), phospholipase A<sub>2</sub> (PLA<sub>2</sub>) from porcine pancreas and sucrose (>99.5%) were purchased from Sigma Aldrich (St. Louis, MO, USA). 1,2 -Dioleoyl-sn-glycero-3-PC (DOPC) was purchased from Cayman Chemical Company (Michigan, USA). Hydrogenated soy phosphatidylcholine (HSPC) was obtained from Lipoid GmbH (Ludwigshafen, Germany). Calcium chloride (>99%) and sodium hydroxide pellets (reagent grade) was obtained from Ajax Finechem (Seven Hills, NSW, Australia). Sodium chloride (>99%), ciprofloxacin hydrochloride monohydrate, ciprofloxacin and orthophosphoric acid (85% w/w) were purchased from Chem Supply (Gillman, SA, Australia). Sodium azide was purchased from Merck Schuchardt OHG (Eduard-Buchner-StraÙe, Hohenbrunn, Germany). Hydrochloric acid 36% (analytical grade) was purchased from Biolab Aust Ltd (Clayton, VIC, Australia). Water was sourced from a Millipore water purification system using a Quantum™ EX Ultrapure Organex cartridge (Millipore, Australia). HPLC grade methanol and acetonitrile were purchased from Merck (MA, USA).

### 4.2.2 Preparation of digestion medium, bile salt buffers and enzymes

Tris buffer was prepared with 50 mM Tris maleate, 5 mM CaCl<sub>2</sub>·2H<sub>2</sub>O, 150 mM NaCl, 6 mM NaN<sub>3</sub> as anti-microbial agent, and adjusted to pH 6.5 using NaOH and HCl solutions. This buffer was used to prepare both the digestion medium (used in the *ex situ* digestion SAXS studies and *in vitro* drug release studies) as well as to prepare the concentrated bile salt buffer (used for the *in situ* bile salt titration SAXS study). The digestion medium consisting of 5 mM NaTDC and 1.25 mM DOPC to represent the fasted intestinal conditions (19). The DOPC was first dissolved with 1 mL of chloroform in a round-bottom flask, a thin lipid film was formed after excess chloroform was removed under vacuum. The required amount of Tris buffer and NaTDC were then added to the DOPC lipid film and the preparation was sonicated to dissolve any remaining solid particles. The final digestion medium was stored at 4 °C before use with a shelf life of 7 days at 4 °C storage conditions. For the *in situ* bile salt titration SAXS studies (Refer to

section 2.4.2), 150 mM sodium taurodeoxycholate was dissolved in the Tris digestion buffer and sonicated to dissolve the bile salts before being vortex mixed to form a homogenous solution.

Pancreatic lipase was prepared at the equivalent of approximately 1000 TB units/mL of digest by weighing 4 g of pancreatin and adding 5 mL of Tris buffer to form a suspension in a 12 mL plastic centrifuge tube and centrifuged at 2013 g at 4 °C for 15 min. This roughly produced 4 mL of supernatant, which was stored at 4 °C prior to addition to the digestion vessel to initiate digestion.

#### 4.2.3 Preparation of liposomal ciprofloxacin nanocrystals for SAXS analysis

GMP-manufactured ciprofloxacin liposomes gifted by Aradigm Corporation (Hayward, CA, USA) at 50 mg/mL (ciprofloxacin hydrochloride concentration) were diluted four fold with 180 mg/mL sucrose and Tris digestion buffer (adjusted to pH 6.0) to produce liposomes containing ciprofloxacin at 12.5 mg/mL. The choice of sucrose as the cryoprotectant was kept constant from previous studies (12, 14). The resulting dispersions were transferred in 1 mL aliquots to 2 mL HPLC glass vials for the freeze-thawing process. The samples were snap frozen in liquid nitrogen and then stored in the -80 °C freezer for at least 2 days. The samples were then thawed in a water bath at room temperature (~20 °C) to form liposomal ciprofloxacin nanocrystals. All experiments conducted on the liposomal ciprofloxacin nanocrystal formulations were performed within 24 hrs post thawing.

Because of the dilute nature of the samples in the bile salt titration SAXS studies, in order to obtain higher signals for the solid state characterization of the drug inside the liposomes, a higher concentration of liposomal nanocrystal formulations were also prepared as reported previously(14). Briefly, the liposomal ciprofloxacin nanocrystals formulations were prepared by freeze-drying the freeze-thawed 12.5 mg/mL dispersions and reconstitution in a smaller volume of buffer to yield a dispersion at 25 mg/mL drug concentration. In order to achieve this, the liposomes containing drug at 12.5 mg/mL were frozen in liquid nitrogen in 2 mL aliquots in 4 mL glass vials. The frozen samples were then placed in the freeze drier (VirTis Wizard 2.0 Lyophilizer, SP Scientific, NY, USA) precooled to a -40 °C shelf temperature. Primary drying was performed at a pressure of <12 mTorr, condenser temperature of -93 °C, and shelf temperature of -40 °C for 48 h, followed by secondary drying at a pressure of <12 mTorr and shelf temperature of 25 °C for 12 h. The

lyophilized liposome powders were redispersed in Tris buffer at a concentration of 25 mg/mL, i.e., double the concentration of the original preparation.

#### 4.2.4 Small angle X-ray scattering (SAXS)

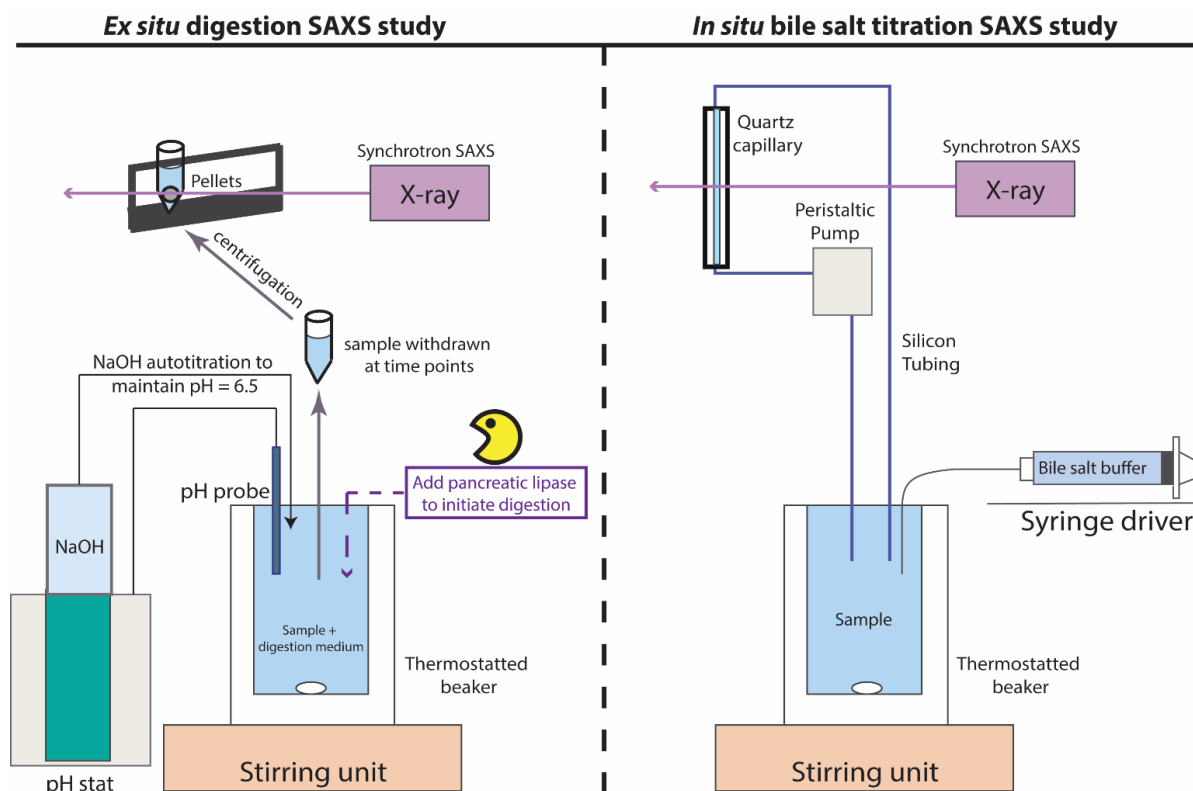
Solid state characterization was performed at the SAXS/WAXS beamline at the Australian Synchrotron. The X-ray beam had a wavelength of 0.6199 Å (20.0 keV) and was calibrated using silver behenate to give a camera to detector distance of 567.5 mm and a  $q$ -range of the magnitude of the scattering vector from 0.03 to 1.9 Å<sup>-1</sup>. A 1-s acquisition period was used, and the two-dimensional SAXS scattering patterns were acquired using a Pilatus 1 M detector with a pixel size of 172 µm. The scattering patterns were then integrated into the one-dimensional scattering function  $I(q)$  vs  $q$  using the ScatterBrain Analysis software. Identification of the drug solid state was determined from the positions of the diffraction peaks in the scattering function and compared to the published diffractograms of different crystalline forms of ciprofloxacin.

##### 4.2.4.1 *Ex Situ* digestion SAXS study

The physical setup of the *ex situ* digestion SAXS study is depicted in Schematic 1 (left), and performed according to previously established method(19). The pH stat auto titrator (Metrohm, Switzerland) was coupled to a dosing unit with autoburette, stirring unit and a glass pH electrode (iUnitrode) (Metrohm AG, Herisau, Switzerland). Tiamo 2.0 software was used to control the pH stat apparatus. The thermostatted glass beaker (37 °C) was placed on a magnetic stirring unit with a stirring bar. To start a digestion study, 9 mL of digestion medium was added to the glass beaker, followed by 2 mL of liposomal dispersions. The mixture was mixed for 1 min and pH was adjusted to 6.5 ± 0.003. An aliquot of 200 µL was withdrawn from the mixing glass beaker as time point zero. 1 mL of pancreatic lipase solution or PLA<sub>2</sub> was added to initiate the digestion process. A 0.6 M NaOH solution was used as titrant to maintain the pH at 6.500. The duration of the digestion experiment was set to 30 min. Samples (200 µL) were retrieved from the vessel at various time points during the digestion studies (5, 10, 20, 30 min after the addition of enzyme) and placed in glass HPLC inserts (6 x 31 mm, conical point, 250 µL purchased from Sigma Aldrich) containing lipase inhibitor (10 µL of 0.1 M 4-BPBA in methanol) followed by placing the insert inside an Eppendorf tube (Sigma 1-14 microfuge, Sigma laborzentrifugen GmbH, Germany) for centrifugation of 1 min at 7378 g. The insert was then placed inside a 3D printed-custom-built sample holder in line with the X-ray beam for

Chapter 4: Exposure of nanocrystallised ciprofloxacin liposomes to digestive media induces solid state transformation and altered *In vitro* drug release

SAXS measurement. The pellet phase was analyzed by acquiring the scattering pattern immediately after centrifugation was completed (within 3 min of taking the sample). This setup allowed for the real-time solid state characterization of the liposomal formulations during the digestion process with increased sensitivity by acquiring scattering patterns from the pellet phase.



**Schematic 1.** (Left) Experimental configuration for the *ex situ* digestion synchrotron SAXS studies. The liposomal dispersion and the digestion medium were placed inside the thermostatted beaker (37 °C). The beaker was connected to a stirring unit and a pH stat which maintained the pH within the beaker at pH 6.500 by titrating 0.6 M NaOH solutions automatically into the beaker. The pancreatic lipase or PLA<sub>2</sub> was added to initiate digestion and at set time points, 200 µL of aliquots were withdrawn and centrifuged for SAXS measurements. (Right) Experimental configuration for the *in situ* bile salt titration SAXS studies. Liposomal dispersions were magnetically stirred in a thermostatted beaker (37 °C). The peristaltic pump circulated the aqueous sample through the quartz capillary aligned with the X-ray beam. The bile salt buffer solution was delivered into the beaker using a syringe driver. SAXS measurements were acquired at increasing bile salt to ciprofloxacin molar ratios with an equilibration time of 1 min after each addition.

## Chapter 4: Exposure of nanocrystallised ciprofloxacin liposomes to digestive media induces solid state transformation and altered *In vitro* drug release

### 4.2.4.2 *In Situ* bile salt titration SAXS study

Schematic 1 (right) depicts the configuration of the *in situ* bile salt titration SAXS study. Briefly, a thermostatted glass beaker (37 °C) was connected to a magnetic stirrer with a mixing speed of 100 rpm. Tiamo 2.0 software was used to monitor the temperature. A 10 mL aliquot of the liposomal dispersion (25 mg/mL ciprofloxacin concentration) was added to the glass beaker. A peristaltic pump connected with silicon tubing that circulated the contents of the beaker through a 1.5 mm diameter quartz capillary aligned with the X-ray beam at approximately 10 mL/min. This allows for the real time *in situ* solid state characterization of the liposomal formulation when exposed to increasing concentration of bile salt. Concentrated bile salt solution in Tris buffer (150 mM NaTDC) was loaded into a 10 mL syringe and delivered to the beaker via a cannula using a remotely controlled syringe driver. The position of the syringe driver was recorded after each addition until all 10 mL of bile salt buffer was delivered to the glass beaker. For each addition, the syringe driver was moved at 1 unit difference to ensure same volume (~0.2 mL) of bile salt solution was introduced to the glass beaker and the sample within the glass beaker was allowed to equilibrate for 1 min before scattering patterns were acquired at each increased bile salt concentration. The molar ratio of NaTDC to ciprofloxacin HCl was then calculated to study the bile salt-dependent solid state changes to the liposomal ciprofloxacin formulations.

### 4.2.4.3 Temperature dependent SAXS study

For the temperature-dependent SAXS study, the FP82HT hot stage unit (Mettler Toledo, VIC, Australia) was vertically mounted onto a stage holder aligned with the X-ray beam and connected to a Mettler Toledo FP90 central processor. Isolated ciprofloxacin bile salt precipitate samples (~100 mg) (refer to section 2.6) were packed onto a quartz slide (Proscitech, G380 50.8 × 25.4 mm), which was placed inside the hot stage. The quartz slide was chosen to reduce background scattering. Heating scans were conducted from 30°C to 250°C at 10°C/min. Real temperature was monitored both on the hot stage as well as from a K-type thermocouples and a lakeshore model 340 temperature control unit at the synchrotron. SAXS patterns were acquired at every 30 sec and temperatures were recorded at each measurements.

### 4.2.5 Cryogenic Transmission Electron Microscopy (Cryo-TEM)

Samples were prepared for cryo-TEM using a laboratory-built humidity-controlled vitrification system, with humidity kept close to 80% for all experiments, and ambient temperature of 22 °C.

## Chapter 4: Exposure of nanocrystallised ciprofloxacin liposomes to digestive media induces solid state transformation and altered *In vitro* drug release

200-mesh copper grids coated with perforated carbon film (Lacey carbon film: ProSciTech, Qld, Australia) were glow discharged in nitrogen to ensure a hydrophilic supporting substrate. 4  $\mu$ L aliquots of the sample were pipetted onto each grid and 30 s adsorption time allowed prior to plunging. Grids were blotted manually using Whatman 541 filter paper, for approximately 2 s. Blotting time was optimised for each sample. Grids were then plunged into liquid ethane cooled by liquid nitrogen. Frozen grids were stored in liquid nitrogen until required.

The samples were examined using a Gatan 626 cryoholder (Gatan, Pleasanton, CA, USA) and Tecnai 12 Transmission Electron Microscope (FEI, Eindhoven, The Netherlands) at an operating voltage of 120 KV. At all times low dose procedures were followed, using an electron dose of 8-10 electrons/ $\text{\AA}^2$  for all imaging. Images were recorded using a FEI Eagle 4k x 4k CCD camera at magnifications ranging from 15 000x to 50 000x.

### 4.2.6 Isolation of Ciprofloxacin bile salt precipitate

Liposomal ciprofloxacin at 50 mg/mL and ciprofloxacin HCl suspension at 50 mg/mL were mixed with NaTDC buffer separately (pH 6.0) at equal ciprofloxacin to NaTDC molar ratios. The mixtures were then magnetically stirred for 24 hrs at room temperature. The drug suspension with bile salt mixture was filtered with a 5.5 cm Whatman 1 filter paper under vacuum to separate the precipitate dried at 25 °C for 24 hrs in a vacuum oven. To separate the liposomes from the precipitate, the liposomal ciprofloxacin with bile salt mixture were transferred to centrifuge tubes (Beckman Coulter, CA). The tubes were placed into the buckets of a SW 60Ti rotor (Beckman Coulter, CA) and subsequently centrifuged at 58,000 rpm, 15°C for 1 hr (Beckman Optima XE-90, Beckman Coulter, CA). The supernatant liquid and liposomal gel were discarded, and white solid precipitate resulting from centrifugation was collected into a glass vial. The collected precipitate was also dried at 25 °C for 24 hrs in a vacuum oven. These samples were used to characterise the salt formation using FTIR.

For temperature-dependent SAXS and CPLM studies, liposomal ciprofloxacin nanocrystals were mixed with excess bile salt buffer at 1:3 CIP : NaTDC molar ratio. The mixture was magnetically stirred for 24 hrs at room temperature and the precipitate was collected from the centrifugation method as described above and further dried at 25 °C under vacuum for 24 hrs.

#### 4.2.7 FTIR to investigate formation of ciprofloxacin salt

The isolated ciprofloxacin bile salt precipitate (CIPTDC) as well as the liposomal ciprofloxacin bile salt precipitate (refer to section 2.6) were analysed using a PerkinElmer Frontier FTIR with attenuated total reflectance (ATR) crystal (Waltham, Massachusetts). The sample (~ 2-3 mg) was placed on the ATR crystal, then the pressure valve was placed on top of the sample to increase sensitivity and contact with the ATR crystal. A background scan was performed first and used to subtract from the sample spectrum collected. NaTDC, ciprofloxacin and ciprofloxacin HCl were scanned as reference IR spectrum for comparison. The spectra for all samples were acquired from 650 to 3650  $\text{cm}^{-1}$  at the resolution of 2  $\text{cm}^{-1}$  using 15 scans setting.

#### 4.2.8 Cross polarized light microscopy (CPLM) and hot stage microscope

A Nikon ECLIPSE Ni-U upright microscope fitted with crossed polarising filters, Plan Fluorite objective and a DS-U3 digital camera control unit (Nikon, Tokyo, Japan) was used for CPLM imaging. CPLM was performed on liposomal ciprofloxacin nanocrystals before and after exposure to bile salt solution. This technique was used to determine whether macroscopic crystals had precipitated exterior of the liposome upon exposure to bile salt buffer. Large crystalline precipitate would show birefringence under crossed polarised light.

Hot stage microscopy was used to examine the thermal properties of the ciprofloxacin bile salt precipitate formed when liposomal ciprofloxacin nanocrystals were exposed to bile salt. Isolated precipitate (~ 2 mg) was spread across the microscope glass slide covered by glass coverslip. The glass slide was placed onto the FP82HT hot stage unit (Mettler-Toledo, Greifense, Switzerland) observed under the Nikon ECLIPSE Ni-U upright microscope. The heating of the precipitate was controlled by the FP 90 Central processor (Mettler-Toledo, Greifense, Switzerland). Samples were heated from 30 °C to 250 °C at 10 °C/min. Images were captured at every 10 °C.

#### 4.2.9 Preparation of sample for *in vitro* drug release studies

Liposomes were prepared by dissolving HSPC and cholesterol at a 1.0 : 0.87 molar ratio in chloroform. The lipid mixtures were then dried with nitrogen gas for 3 hrs and residual solvent was extracted by placing the mixture under vacuum at 50 °C overnight. The dried lipid film was hydrated with 500 mM ammonium sulfate pH 3.0 solution to obtain

## Chapter 4: Exposure of nanocrystallised ciprofloxacin liposomes to digestive media induces solid state transformation and altered *In vitro* drug release

a 10% w/w lipid dispersion and incubated at 60 °C oven for 30 min before vortex mixed to form a coarse dispersion (multilamellar liposomes). The lipid dispersions were then extruded 20 times through 0.1 µm polycarbonate membrane filters (Nucleopore®, Whatman, USA) using an extruder (Avanti Polar Lipids Inc, Alabaster, USA) to generate unilamellar vesicles. To perform active drug loading, the external medium of the liposomal dispersion was dialfiltrated with 10 volumes of 5 mM histidine buffer (pH 6.0) containing 145 mM NaCl and 6 mM NaN<sub>3</sub> using a 10 mL Amicon® stirred ultrafiltration cell (Merck, Australia) through a Ultracel® 30 kDa regenerated cellulose ultrafiltration discs, diameter 25 mm (EMD Millipore Corporation, Billerica, MA, USA). The dialfiltrated liposomes were analysed for the lipid concentration using the Wako Phospholipid C assay kit (FUJIFILM Wako Diagnostics U.S.A). Ciprofloxacin solutions at the required concentration (0.3 : 1 drug to lipid ratio) were prepared in water and were used for drug loading by mixing the pre-prepared drug solution and dialfiltrated liposome solution at 1:1 v/v ratio. The liposome and drug mixtures were then vortex mixed and stored in an oven at 60 °C for 1 hr to complete drug loading.

To generate liposomal ciprofloxacin nanocrystals, the drug-loaded liposomes were diluted 4-fold with Tris buffer (pH 6.0) and 180 mg/mL sucrose solutions. The prepared dispersions were vortex mixed and 650 µL of sample was transferred into each 1.5 mL HPLC glass vials. The samples were then snap frozen in liquid nitrogen for 5 min and immediately stored in the -80 °C freezer for at least 2 days. The samples were then thawed in water at room temperature just prior to the *in vitro* drug release studies.

### 4.2.10 *In vitro* drug release studies

The *in vitro* drug release studies were conducted using the digestion setup with the pH stat apparatus described in 2.4.1. Digestion medium (16.8 mL) was added to the thermostatted beaker along with 1.2 mL of liposomal dispersion sample and 2 mL of pancreatic lipase solution to make up to a 20 mL digestion volume. For the control study of Tris buffer only, 1.2 mL of liposomal dispersion was added to 18.8 mL of Tris buffer (pH 6.5) within the beaker. The pH of the mixture was adjusted to pH 6.5 ± 0.003 and the digestion time was set at 24 hrs. To quantify the amount of ciprofloxacin release from the liposome, a previously reported assay was used (20). Briefly, at predetermined time points (t = 0, 0.5, 1, 2, 4, 8, 12, 24 hr after pancreatic lipase addition), 400 µL of aliquot was withdrawn from the beaker and transferred to a 10 K Nanosep centrifugal device with Omega Membrane (Pall Laboratory Australia, Cheltenham, Victoria) and centrifuged at

8100 g for 18 min. The filtrate from the centrifugal device was assayed for the free drug release from the liposome using HPLC method described below. The residual sample left on top of the filter was assayed for the total amount of drug present within the liposomes withdrawn from the drug release experiment by dilution into 80% methanol to dissolve the liposomes. The original liposomal dispersion was also diluted into 80% methanol to allow for quantification of the total amount of ciprofloxacin introduced in the drug release experiment by HPLC. The percent release at each time point was calculated by the amount of free drug released to the total drug present. The drug release experiment was designed and conducted under complete sink conditions.

#### 4.2.11 Quantification of ciprofloxacin using HPLC

The amount of ciprofloxacin present in the filtrate of the centrifugal device was quantified using a previously reported HPLC method (20). Shimadzu Nexera binary UPLC system fitted with diode array detectors (DAD) was used to perform the HPLC studies (Shimadzu Corporation, Kyoto, Japan). The column temperature was set at 35 °C and a Symmetry reversed-phase C18 column (3.5 µm, 4.6 x 75 mm<sup>2</sup>, Waters Symmetry®, MA, USA) was used. The detector for integration was set at 280 nm for detection of ciprofloxacin. The mobile phase consisted of a mixture of 0.5% TEA in water, pH 3.0 and 100% methanol at 83:17 v/v ratio and eluted at a flow rate of 1.3 mL/min. Sample injection volume was set at 10 µL and a run time of 12 min. A standard curve was constructed from ciprofloxacin in the mobile phase at concentrations of 10, 25, 50, 100, 250 and 500 µg/mL, diluted from a stock solution of 500 µg/mL. To prepare the stock solution of ciprofloxacin, 12.5 mg of ciprofloxacin HCl monohydrate was weighed into a 25 mL volumetric flask, then 0.1 mL of 7% phosphoric acid was added and the prepared mobile phase was used to make up the rest of the volume. The sample collected from the *in vitro* release experiments were diluted at least 4-fold with the mobile phase before injecting into the HPLC.

### 4.3 Results and discussion

#### 4.3.1 *Ex situ* solid state transformation of liposomal ciprofloxacin nanocrystal during *in vitro* digestion

The solid state characteristics of drug encapsulated inside the liposomes when the liposomal formulations were exposed to simulated digestive environment (i.e. in the

presence of bile salt and various enzymes) were evaluated using *ex situ* digestion SAXS studies. **Figure 1** shows the scattering patterns acquired for different liposomal formulations before and during the *in vitro* digestion studies. Before digestion, ciprofloxacin liposomes with drug nanocrystals showed a crystal form of the ciprofloxacin hydrate form consistent with previous study at pH 6.5 (pH of the digestion study to simulate the fasted intestinal pH) (14). The signature peak for the ciprofloxacin hydrate crystal at  $q = 0.46 \text{ \AA}^{-1}$  is highlighted in blue in **Figure 1 a and 1 c**. When nanocrystallised ciprofloxacin liposomes were exposed to the digestive environment representative of the fasted state, a new crystal form is identified with two prominent peaks shown at  $q = 0.35$  and  $0.62 \text{ \AA}^{-1}$  (highlighted in green in **Figure 1 a and 1 c**). This new crystal transformation was seen for the nanocrystallised ciprofloxacin liposomes when digested using either pancreatic lipase or PLA<sub>2</sub>. On taking closer look at the scattering patterns for nanocrystallised ciprofloxacin liposomes during *in vitro* digestion, the new crystal formation was actually observed at time point zero in both **Figure 1 a and 1 c**. At this time point, the liposomes were dispersed in the digestion medium, however, neither pancreatic lipase nor PLA<sub>2</sub> had been added into the digestion vessel. This meant that the polymorphic transformation from the encapsulated ciprofloxacin hydrate nanocrystals to the new crystal was not due to the digestion of the liposomes by the pancreatic lipase or the PLA<sub>2</sub>. It was an interaction of the components present in the digestion medium with the ciprofloxacin within the liposomes.

Further digestion with the pancreatic lipase or PLA<sub>2</sub> did not induce further changes to the new crystal form during the 30 min digestion studies. For the ciprofloxacin liposomes without nanocrystals (i.e. not subject to freeze/thaw) and empty liposomes (no ciprofloxacin present), there were no crystalline drug peaks identified resembling either the ciprofloxacin hydrate nanocrystal or the new crystal form. This indicates that the drug inside the ciprofloxacin liposome is either dissolved in solution or presented as an amorphous form. The addition of bile salt and pancreatic lipase did not modify the solid state characteristics of the drug inside the liposome for the ciprofloxacin liposomes without nanocrystals.

Overall, the liposomal ciprofloxacin nanocrystals digested with pancreatic lipase showed a lower scattering intensity for the ciprofloxacin hydrate crystals peaks than liposomes digested with PLA<sub>2</sub> after digestion of 30 min. This indicated that the transformation from the ciprofloxacin hydrate crystal to the new drug crystal is close to completion with only trace amount of ciprofloxacin hydrate crystals present by the end of

the digestion period (**Figure 1 a**). For the liposomes digested with PLA<sub>2</sub>, the peak intensity for the ciprofloxacin hydrate crystal was still very strong at the end of the digestion period (**Figure 1 d**). One possible explanation for this can be that the pancreatic lipase in this digestion environment has a stronger disruption effect on the liposomal bilayer than the PLA<sub>2</sub>. This is evident in the scattering intensity of the liposomal bilayers shown in **Figure 1 a and 1 c**. For **Figure 1 a**, the liposome scattering peaks previously reported at  $q = 0.39$  and  $0.83 \text{ \AA}^{-1}$  cannot be identified after 10 min of digestion of liposome with pancreatic lipase. However in **Figure 1 c**, the liposome scattering peaks are observed even after 30 min of digestion. The disruption of the liposomal bilayer induced by the pancreatic lipase that is not observed with PLA<sub>2</sub> could mean that as the bilayer is disrupted, more encapsulated drugs nanocrystals are exposed and leaked out of the lipid membrane, which allowed for more drug interaction with the digestion medium component that enabled complete drug polymorphic transformation to the new crystal form, hence a more complete transformation. For the PLA<sub>2</sub> digested sample, although the polymorphic transformation was observed, the presence of the ciprofloxacin hydrate crystals means that there are still a population of liposomes not been disrupted by the digestion with PLA<sub>2</sub>. This allowed for the preservation of the original ciprofloxacin hydrate nanocrystals encapsulated inside the liposomes.

Revisiting the composition of the digestion medium, it consisted of sodium taurodeoxycholate (NaTDC), DOPC and Tris buffer. DOPC is presented as vesicles in the buffer and should not have influenced the drug crystal form. With Tris buffer, from previous pH-dependent solid state SAXS measurements performed on the nanocrystallised ciprofloxacin liposomes (Chapter 2), there were no polymorphic transformation identified when the nanocrystallised ciprofloxacin liposomes were dispersed in Tris buffer at different pH environment (14). Hence, it is most likely that the bile salt (NaTDC) presented in the digestion medium is responsible for the new crystal formation. In order to confirm this hypothesis and evaluate the effect of NaTDC on the ciprofloxacin liposomes, *in situ* bile salt titration SAXS studies were performed in non-sink condition.

## Chapter 4: Exposure of nanocrystallised ciprofloxacin liposomes to digestive media induces solid state transformation and altered *In vitro* drug release

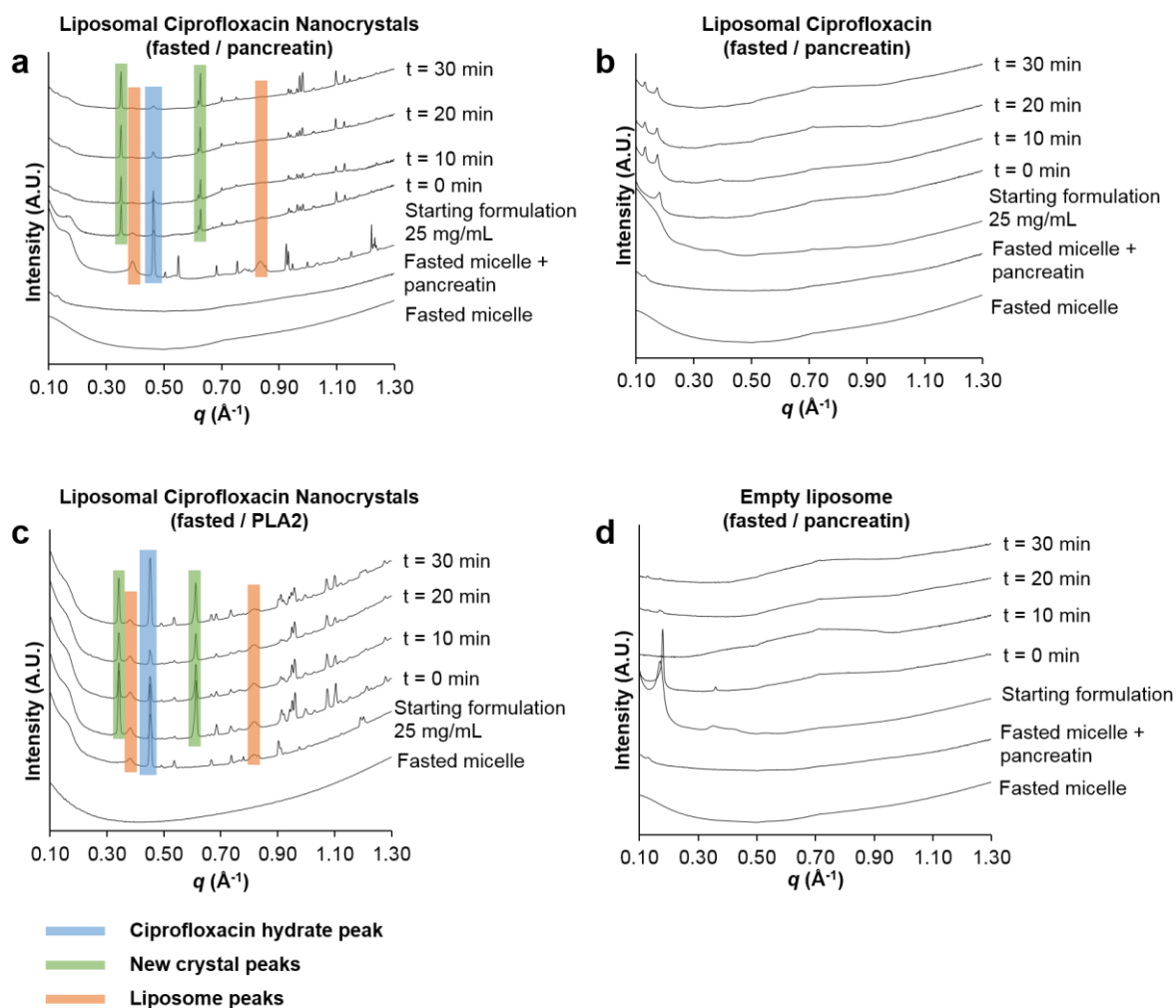


**Figure 1.** *Ex situ* digestion SAXS scattering patterns of liposomal dispersions. a) Digestion of liposomal ciprofloxacin nanocrystals in fasted state with pancreatic lipase. b) Digestion of liposomal ciprofloxacin (not freeze/thawed) in fasted state with pancreatic lipase. c) Digestion of liposomal ciprofloxacin nanocrystals in fasted state with PLA<sub>2</sub>. d) Digestion of empty liposome (no drug) in fasted state with pancreatic lipase. The areas highlighted in blue is the signature peak at  $q = 0.46 \text{ \AA}^{-1}$  of ciprofloxacin hydrate crystals. The areas highlighted in green is the signature peaks at  $q = 0.35$  and  $0.62 \text{ \AA}^{-1}$  of the new crystal form. The areas highlighted in orange is the liposome peaks at  $q = 0.39$  and  $0.83 \text{ \AA}^{-1}$ .

### 4.3.2 *In situ* polymorphic transformation of nanocrystallised ciprofloxacin liposomes upon exposure to biorelevant media

Flow through synchrotron SAXS was used to track the *in situ* drug solid state characteristics of the ciprofloxacin liposomes upon exposure to increasing concentration of bile salt (NaTDC) buffer. The scattering patterns for Tris buffer solution was subtracted

Chapter 4: Exposure of nanocrystallised ciprofloxacin liposomes to digestive media induces solid state transformation and altered *In vitro* drug release

from the acquired scattering patterns for the *in situ* study. Due to the low sensitivity of the formulation at 12.5 mg/mL in suspension and dilution introduced through titration of bile salt solution, a higher formulation concentration (25 mg/mL of nanocrystallised ciprofloxacin liposome) was used as a starting point of the titration. The titration experiment was conducted in a non-sink condition to allow high detection sensitivity as only the solid state form is of interest for this study. The scattering patterns acquired for the titration experiment on different liposomal dispersions are presented in **Figure 2**.

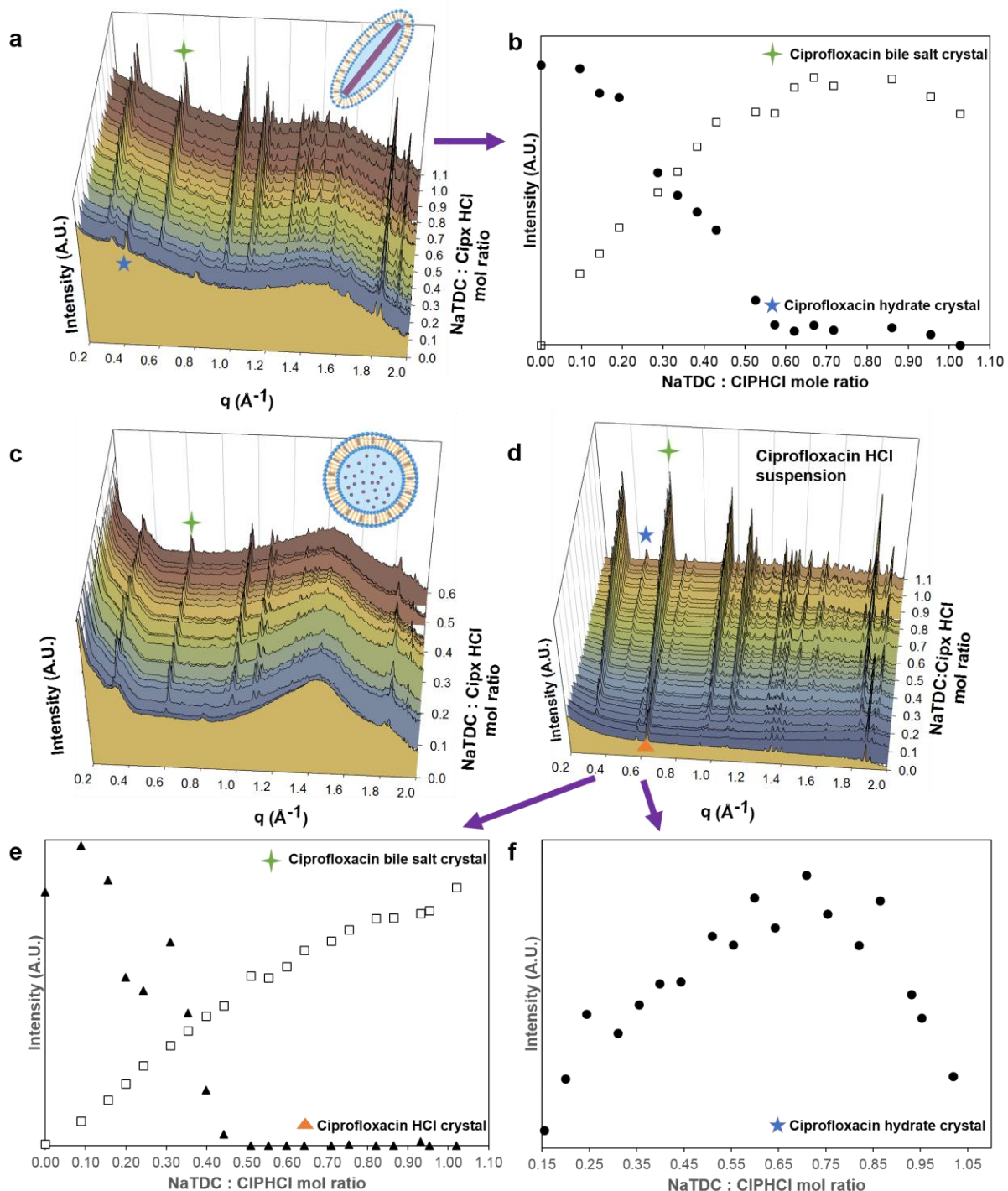


**Figure 2.** (a) *In situ* bile salt-dependent SAXS scattering patterns for liposomal ciprofloxacin nanocrystals. b) Change in relative intensity of the CIPH<sub>2</sub>O signature peak at  $q = 0.46 \text{ \AA}^{-1}$  versus the CIPTDC peak at  $q = 0.62 \text{ \AA}^{-1}$  at increasing NaTDC to CIPHCl molar ratio. c) *In situ* bile salt dependent SAXS scattering patterns for liposomal ciprofloxacin w/o nanocrystals, presence of the CIPTDC peaks are observed from 0.02 NaTDC : CIPHCl molar ratio. d) *In situ* bile salt dependent SAXS scattering patterns for CIPHCl suspension e) Change in relative intensity of the CIPHCl signature peak at  $q = 0.64 \text{ \AA}^{-1}$  versus the CIPTDC peak at  $q = 0.62 \text{ \AA}^{-1}$  at increasing NaTDC to CIPHCl molar ratio. f) Change in relative intensity of the CIPH<sub>2</sub>O signature peak at  $q = 0.46 \text{ \AA}^{-1}$  at increasing NaTDC to CIPHCl molar ratio.

**Figure 2 a** shows the *in situ* solid state transformation of the liposomal ciprofloxacin nanocrystals when exposed to NaTDC. The initial formulation showed the ciprofloxacin hydrate nanocrystals (at  $q = 0.46 \text{ \AA}^{-1}$ ) presented inside the liposomal dispersion. This is consistent with the *ex situ* digestion study and previous study(14). At approximately NaTDC : Ciprofloxacin hydrochloride (CIPHCl) molar ratio of 0.1, the new crystal peaks (observed above in **Figure 1 a and c**) are identified at  $q = 0.35$  and  $0.62 \text{ \AA}^{-1}$  and will be referred to as the ciprofloxacin taurodeoxycholate (CIPTDC) salt crystal. The concentration dependent polymorphic transition for the liposomal ciprofloxacin nanocrystal sample are depicted more clearly in **Figure 2 b**, where the relative scattering intensity from the ciprofloxacin hydrate (CIPH<sub>2</sub>O) at  $q = 0.46 \text{ \AA}^{-1}$  and ciprofloxacin taurodeoxycholate (CIPTDC) at  $q = 0.62 \text{ \AA}^{-1}$  crystal forms are plotted at increasing NaTDC: CIPHCl molar ratio. The transition was completed at approximately 0.62 NaTDC: CIPHCl molar ratio where the peak for CIPH<sub>2</sub>O disappeared completely leaving only the CIPTDC crystal form. The scattering patterns of this new (CIPTDC) salt crystal upon exposure to digestion medium were compared with known ciprofloxacin salt and polymorphic forms published in the literature. No matching crystal form was found.

The ciprofloxacin liposomes without nanocrystals were also titrated with NaTDC under non-sink condition and the scattering patterns with increasing NaTDC concentration are presented in **Figure 2 c**. Initially, there was no crystalline peaks identified with the formulation before addition of NaTDC, which is consistent with previous cryo-TEM and SAXS studies, that the drug is solubilised or in an amorphous state inside the liposome. As soon as NaTDC was titrated into the sample (as low as 0.02 NaTDC : CIPHCl molar ratio), the two signature peaks for CIPTDC at  $q = 0.35$  and  $0.62 \text{ \AA}^{-1}$  were identified in the

scattering pattern. The new crystal form was retained throughout the titration study. Since the drug inside the liposome before bile salt addition is in a dissolved state, it is more prone to complexation and salt crystal formation. In order to further prove that the complexation between ciprofloxacin and NaTDC in a concentration dependent manner was not due to the solubilisation of the liposome by the bile salt, a saturated drug suspension of CIPHCl was titrated with NaTDC buffer. **Figure 2 d** depicts the scattering patterns acquired during the *in situ* bile salt titration experiment for CIPHCl suspension. Briefly, the CIPHCl suspension exhibited the CIPHCl crystal form where the signature peak is identified at  $q = 0.64 \text{ \AA}^{-1}$ . The relative scattering intensity from the CIPHCl crystal at  $q = 0.64 \text{ \AA}^{-1}$  and the CIPTDC crystal at  $q = 0.62 \text{ \AA}^{-1}$  were plotted with increasing NaTDC : CIPHCl molar concentration in **Figure 2 e**. The CIPHCl crystal peak gradually decreased in intensity until disappearing at approximately 0.47 NaTDC : CIPHCl molar ratio. During the titration, the CIPTDC crystals started to form at 0.04 NaTDC : CIPHCl molar ratio and the scattering intensity of the CIPTDC peaks increased with concentration of NaTDC in the mixture. Another point to note is that CIPH<sub>2</sub>O crystal forms were also present during the bile salt titration experiment and the relative intensity from the CIPH<sub>2</sub>O crystal at  $q = 0.46 \text{ \AA}^{-1}$  with increasing NaTDC is illustrated in **Figure 2 f**. From approximately NaTDC : CIPHCl molar ratio of 0.15, the CIPH<sub>2</sub>O crystal was present in the mixture. The scattering intensity of the CIPH<sub>2</sub>O crystal increased with increasing NaTDC concentration and peaked at 0.71 NaTDC : CIPHCl molar concentration. Then the scattering intensity decreased but there was still existence of the CIPH<sub>2</sub>O form at the end of the titration experiment.

It is known that sodium taurodeoxycholate (NaTDC) has the ability to solubilise the phospholipid bilayers and that the effect of solubilisation increases as phase transition temperature of the phospholipid decreases (21, 22). For liposomal ciprofloxacin nanocrystals, the full transformation from the CIPH<sub>2</sub>O to CIPTDC salt crystal was achieved at around NaTDC : CIP mol ratio of 0.62 (NaTDC to phospholipid mol ratio is 0.98). This represented a total concentration of 31 mM NaTDC within the mixture. A previous study reported that the effective detergent to lipid molar ratio for sodium cholate to egg phosphatidylcholine liposomes is 0.3 and full solubilisation into mixed micelles was achieved at detergent to lipid mol ratio of 0.9 (23). The proposed mechanism is that when bile salt (NaTDC) is mixed with the liposomal dispersions with nanocrystals, it inserts into the phospholipid bilayer, solubilising the lipid bilayer forming mixed micelles, the drug

nanocrystals would leak into the exterior bulk phase and forming drug bile salt crystals. The CIPTDC crystal intensity increased as more bile salt was titrated to the liposome (**Figure 8**). At a NaTDC concentration of 31 mM, the liposomes should be fully solubilised leaving the originally encapsulated CIPH<sub>2</sub>O nanocrystals to be fully exposed to the bile salt buffer environment. From the SAXS *in situ* scattering profiles in 2 a and 2 d, at this concentration the crystalline peak for the CIPTDC crystal had reached its maximum whereas the CIPH<sub>2</sub>O peak intensity was at its lowest. To put this into perspective of the real intestinal environment, the average bile salt concentration reported in human duodenum is around 10.8 mM for the fasted state (24). In the titration experiment performed, at around 0.19 molar ratio of NaTDC: CIPH<sub>2</sub>O, the NaTDC concentration is around 11 mM. It is evident at this bile salt concentration, formation of the new CIPTDC crystal is already observed through SAXS that coexist with CIPH<sub>2</sub>O crystals. This means that the bile salt present in the intestines could induce the CIPTDC crystal formation which may impact the solubility of the parent drug ciprofloxacin when administering the liposomal ciprofloxacin nanocrystals in the gastric intestinal tract (GIT).

To investigate the changes to the structure of the liposomes and the drug crystal shape before and after the nanocrystallised ciprofloxacin liposomes were exposed to bile salt, CPLM and cryo-TEM were performed. CPLM is used to identify any large crystals formed in the dispersion, which would contribute to the crystals formed outside of the liposome (in the bulk aqueous phase). The results are shown in **Figure 3 a and b** representing before and after bile salt exposure respectively. At 10x magnification (Plan Fluorite objective), the resolution threshold is 920 nm, the nanocrystals within the liposomes of the original nanocrystallised ciprofloxacin liposomes are around 100-200 nm so no birefringence should be observed attributable to the nanocrystals inside the liposome. Before exposure to bile salt, there was no birefringence identified (**Figure 3 a**). Upon incubation with NaTDC buffer at 0.3 NaTDC : CIPHCl molar ratio in a non-sink condition (**Figure 3 c**), birefringence were observed throughout the sample indicating crystal precipitation in the bulk aqueous phase of the sample due to the CIPTDC salt crystallisation. The CIPTDC precipitated in a crystalline form with needle-like structures (micrometres in size). Cryo-TEM studies were also conducted to study the effect of bile salt on the liposomal bilayer and the nanocrystals inside the liposome. Before exposure to the bile salt, the nanocrystallised ciprofloxacin liposomes showed a one nanocrystal per liposome structure consistent with previous studies (12, 14) (**Figure 3 b**). When the

formulation is exposed to the bile salt (**Figure 3 d**), there were still a number of liposomes with nanocrystals encapsulated, however, there were also a few circular liposomes with no drug nanocrystals as well as micron sized needle-like crystal that were not encapsulated within a liposomal shell. These micron-sized rod-like structure aligns well with the observation from the CPLM results possibly due to the formation of the CIPTDC crystals in the bulk aqueous phase.

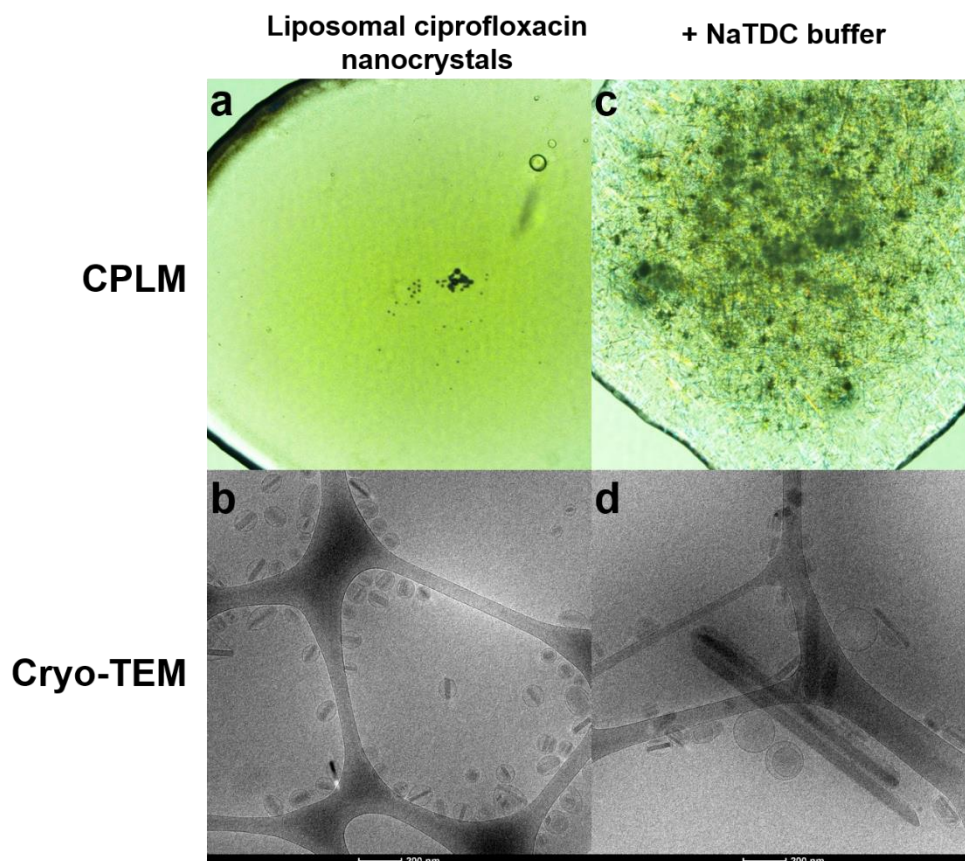


**Figure 3.** Cross polarised light microscopy images (CPLM) (a, c) and cryo -TEM images (b, d) for liposomal ciprofloxacin nanocrystals exposed to NaTDC at NaTDC : CIPHCl molar concentration of 0.3. Liposomal ciprofloxacin nanocrystals before addition of NaTDC under CPLM (a) and cryo-TEM (b). Liposomal ciprofloxacin nanocrystal after exposure to bile salt buffer at NaTDC : CIPHCl molar ratio of 0.3 under CPLM (c) and cryo-TEM (d). The scale bar represents 200 nm for the cryo-TEM images.

#### 4.3.3 pH dependent CIPTDC crystallisation

In order to understand the mechanism of the ciprofloxacin and bile salt crystallisation, the effect of pH on the new crystal formation was investigated in suspension using SAXS. Liposomal ciprofloxacin nanocrystals were exposed to NaTDC buffer at excess bile salt

concentration (3:1 NaTDC: CIPH<sub>2</sub>O molar concentration to allow complete transformation) and pH was adjusted to 7.5 as a starting point. The pH of the suspension mixture was gradually reduced with HCl solution. Aliquots of sample were taken at different pH and immediately assessed with SAXS static measurements which is presented as stacked scattering patterns in **Figure 4 a**. At pH 7.5, only the CIPH<sub>2</sub>O crystal with the signature peak at  $q = 0.46 \text{ \AA}^{-1}$  (highlighted in blue) was identified for the bile salt exposed nanocrystallised ciprofloxacin liposomes. When pH was reduced to 6.5, CIPTDC crystal peaks (the signature peak at  $q = 0.62 \text{ \AA}^{-1}$  highlighted in green) were identified and complete transformation to the new CIPTDC crystal is observed at pH 6.0 with absence of the diffraction peaks from the CIPH<sub>2</sub>O crystal form.

Similar experiments were also performed for ciprofloxacin suspension (refer to supporting information Figure S2) and results were similar to that of the liposomal ciprofloxacin nanocrystals. Interestingly, when the ciprofloxacin liposomes without nanocrystals were exposed to bile salt in a non-sink environment, the formation of the CIPTDC salt crystals was instantaneous and pH had no effect on the CIPTDC formation (Figure S1). This indicates that the ionisation state of the ciprofloxacin is a determining factor for the bile salt complexation. For liposomal ciprofloxacin nanocrystals, pH affect the ionisation state of the ciprofloxacin nanocrystals within the liposome which determines the ability of ciprofloxacin salt formation with taurodeoxycholate anion (**Figure 4 b**). At pH of 6.0 and below, the carboxylic acid group ( $pK_a = 6.08(25)$ ) is only half (or less) deprotonated and the nitrogen within the piperazine group ( $pK_a = 8.74$ ) are protonated (26). It has been reported that at pH 6, ciprofloxacin is around 50% zwitterionic or charge neutral and 50% cationic (27). This ionisation of ciprofloxacin into its cationic form allows it to interact with the anionic sulfonate group of the taurodeoxycholic acid forming the salt complex, which precipitates in a crystalline form. In the GIT, the pH in the duodenum is around 6, and gradually increases in the small intestine from pH 6 to about pH 7.4 in the terminal ileum (28). Therefore the chances of the CIPTDC formation is quite high *in vivo* especially during the transition from the highly acidic stomach to the duodenum.

Chapter 4: Exposure of nanocrystallised ciprofloxacin liposomes to digestive media induces solid state transformation and altered *In vitro* drug release

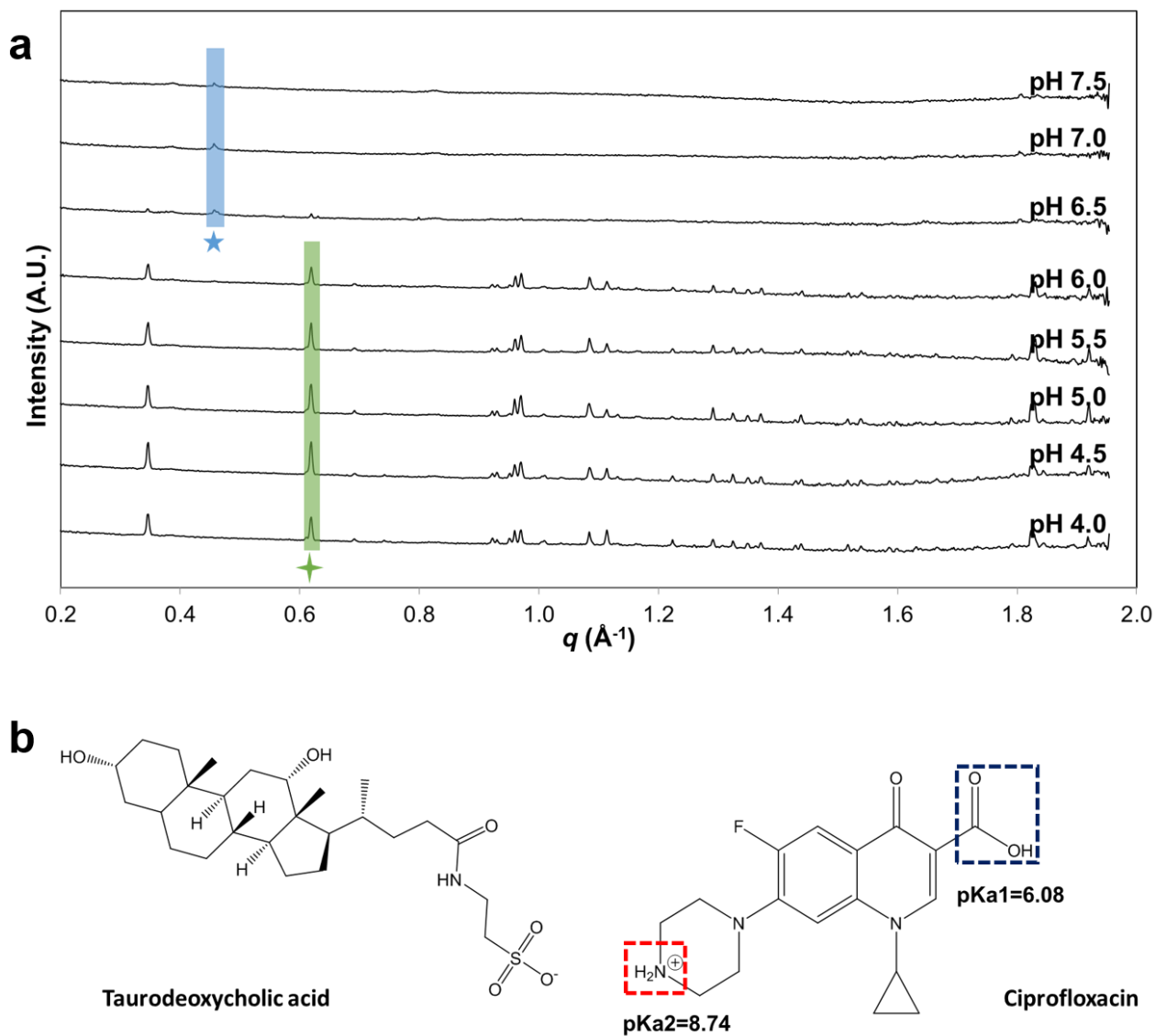


**Figure 4.** a) *Ex situ* SAXS scattering patterns of liposomal ciprofloxacin nanocrystals exposed to sodium taurodeoxycholate (NaTDC) solution at different pH values. The region highlighted in blue represents the CIPH<sub>2</sub>O peak at  $q = 0.46 \text{ \AA}^{-1}$  and the region highlighted in green represents the CIPTDC peak at  $q = 0.62 \text{ \AA}^{-1}$ . b) Chemical structure of taurodeoxycholic acid and ciprofloxacin, the ionisable functional groups of ciprofloxacin is highlighted.

#### 4.3.4 FTIR assessment of ciprofloxacin and sodium taurodeoxycholate salt formation

To investigate the complexation interaction of ciprofloxacin and NaTDC and the thermal properties of the crystalline salt precipitate, the CIPTDC salt crystals were first isolated and dried followed by FTIR analysis and temperature-dependent SAXS measurements. The infrared spectrum of the ciprofloxacin, CIPHCl, NaTDC, and CIPTDC precipitate isolated from both liposomal ciprofloxacin (LipoCIP) and ciprofloxacin suspension (CIP) are presented in **Figure 5**.

From FTIR, the protonation of the carboxylic group of the ciprofloxacin in the new CIPTDC salt was confirmed by the strong absorption band at around  $1728\text{ cm}^{-1}$  in CIP+NaTDC (**Figure 5 b**) and  $1730\text{ cm}^{-1}$  in LipoCIP+TDC (**Figure 5 c**). These peaks are very similar to the FTIR band of ciprofloxacin HCl which is at  $1700\text{ cm}^{-1}$ . It has been reported that the signature band correlated to the protonated C=O group, stretch around the  $1700\text{-}1780\text{ cm}^{-1}$  wavenumber region (29). The band stretch is also identified in ciprofloxacin succinic acid formation (30). Apart from the protonation of the carboxylic acid group, the nitrogen (NH group) of the piperazine within ciprofloxacin was also protonated making it positively charged. For the free base, the peak at  $834\text{ cm}^{-1}$  shown for CIP (**Figure 5 e**) was absent for the CIPHCl (**Figure 5 d**) and CIPTDC salts crystals (**Figure 5 b and c**) spectra. This band aligns with the IR absorption of piperazine at  $835\text{ cm}^{-1}$ . It was reported for piperazine hydrochloride (ionised piperazine), the formation of the amine salt of the piperazine group would make the absorption band at  $835\text{ cm}^{-1}$  vanish (31). For the nitrogen in the piperazine group, formation of the salt can be identified as medium to strong absorption peak near  $1600\text{ cm}^{-1}$ . LipoCIP+TDC have shown bands at  $1628$  and  $1545\text{ cm}^{-1}$  and CIP + TDC shown at bands at  $1629$  and  $1545\text{ cm}^{-1}$ ,  $1622$  and  $1552\text{ cm}^{-1}$  were identified for CIPHCl. These peaks are absorption due to the  $\text{-NH}_2^+$  deformation on the piperazine group(31). From the FTIR results, it is evident that the CIPTDC salt crystals have an ionised piperazine group and carboxylic acid group. The deformed secondary amine band indicated the complexation of the nitrogen (in the piperazine group of ciprofloxacin) with the taurodeoxycholate anion forming the CIPTDC salt crystals. The crystalline salt formation of ciprofloxacin is not a rare phenomenon, it has been previously reported, that ciprofloxacin has a tendency to form salt crystals with dicarboxylic acids (32,

33). The use of synthesised salts of ciprofloxacin is also a common approach to increase the aqueous solubility of ciprofloxacin.

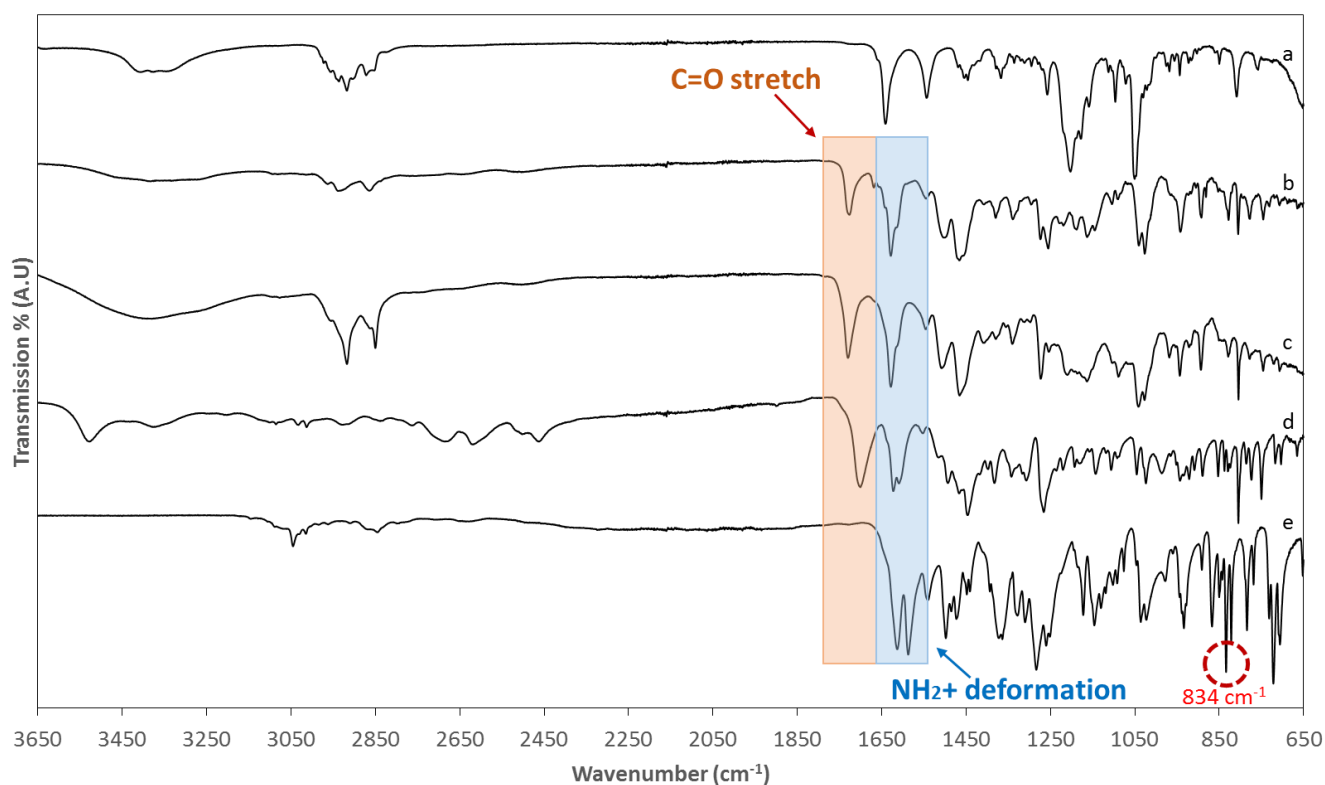


**Figure 5.** FTIR spectroscopy of a) sodium taurodeoxycholate (NaTDC). b) Ciprofloxacin HCl + taurodeoxycholate precipitate (CIP+TDC). c) Liposomal ciprofloxacin + taurodeoxycholate precipitate (LipoCIP+TDC) d) Ciprofloxacin hydrochloride monohydrate (CIPHCl) e) Ciprofloxacin (CIP).

#### 4.3.5 Thermal properties of crystalline CIPTDC salt

The isolated CIPTDC salt precipitate from liposomal ciprofloxacin nanocrystals exposed to bile salt buffer suspension was analysed for its thermal properties using both temperature-dependent SAXS and hot stage CPLM. **Figure 6** a shows the microscope images taken at 30, 130 and 150 °C, where changes to the structures were observed. At 30 °C, the precipitate showed no birefringence, this remained the same until when the temperature reaches 130 °C. At about 130 °C, birefringence was observed throughout the precipitates signifying some changes with the crystallinity and the structure. From 130 °C the solid precipitate started to melt until at about 150 °C, all the solids had melted and turned into a liquid state with a tinge of brown colour indicating the occurrence of decomposition.

#### Chapter 4: Exposure of nanocrystallised ciprofloxacin liposomes to digestive media induces solid state transformation and altered *In vitro* drug release

To investigate the solid state characteristics of the CIPTDC salt crystals at different temperatures, temperature-dependent SAXS were conducted and scattering patterns are presented in **Figure 6 b**. The CIPTDC crystalline salt maintained its crystallinity and strong diffraction peaks ( $q = 0.62 \text{ \AA}^{-1}$  highlighted in green) from 30 °C to 150 °C. From about 150 °C, the CIPTDC crystalline peaks started to diminish and no diffraction peaks were observed at 170 °C and above. This results showed similar trends observed with the hot stage CPLM experiment. It could be explained that the structural changes observed at around 120 -130 °C in CPLM could indicate dehydration of the CIPTDC crystal and the melting point is observed to be around 150 - 170 °C.

The melting point of the parent drug ciprofloxacin is around 225 - 257 °C (34), whereas the CIPTDC crystals formed due to exposure of the liposomal ciprofloxacin nanocrystals to bile salt is around 150 - 170 °C. Since the melting point of a solid indicates the strength of intermolecular forces, a lower melting point would indicate the crystal lattice with a weaker intermolecular forces. This means that potentially the formation of the CIPTDC crystals upon ingestion of the nanocrystallised ciprofloxacin liposomes within the small intestine, it could ultimately increase the solubility of the parent drug ciprofloxacin.

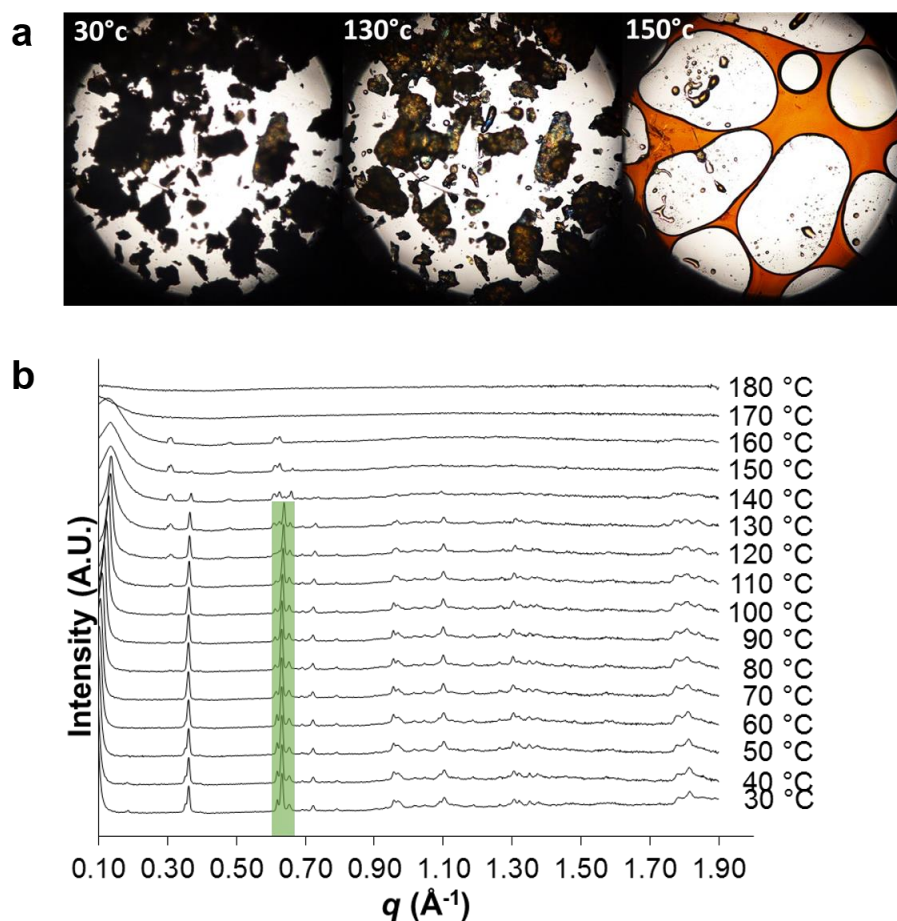


**Figure 6.** Thermal characteristics of the isolated CIPTDC crystals formed when liposomal ciprofloxacin liposomes were exposed to NaTDC buffer. a) Hot stage CPLM images of the precipitate at temperatures where the structures have changed. b) Temperature dependent SAXS scattering patterns. Both method used the same heating rate of 10 °C/min.

#### 4.3.6 *In vitro* drug release from liposomal ciprofloxacin formulation in simulated digestive environment

In order to investigate the rate of drug release from the ciprofloxacin liposomes with and without nanocrystals under simulated digestion environment, *in vitro* drug release studies were performed and results are shown in **Figure 7**. For the control with liposomes dispersed in Tris buffer alone at pH 6.5 (**Figure 7 a**), ciprofloxacin liposomes without nanocrystals showed a close to complete drug release at 24 hrs ( $88.6 \pm 4.9$  %). On the contrary, liposomal ciprofloxacin formulation with drug nanocrystals only showed a release of  $25.4 \pm 11.6$  % ciprofloxacin by the 24 hrs. When the majority of the drug is crystallised inside the liposome (from cryo-TEM images), less solubilised drug is available for diffusion out of the liposomal bilayer, hence limiting the drug release. The slow drug release from the nanocrystallised ciprofloxacin liposomes also indicates that faster drug leakage of ciprofloxacin from liposomes can be prevented.

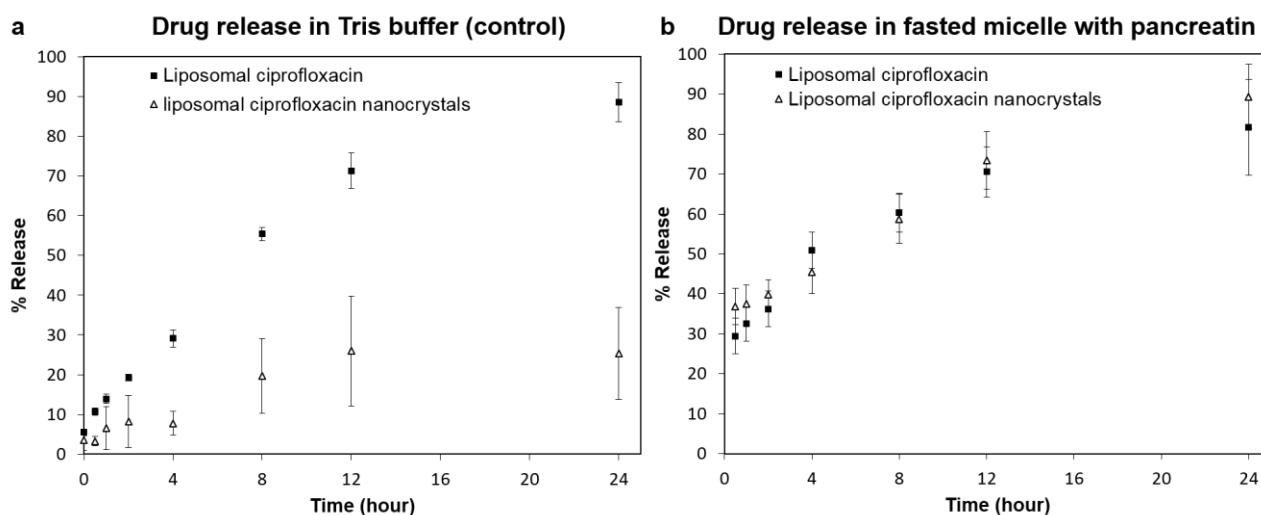


**Figure 7.** Comparison of the ciprofloxacin (CIP) release from liposomal ciprofloxacin formulations when dispersed in different medium *in vitro*. *In vitro* drug release profiles were performed at 37 °C in the pH stat apparatus over 24 hrs under stirring (setting 8). a) Percentage CIP release when

#### Chapter 4: Exposure of nanocrystallised ciprofloxacin liposomes to digestive media induces solid state transformation and altered *In vitro* drug release

liposomal ciprofloxacin and liposomal ciprofloxacin nanocrystals are dispersed in Tris buffer.b) Percentage CIP release when liposomal ciprofloxacin and liposomal ciprofloxacin nanocrystals are dispersed in digestion medium simulating the fasted state with addition of pancreatic lipase. The experiments were conducted in triplicates and the average percentage drug release relative to the total drug present is plotted. The error bar represents the standard deviation from the average results.

*In vitro* drug release studies were also performed under the simulated intestinal environment representing the fasted state for the ciprofloxacin liposomes and is depicted in **Figure 7 b**. The initial drug release at 30 min was around  $29.3 \pm 4.2$  % for ciprofloxacin liposomes without nanocrystals and  $37.6 \pm 6.1$  % for ciprofloxacin liposomes with drug nanocrystals. Both formulations showed a complete drug release at the end of the study. The final percentage drug release from ciprofloxacin liposomes without nanocrystals in the digestive environment was  $81.6 \pm 11.4$  % and from ciprofloxacin liposomes with nanocrystals was  $89.4 \pm 8.1$  %. The initial burst release of around 30 – 40 % of drug at 30 min could be due to the solubilisation effect of the bile salt and pancreatic lipase present in the mixture. The close to complete drug release from the liposomes without nanocrystals under digestive environment was very similar to the control. Fast drug release was observed in both the crystallised state and non-crystallised state of the drug inside the liposome upon dispersion into the digestion environment. Since we know from the *in situ* bile salt titration experiment, that bile salt (NaTDC) can induce polymorphic transformation from the CIPH<sub>2</sub>O nanocrystals form to the CIPTDC crystal form, this could explain the near identical fast and close to complete drug release observed in **Figure 7 b**.

These results indicated that the liposomal ciprofloxacin nanocrystal formulation exhibited a bile salt-induced-stimulated drug release behaviour. In terms of drug release inside the body, we can assume that when the liposomal drug nanocrystals is ingested, it will have a slow release or minimal drug leakage depending on the circulation time. When the formulation reaches the intestine where bile salt and enzymes are present, the transformation of the CIPH<sub>2</sub>O nanocrystals to the CIPTDC crystal formation would induce a faster drug release from the liposomes.

**Figure 8** showed a schematic summarizing the mechanism observed for the liposomal ciprofloxacin formulation with different drug solid state characteristics when exposed to the bile salt (NaTDC). For the ciprofloxacin liposomes without drug

Chapter 4: Exposure of nanocrystallised ciprofloxacin liposomes to digestive media induces solid state transformation and altered *In vitro* drug release

nanocrystals, addition of bile salt would solubilize some of the liposomes making them rupture and the ciprofloxacin leaked from the liposome would form the CIPTDC salt crystals outside the liposome. Although there might still be empty liposomes or liposomes where some drug remains solubilized inside the liposome. For the nanocrystallised ciprofloxacin liposomes, bile salt played a similar effect in solubilizing the membrane, and when the CIPH<sub>2</sub>O nanocrystals leaked out of the liposome, the CIPTDC salt crystals were formed outside of the liposome. The extent of the transformation would highly depend on the bile salt to liposome ratio and the bile salt to drug ratio.

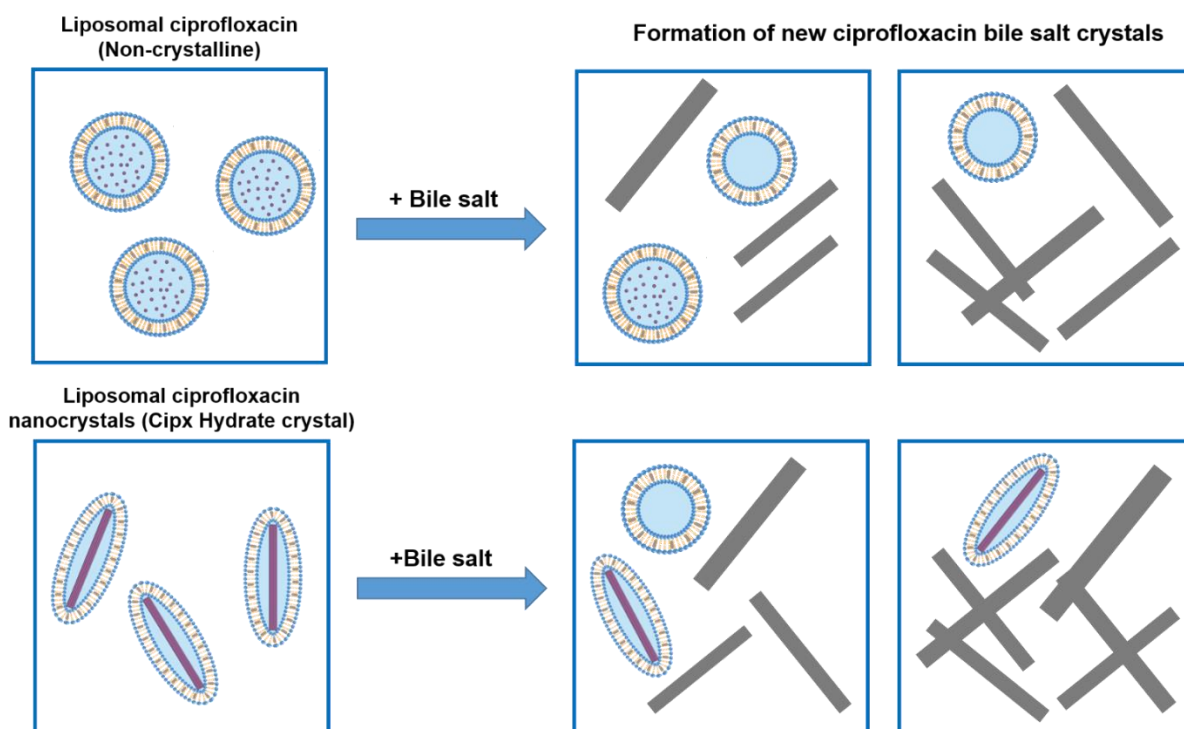


**Figure 8.** Schematic illustrating the effect of bile salt (NaTDC) on the liposomal ciprofloxacin formulations with different drug solid state characteristics. When the drug inside the liposome is not crystallised, it is believed to be solubilised in the inner aqueous core of the liposome. Exposing the liposomes with no nanocrystals to NaTDC, would allow for the bile salt to insert itself into the liposome and solubilise and rupture the liposomal bilayer. The encapsulated drug then leaks out of the liposomes and forms ciprofloxacin bile salt (CIPTDC) crystals in the bulk aqueous phase. For the liposomal ciprofloxacin with nanocrystals, when it is exposed to NaTDC, the encapsulated drug is in the CIPH<sub>2</sub>O crystal form, as the NaTDC solubilises the liposomal bilayer, the drug nanocrystals transitions from the CIPH<sub>2</sub>O crystals form to the CIPTDC crystal form. There are also liposomes that remained stable with drug nanocrystals inside.

## 4.4 Conclusion

This work presented an in depth understanding on the solid state transformation of the nanocrystallised ciprofloxacin liposome in the presence of biorelevant media (especially in terms of the drug interaction with a particular bile acid). The use of SAXS to study the real time polymorphic transformation of drug from liposomes under digestive environment is new and powerful. It provided better understanding of the drug solid state inside the liposome and any potential changes that could have occurred if ingested orally. From the results, few conclusions can be drawn. Firstly, ciprofloxacin nanocrystals inside the liposome can undergo polymorphic transformation during *in vitro* digestion. Secondly, it was found that the new crystal is formed between the ionised ciprofloxacin complexing with the sodium taurodeoxycholate (bile salt component) in the digestion medium. In retrospective, the duodenal bile acid concentration is around 5.4 – 21.5 mM with a mean concentration of 10.8 mM (containing 1.3 – 6.4 mM tauro-conjugated bile salts) (24), and the pH in the small intestine also varies from pH 6-7.4 (28). This means that depending on the solid state of the ciprofloxacin in the liposomes and the drug concentration, the new CIPTDC salt crystal formation is highly possible *in vivo* when ciprofloxacin liposomes are ingested orally. This effect of CIPTDC formation would be pronounced in the fed state where higher bile acid are present in the intestinal fluid.

Lastly, it is evident that the solid state of the drug would dictate the amount of drug release from the liposomes. In addition to that, the observed approximate 3.5-fold increase of ciprofloxacin from the nanocrystallised formulation, due to the new CIPTDC crystal formation also indicate that the change in the crystal form of the drug could also affect the percentage of drug release. This understanding would help researchers designing towards better liposomal formulation for oral drug delivery. It would also inspire future research into the study of bile salt responsive drug release from nanocarrier formulations.

## Acknowledgments

This study was funded under the Australian Research Council Centre of Excellence in Convergent Bio-Nano Science and Technology. SAXS studies were conducted on the SAXS/WAXS beamline at the Australian Synchrotron, Victoria, Australia. BB is the recipient of an ARC Future Fellowship. Cryo-TEM was conducted at the CSIRO Materials Science and Engineering under the help of Dr. Lynne Waddington.

## Supporting Information

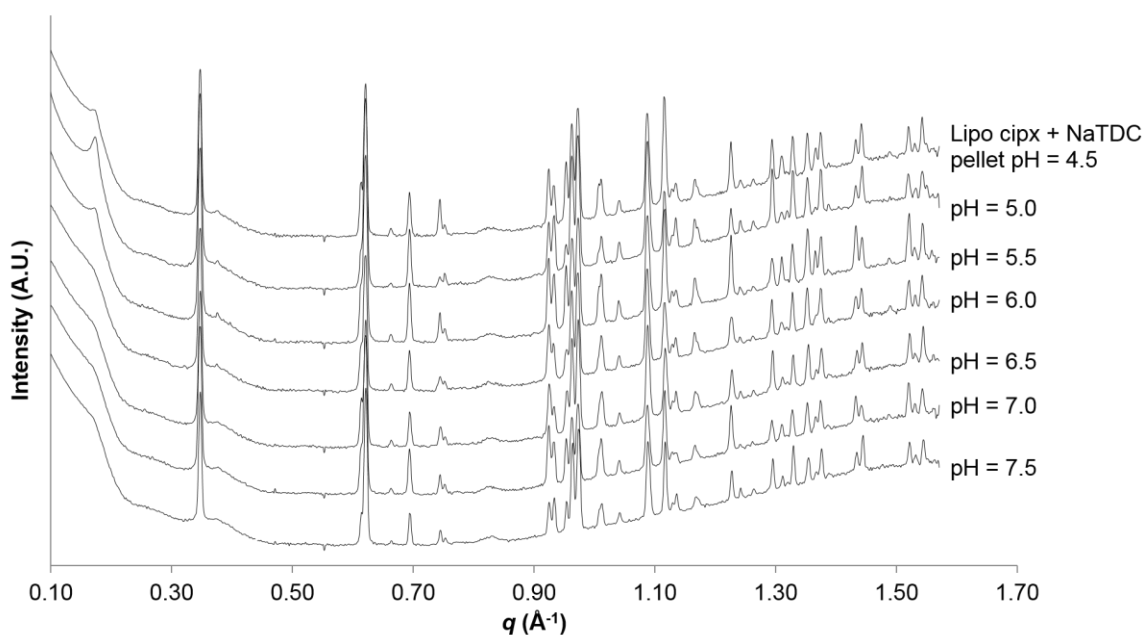


**Figure S1.** *Ex situ* static SAXS measurements of liposomal ciprofloxacin liposome (non-crystallised) dispersed in NaTDC buffer in non-sink condition at different pH. Varying the pH did not change the formation of the new CIPTDC salt precipitate.

Chapter 4: Exposure of nanocrystallised ciprofloxacin liposomes to digestive media induces solid state transformation and altered *In vitro* drug release

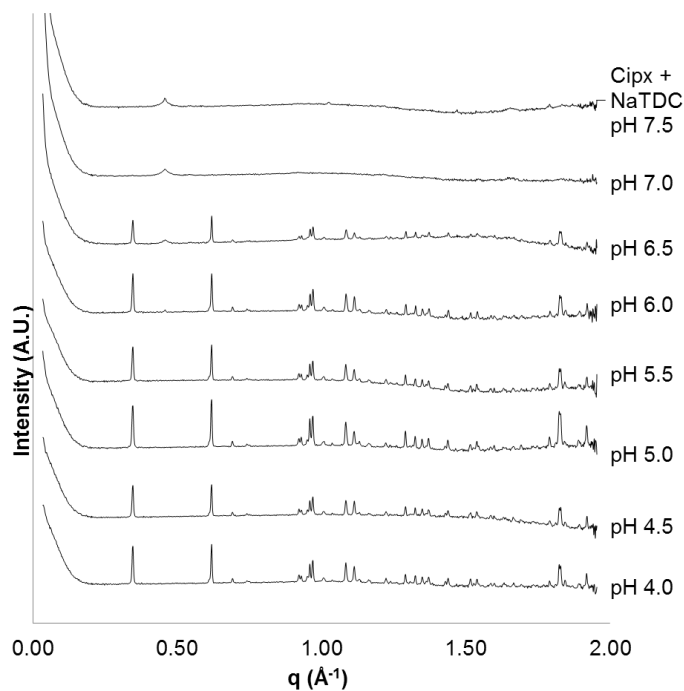


**Figure S2.** *Ex situ* static SAXS measurements of ciprofloxacin base suspension with excess NaTDC buffer with varying pH. The presence of the CIPTDC precipitate is observed from pH 6.5.

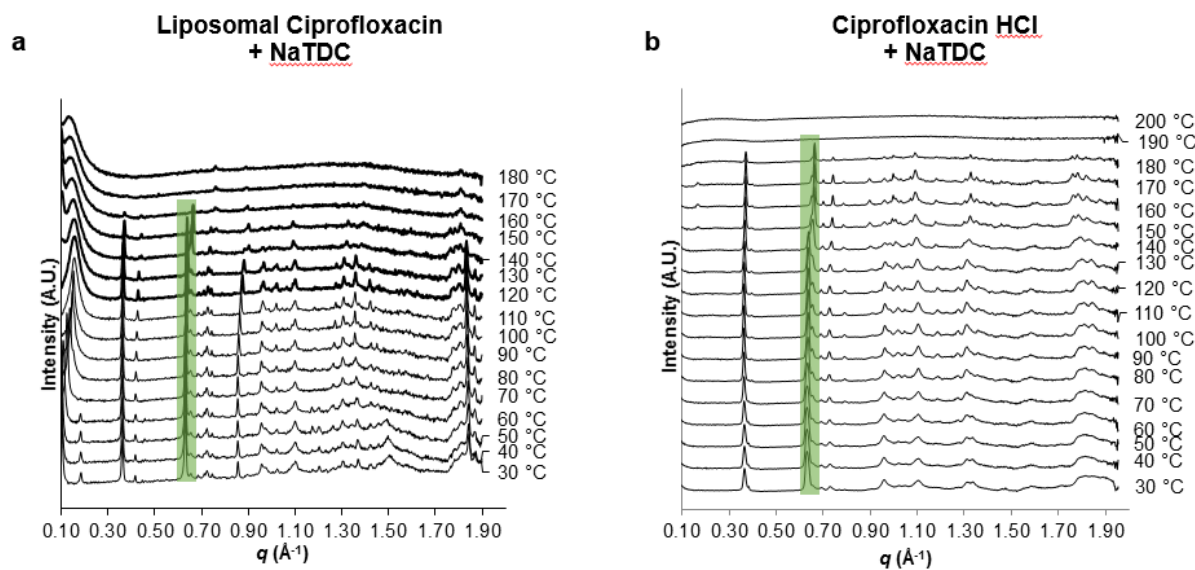


**Figure S3.** Temperature-dependent SAXS of liposomal isolated precipitate from liposomal ciprofloxacin w/o nanocrystals exposed to bile salt and ciprofloxacin HCl suspension exposed to bile salt.

## References

1. Savjani KT, Gajjar AK, Savjani JK. Drug solubility: importance and enhancement techniques. *ISRN pharmaceutics*. 2012;2012:195727-.
2. Williams HD, Trevaskis NL, Charman SA, Shanker RM, Charman WN, Pouton CW, et al. Strategies to address low drug solubility in discovery and development. *Pharmacological reviews*. 2013;65(1):315-499.
3. Porter CJ, Trevaskis NL, Charman WN. Lipids and lipid-based formulations: optimizing the oral delivery of lipophilic drugs. *Nature reviews drug discovery*. 2007;6(3):231-48.
4. Junghanns JU, Müller RH. Nanocrystal technology, drug delivery and clinical applications. *International Journal of Nanomedicine*. 2008;3(3):295-310.
5. Rezhdo O, Speciner L, Carrier RL. Lipid-associated oral delivery: mechanisms and analysis of oral absorption enhancement. *Journal of controlled release*. 2016;240:544-60.
6. Jinno J, Kamada N, Miyake M, Yamada K, Mukai T, Odomi M, et al. Effect of particle size reduction on dissolution and oral absorption of a poorly water-soluble drug, cilostazol, in beagle dogs. *Journal of controlled release*. 2006;111(1-2):56-64.
7. Shegokar R, Muller RH. Nanocrystals: industrially feasible multifunctional formulation technology for poorly soluble actives. *International journal of pharmaceutics*. 2010;399(1-2):129-39.
8. O'Brien MER, Wigler N, Inbar M, Rosso R, Grischke E, Santoro A, et al. Reduced cardiotoxicity and comparable efficacy in a phase III trial of pegylated liposomal doxorubicin HCl (CAELYX/Doxil) versus conventional doxorubicin for first-line treatment of metastatic breast cancer. *Annals of oncology*. 2004;15(3):440-9.
9. Gabizon A, Shmeeda H, Barenholz Y. Pharmacokinetics of pegylated liposomal doxorubicin: review of animal and human studies. *Clinical pharmacokinetics*. 2003;42(5):419-36.
10. Gabizon A, Chemla M, Tzemach D, Horowitz AT, Goren D. Liposome longevity and stability in circulation: effects on the in vivo delivery to tumors and therapeutic efficacy of encapsulated anthracyclines. *Journal of drug targeting*. 1996;3(5):391-8.
11. Li T, Cipolla D, Rades T, Boyd BJ. Drug nanocrystallisation within liposomes. *Journal of Controlled Release*. 2018;288:96-110.

Chapter 4: Exposure of nanocrystallised ciprofloxacin liposomes to digestive media induces solid state transformation and altered *In vitro* drug release

12. Cipolla D, Wu H, Salentinig S, Boyd B, Rades T, Vanhecke D, et al. Formation of drug nanocrystals under nanoconfinement afforded by liposomes. *RSC Advances*. 2016;6(8):6223-33.
13. Cipolla D, Wu H, Eastman S, Redelmeier T, Gonda I, Chan H-K. Tuning ciprofloxacin release profiles from liposomally encapsulated nanocrystalline drug. *Pharmaceutical research*. 2016;33(11):2748-62.
14. Li T, Mudie S, Cipolla D, Rades T, Boyd BJ. Solid state characterization of ciprofloxacin liposome nanocrystals. *Molecular Pharmaceutics*. 2019;16(1):184-194.
15. Barenholz Y. Doxil® — The first FDA-approved nano-drug: lessons learned. *Journal of Controlled Release*. 2012;160(2):117-34.
16. Li X, Hirsh DJ, Cabral-Lilly D, Zirkel A, Gruner SM, Janoff AS, et al. Doxorubicin physical state in solution and inside liposomes loaded via a pH gradient. *Biochimica et Biophysica Acta (BBA) - Biomembranes*. 1998;1415(1):23-40.
17. Schilt Y, Berman T, Wei X, Barenholz Y, Raviv U. Using solution X-ray scattering to determine the high-resolution structure and morphology of PEGylated liposomal doxorubicin nanodrugs. *Bba-Gen Subjects*. 2016;1860(1):108-19.
18. Khan J, Rades T, Boyd BJ. Lipid-based formulations can enable the model poorly water-soluble weakly basic drug cinnarizine to precipitate in an amorphous-salt form during *in vitro* digestion. *Molecular Pharmaceutics*. 2016;13(11):3783-93.
19. Khan J, Hawley A, Rades T, Boyd BJ. *In situ* lipolysis and synchrotron small-angle X-ray scattering for the direct determination of the precipitation and solid-state form of a poorly water-soluble drug during digestion of a lipid-based formulation. *Journal of Pharmaceutical Sciences*. 2016;105(9):2631-2639.
20. Cipolla D, Wu H, Eastman S, Redelmeier T, Gonda I, Chan HK. Development and characterization of an *in vitro* release assay for liposomal ciprofloxacin for inhalation. *Journal of Pharmaceutical Sciences*. 2014;103(1):314-27.
21. Richards MH, Gardner CR. Effects of bile salts on the structural integrity of liposomes. *Biochimica et biophysica acta*. 1978;543(4):508-22.
22. Rowland RN, Woodley JF. The stability of liposomes *in vitro* to pH, bile salts and pancreatic lipase. *Biochimica et biophysica acta*. 1980;620(3):400-9.
23. Paternostre MT, Roux M, Rigaud JL. Mechanisms of membrane protein insertion into liposomes during reconstitution procedures involving the use of detergents. 1. Solubilization of large unilamellar liposomes (prepared by reverse-phase evaporation) by Triton X-100, octyl glucoside, and sodium cholate. *Biochemistry*. 1988;27(8):2668-77.

Chapter 4: Exposure of nanocrystallised ciprofloxacin liposomes to digestive media induces solid state transformation and altered *In vitro* drug release

24. Westergaard H. Duodenal bile acid concentrations in fat malabsorption syndromes. *Scandinavian journal of gastroenterology*. 1977;12(1):115-22.
25. Ross DL, Riley CM. Physicochemical properties of the fluoroquinolone antimicrobials. II. Acid ionization constants and their relationship to structure. *International Journal of Pharmaceutics*. 1992;83(1):267-72.
26. Torniainen K, Tammilehto S, Ulvi V. The effect of pH, buffer type and drug concentration on the photodegradation of ciprofloxacin. *International Journal of Pharmaceutics*. 1996;132(1):53-61.
27. Ross DL, Riley CM. Dissociation and complexation of the fluoroquinolone antimicrobials — an update. *Journal of Pharmaceutical and Biomedical Analysis*. 1994;12(10):1325-31.
28. Fallingborg J. Intraluminal pH of the human gastrointestinal tract. *Danish medical bulletin*. 1999;46(3):183-96.
29. Dioumaev AK. Infrared methods for monitoring the protonation state of carboxylic amino acids in the photocycle of bacteriorhodopsin. *Biochemistry Biokhimiia*. 2001;66(11):1269-76.
30. Paluch KJ, McCabe T, Müller-Bunz H, Corrigan OI, Healy AM, Tajber L. Formation and Physicochemical Properties of Crystalline and Amorphous Salts with Different Stoichiometries Formed between Ciprofloxacin and Succinic Acid. *Molecular Pharmaceutics*. 2013;10(10):3640-54.
31. Heacock RA, Marion L. The infrared spectra of secondary amines and their salts. *Canadian Journal of Chemistry*. 1956;34(12):1782-95.
32. Surov AO, Manin AN, Voronin AP, Drozd KV, Simagina AA, Churakov AV, et al. Pharmaceutical salts of ciprofloxacin with dicarboxylic acids. *European Journal of Pharmaceutical Sciences*. 2015;77:112-21.
33. Zhang G, Zhang L, Yang D, Zhang N, He L, Du G, et al. Salt screening and characterization of ciprofloxacin. *Acta crystallographica Section B, Structural science, crystal engineering and materials*. 2016;72(Pt 1):20-8.
34. Greenstein GR. The Merck Index: An Encyclopedia of Chemicals, Drugs, and Biologicals (14th edition). In: O'Neil MJ, editor.: Merck & Co.; 2007. p. 40.



## **Chapter 5: Summary and Future Outlook**

## 5.1 Summary and Findings

Liposomes are widely researched phospholipid-based drug delivery nanocarriers that provide benefit in the ability to encapsulate drugs of various physiochemical properties. These systems are versatile in their ability to modify the pharmacokinetics of drug actives through the modification of the liposome surface. Many research efforts have focused on the design of the liposome surface, to enable stimuli-responsive drug release and active-targeting drug delivery. However, the modification of what goes inside the liposome is not well studied. Considering the encapsulated drug inside the liposomes, the physical states can vary for different drugs and different method of drug loading into the liposomes. However, the physical state of the drugs inside the liposome has rarely been reported as discussed in Chapter 1 of this thesis. The physical state of the drug, especially when it is precipitated as drug nanocrystals inside the liposomes versus when it is dissolved in solution or present as an amorphous precipitate would affect both the drug release kinetics from the liposomal nanocarriers as well as affecting the overall morphology of the liposomal nanocarriers. When drugs are precipitated inside the liposomes as drug nanocrystals; like that of the Doxil formulation or the nanocrystallised ciprofloxacin liposomes studied in this thesis, the growth of the drug nanocrystals under the confinement of the liposomal bilayer often results in the deformation of the liposomal vesicle. This deformation caused by the drug nanocrystals, would stretch the liposomal bilayer to form an ellipsoidal-shaped nanoparticle from its natural spherical-shape spontaneously formed by the phospholipids. The nanoparticle shape has been reported to affect its ability to interact with cells, hence the change in the physical state of the drug inside the liposome for example when it is precipitated as drug nanocrystals, it would modify the *in vivo* fate of the liposomes. The other reason why the physical state of the drug is important is that, if it has precipitated as drug nanocrystals, then the amount of freely soluble drug would be affected, as most drugs would have been precipitated, hence affecting the drug release kinetics out of the liposome.

Ciprofloxacin liposome is an interesting formulation, where the physical state of the drug can be modified using a freeze-thawing technique that converts the non-crystalline ciprofloxacin to drug nanocrystals inside the liposome. This enables the drug to exist in different physical state inside the liposome, depending on the preparation. This formulation is an ideal model system that can be used to investigate how the physical state of the drug is changed when the liposome is exposed to different bio-relevant physical parameters,

such as pH, bile salt, enzymes. The physical state of the drug would affect the amount of drug that is solubilised, which would affect the drug release kinetics. Together, the benefit of such formulation and its potential in oral drug delivery were also further discussed in chapter 1.

In Chapter 2, using the powerful synchrotron-based solution small angle X-ray scattering (SAXS) and cryogenic transmission electron microscopy (Cryo-TEM), the physical state of the drug inside the ciprofloxacin liposome after the freeze-thawing was studied. SAXS was able to identify the crystalline nature of the drug precipitate observed inside the ciprofloxacin liposome. The exact crystal form of the precipitate was also confirmed, where the ciprofloxacin have precipitated in the ciprofloxacin hydrate form with a unit cell dimension of 16.7 Å after freeze-thawing inside the liposome. SAXS were also coupled with a hot stage to study the temperature dependent solid-state properties of the nanocrystals inside the liposome *in situ*, this novel setup has not been previously reported to study such small nanocrystals in dispersions. The results showed the nanocrystals melted at 93 °C, which correlates with the dehydration of the ciprofloxacin hydrate crystals to the anhydrate form of ciprofloxacin. Furthermore, the pH dependent-solid state characteristics of the drug inside the liposomes were also studied *in situ*. It was found that for the crystallised drug inside the liposome, the physical state of the drug can be different depending on the pH. This is mainly due to the pH-dependent solubility nature of ciprofloxacin, as this would affect the supersaturation ratio, affecting the amount of solubilised drug versus amount of drug in crystalline form. Nanocrystallised ciprofloxacin liposomes were found to have a crystalline precipitate at pH 6-10, whereas, when pH is 5 and below, the crystalline precipitate is not identified. This could be used to predict the physical state of the drug inside the liposome at different locations of the gastrointestinal tract if the formulation were ingested orally. These SAXS experiments confirmed the wide application of synchrotron based SAXS in study of the fine nanostructures in solution in a time resolved manner. It provide a precedent for future researchers to use such technique to identify and screen for changes in solid state properties in drug delivery nanocarriers *in situ*.

After the crystal form of the nanocrystallised ciprofloxacin liposomes was identified, the ability to change the dimension and shape of the nanocrystals was investigated. In order to accurately, quantitatively and effectively analyse the nanocrystal dimension, a quantitative standard TEM assay was developed. To validate the accuracy of such an assay, direct comparison to cryo-TEM was studied and can be found in Chapter 3 A. It is

well known that for nanoparticles, the size and shape characterisation is crucial in its clinical applications and different imaging techniques are used by different researchers. Often, due to resource limitation, researchers would only use one type of microscopy technique, however the suitability of the chosen technique is often overlooked. In Chapter 3 A, TEM and cryo-TEM as imaging methods were used to visualize ciprofloxacin nanocrystals inside liposomes after freeze-thawing. In addition, the effect of thawing temperature on the size of nanocrystal formed has been evaluated. In pharmaceutical sciences, a wide range of nanoparticles and drug delivery systems are used, the reliable and appropriate analysis techniques are required to characterize these systems. TEM and cryo-TEM methods have their inherent benefits and disadvantages. TEM offers a quantitative approach for nanocrystal characterisation, since higher number of nanocrystals can be analysed resulting in more data for particle size analysis. On the other hand, cryo-TEM offers a qualitative approach, since it can be used to visualize the nanoparticle drug delivery systems while preserving the fine structure of the systems such as liposomal bilayer. Cryo-TEM is however, a much more expensive and demanding imaging method and is not the most appropriate method for quantitative purposes. Therefore, head-to-head comparison of these techniques is very important so that researchers can select appropriate imaging methods for appropriate purposes with high confidence. From the study, it was found that particle size data obtained from both imaging methods are closely aligned and that ciprofloxacin nanocrystals formed shorter and thinner crystals inside the liposomes when thawed at higher temperatures. The results provide confidence in the use of standard TEM to determine the size and shape distribution of nanocrystals inside the liposome without fear of sample preparation altering the conclusions.

The quantitative standard TEM assay was then used to evaluate the ciprofloxacin drug nanocrystals formed with liposomes of varying membrane and drug concentration in Chapter 3 B. SAXS modelling were also used and compared with the quantitative TEM assay to analyse the size distributions of the drug nanocrystals. Liposomal bilayer rigidity was controlled through the use of different membrane phospholipids and varying cholesterol content, and the impact of bilayer rigidity on the size distribution of ciprofloxacin nanocrystals was investigated. The results showed that the phospholipid gel-to-liquid crystalline phase transition temperature has a direct effect on the nanocrystal size. Shorter and thinner nanocrystals were formed in liposomes made from HSPC and DPPC phospholipids with a higher phase transition temperatures than DMPC and DOPC

with lower transition temperatures. The addition of cholesterol, which increases the rigidity of the liposomal bilayer, was also shown to restrict the growth of the ciprofloxacin nanocrystals. By increasing the drug loading of the liposomes made from HSPC and DPPC phospholipid, longer and wider nanocrystals were generated. These findings further exploit the ability to modify the crystals size inside the liposome. This would affect the overall nanoparticle shape, as well as the aspect ratio of the enclosing liposomes with potential to alter drug release and *in vivo* behaviour. Chapter 3 B also concluded that SAXS can be used as a complimentary method in analysing the nanocrystal size distributions but due caution must be applied when analysing samples containing larger nanocrystals with broader size distributions and in cases where it appears that significant disruption of the liposome shape has occurred.

Finally in Chapter 4, to explore the potential application of the nanocrystallised drug liposomes in oral delivery applications, *in vitro* digestion coupled with SAXS was used to study the effect of the simulated digestion on the physical state of the drug inside the ciprofloxacin liposomes with and without drug nanocrystals. Results identified a polymorphic transformation when the nanocrystallised ciprofloxacin liposomes were dispersed in simulated intestinal fluid at fasted state prior to the addition of enzymes. Further bile salt dependent solid state SAXS was used to identify the effect of bile salt on the transformation of the new crystal. It was found that a complete polymorphic transformation of the ciprofloxacin hydrate nanocrystals to a new crystal form were identified at a NaTDC : CIP molar ratio of 0.6. The new salt crystal has two signature peaks at  $q = 0.35$  and  $0.62 \text{ \AA}^{-1}$ , and was named the ciprofloxacin bile salt crystals (CIPTDC). The formation of the CIPTDC crystal is due to the complexation of the nitrogen on the ciprofloxacin piperazine functional group with the sulfonate group of the bile salt (sodium taurodeoxycholate NaTDC) and was confirmed with Fourier Transform Infrared Spectroscopy (FTIR). This complexation is also pH dependent, where the CIPTDC is only formed when the pH <6. This is because at this pH, the nitrogen on the ciprofloxacin piperazine group would be ionised and able to complex with the bile acid. The new CIPTDC salt crystal when isolated and dried, also had a melting point of 150-170 °C from temperature-dependent SAXS analysis and hot stage cross-polarised microscopy (CPLM) measurements. The *in vitro* drug release from nanocrystallised ciprofloxacin liposomes showed controlled drug release behaviour under non-digestive environment and a 3.5-fold increase in the drug release when the liposomes were exposed to the simulated digestive environment. For the non-crystallised ciprofloxacin liposomes, the drug release was fast

even when under non-digestive environment. These findings further confirm the importance of the physical state of the drug inside the liposome and how it could dictate the drug release behaviour from the liposomes. The use of SAXS to identify any polymorphic transformation is also useful in future drug research as these would help the formulator to identify any underlying polymorphic transformation due to the inherent nature of the formulation or due to external stimuli. In this case, it can be used to screen for any other drug polymorphic changes due to digestion or bile salt if the formulation was designed for oral administration.

## 5.2 Future Outlook

The work reported in this thesis has demonstrated the importance of drug solid state inside the liposome, especially when it is presented as drug nanocrystals inside the liposome. It confirmed how the solid state can be affected by different factors such as the pH, temperature and digestive components *in vitro*. Although these factors could have correlations *in vivo*, however, the biological systems are much more complicated. The research used the ciprofloxacin liposome as a model formulation to provide a proof of concept study that solid state of the drug inside the liposome and the crystal form it is present would affect the amount of drug release *in vitro*. To study the full potential of nanocrystallised drug liposomes in oral drug delivery, ciprofloxacin would not be an ideal candidate to investigate due to the high bioavailability of the drug. For future study, one should investigate on exploring other drug candidates with low bioavailability, which could be actively loaded, into the liposome and forming drug nanocrystals after freeze-thawing. Once these drug candidates are identified, interaction of different aspect ratio drug nanocrystal liposomes with intestinal cells can be explored for uptake and toxicity related studies. These studies would help researchers to understand the influence of drug solid state and/or the shape and the size of the liposome with the intestinal cells.

Once a low bioavailability drug candidate is selected and drug nanocrystals are successfully formed inside the liposome with the freeze-thawing method, researchers could also explore whether the crystallised drug inside the liposome would provide an improvement on the drug bioavailability *in vivo*. Further, by controlling the size and aspect ratio using the formulation approaches discussed in chapter 3 A and 3 B. One can also investigate how different shape, aspect ratio and size drug nanocrystallised liposomes would affect the overall bioavailability of the drug *in vivo*.

Moreover, apart from the oral application of the nanocrystallised drug liposomes, these asymmetric nanocarriers can be investigated for their potential in other application routes. The highlight of these nanocarriers is the ability to control the nanocrystal size and aspect ratio, which would affect the overall liposome shape forming high aspect ratio non-spherical nanoparticles. Previous studies have shown that high aspect ratio elongated microparticles can successfully penetrate the epidermis and upper dermis of the pig skin *ex vivo* and *in vivo*, resulting in enhanced topical delivery of vitamin A and vitamin B3 to the skin (1). These particles also showed an enhanced topical delivery to human volunteers (2). Hence nanocrystallised drug liposomes with high aspect ratios could be evaluated for their penetration ability through the skin, and studies can be done *ex vivo* and *in vivo* to evaluate whether different shape or aspect ratio liposomes can enhance skin penetration and topical delivery to the skin.

Furthermore, liposomes are widely applied in the intravenous route of administration. As discussed in chapter 3 B, the nanoparticle shape plays a dominant role in phagocytosis (3). Rod-shaped micelles showed a ten-fold longer circulation lifetime than spherical micelles (4). Also high aspect ratio non-spherical polymer particles showed an inhibition of phagocytosis by macrophages (5). Inhibition of phagocytosis by either PEGylation or shape modification of the liposome would enhance the circulation time of the liposome *in vivo*, which could provide benefit in the therapeutic efficacy.

Future research on these liposomal drug nanocrystals should focus on the exploration of how drugs of different bioavailability can be encapsulated and crystallised inside the liposome in order to draw more conclusion on the crystallisation mechanism. Also this exploration would enable one to identify the correlation between the drug candidate's molecular structure/physicochemical properties to the active loading and crystallisation behaviour inside the liposome. Another aspect would be to identify an ideal drug candidate that can be crystallised inside the liposome with bioavailability lower than ciprofloxacin. Then to evaluate the *in vivo* oral drug delivery of the crystallised liposomal drug versus the non-crystallised liposomal drug formulation to explore the potential benefit of these nanoparticles in oral drug delivery applications. Moreover, the ability to control the size of the nanocrystals for these formulations means once an ideal drug candidate is selected, one can also evaluate how the size and aspect ratio of drug nanocrystals inside the liposome would affect its *in vivo* performance for oral drug delivery or other route of administration.

## References

1. Raphael AP, Primiero CA, Ansaldo AB, Keates HL, Soyer HP, Prow TW. Elongate microparticles for enhanced drug delivery to ex vivo and in vivo pig skin. *Journal of Controlled Release*. 2013;172(1):96-104.
2. Raphael AP, Primiero CA, Lin LL, Smith RF, Dyer P, Soyer HP, et al. High aspect ratio elongated microparticles for enhanced topical drug delivery in human volunteers. *Advanced healthcare materials*. 2014;3(6):860-6.
3. Champion JA, Mitragotri S. Role of target geometry in phagocytosis. *Proceedings of the National Academy of Sciences of the United States of America*. 2006;103(13):4930.
4. Geng Y, Dalhaimer P, Cai S, Tsai R, Tewari M, Minko T, et al. Shape effects of filaments versus spherical particles in flow and drug delivery. *Nature nanotechnology*. 2007;2(4):249-55.
5. Champion JA, Mitragotri S. Shape induced inhibition of phagocytosis of polymer particles. *Pharmaceutical Research*. 2009;26(1):244-9.